PNC TN9600 92-004

分 置

海外出張報告
ＪＡＳＰＥＲレビュー会議、米国遮蔽専門家会議

１９９２年6月

動力炉・核燃料開発事業団
大洗工学センター

動力炉・核燃料開発事業団（Power Reactor and Nuclear Fuel Development Corporation）

PNC TN9600 92-004
１９９２年６月

海　外　出　張　報　告
JASPERレビュー会議、米国遮蔽専門家会議

報告者　吉田　昌宏*)

要　　旨

米国のオークリッジ国立研究所で開催された日米共同大型炉遮蔽ベンチマーク実験計画（JASPER計画）レビュー会議に出席し、日米双方の実験者を交えた解析担当者レベルの打合せにより、

・実験に密接した解析結果の検討評価
・日米相互比較による日本固有の解析精度上の課題の摘出
・モックアップ実験を大型炉設計へ外挿または適用する上での問題点の把握
・大型炉の遮蔽設計解析手法の高度化に関する技術討論、意見交換

を細部に渡って行った。また、残りの実験項目について、これまでの解析評価を踏まえたレビューを行い、実験体系、測定項目および工程等に関して技術的内容の確認を行った。

米国ワシントン州パスコで開催された米国遮蔽専門家会議（米国原子力学会主催）に出席し、「常陽」で計画中のB_4Cを用いた遮蔽集合体の設計研究に関する発表を行った。

*)　大洗工学センター　実験炉部　技術課

目　　次

1. 概　　要 …… 1

2. 会議の内容 …… 2

3. 添付資料 …… 16

1. 概　　要

1．1　出張先

米国（オークリッジ国立研究所、ワシントン州パスコ）

1．2　出張目的

1)　JASPER計画レビュー会議への出席

2)　米国遮蔽専門家会議への出席、論文発表

1．3　出張期間

平成4年4月21日（火）～5月3日（日）

2. 会 議 の 内 容

2．1　JASPER計画レビュー会議

日時：平成４年４月２３日（木）～２４日（金）

場所：米国オークリッジ国立研究所（ORNL）

出席者

Pace, Bucholz, Muckenthaler, Slater, Spencer, Hunter, Ingersoll（以上、ORNL）
Hemmig（DOE）
庄野、吉田（以上、PNC）、角田（MRI）、半田（HEC）、多田（MAPI）、清水（KHI）

概要

大型高速炉の遮蔽解析精度を向上させて設計合理化に資するため、米国ORNLのTSF施設（Tower Shielding Facility）を用いた日米共同大型炉遮蔽ベンチマーク実験（JASPER計画）を実施している。

本計画に基づく遮蔽モックアップ実験は、径方向遮蔽実験、燃料集合体内ガスプレナム部ストリーミング実験が予定通り完了したが、その後、ＤＯＥの指示により1987年３月から1990年８月までの間、実験が中断した。実験再開後、集合体内の軸方向遮蔽実験と炉内貯蔵燃料の遮蔽実験を終了し、1991年10月から、中間熱交換器内の２次系Ｎａ放射化実験が進行中である。

実験工程は、炉内貯蔵燃料の遮蔽実験の開始がＤＯＥからの実験開始の許可取得が遅れたこと及び測定上の課題の解決のために測定体系を追加したことにより、当初の予定より遅れているが、今後、遮蔽プラグ部のギャップストリーミング実験、中性子検出器応答実験、及び新遮蔽材透過実験を実施する予定である。別紙にＪＡＳＰＥＲ実験計画の概要及び実験工程を示す。

今回の会議はインフォーマルではあるが、1987年のフォーマル会議以来、５年ぶりに開かれた日米のJASPER計画担当者会議である。本会議において、PNCにおける遮蔽設計の現状、米国

で実施中のJASPER実験の現状、及び日米各々のJASPER実験解析結果等に関して技術的討論と情報交換を行った。また、契約期間内に実施する予定の実験項目について、その目的、内容及び工程に関して技術的なディスカッションを行った。

詳細な議事内容を以下に示す。

議事内容

4月23日

(1) 実験計画について（資料1-1）

C(U.S.A.)： ギャップストリーミング実験は順調に進めば、5月中旬に終了する。終了次第、次の実験の準備を開始したいので、早急に実験計画を詰めたい。

A(Japan)： 実験項目の正式な決定は本会議終了後、日本側関係者と打合した上で決定する必要がある。なお、現在、5月19日に本会議の日本国内での報告会を予定している（その後、5月13日に変更）。

C(U.S.A.)： 5月下旬では次の実験準備作業に食い込むことになるので、実験計画の決定を早めて欲しい。

A(Japan)： 検討する（本件に関しては、翌24日に再度詳細な打合を行った）

(2) ギャップストリーミング実験経過報告（資料1-2）

C(U.S.A.)： 他のreferenceと比較するため、工程上余裕があれば、ギャップを鉄で埋めたスリットなしの体系の測定を行う予定である。

体系ⅡＣでは、ギャップ内のＨＢ応答に傾きが見られたが、これはＴＳＦが面線源ではなく点線源に近いためではないかと考えられる。なお、体系ⅢはＳＭを含むため、ピークが約2倍に広がる。また、ＨＢ測定は計数率が低く、割愛する。

(3) INTRODUCTION（資料1-0）

Q(U.S.A.)： 日本側でJASPERに関係している人員はどの程度か。

A(Japan)： 日本側解析に直接関与しているのは、各社（MRI、HEC、KHI）1～2名程度で、ＰＮＣ関係者を含めて１０名程度である。

(4) 新遮蔽材実験 PRE-ANALYSIS結果報告（資料1-0）

Q(U.S.A.)： 1次元解析結果で体系後方(B_4C後方等）のスペクトル解析結果のZr体系とZrHx体系の比較はないか。

A(Japan)： ここには持ってきていないが、日本にFLUX FILEがある。

Q(Japan)： 今回示したB.B.の計数率予想結果では、実験においてＢＧ等の面から問題

となるようなことはないか。

A(U.S.A.)： 透過層が薄いため、問題無いと考えられる。

Q(Japan) ： 実験で使用予定のポリエチレンスラブはボロンを含んだものか。

A(U.S.A.)： 確認を行うが、おそらく含んでいないと思われる。もし、ボロンを含んでいた場合何か問題があるのか。

C(Japan) ： 実験の本質からは問題ない。ただし、ボロン含有の有無がC／Eの評価精度に影響するため、ボロン含有の有無だけではなく、組成データを速やかに提示してほしい。

A(U.S.A.)： 了解。組成分析を行うこととする。

(5) 日本における大型炉設計の進捗状況報告（資料1-0）

Q(U.S.A.)： 径方向遮蔽構成を4層とすることは確定事項か。

A(Japan) ： 設計研究の中での最確なものとされている。

Q(U.S.A.)： 可動型ＵＩＳに導入により何故Ｒ／Ｖの径を小さくできるのか。

A(Japan) ： 従来の大回転Ｐ、小回転Ｐの組合せによるＲ／Ｐはさらに大きな径を必要とするためである。

Q(U.S.A.)： ＵＩＳの放射化量評価の詳細化とは具体的に何を行う予定か。

A(Japan) ： 炉心上部方向の中性子束の予測精度を向上する。そのためには、JASPER計画のガスプレナム実験、軸方向遮蔽実験等の解析の成果を反映したい。

(6) 径方向遮蔽実験解析日本側結果報告（資料1-0）

Q(U.S.A.)： JSD100、JSDJ2について説明してほしい。

A(Japan) ： JSD100はENDF/B-IV をベースとし、JSDJ2 はJENDL2（JAPANESE EVALUATED NUCLEAR DATA LIBRARY Version-2）をベースとした定数セットである。

Q(U.S.A.)： Fig.3.2-3について説明してほしい。

A(Japan) ： Ｘ軸の単位はWidthとなっているが、これはNumberの誤りである。また、Ｙ軸の中性子束は相対値であり、数値には特に意味はない。この図はメッシュを詳細にする程、フラックスが増加する傾向を示している。

Q(U.S.A.)： メッシュの詳細化による効果は逆の傾向ではないか。

A(Japan) ： Ｎｏ。間違いはない（この後、本件の詳細な資料：ボーンマスでの会議で

の論文をU.S.A.側へ提示した）。

(7) 径方向遮蔽実験U.S.A.側解析結果報告（資料1-3）

Q(U.S.A.)： U.S.A.の解析結果では、C／E値はすべて1を下回る傾向であったが、日本側解析ではどうか。

A(Japan)： C／E値は0.8～1.6の範囲であった。日本側の解析は米国側と比較して全体的に高目の傾向である。なお、それとは別に、日本側解析では透過厚さを増やすと、C／Eが1より小さくなる傾向が見られた。

(8) ガスプレナム実験日本側解析結果報告（資料1-0）

日本側の解析でコンクリート組成の最適化によりC／E値が改善されたことを発表した。コンクリートの組成に関して詳細なデータを要求したところ、米国側よりギャップストリーミング実験体系の供試体製造時にサンプリングした液体状のコンクリートを缶に入れて固化したものを提供された。これは後日、日本へ郵送し、日本側で成分分析する予定である。

なお、U.S.A.側から本サンプルと実験時のコンクリートスラブの水分含有率に関しては、ほぼ一致するものと考えているとのコメントがあった。また、U.S.A.側では、このコンクリートの化学分析は行っていないが、実施は検討中とのことであった。

(9) ガスプレナム実験U.S.A.側解析結果報告（資料1-4）

C(U.S.A.)： コンクリートの数密度はレポートの組成記載値より求めて使用したが、計算と実測はよく一致した。

Q(Japan)： 数密度計算手法について教えて欲しい。

A(U.S.A.)： ＬＯＩの取扱等複雑なので、後日、導出過程を示したメモを渡す（4/24に資料2-3を提出）。

Q(Japan)： 計算に用いている"Streaming correction"に関して教えて欲しい。

A(U.S.A.)： 非均質領域を取り出して、ＤＯＴとＭＯＲＳＥとの比較より係数を評価したものである。なお、ＭＯＲＳＥでは一次元角度束（極角）に対応して、線束を求め、同じくＤＯＴの線束も一次元角度束毎にまとめて両者を比較し、角度依存の係数とした。これを境界線束に補正項として与えた。

(10) 軸方向遮蔽実験日本側解析結果報告（資料1-0）

C(U.S.A.)： 日本側の水分含有率８％との評価結果はU.S.A.側のCfによる測定結果とほぼ一致している。なお、測定結果の詳細は後程詳細に報告する（資料1-6）。

Q(U.S.A.)： Ｃ／Ｅが体系の中心について左右対称でないのは何故か。

A(Japan)： 計算値は左右対称である。実測値が左右対称とはなっていなかった。ＨＢの測定結果では約15%の差が見られる。

A(U.S.A.)： 左右でB_4C層の厚さに差があった可能性があるので、後日チェックする。

Q(U.S.A.)： 資料1-０のＰ80の図で、２次元計算と３次元計算では、何故３次元計算算の方がＣ／Ｅが小さいのか。

A(Japan)： 原因は現在検討中である。なお、後日、ＭＯＲＳＥによる追加解析を計画中である。

(11) 軸方向遮蔽実験U.S.A.側解析結果報告（資料1-5）

C(U.S.A.)： UO_2 ブランケット領域に従来の"Standard weighted"断面積に代えて"Self-shielding"断面積を適用したところ、低エネルギーサイド（3"、4"）ではＣ／Ｅが１から＋側にずれるが、5～12"の側のＣ／Ｅはよく揃った。また、高速領域の中性子スペクトルも良く一致した。

Q(Japan)： "Self-shielding"断面積の作成方法を教えて欲しい。

A(U.S.A.)： AMPXでピン領域を微細群解析し、そのスペクトルで重みづけして、61群の実効断面積を作成した。一方の"Standard weighted"断面積は標準的な１／ＥΣtrを縮約スペクトルとしている。

Q(Japan)： "Self-shielding"断面積を使用した目的は何か。

A(U.S.A.)： 特に従来の手法に問題があったためではなく、Ｃ／Ｅの改善を目的とした試みの一つである。なお、これは今回初めて試みたものである。

(12) コンクリートスラブ水分測定結果報告（資料1-6）

Q(Japan)： 本測定結果の誤差はどの程度か。

A(U.S.A.)： 様々な誤差要因の定量的な分析は行っていない。なお、評価に使用したCaの励起γ線エネルギーに関するデータベースに２種類あり、今回は確からしいとされている方を使用した結果、含有率が7.8%となったが、もう一方の

データを使用した場合は7.3%となった。他の誤差要因は、あくまで推測ではあるが、この0.5%の差より小さいか同程度ではないかと考えている。

C(U.S.A.)： この測定結果は後日いずれかのレポートに記載する予定でいるので、それまでは公開の場での引用は行わないこと。

Q(Japan)： ガスプレナムコンクリートの測定結果はどうであったか。

A(U.S.A.)： 測定結果は約10.3%と大きかった。なお、この測定結果には雨により湿分の混入の可能性等が考えられるので、後日再測定を検討中である。ただし、本供試体はコンクリートの厚さが小さいため、本手法による評価に適していない可能性も考えられる。

(13) 軸方向遮蔽体実験の再測定に関する計算結果報告（資料1-7）

U.S.A.側より、軸方向遮蔽実験の再測定体系に関して、予備解析を行ったところ、コンクリートからの回り込みは小さく、また、再測定体系における回り込み成分の減少効果は小さいことが示された。しかし、本会議終了後、日本側とPace氏とでさらに検討を行った結果、日本側とU.S.A.側では角度束の評価点が異なっていることが確認された。U.S.A.側の計算結果は再測定の有効性の評価を行う上での根拠となるものではないことが確認され、再測定の必要性が再確認された。

4月24日

(1) 今後の実験計画について（資料2-3）

今後の実験計画は日本国内での会議終了後に正式に決定すろこととなっているが、本会議の席上で、技術的なディスカッションを行い、できるだけ確度の高い実験計画案を作成しておくこととした。そのため、まず、日本側の要望を以下のとおり説明した。

- 軸方向遮蔽実験については、Li入りパラフィンをコンクリート前後に配置した体系で、SM、B_4C均質、B_4Cロッドバンドルの再測定を行って欲しい。
- ＮＩＳ実験では、体系Ⅲのコンクリートの前のみにLi入りパラフィンを配置した体系で測定を行い、さらに体系ⅢＢ、Ｃ、Ｅ、及びＦについてはボイド領域のB.B.測定を追加して欲しい。この要望が受け入れられれば、体系Ⅲは全て削除してもかまわない。
- 新遮蔽材実験は、予定通り行って欲しい。なお、実験期間の関係で、全ての測定項目

の実施が不可能となった場合、3”と8”B.B.のトラバース測定は最もプライオリティが低いので、削除してもかまわない。

① 軸方向遮蔽実験の再測定について

C(U.S.A.)： 軸方向遮蔽再測定で使用するLi入りパラフィンが足りるかどうか確認する。

C(Japan)： Li入りパラフィンはＳM後方のみをカバーすればよい。10×7×7ftブロックを使用した場合、概算ではコンクリート前後に約200＋200個で足りると考えられる。

C(U.S.A.)： 他領域の遮蔽に必要なため、あと100個づつは必要であろう。その程度であればおそらく、十分足りると考えられる。

② ＮＩＳ実験について

C(U.S.A.)： ＨＢ測定は少なくとも45cm以上のボイドが必要であり、現在の体系のボイド幅では測定は不可能である。

A(Japan)： 了解。

C(U.S.A.)： B.B.は重量が重く、また、ケーブルの引き回しの関係などにより、10”は可能であると思われるが、12”はコントロールできないであろう。

A(Japan)： 了解。B.B.径はできるだけ大きなものでの測定が望ましいが、小さい径での測定結果も有効であるため、実験はできるだけ多くの径のB.B.について行って欲しい。

③ 新遮蔽材実験について

C(U.S.A.)： 新遮蔽材実験は順調な進捗を前提とすれば、従来予定の1.5カ月で実施可能であると考えられる。

C(U.S.A.)： 日本側で指定した3”と8”B.B.のトラバース測定を削除しても実験期間の短縮効果は比較的小さい。それより、センターラインの測定は短時間の測定の繰り返し回数が増大するため、この測定でのB.B.の測定ケースを減らした方が効果が大きい。

Q(U.S.A.)： エネルギー分布の変化を見るため、6種類のB.B.径の測定を計画したとのことだが、エネルギー分布は別途ＮＥ２１３の測定も実施するので、削除できないのか。

A(Japan)： B.B.は低エネルギー領域、ＮＥ２１３は高エネルギー領域を見るため、重複するとは思っていない。

C(Japan) : センターラインの測定は、できるだけ全ての径について実施してもらいたいが、もし、実験期間に間に合わなくなった場合は、4”と12”径のB.B.測定を削除してもよいものとする。

③ まとめ

C(U.S.A.): 日本側で指定した計画に従って、今後実験を実施していくものとする。ただし、U.S.A.側としては、ＮＩＳ実験と新遮蔽材実験は協定で明記されているので、確実に終了させたい。そのため、ＮＩＳ実験→新遮蔽材実験→軸遮蔽実験再測定の順に実験を実施し、最悪の場合でも、再測定の中止のみで済ませたい。

ただし、Li入りパラフィン設置の関係上、ＮＩＳ実験と軸遮蔽実験再測定の体系が類似しているため、両者を続けて実施した方が実験期間の短縮効果が大きい。

そこで、実験体系準備期間、測定実施時間等を詳細に考慮した上で、実験の実施順番や、内容に関するU.S.A.側の案を検討したい。

なお、結果は来週以降、駐在員の庄野氏を通じて日本側に連絡する。

(2) ＩＶＦＳ実験U.S.A.側 Pre-analysis結果報告（資料2-1、2-2）

Q(Japan) : ＴＯＲＴの計算時間はどの程度であったか教えて欲しい。

A(U.S.A.): メッシュ数、群数、SN分点数等を単位にとると、ＤＯＲＴと同程度である。クレイでは体系ⅢＢで14～15時間程度であったと記憶している。

(3) ＩＶＦＳ実験日本側 Post-analysis結果報告（資料1-0）

Q(Japan) : 日本側の解析は、Hydrogen counterの測定結果を過小評価し、ＮＥ２１３の測定結果を過大評価した。なお、B.B.の測定結果についても同様の傾向が見られたが、U.S.A.側の解析にはこのような傾向は見られなかったか。

A(U.S.A.): 径方向遮蔽実験の体系ⅡＤの解析で同様の傾向が見られた。

(4) JENDL 3 の適用に関して（資料1-0）

Q(U.S.A.)： JENDL3のＮａの非弾性散乱断面積の詳細について教えて欲しい。

A(Japan)： JENDL3ではスレッショールドエネルギー近傍の値がほぼENDF/B-IVと同じであり、他の領域はJENDL2と同じである。

Q(U.S.A.)： JENDL3は完全に公開されたものか。

A(Japan)： 公開されている。

Q(U.S.A.)： 今後、遮蔽用定数セットをJENDL2ベースからJENDL3ベースに変更する予定はあるか。

A(Japan)： JENDL2をベースとしたJSDJ2は日本の高速炉設計のスタンダードであるため、当面切り替えの予定はない。

C(U.S.A.)： 今後、POST-JASPERのテーマとしてJENDL 3 とENDF/B-V,VI等と核データを交換した解析を考えてはどうか。

C(Japan)： このような交換解析は基礎的研究であり、解析者として興味はあるが、ＰＮＣとしてはプログラムを組みにくい面があるのではないかと考えられる。

(6) その他

Q(Japan)： ＩＨＸ実験ではＮａ放射化量の測定結果が20～30%程度の差で非対称となったが、この解析に関して何かアイディアはあるか。

A(U.S.A.)： 特にアイディアはない。なお、ＩＨＸ実験の解析はFY93（U.S.A.年度）より行う予定である。

Q(Japan)： U.S.A.側の今後の解析の計画を教えて欲しい。

A(U.S.A.)： FY92内にIVSF、軸方向遮蔽実験の解析の実施を予定している。ＩＨＸ以降の実験はFY93に実施の予定である。

Q(Japan)： 日本側体系の解析の予定はないか。

A(U.S.A.)： 予定はない。

C(Japan)： 日本とU.S.A.の解析精度の比較のため、数ケースの日本側体系の解析を実施してもらいたい。なお、日本では数ケースのU.S.A.体系を解析する予定である。

A(U.S.A.)： 了解。

Q(U.S.A.)： 特に比較を行いたい日本側体系を指定してほしい。

C(Japan) : 了解。本比較はJASPERの正式打合の際にディスカッションしたいと考えている。U.S.A.では正式打合の実施はいつごろを想定しているか。

A(U.S.A.): 来年の夏か秋頃を考えている（1993年9月末以前）。

C(Japan) : 日本側も来年の夏より前の開催は考えていない。米国側で解析してもらいたい日本側体系に関しては年内に指定することとする。

A(U.S.A.): 了解。

以上

ま　と　め

主な検討結果を以下に示す。

- 1990年の実験再開以降、実験は順調に実施され、現在も順調に進行中であることを確認した。
- 日米の担当者間で、実験及び解析に関する解釈等に大きなギャップが無かったことが確認された。
- 軸遮蔽実験で予想以上にバックグラウンドの寄与が大きく、実験本来の目的である均質体系と非均質体系の中性子ストリーミング効果の違いの評価に有効な結果が得られなかった体系についてはバックグラウンドの除去を考慮した体系での再測定を実施することとなった。
- 上記再測定と残り２つの実験項目をPNC側の計画通りに実験期間内に完遂することはほぼ可能であることが、非公式ではあるが、確認された。
- 今回検討した工程が実際に可能か否かを判断するには、さらに検討を行う必要があるため、現在、ORNLのPNC駐在員を通じて詳細を調整中である。

表２．１　ＪＥＳＰＥＲ計画の実施状況

実験項目	実験	解析・評価
(1)　径方向遮蔽実験	終了	終了
(2)　燃料集合体内ｶﾞｽﾌﾟﾚﾅﾑ部ストリーミング実験	終了	終了
(3)　軸方向遮蔽実験	終了	ほぼ終了
(4)　炉内燃料貯蔵実験	終了	実施準備中
(5)　２次ﾅﾄﾘｳﾑ 放射化実験	終了	—
(6)　遮蔽プラグ部のギャップストリーミング実験	実施中	—
(7)　中性子検出器応答実験	—	—
(8)　新遮蔽材透過実験	—	—

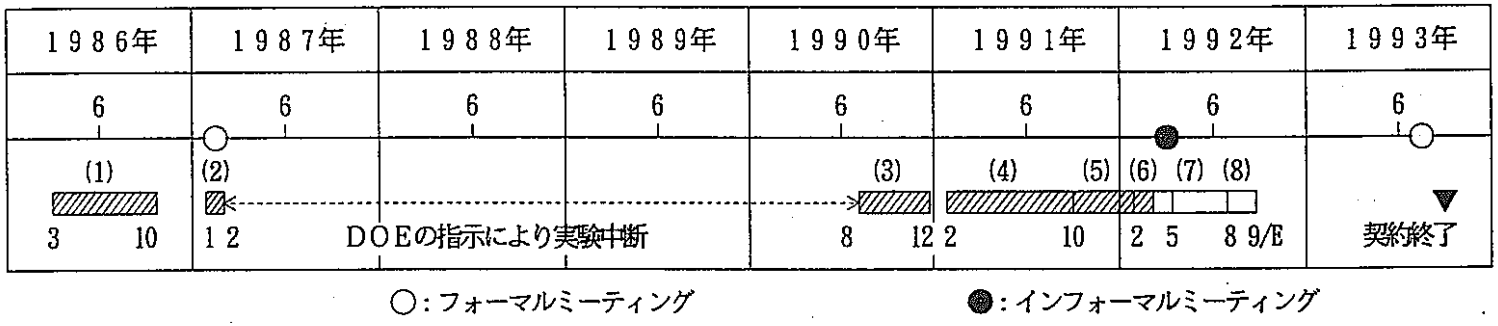

2．2　米国遮蔽専門家会議

主催：　米国原子力学会

日時：　平成4年4月26～5月1日

場所：　ワシントン州パスコ

概要

本会議は米国原子力学会が2年に1回の頻度で開催する放射線遮蔽全般について討論する国際会議である。

会議には米、英、仏、独、フィンランド、カナダ及び日本から約150名が参加し、日本からの参加者は17名であった。今回の会議では、計算機の高速化、並列化及びワークステーションの活用等の計算技術の高度化を反映した解析に関する報告が活発になされ、中でもモンテカルロ計算コード"MCNP"に関する報告が多く、会場の関心も集中していた。

今回、動燃より下記の2件の発表を行った。JANUS計画（英、仏、独による主にEFR遮蔽設計を目的とした共同研究）の関係者より、「常陽」で計画中の B_4Cを装填した遮蔽体に関して、その使用形態及び使用寿命評価方法に関しての質問があった。「常陽」では、高速炉の径方向遮蔽として B_4Cを使用する計画であるが、EFRにおいても、径方向遮蔽には B_4Cの使用が検討されており、本発表への関心が高かった。

高速炉遮蔽のセッションでは、JASPER、JANUS のベンチマーク実験解析及びFFTFの遮蔽計算に関する発表があった。ORNLからのJASPER計画に関する発表に対し、計画終了後の TSFの運用に関する質問があり、実験計画はなく閉鎖する旨の回答がなされた。また、FFTFの発表は遮蔽体、炉内構造物の照射損傷からの余寿命評価を目的とした"MCNP"を用いた全炉心解析に関するものであった。

① " Experiment and Analysis of Neutron Streaming through an Axial Shield in a FBR Fuel Subassembly"

② " B_4C Shielding Design Study for the JOYO Reactor"

3. 添 付 資 料

3．1 JASPERレビュー会議資料

Ⅰ AGENDA

Ⅱ ORNL資料リスト

4/23使用分

2-1 Program plan for remaining JASPER experiments(J.V.Pace III)

2-2 On-going measurements for the JASPER program(F.J.Muckenthaler)

2-3 Analysis of the JASPER program radial shield attenuation experiment (C.O.Slater)

2-4 Analysis of the JASPER fission gas plenujm experiment(C.O.Slater)

2-5 Results of the analysis of the axial shield experiment(C.O.Slater)

2-6 Measurements of wt% in axial shields and fission gas plenum concrete slabs(R.R.Spencer)

2-7 Calculational results of re-confugurations of the JASPER axial shield (J.V.Pace III)

4/24使用分

2-8 The JASPER in-vessel fuel storage(IVFS) experiment(J.A.Bucholz)

2-9 Partial list of IVFS report(J.A.Bucholz)

2-10 Calculational method of the number density of the concrete slabs (C.O.Slater)

Ⅲ 日本側資料リスト

4/23使用分

3-1 Summary of the analysis of the JASPER experiment in JAPAN (PNC TN9410 92-083：社内資料化されているため、ここには添付しない)

4/24使用分

3-2 PNC's request about the data plan for future experiments

※（ ）内は発表者を示す。

I AGENDA

U.S.-JAPAN INFORMAL JASPER MEETING

APRIL 23-24, 1992

BUILDING 6025 CONFERENCE ROOM
OAK RIDGE NATIONAL LABORATORY
OAK RIDGE, TENNESSEE

AGENDA

THURSDAY, 23 APRIL 1992

0830 - 0900	Coffee/Sweet Rolls	
0900 - 0910	Welcome	US (ORNL-DTI)
0910 - 0925	Presentation of Ongoing Measurements	US (ORNL-FJM)
0925 - 0945	Program Plan for Remaining Experiments	US (ORNL-JVP)
0945 - 1000	Special Materials Experiment Plans	Japan (PNC-AY)
1000 - 1010	Introduction of Japanese Analyses	Japan (PNC-AY)
1010 - 1040	Shielding Design Study in Japan	Japan (PNC-AY)
1040 - 1100	Japanese Post Analysis of the Radial Shield Attenuation Experiment	Japan (KHI-YS)
1100 - 1130	U.S. Post Analysis of the Radial Shield Attenuation Experiment	US (ORNL-COS)
1130 - 1200	Radial Shield Attenuation Experiment Discussion	Japan, US
1200 - 1300	Catered Lunch	
1300 - 1320	Japanese Post Analysis of the Fission Gas Plenum Experiment	Japan (MAPI-KT)
1320 - 1340	U.S. Post Analysis of the Fission Gas Plenum Experiment	US (ORNL-COS)
1340 - 1400	Fission Gas Plenum Experiment Discussion	Japan, US

U.S.-JAPAN INFORMAL JASPER MEETING AGENDA (cont'd)

1400 - 1530	Japanese Post Analysis of the Axial Shield Experiment		Japan
	1400 - 1420	Homogeneous Shield Mockup	(PNC-AY)
	1420 - 1440	Central Blockage Shield Mockup	(KHI-YS)
	1440 - 1500	Rod Bundle Shield Mockup	(HEC-HH)
	1500 - 1530	Central Sodium Channel Mockup	(MRI-HT)
1530 - 1550	U.S. Post Analysis of the Axial Shield Experiment		US (ORNL-COS)
1550 - 1600	Measurement of Water Content in Concrete Shields		US (ORNL-RRS)
1600 - 1700	Axial Shield Experiment Discussion		Japan, US

FRIDAY, 24 APRIL 1992

0830 - 0900	Coffee/Sweet Rolls		
0900 - 0940	Japanese Post Analysis of the In-Vessel Fuel Storage Experiment		Japan
	0900 - 0920	Spectrum Modifier (SM-2)	(MRI-HT)
	0920 - 0940	Shield Mockup (Config.II-M,N,O)	(HEC-HH)
0940 - 1000	U.S. Post Analysis of the In-Vessel Fuel Storage Experiment		US (ORNL-JAB)
1000 - 1045	In-Vessel Fuel Storage Experiment Discussion		Japan, US
1045 - 1100	Improvement of shielding Analysis Method		Japan (KHI-YS)
1100 - 1200	General Discussion		Japan, US
1200 - 1300	Lunch		
1300 - 1500	Tour of the Tower Shielding Facility		Japan, US

U.S.-JAPAN INFORMAL JASPER MEETING AGENDA (cont'd)

Alpahbetical Listing of Acronyms

HEC-HH	Hitachi Engineering, Co., Ltd.	- Hiroyuki Handa
KHI-YS	Kawasaki Heavy Industries, Ltd.	- Yasuyuki Shimizu
MAPI-KT	Mitsubishi Atomic Power Industry, Inc.	- Keiko Tada
MRI-HT	Mitsubishi Research Institute, Inc.	- Hirokazu Tsunoda
ORNL-COS	Oak Ridge National Laboratory	- Charles O. Slater
ORNL-DTI	Oak Ridge National Laboratory	- Dan T. Ingersoll
ORNL-FJM	Oak Ridge National Laboratory	- F.J. (Buzz) Muckenthaler
ORNL-JAB	Oak Ridge National Laboratory	- Jim A. Bucholz
ORNL-JVP	Oak Ridge National Laboratory	- Joe V. Pace III
ORNL-RRS	Oak Ridge National Laboratory	- R.R. (Bob) Spencer
PNC-AY	Power Reactor & Nulcear Fuel Development Corp, O-arai Engr Center	- Akihiro Yoshida

Ⅱ ＯＲＮＬ資料リスト

Program Plan For Remaining JASPER Experiments

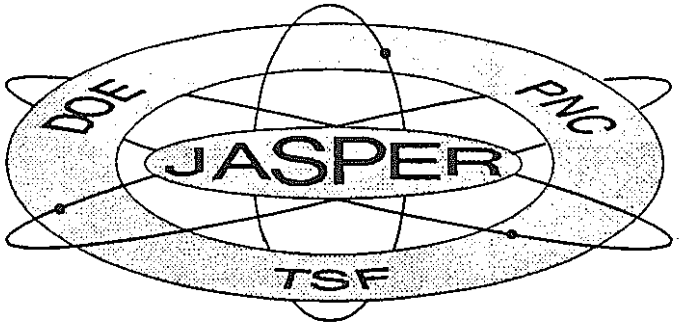

J.V. Pace III

ornl

US-JAPAN INFORMAL JASPER MEETING
ORNL, Oak Ridge, TN
April 23-24, 1992

TABLE 1. Summary Program Plan For Flu.. Monitor Experiment

Configuration*	Measurements**				
	Spectra & BB	Bonner Ball		Fission Counter	
		Centerline	Traverse	Traverse	In void
I. Spectrum Modifier and Removable Radial Shield (RRS) Mockups					
A. SM (10cm Fe + 9cm Al + 2.54cm boral + 20cm Radial Blanket)		x			
B. I.A + 1.3cm Al + 15cm SS	x	x	x	x	
C. I.B + 1.3cm Al + 10cm C + 5cm SS + 1.3cm Al + 10cm C + 5cm SS	x	x	x	x	
II. RRS plus 15cm-dia Neutron Guide (Tank Type)					
A. I.C + 13.05cm B4C with aluminum guide		x	x	x	
B. II.A + 30cm void + 30cm C		x	x	x	x
C. II.A + 30cm void + 15cm B4C		x			
D. II.A + 30cm void + 15cm B4C + 20cm C		x			
E. II.A + 30cm void + Thick IVFS Mockup		x	x	x	
F. II.E + 30cm C		x	x	x	x
G. II.E + 15cm B4C		x			
H. II.E + 15cm B4C + 20cm C		x			
III. RRS plus 15cm-dia Neutron Guide (Loop Type)					
A. I.B + Axial Shield with aluminum center	x	x	x	x	
B. III.A + 30cm void + 15cm B4C		x			
C. III.A + 30cm void + 15cm B4C + 20cm C		x	x	x	x
D. III.A + 30cm void + Thick IVFS Mockup		x	x	x	
E. III.D + 15cm B4C		x			
F. III.D + 15cm B4C + 20cm C		x	x	x	x

* Nominal Dimensions

** Spectra & BB: NE-213/Benjamin spectrometer measurements on beam centerline as close as feasible and 3-, 5-, and 10-in Bonner balls at same location.
BB Centerline: bare, Cd-covered, 3-, 5-, 8-, and 10-in. Bonner ball measurements on centerline at 30cm and at 150cm.
BB Traverse: 5-in. Bonner ball traverse at 30cm behind the shield mockups.
Fission Counter Traverse: U-235 fission chamber in horizontal traverse at 30cm behind mockup.
Fission Counter in Void: U-235 fission chamber traverse along beam centerline in void.

TABLE 1. Summary Program Plan For Flux Monitor Experiment (Rev. 1)

Configuration*	Measurements**						
	Spectra & BB	Bonner Ball		Fission Counter		Hornyak Button	
		Center-line	Traverse	Traverse	In Void	Traverse	In Void
III. RRS plus 15cm-dia Neutron Guide (Loop Type)							
A. I.B + Axial Shield with hexagonal Al center	x	x	x	x			
B. III.A + 30cm void + 15cm B4C		x					
C. III.A + 30cm void + 15cm B4C + 20cm C		x	x	x	x		
D. III.A + 30cm void + Thick IVFS Mockup		x	x	x			
E. III.D + 15cm B4C		x					
F. III.D + 15cm B4C + 20cm C		x	x	x	x		

* Nominal Dimensions

** Spectra & BB: NE-213/Benjamin spectrometer measurements on beam centerline as close as feasible and 3-, 5-, and 10-in Bonner balls at same location.
BB Centerline: bare, Cd-covered, 3-, 5-, 8-, and 10-in. Bonner ball measurements on centerline at 30cm and at 150cm.
BB Traverse: 5-in. Bonner ball traverse at 30cm behind the shield mockups.
Fission Counter Traverse: U-235 fission chamber in horizontal traverse at 30cm behind mockup.
Fission Counter in Void: U-235 fission chamber traverse along beam centerline in void.
Hornyak Button Traverse: Hornyak Button in horizontal traverse as close as feasible behind mockup.
Hornyak Button In Void: Hornyak Button in horizontal traverse in the void.

TABLE 1. Summary Program Plan For Flux Monitor Experiment (Rev. 2)

Configuration*	Measurements**						
		Bonner Ball		Fission Counter		Hornyak Button	
	Spectra & BB	Centerline	Traverse	Traverse	In Void	Traverse	In Void
I. Spectrum Modifier and Removable Radial Shield (RRS) Mockups							
A. SM (10cm Fe + 9cm Al + 2.54cm boral + 20cm Radial Blanket)		x					
B. I.A + 1.3cm Al + 15cm SS	x	x	x	x			
II. RRS plus 15cm-dia Neutron Guide (Loop Type)							
A. I.B + Axial Shield with hexagonal Al center	x	x	x	x		?	
B. III.A + 30cm void + 15cm B4C		x				?	?
C. III.A + 30cm void + 15cm B4C + 20cm C		x	x	x	x		?
D. III.A + 30cm void + Thick IVFS Mockup		x	x	x		?	
E. III.D + 15cm B4C		x				?	?
F. III.D + 15cm B4C + 20cm C		x	x	x	x		?

* Nominal Dimensions

** Spectra & BB: NE-213/Benjamin spectrometer measurements on beam centerline as close as feasible and 3-, 5-, and 10-in Bonner balls at same location.

BB Centerline: bare, Cd-covered, 3-, 5-, 8-, and 10-in. Bonner ball measurements on centerline at 30cm and at 150cm.

BB Traverse: 5-in. Bonner ball traverse at 30cm behind the shield mockups.

Fission Counter Traverse: U-235 fission chamber in horizontal traverse at 30cm behind mockup.

Fission Counter in Void: U-235 fission chamber traverse along beam centerline in void.

Hornyak Button Traverse: Hornyak Button in horizontal traverse as close as feasible behind mockup.

Hornyak Button In Void: Hornyak Button in horizontal traverse in the void.

TABLE 1. Summary Program Plan For Re-Measurement* of a Subset of the Axial Shield Experiment (Rev. 1)

Configuration**	Measurements***			
	Spectra & BB	Bonner Ball		Hornyak Button
		Centerline	Traverse	
I. Neutron Spectrum Modifier (SM-1)				
A. SM-1 (10cm Fe + 9cm Al + 2.5cm boral + 20cm Radial Blanket)		x		
II. Homogeneous Shield Mockup				
A. I.A + 7 B_4C homogeneous type assemblies	x	x	x	x
III. Rod Bundle Shield Mockup				
A. I.A + 6 B_4C homogeneous type hexagonal assemblies around 1 B_4C rod bundle type hexagonal assembly	x	x	x	x

* Using reformed Axial Shield configuration

** Nominal Dimensions

*** Spectra & BB: NE-213/Benjamin spectrometer measurements on beam centerline as close as feasible and 3-, 5-, and 10-in Bonner balls at same location.
BB Centerline: 3-, 4-, 5-, 8-, 10-, and 12-in. Bonner ball measurements on centerline at 30 & 150cm.
BB Traverse: 3-, 5-, and 8-in. Bonner ball traverses at 30cm behind the shield mockups.
Hornyak Button: Hornyak button (0.25-in-diameter) traverse as close as feasible behind shield mockup.

ON-GOING MEASUREMENTS FOR THE JASPER PROGRAM

F. J. Muckenthaler
Oak Ridge National Laboratory*

Paper to Presented at the
US-JAPAN Informal JASPER Meeting
ORNL, Oak Ridge, TN
April 23-24, 1992

*Managed by Martin Marietta Energy Systems, Inc. under Contract No. DE-AC05-84OR21400 for the U.S. Department of Energy.

I. EXPERIMENTAL PROGRAMS

	Program	Status
1.	Radial Shield Attenuation Experiment	Completed, Reported
2.	Fission Gas Plenum Experiment	Completed, Reported
3.	Axial Shield Experiment	Completed, Reported
4.	In-Vessel Fuel Storage Experiment	Completed, Reported
5.	Intermediate Heat Exchanger Experiment	Completed, First Draft
6.	Gap Streaming Experiment	In Progress
7.	Flux Monitor Experiment	Scheduled for May
8.	Special Materials Experiment	Scheduled for August

II. GAP STREAMING EXPERIMENT

Purpose: The experiment is designed to study the magnitude and shape of the neutron distribution streaming in narrow voids that are typical of gaps anticipated in the design of enclosure systems for the LMRs.

Mockups: The mockups that are being studied contain cylindrical voids, both straight and with single offsets that vary in width and location. The cylindrical sleeves used to form the voids contain either iron or concrete enclosed in iron shells. Concrete is the primary shield material within the vessel. A similar vessel of solid concrete is also included to provide a study of just concrete.

Detectors: The fast neutron spectra were measured using an NE-213 liquid scintillator whose response has a low energy cutoff at about 0.8 MeV. The low-energy neutron spectra 50 keV to about 1.5 MeV, were measured with a series of hydrogen-filled proton recoil detectors with different gas pressures.

The Bonner ball detector contains ^{10}B enriched BF_3 gas that can be surrounded by different thicknesses of polyethylene whose responses are sensitive to different neutron energy ranges. These response functions provide a method for converting the calculated spectra to flux values for comparison with the measured values.

The Hornyak button is a 0.635-cm-diameter, 0.158-cm-thick mixture of lucite and zinc sulfide, mounted on a photomultiplier tube. Its small size provides a means for determining the shape of the neutron flux leaving small voids.

III. SUMMARY PROGRAM PLAN FOR GAP STREAMING EXPERIMENT

Configuration*	Measurements**			
	Spectra & BB	Bonner Ball		Hornyak Button
		Centerline	Traverse	
I. Neutron Spectrum Modifier				
A. SM-2 (10 cm Fe + 9 cm Al + 2.5 cm boral + 180 cm Na		X	X	
II. Bare Beam + Mockups				
A. 100 cm concrete slab	X	X	X	X
B. 1 cm straight annular slit		X	X	X
C. 3 cm straight annular slit	X	X	X	X
D. 2 cm slit, 4 cm offset		X	X	X
E. 2 cm slit, 8 cm offset		X	X	X
F. No slits		X	X	
III. SM-2 + Mockups				
A. 100 cm concrete		X	X	X
B. 1 cm straight annular slit		X	X	X
C. 3 cm straight annular slit		X	X	X
D. III.C + 5 cm SS		X	X	X
E. III.C + 10 cm SS		X	X	X
F. 2 cm slit, 4 cm offset		X	X	X
G. 2 cm slit, 8 cm offset		X	X	X
H. No slits		X	X	

*Nominal Dimensions

**Spectra & BB: NE-213/Benjamin spectrometer measurements on beam centerline as close as feasible and 3-, 5-, and 10-in Bonner balls at same location.
BB Centerline: 3-, 5-, and 8-in Bonner ball measurements on centerline at 150 cm.
BB Traverse: 3-, 5-, and 8-in Bonner ball traverses at 30 cm behind the shield mockups.
Hornyak Button: Hornyak button (0.25-in-diameter) traverse as close as feasible behind shield mockup and at 30 cm.

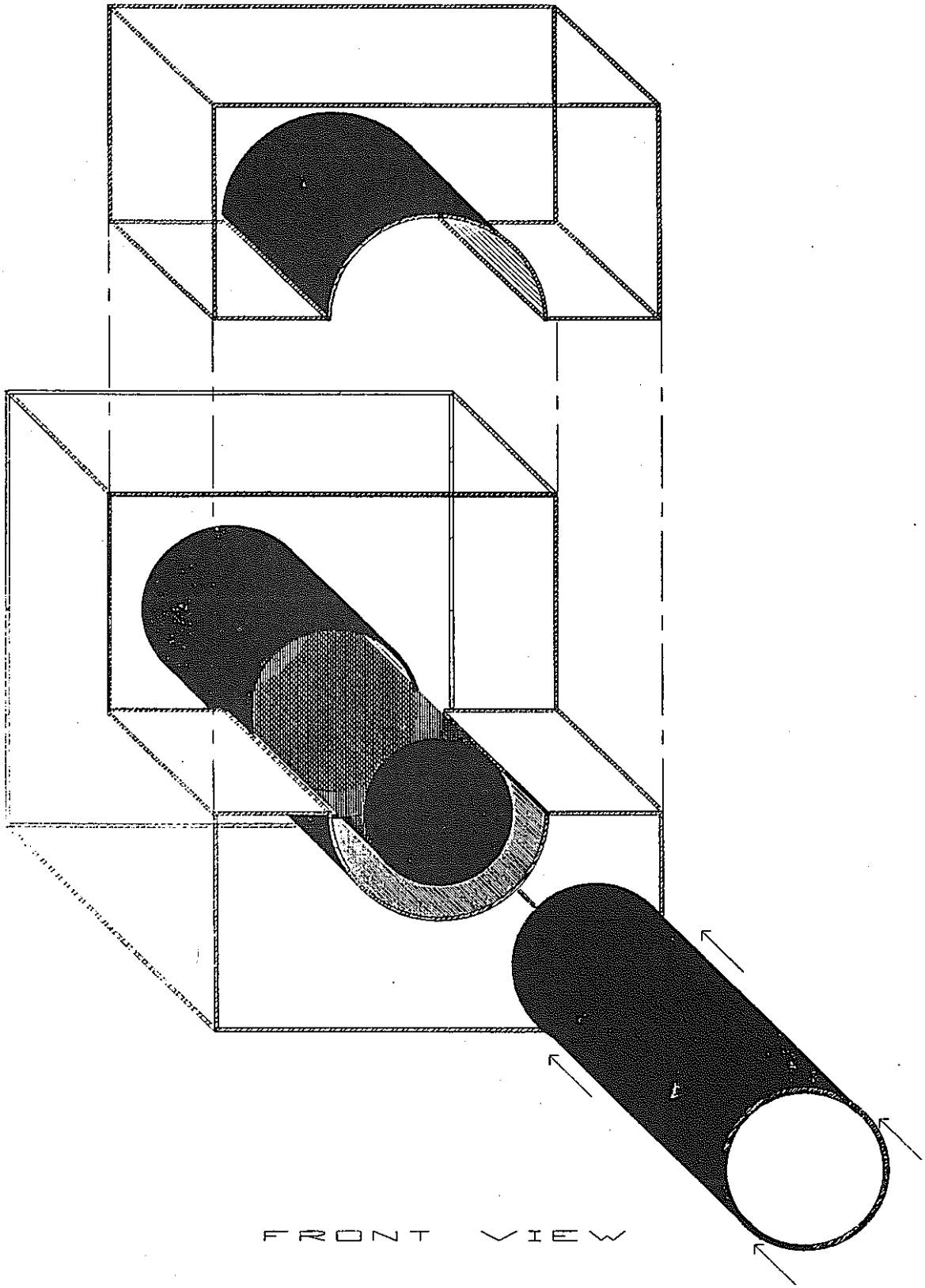

FRONT VIEW

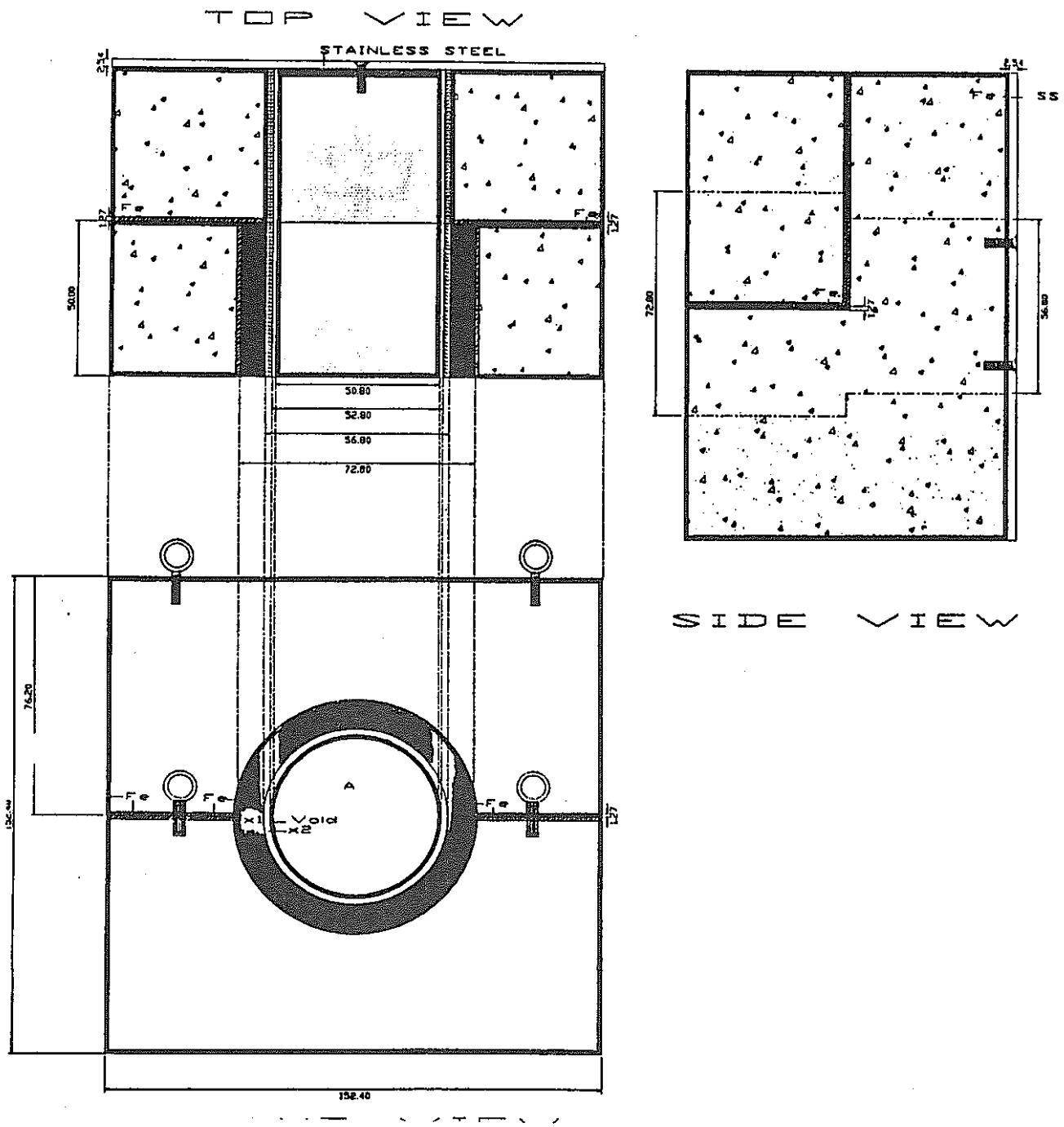
TOP VIEW
STAINLESS STEEL
50.80
52.80
56.80
72.80
76.20
Fe
Void
x1
x2
A
152.40
SIDE VIEW
72.80
56.80

TOP CUTAWAY VIEW
(configuration #2)

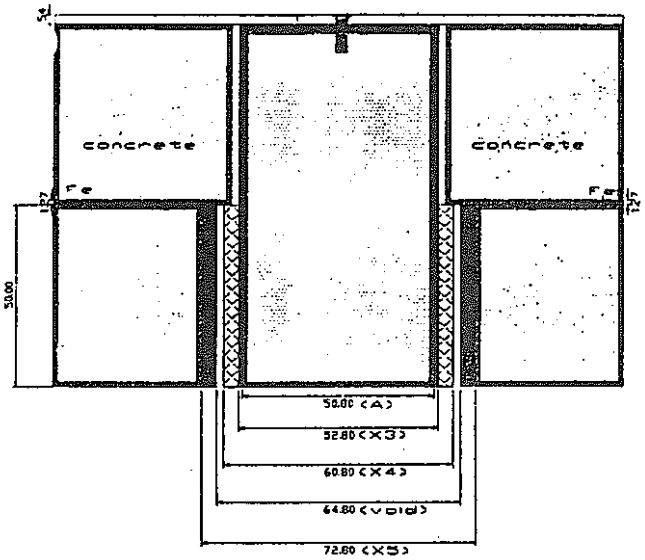

TOP CUTAWAY VIEW
(configuration #3)

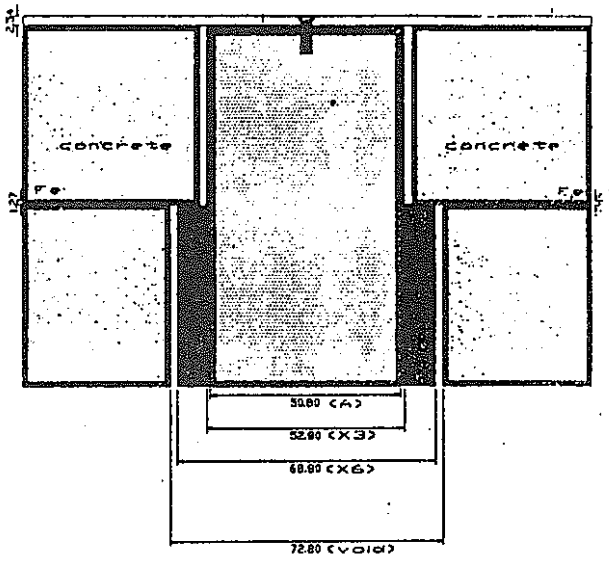

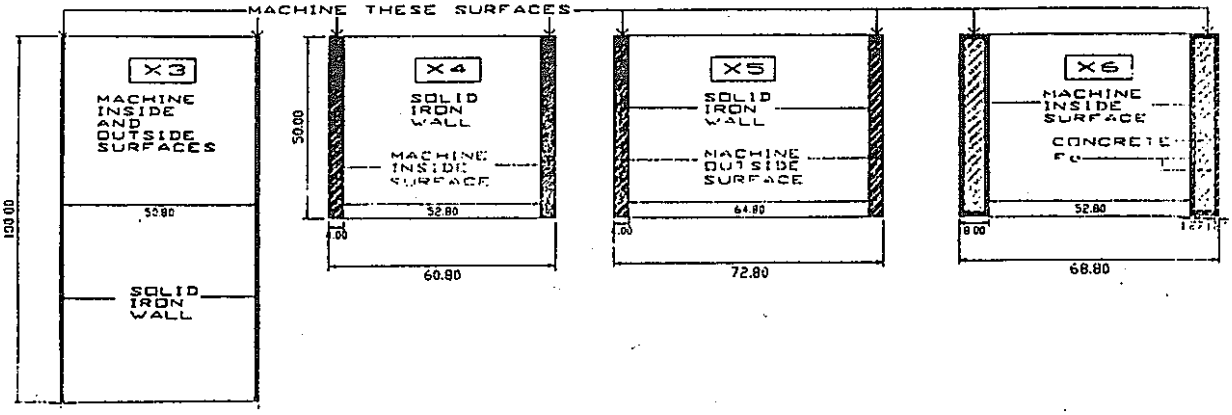

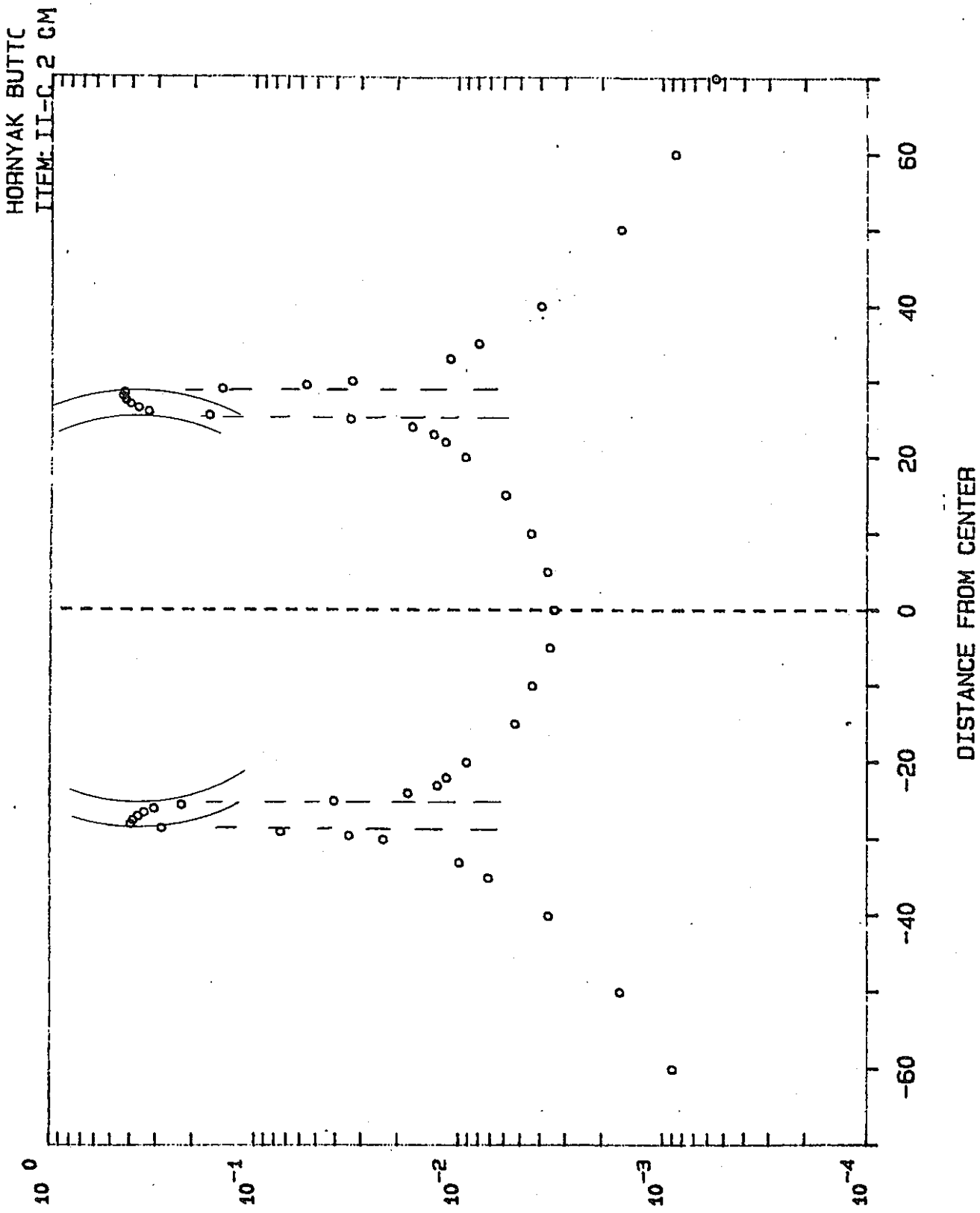
HORNYAK BUTTC
ITEM: II-C 2 CM
60
40
20
0
-20
-40
-60
DISTANCE FROM CENTER
10^0
10^-1
10^-2
10^-3
10^-4

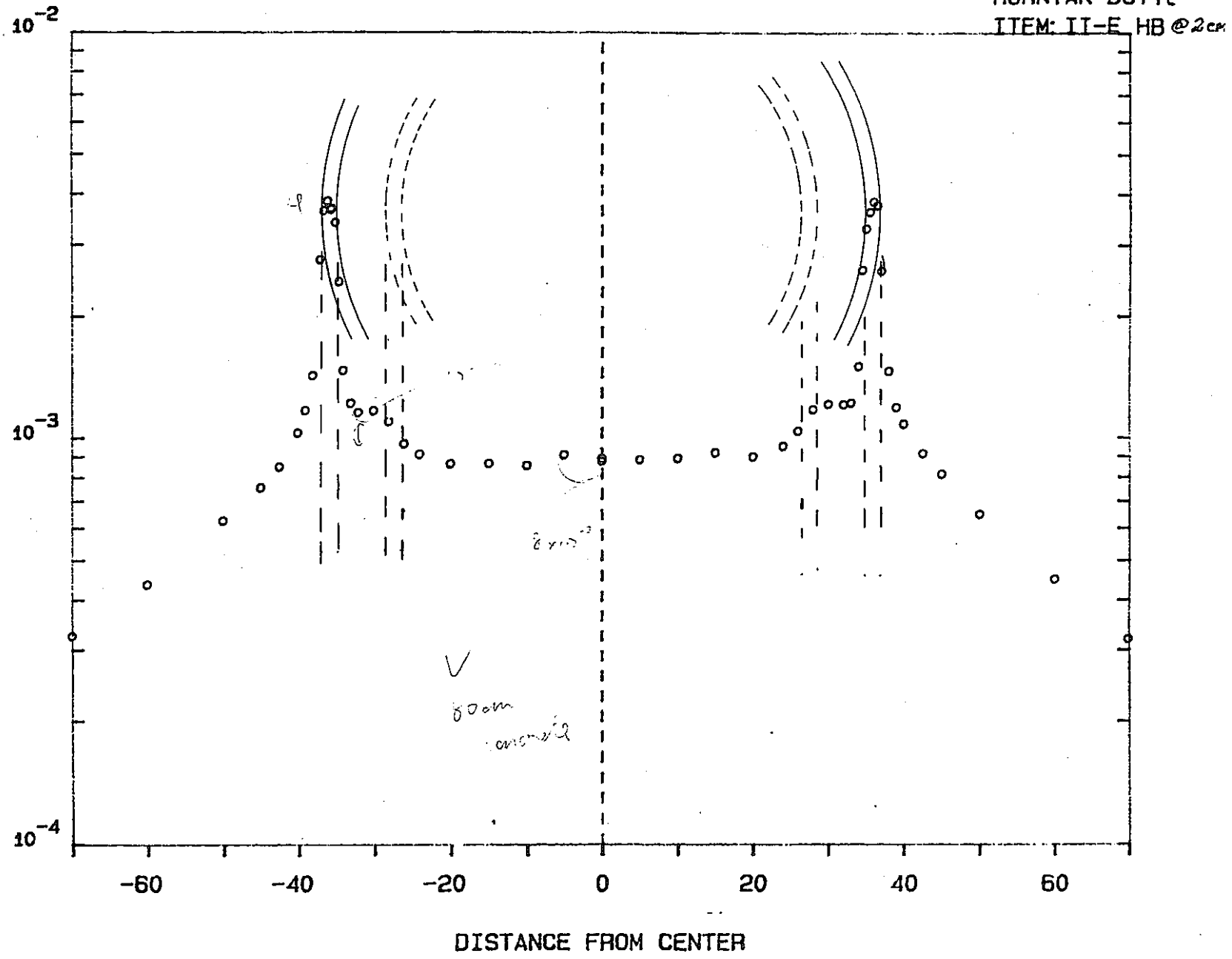
HORNYAK BUTTC
ITEM: II-E HB @2cm
10^{-2}
10^{-3}
10^{-4}
-60
-40
-20
0
20
40
60
DISTANCE FROM CENTER

III. SUMMARY PROGRAM PLAN FOR GAP STREAMING EXPERIMENT

Status	Configuration*	Measurements**			
		Spectra & BB	Bonner Ball		Hornyak Button
			Centerline	Traverse	
	I. Neutron Spectrum Modifier				
Completed	A. SM-2 (10 cm Fe + 9 cm Al + 2.5 cm boral + 180 cm Na		X	X	
	II. Bare Beam + Mockups				
Completed	A. 100 cm concrete slab	X	X	X	X
Completed	B. 1 cm straight annular slit		X	X	X
Completed	C. 3 cm straight annular slit	X	X	X	X
Completed	D. 2 cm slit, 4 cm offset		X	X	X
Completed	E. 2 cm slit, 8 cm offset		X	X	X
	F. No slits		X	X	
	III. SM-2 + Mockups				
Completed	A. 100 cm concrete		X	X	X
	B. 1 cm straight annular slit		X	X	X
Completed	C. 3 cm straight annular slit		X	X	X
Completed	D. III.C + 5 cm SS		X	X	X
Completed	E. III.C + 10 cm SS		X	X	X
	F. 2 cm slit, 4 cm offset		X	X	X
	G. 2 cm slit, 8 cm offset		X	X	X
	H. No slits		X	X	

*Nominal Dimensions

**Spectra & BB: NE-213/Benjamin spectrometer measurements on beam centerline as close as feasible and 3-, 5-, and 10-in Bonner balls at same location.
BB Centerline: 3-, 5-, and 8-in Bonner ball measurements on centerline at 150 cm.
BB Traverse: 3-, 5-, and 8-in Bonner ball traverses at 30 cm behind the shield mockups.
Hornyak Button: Hornyak button (0.25-in-diameter) traverse as close as feasible behind shield mockup and at 30 cm.

ORNL/TM-10701

ENGINEERING PHYSICS AND MATHEMATICS DIVISION

Analysis of the JASPER Program Radial Shield Attenuation Experiment

C. O. Slater

This work Sponsored by the
Defense Nuclear Agency
under
Interagency Agreement No. 40-65-65

NOTICE:	This document contains information of a preliminary nature. It is subject to revision or correction and therefore does not represent a final report.

Prepared by the
OAK RIDGE NATIONAL LABORATORY
Oak Ridge, Tennessee 37831
managed by
MARTIN MARIETTA ENERGY SYSTEMS, INC.
for the
U.S. DEPARTMENT OF ENERGY
under Contract No. DE-AC05-84OR21400

ABSTRACT

The results of the analysis of the JASPER Program Radial Shield Attenuation Experiment are presented. The experiment was performed in 1986 at the ORNL Tower Shielding Facility. It is the first of six experiments in this cooperative Japanese and American program in support of shielding designs for advanced sodium-cooled reactors. Six different shielding configurations and subconfigurations thereof were studied. The configurations were calculated with the DOT-IV two-dimensional discrete ordinates radiation transport computer code using the R-Z geometry option, a symmetric S_{12} quadrature (96 directions), and cross sections from ENDF/B versions IV and V in either a 51- or 61-group structure. Auxiliary codes were used to compute detector responses and prepare cross sections and source input for the DOT-IV calculations. Calculated detector responses were compared with measured responses and the agreement was good to excellent in many cases. However, the agreement for configurations having thick steel or B_4C regions or for some very large configurations was fair to poor. The disagreement was attributed to cross-section data, broad-group structure, or high background in the measurements. In particular, it is shown that two cross-section sets for 11_B give very different results for neutron transmission through the thick B_4C regions used in one set of experimental configurations. Implications for design calculations are given.

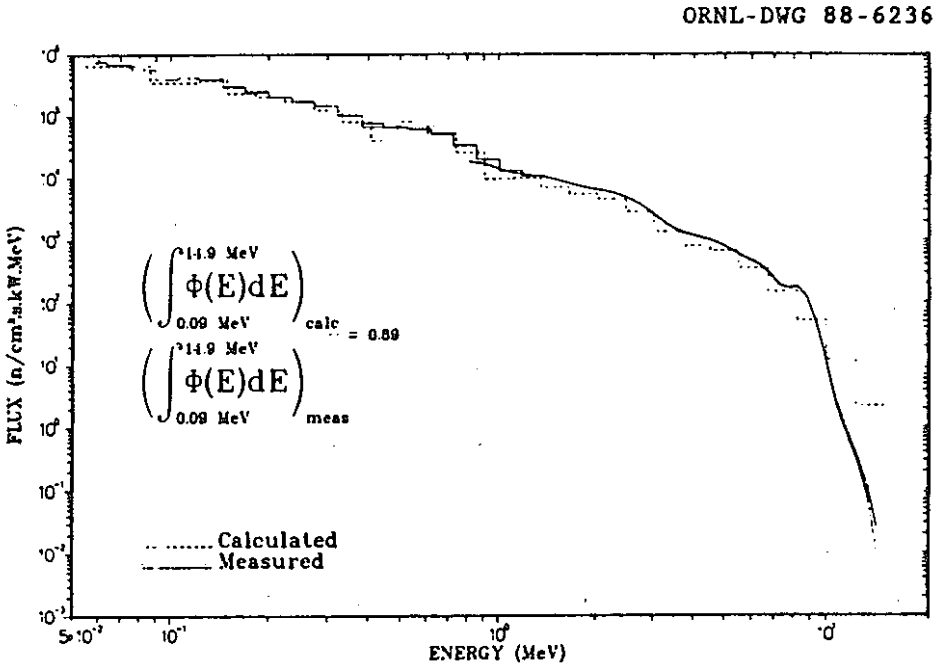

Figure 3. Calculated versus measured E > 0.05 MeV neutron spectra on centerline 178.8 cm behind Configuration I.A.

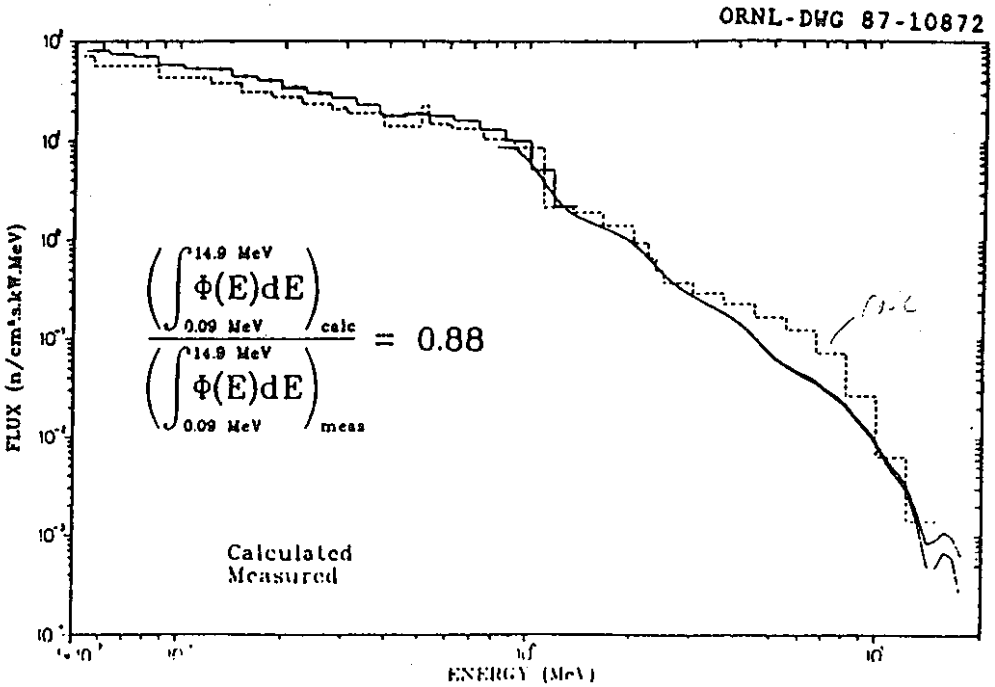

Fig. 4. Calculated versus measured E > 0.05 MeV neutron spectra on centerline 47.3 cm behind Configuration II.D.

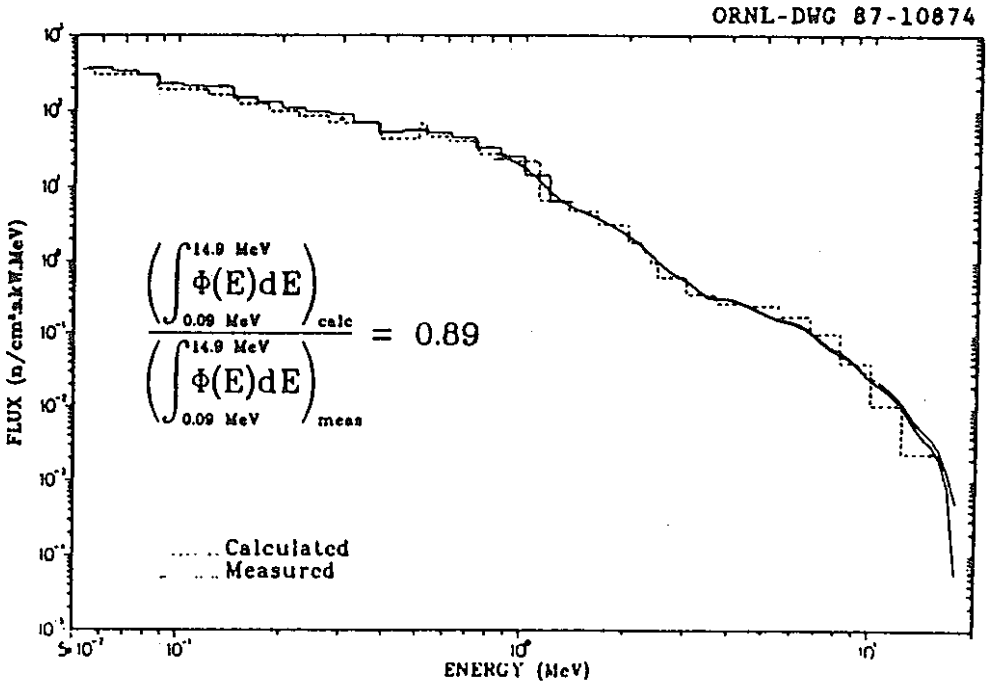

Fig. 5. Calculated versus measured E > 0.05 MeV neutron spectra on centerline 42.8 cm behind Configuration IV.C.

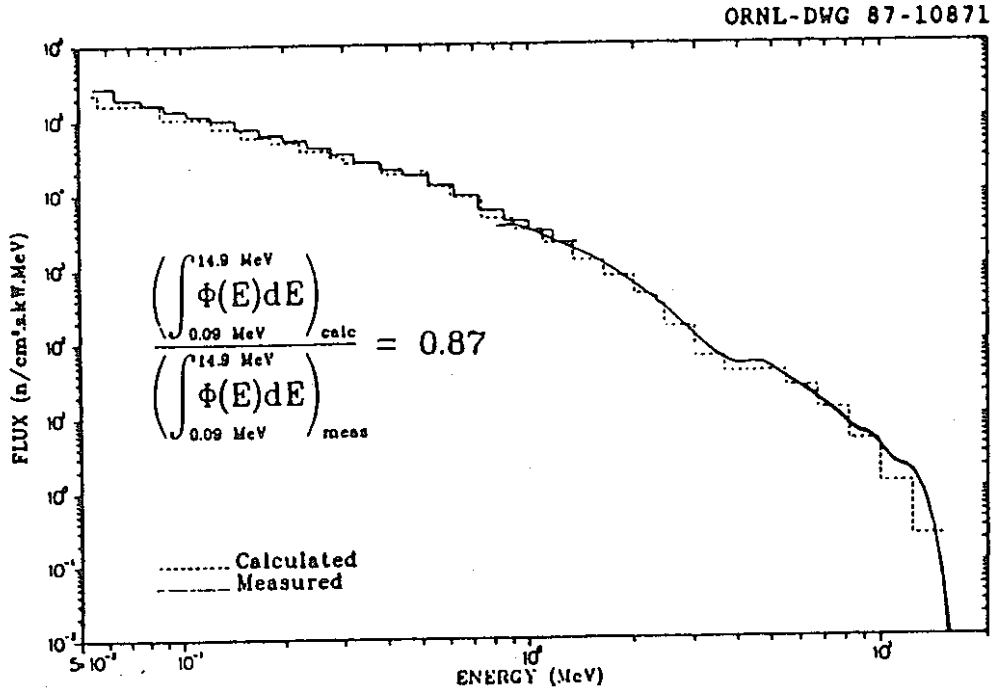

Fig. 6. Calculated versus measured E > 0.05 MeV neutron spectra on centerline 51.1 cm behind Configuration VI.A.

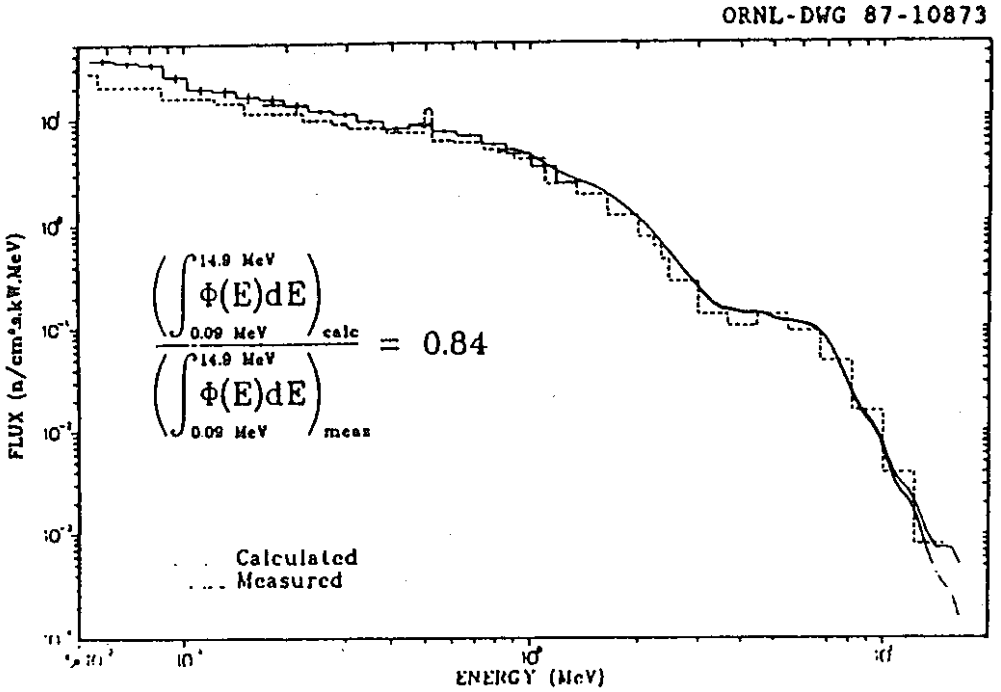

Fig. 7. Calculated versus measured E > 0.05 MeV neutron spectra on centerline 63.2 cm behind Configuration VI.F.

Table 3. Comparison of Calculated and Measured Bonner Ball Count Rates ($s^{-1} \cdot W^{-1}$) at the Spectrum Measurement Locations

	Detector			
Configuration	3-in. BB	4-in. BB	5-in. BB	10-in. BB
I.A				
Calculated	6.44(+1)[a]		3.03(+2)	1.02(+2)
Measured	6.86(+1)		3.13(+2)	1.20(+2)
C/E[b]	0.94		0.97	0.85
II.D				
Calculated	4.58(-3)		3.26(-2)	1.77(-2)
Measured	6.68(-3)		4.10(-2)	2.07(-2)
C/E	0.69		0.80	0.86
IV.C				
Calculated	2.61(-2)		1.44(-1)	5.90(-2)
Measured	3.36(-2)		1.76(-1)	6.95(-2)
C/E	0.78		0.82	0.85
VI.A				
Calculated		2.04(+2)	2.25(+2)	4.42(+1)
Measured		2.56(+2)	2.82(+2)	6.00(+1)
C/E		0.80	0.80	0.74
VI.F				
Calculated	3.34(-3)		1.80(-2)	9.54(-3)
Measured	4.51(-3)		2.22(-2)	1.12(-2)
C/E	0.74		0.81	0.85

[a] Read as $6.44 \times 10^{+1}$.
[b] Calculation-to-experiment ratio.

Table 4. Comparison of Calculated and Measured Bare BF_3 Detector Count Rates ($s^{-1} \cdot W^{-1}$) Close Behind Configurations

Configuration	Distance (cm) behind configuration	Calculated	Measured	C/E[a]
I.A	30	7.73(-5)[b]	1.30(-3)	0.06
V.A	30	4.79(+0)	5.98(+0)	0.80
V.B	30	1.25(+0)	1.61(+0)	0.78
V.C	30	7.46(-1)	9.37(-1)	0.80
V.D	30	3.41(-1)	4.12(-1)	0.83
V.E	30	2.27(-3)	1.09(-2)	0.21
V.F	30	6.14(-3)	1.33(-2)	0.46
V.G	30	3.64(-3)	8.53(-3)	0.43
V.H	30	5.53(-4)	3.77(-3)	0.15
V.I	30	1.62(-3)	3.79(-3)	0.43
V.J	30	1.41(-3)	3.11(-3)	0.45
VI.A(3-5)	30	2.41(+1)	2.87(+1)	0.84
VI.B	30	7.65(+1)	8.40(+1)	0.91
VI.C	30	9.70(+1)	1.19(+2)	0.82
VI.D	30	8.76(+1)	1.13(+2)	0.78
VI.E	30	6.63(+1)	9.70(+1)	0.68
VI.F(3-5)	30	4.50(+1)	7.52(+1)	0.60
VII.D	30	3.78(-3)	1.01(-2)	0.37

[a] Calculation-to-experiment ratio.
[b] Read as 7.73×10^{-5}.

Table 5. Comparison of Calculated and Measured Cd-Covered BF_3 Detector Count Rates ($s^{-1} \cdot W^{-1}$) Close Behind Configurations

Configuration	Distance (cm) behind configuration	Calculated	Measured	C/E[a]
I.A	30	4.28(-5)[b]	1.53(-4)	0.28
V.A	30	2.73(+0)	2.92(+0)	0.93
V.B	30	9.97(-1)	1.11(+0)	0.90
V.C	30	4.72(-1)	5.23(-1)	0.90
V.D	30	2.01(-1)	2.21(-1)	0.91
V.E	30	2.22(-3)	4.32(-3)	0.51
V.F	30	3.20(-3)	4.91(-3)	0.65
V.G	30	2.38(-3)	3.49(-3)	0.68
V.H	30	5.12(-4)	1.02(-3)	0.50
V.I	30	9.35(-4)	1.18(-3)	0.79
V.J	30	8.73(-4)	9.23(-4)	0.95
VI.A(3-5)	30	9.28(+0)	1.25(+1)	0.74
VI.B	30	9.93(+0)	1.30(+1)	0.76
VI.C	30	5.68(+0)	7.42(+0)	0.77
VI.D	30	2.44(+0)	3.09(+0)	0.79
VI.E	30	8.61(-1)	1.08(+0)	0.80
VI.F(3-5)	30	2.65(-1)	3.39(-1)	0.78
VII.D	30	2.19(-3)	4.00(-3)	0.55

[a] Calculation-to-experiment ratio.
[b] Read as 4.28×10^{-5}.

Table 6. Comparison of Calculated and Measured 3-in Bonner Ball Count Rates ($s^{-1}.W^{-1}$) Close Behind Configurations

Configuration	Distance (cm) Behind Configuration	Calculated	Measured	C/E[a]
I.A	30	6.06(+2)[b]	5.92(+2)	1.02
II.A[c]	30	1.91(+2)	2.00(+2)	0.96
II.A[d]	30	1.79(+2)	2.00(+2)	0.90
II.B	30	3.86(+0)	4.35(+0)	0.89
II.C	30	1.41(-1)	1.78(-1)	0.79
II.D(3-5)	30	6.19(-3)	1.03(-2)	0.60
II.E	30	3.10(-3)	5.20(-3)	0.60
III.A	30	3.22(+2)	2.88(+2)	1.12
III.B	30	7.07(+1)	7.26(+1)	0.97
III.C	30	1.44(+2)	1.55(+2)	0.93
III.D	30	3.10(+1)	3.49(+1)	0.89
III.E	30	9.10(+0)	1.07(+1)	0.85
IV.A	30	9.65(+1)	1.06(+2)	0.91
IV.B	30	2.15(+1)	2.40(+1)	0.90
IV.C(3-5)	30	4.54(-2)	5.09(-2)	0.89
IV.D	30	2.83(-2)	3.11(-2)	0.91
IV.E	30	1.80(-2)	1.91(-2)	0.94
IV.F	30	4.51(-3)	5.43(-3)	0.83
IV.F[e]	72.4	2.08(-3)	2.41(-3)	0.86
IV.G	30	7.68(-4)	1.26(-3)	0.61
IV.G[e]	53.6	4.65(-4)	6.67(-4)	0.70
IV.H	30	2.84(-4)	7.15(-4)	0.40
IV.H[e]	52.1	1.78(-4)	2.95(-4)	0.60
IV.I	30	1.20(-4)	5.07(-4)	0.24
IV.I[e]	49.5	8.17(-5)	1.52(-4)	0.54
V.A	30	3.84(+1)	3.44(+1)	1.12
V.B	30	1.33(+1)	1.25(+1)	1.06
V.C	30	5.52(+0)	5.42(+0)	1.02
V.D	30	2.13(+0)	1.97(+0)	1.08
V.E	30	2.25(-1)	1.99(-1)	1.13
V.F	30	1.32(-1)	1.27(-1)	1.04
V.G	30	6.85(-2)	6.33(-2)	1.08
V.H	30	6.38(-2)	5.43(-2)	1.17
V.I	30	4.26(-2)	3.40(-2)	1.25
V.J	30	2.46(-2)	1.34(-2)	1.84
VI.A(3-5)	30	1.89(+2)	2.01(+2)	0.94
VI.B	30	1.25(+2)	1.35(+2)	0.93
VI.C	30	5.70(+1)	6.30(+1)	0.90
VI.D	30	2.11(+1)	2.23(+1)	0.95
VI.E	30	6.74(+0)	7.44(+0)	0.91
VI.F(3-5)	30	1.93(+0)	2.10(+0)	0.92
VII.A	30	5.82(+1)	6.57(+1)	0.89
VII.B	30	1.57(+1)	1.92(+1)	0.82
VII.C	30	2.31(-1)	3.04(-1)	0.76
VII.D	30	1.25(-1)	1.52(-1)	0.82

[a]Calculation-to-experiment ratio.
[b]Read as $6.06 \times 10^{+2}$.
[c]Calculated result obtained using 51 groups.
[d]Calculated result obtained using 61 groups.
[e]The measured result has background subtracted.

Table 7. Comparison of Calculated and Measured 5-in. Bonner Ball Count Rates ($s^{-1} \cdot W^{-1}$) Close Behind Configurations

Configuration	Distance (cm) behind configuration	Calculated	Measured	C/E[a]
I.A	30	2.94(+3)[b]	2.86(+3)	1.08
II.A[c]	30	7.64(+2)	8.31(+2)	0.92
II.A[d]	30	7.50(+2)	8.31(+2)	0.90
II.B	30	2.18(+1)	2.64(+1)	0.83
II.C	30	8.65(-1)	1.26(+0)	0.69
II.D(3-5)	30	4.20(-2)	7.16(-2)	0.59
II.E	30	1.47(-2)	2.47(-2)	0.60
III.A	30	1.32(+3)	1.33(+3)	0.99
III.B	30	3.76(+2)	4.12(+2)	0.91
III.C	30	5.59(+2)	6.26(+2)	0.89
III.D	30	1.68(+2)	2.02(+2)	0.83
III.E	30	5.07(+1)	6.13(+1)	0.83
IV.A	30	2.18(+2)	2.45(+2)	0.89
IV.B	30	3.81(+1)	4.42(+1)	0.86
IV.C(3-5)	30	2.61(-1)	2.98(-1)	0.88
IV.D	30	1.44(-1)	1.64(-1)	0.88
IV.E	30	4.45(-2)	4.93(-2)	0.90
IV.F	30	8.55(-3)	1.08(-2)	0.79
IV.F[e]	72.4	3.97(-3)	4.72(-3)	0.84
IV.G	30	1.30(-3)	2.20(-3)	0.59
IV.G[e]	53.6	7.98(-4)	1.14(-3)	0.70
IV.H	30	5.42(-4)	1.32(-3)	0.41
IV.H[e]	52.1	3.44(-4)	5.57(-4)	0.62
IV.I	30	2.08(-4)	8.95(-4)	0.23
IV.I[e]	49.5	1.42(-4)	2.91(-4)	0.49
V.A	30	6.04(+1)	5.61(+1)	1.08
V.B	30	2.08(+1)	2.03(+1)	1.02
V.C	30	7.97(+0)	7.66(+0)	1.04
V.D	30	2.88(+0)	2.68(+0)	1.07
V.E	30	1.03(+0)	9.02(-1)	1.14
V.F	30	4.16(-1)	3.91(-1)	1.06
V.G	30	1.69(-1)	1.50(-1)	1.13
V.H	30	3.37(-1)	2.83(-1)	1.19
V.I	30	1.47(-1)	1.19(-1)	1.24
V.J	30	6.31(-2)	4.94(-2)	1.28
VI.A(3-5)	30	4.58(+2)	5.15(+2)	0.89
VI.B	30	2.16(+2)	2.46(+2)	0.88
VI.C	30	8.23(+1)	9.45(+1)	0.87
VI.D	30	2.71(+1)	2.97(+1)	0.91
VI.E	30	8.00(+0)	9.04(+0)	0.88
VI.F(3-5)	30	2.19(+0)	2.42(+0)	0.90
VII.A	30	2.13(+2)	2.61(+2)	0.82
VII.B	30	5.59(+1)	7.69(+1)	0.73
VII.C	30	1.20(+0)	1.61(+0)	0.75
VII.D	30	4.36(-1)	5.46(-1)	0.80

[a]Calculation-to-experiment ratio.
[b]Read as $2.94 \times 10^{+3}$.
[c]Calculated result obtained using 51 groups.
[d]Calculated result obtained using 61 groups.
[e]The measured result has background subtracted.

Table 8. Comparison of Calculated and Measured 8-in. Bonner Ball Count Rates ($s^{-1} \cdot W^{-1}$) Close Behind Configurations

Configuration	Distance (cm) behind configuration	Calculated	Measured	C/E[a]
I.A	30	2.01(+3)[b]	2.10(+3)	0.96
II.A[c]	30	4.95(+2)	5.68(+2)	0.87
II.A[d]	30	5.02(+2)	5.68(+2)	0.88
II.B	30	1.62(+1)	2.04(+1)	0.79
II.C	30	6.94(-1)	1.02(+0)	0.68
II.D(3-5)	30	3.73(-2)	6.68(-2)	0.56
II.E	30	1.08(-2)	1.85(-2)	0.58
III.A	30	8.65(+2)	9.17(+2)	0.94
III.B	30	2.71(+2)	3.17(+2)	0.85
III.C	30	3.60(+2)	4.24(+2)	0.85
III.D	30	1.18(+2)	1.47(+2)	0.80
III.E	30	3.61(+1)	4.57(+1)	0.79
IV.A	30	1.06(+2)	1.25(+2)	0.85
IV.B	30	1.60(+1)	1.87(+1)	0.86
IV.C(3-5)	30	2.03(-1)	2.15(-1)	0.94
IV.D	30	1.06(-1)	1.21(-1)	0.88
IV.E	30	2.34(-2)	2.64(-2)	0.89
IV.F	30	3.86(-3)	4.82(-3)	0.80
IV.F[e]	72.4	1.82(-3)	2.20(-3)	0.83
IV.G	30	5.52(-4)	9.34(-4)	0.59
IV.G[e]	53.6	3.44(-4)	4.90(-4)	0.70
IV.H	30	2.52(-4)	5.83(-4)	0.43
IV.H[e]	52.1	1.63(-4)	2.48(-4)	0.66
IV.I	30	8.67(-5)	3.73(-4)	0.23
IV.I	49.5	6.03(-5)	1.20(-4)	0.50
V.A	30	2.20(+1)	2.12(+1)	1.04
V.B	30	7.86(+0)	7.94(+0)	0.99
V.C	30	2.85(+0)	2.79(+0)	1.02
V.D	30	9.88(-1)	9.37(-1)	1.05
V.E	30	7.06(-1)	5.93(-1)	1.19
V.F	30	2.35(-1)	2.12(-1)	1.11
V.G	30	8.16(-2)	7.20(-2)	1.13
V.H	30	2.58(-1)	2.11(-1)	1.22
V.I	30	9.01(-2)	7.18(-2)	1.25
V.J	30	3.22(-2)	2.52(-2)	1.28
VI.A(3-5)	30	2.25(+2)	2.61(+2)	0.86
VI.B	30	8.76(+1)	1.03(+2)	0.85
VI.C	30	3.03(+1)	3.62(+1)	0.84
VI.D	30	9.46(+0)	1.06(+1)	0.89
VI.E	30	2.72(+0)	3.08(+0)	0.88
VI.F(3-5)	30	7.44(-1)	8.44(-1)	0.88
VII.A	30	1.34(+2)	1.69(+2)	0.79
VII.B	30	3.38(+1)	4.64(+1)	0.73
VII.C	30	7.90(-1)	1.08(+0)	0.73
VII.D	30	2.37(-1)	3.11(-1)	0.76

[a]Calculation-to-experiment ratio.
[b]Read as $2.01 \times 10^{+3}$.
[c]Calculated result obtained using 51 groups.
[d]Calculated result obtained using 61 groups.
[e]The measured result has background subtracted.

Table 9. Comparison of Calculated and Measured 10-in. Bonner Ball Count Rates ($s^{-1} \cdot W^{-1}$) Close Behind Configurations

Configuration	Distance (cm) behind configuration	Calculated	Measured	C/E[a]
I.A	30	1.00(+3)[b]	1.13(+3)	0.89
II.A[c]	30	2.37(+2)	2.71(+2)	0.87
II.A[d]	30	2.44(+2)	2.71(+2)	0.90
II.B	30	8.23(+0)	1.07(+1)	0.77
II.C	30	3.75(-1)	5.76(-1)	0.65
II.D(3-5)	30	2.17(-2)	3.89(-2)	0.56
II.E	30	5.76(-3)	9.63(-3)	0.60
III.A	30	4.18(+2)	4.59(+2)	0.91
III.B	30	1.35(+2)	1.63(+2)	0.83
III.C	30	1.71(+2)	2.13(+2)	0.80
III.D	30	5.68(+1)	7.36(+1)	0.77
III.E	30	1.75(+1)	2.37(+1)	0.74
IV.A	30	4.59(+1)	5.42(+1)	0.85
IV.B	30	6.64(+0)	7.94(+0)	0.84
IV.C(3-5)	30	1.09(-1)	1.16(-1)	0.94
IV.D	30	5.48(-2)	6.35(-2)	0.86
IV.E	30	1.07(-2)	1.20(-2)	0.89
IV.F	30	1.67(-3)	2.10(-3)	0.80
IV.Fe[e]	72.4	7.97(-4)	9.41(-4)	0.85
IV.G	30	2.36(-4)	3.95(-4)	0.60
IV.G[e]	53.6	1.49(-4)	2.03(-4)	0.73
IV.H	30	1.11(-4)	2.48(-4)	0.45
IV.H[e]	52.1	7.26(-5)	1.04(-4)	0.70
IV.I	30	3.60(-5)	1.55(-4)	0.23
IV.I[e]	49.5	2.53(-5)	4.70(-5)	0.54
V.A	30	8.67(+0)	8.24(+0)	1.05
V.B	30	3.19(+0)	3.20(+0)	1.00
V.C	30	1.13(+0)	1.09(+0)	1.04
V.D	30	3.86(-1)	3.65(-1)	1.06
V.E	30	3.57(-1)	2.98(-1)	1.20
V.F	30	1.09(-1)	9.76(-2)	1.12
V.G	30	3.54(-2)	3.13(-2)	1.13
V.H	30	1.39(-1)	1.14(-1)	1.22
V.I	30	4.38(-2)	3.51(-2)	1.25
V.J	30	1.44(-2)	1.16(-2)	1.24
VI.A(3-5)	30	9.66(+1)	1.10(+2)	0.88
VI.B	30	3.57(+1)	4.25(+1)	0.84
VI.C	30	1.21(+1)	1.47(+1)	0.82
VI.D	30	3.78(+0)	4.32(+0)	0.88
VI.E	30	1.10(+0)	1.25(+0)	0.88
VI.F(3-5)	30	3.07(-1)	3.58(-1)	0.86
VII.A	30	6.21(+1)	7.77(+1)	0.80
VII.B	30	1.52(+1)	2.13(+1)	0.71
VII.C	30	3.62(-1)	5.03(-1)	0.72
VII.D	30	1.00(-1)	1.37(-1)	0.73

[a]Calculation-to-experiment ratio.
[b]Read as $1.00 \times 10^{+3}$.
[c]Calculated result obtained using 51 groups.
[d]Calculated result obtained using 61 groups.
[e]The measured result has background subtracted.

Table 10. Comparison of Calculated and Measured Bare BF^3 Detector Count Rates ($s^{-1} \cdot W^{-1}$) Behind Configurations at Large Distances from the TSR-II Core Center

Configuration	Distance (cm) from TSR-II core center	Calculated	Measured	C/E[a]
I.A	304.8	8.23(-5)[b]	3.80(-4)	0.22
V.A	501.3	7.10(-1)	9.40(-1)	0.76
V.B	501.3	1.75(-1)	2.32(-1)	0.75
V.C	501.3	1.71(-1)	1.94(-1)	0.88
V.D	501.3	1.07(-1)	1.45(-1)	0.74
V.E	501.3	5.00(-4)	3.70(-3)	0.14
V.F	501.3	2.12(-3)	3.70(-3)	0.57
V.G	501.3	1.51(-3)	3.21(-3)	0.47
V.H	501.3	1.53(-4)	1.66(-3)	0.09
V.I	501.3	5.87(-4)	9.40(-4)	0.62
V.J	501.3	6.94(-4)	9.00(-4)	0.77
VI.A(3-5)	304.8	3.94(+0)	4.98(+0)	0.79
VI.B	304.8	1.51(+1)	1.69(+1)	0.89
VI.C	304.8	2.12(+1)	2.79(+1)	0.76
VI.D	304.8	2.19(+1)	3.07(+1)	0.71
VI.E	304.8	1.93(+1)	3.10(+1)	0.62
VI.F(3-5)	304.8	1.55(+1)	2.87(+1)	0.54
VII.D	304.8	3.00(-3)	6.44(-3)	0.47

[a]Calculation-to-experiment ratio.
[b]Read as 8.23×10^{-5}.

Table 11. Comparison of Calculated and Measured Cd-Covered BF^3 Detector Count Rates ($s^{-1} \cdot W^{-1}$) Behind Configurations at Large Distances from the TSR-II Core Center

Configuration	Distance (cm) from TSR-II core center	Calculated	Measured	C/E[a]
I.A	304.8	3.95(-5)[b]	8.30(-5)	0.48
V.A	501.3	3.53(-1)	4.34(-1)	0.81
V.B	501.3	1.32(-1)	1.58(-1)	0.84
V.C	501.3	8.91(-2)	1.13(-1)	0.79
V.D	501.3	5.80(-2)	7.14(-2)	0.81
V.E	501.3	3.60(-4)	1.20(-3)	0.30
V.F	501.3	8.34(-4)	1.40(-3)	0.60
V.G	501.3	8.41(-4)	1.34(-3)	0.63
V.H	501.3	9.79(-5)	3.85(-4)	0.25
V.I	501.3	2.61(-4)	3.56(-4)	0.73
V.J	501.3	3.51(-4)	3.65(-4)	0.96
VI.A(3-5)	304.8	1.49(+0)	2.27(+0)	0.66
VI.B	304.8	1.90(+0)	2.72(+0)	0.70
VI.C	304.8	1.23(+0)	1.79(+0)	0.69
VI.D	304.8	6.06(-1)	8.48(-1)	0.71
VI.E	304.8	2.50(-1)	3.51(-1)	0.71
VI.F(3-5)	304.8	9.11(-2)	1.27(-1)	0.72
VII.D	304.8	1.64(-3)	2.77(-3)	0.59

[a]Calculation-to-experiment ratio.
[b]Read as 3.95×10^{-5}.

Table 12. Comparison of Calculated and Measured 3-in. Bonner Ball Count Rates ($s^{-1} \cdot W^{-1}$) Behind Configurations at Large Distances from the TSR-II Core Center

Configuration	Distance (cm) behind configuration	Calculated	Measured	C/E[a]
I.A	304.8	7.39(+1)[b]	7.11(+1)	1.04
I.A	457.2	2.15(+1)	2.12(+1)	1.01
II.A[c]	304.8	2.94(+1)	3.25(+1)	0.90
II.A[d]	304.8	2.77(+1)	3.25(+1)	0.85
II.B	304.8	7.95(-1)	9.80(-1)	0.81
II.C	304.8	3.90(-2)	5.35(-2)	0.73
II.D(3-5)	304.8	2.47(-3)	4.26(-3)	0.58
II.E	304.8	2.43(-3)	3.53(-3)	0.69
III.A	304.8	4.84(+1)	4.34(+1)	1.12
III.B	304.8	1.20(+1)	1.26(+1)	0.95
III.C	304.8	2.41(+1)	2.64(+1)	0.91
III.D	304.8	5.88(+0)	6.92(+0)	0.85
III.E	304.8	1.87(+0)	2.26(+0)	0.83
IV.A	304.8	1.72(+1)	2.07(+1)	0.83
IV.B	304.8	4.74(+0)	6.00(+0)	0.79
IV.C(3-5)	304.8	1.49(-2)	1.81(-2)	0.82
IV.C(3-5)	457.2	2.65(-3)	3.72(-3)	0.71
IV.D	457.2	1.75(-3)	2.36(-3)	0.74
IV.E	457.2	1.31(-3)	1.68(-3)	0.78
IV.F	457.2	3.92(-4)	5.06(-4)	0.77
V.A	501.3	4.77(+0)	5.00(+0)	0.95
V.B	501.3	1.72(+0)	1.76(+0)	0.98
V.C	501.3	1.02(+0)	1.12(+0)	0.91
V.D	501.3	6.09(-1)	6.22(-1)	0.98
V.E	501.3	3.11(-2)	3.52(-2)	0.88
V.F	501.3	2.77(-2)	3.08(-2)	0.90
V.G	501.3	2.21(-2)	2.24(-2)	0.99
V.H	501.3	9.61(-3)	1.11(-2)	0.87
V.I	501.3	9.48(-3)	8.50(-3)	1.12
V.J	501.3	8.76(-3)	6.86(-3)	1.28
VI.A(3-5)	304.8	3.01(+1)	3.68(+1)	0.82
VI.B	304.8	2.37(+1)	2.78(+1)	0.85
VI.C	304.8	1.23(+1)	1.50(+1)	0.82
VI.D	304.8	5.26(+0)	6.05(+0)	0.87
VI.E	304.8	1.96(+0)	2.38(+0)	0.82
VI.F(3-5)	304.8	6.65(-1)	7.92(-1)	0.84
VII.A	304.8	1.15(+1)	1.37(+1)	0.84
VII.B	304.8	3.81(+0)	5.11(+0)	0.75
VII.C	304.8	7.97(-2)	1.18(-1)	0.68
VII.D	304.8	8.44(-2)	1.01(-1)	0.84

[a]Calculation-to-experiment ratio.
[b]Read as $7.39 \times 10^{+1}$.
[c]Calculated result obtained using 51 groups.
[d]Calculated result obtained using 61 groups.

Table 13. Comparison of Calculated and Measured 5-in. Bonner Ball Count Rates ($s^{-1} \times W^{-1}$) Behind Configurations at Large Distances from the TSR-II Core Center

Configuration	Distance (cm) behind configuration	Calculated	Measured	C/E
I.A	304.8	3.48(+2)	3.63(+2)	0.96
I.A	457.2	9.99(+1)	1.13(+2)	0.88
II.A	304.8	1.15(+2)	1.35(+2)	0.85
II.A	304.8	1.13(+2)	1.35(+2)	0.84
II.B	304.8	4.38(+0)	5.94(+0)	0.74
II.C	304.8	2.41(-1)	3.81(-1)	0.63
II.D(3-5)	304.8	1.68(-2)	2.98(-2)	0.56
II.E	304.8	1.16(-2)	1.74(-2)	0.67
III.A	304.8	1.83(+2)	1.93(+2)	0.95
III.B	304.8	5.96(+1)	7.15(+1)	0.83
III.C	304.8	8.88(+1)	1.08(+2)	0.82
III.D	304.8	3.03(+1)	3.90(+1)	0.78
III.E	304.8	1.02(+1)	1.36(+1)	0.75
IV.A	304.8	3.84(+1)	4.85(+1)	0.79
IV.B	304.8	8.40(+0)	1.10(+1)	0.76
IV.C(3-5)	304.8	8.66(-2)	1.07(-1)	0.81
IV.C(3-5)	457.2	1.51(-2)	2.21(-2)	0.68
IV.D	457.2	8.79(-3)	1.23(-2)	0.71
IV.E	457.2	3.20(-3)	4.26(-3)	0.75
IV.F	457.2	7.39(-4)	1.07(-3)	0.69
V.A	501.3	7.37(+0)	8.18(+0)	0.90
V.B	501.3	2.67(+0)	2.75(+0)	0.97
V.C	501.3	1.45(+0)	1.61(+0)	0.90
V.D	501.3	8.18(-1)	8.17(-1)	1.00
V.E	501.3	1.43(-1)	1.46(-1)	0.98
V.F	501.3	8.46(-2)	8.71(-2)	0.97
V.G	501.3	5.36(-2)	5.15(-2)	1.04
V.H	501.3	5.08(-2)	5.05(-2)	1.01
V.I	501.3	3.19(-2)	2.93(-2)	1.09
V.J	501.3	2.20(-2)	1.79(-2)	1.23
VI.A(3-5)	304.8	7.33(+1)	9.29(+1)	0.79
VI.B	304.8	4.09(+1)	5.10(+1)	0.80
VI.C	304.8	1.78(+1)	2.24(+1)	0.79
VI.D	304.8	6.76(+0)	7.94(+0)	0.85
VI.E	304.8	2.34(+0)	2.89(+0)	0.81
VI.F(3-5)	304.8	7.54(-1)	9.70(-1)	0.78
VII.A	304.8	4.10(+1)	5.48(+1)	0.75
VII.B	304.8	1.35(+1)	2.00(+1)	0.68
VII.C	304.8	4.19(-1)	6.07(-1)	0.69
VII.D	304.8	2.95(-1)	3.64(-1)	0.81

[a]Calculation-to-experiment ratio.
[b]Read as $3.48 \times 10^{+2}$.
[c]Calculated result obtained using 51 groups.
[d]Calculated result obtained using 61 groups.

Table 14. Comparison of Calculated and Measured 8-in. Bonner Ball Count Rates ($s^{-1} \cdot W^{-1}$) Behind Configurations at Large Distances from the TSR-II Core Center

Configuration	Distance (cm) behind configuration	Calculated	Measured	C/E[a]
I.A	304.8	2.36(+2)[b]	2.64(+2)	0.89
I.A	457.2	6.68(+1)	8.05(+1)	0.81
II.A[c]	304.8	7.38(+1)	9.18(+1)	0.80
II.A[d]	304.8	7.49(+1)	9.18(+1)	0.82
II.B	304.8	3.30(+0)	4.61(+0)	0.72
II.C	304.8	1.98(-1)	3.17(-1)	0.62
II.D(3-5)	304.8	1.53(-2)	2.84(-2)	0.54
II.E	304.8	8.92(-3)	1.32(-2)	0.68
III.A	304.8	1.18(+2)	1.36(+2)	0.87
III.B	304.8	4.27(+1)	5.46(+1)	0.78
III.C	304.8	5.67(+1)	7.35(+1)	0.77
III.D	304.8	2.13(+1)	2.94(+1)	0.72
III.E	304.8	7.31(+0)	1.00(+1)	0.73
IV.A	304.8	1.87(+1)	2.45(+1)	0.76
IV.B	304.8	3.57(+0)	4.72(+0)	0.76
IV.C(3-5)	304.8	6.94(-2)	7.91(-2)	0.88
IV.C(3-5)	457.2	1.19(-2)	1.67(-2)	0.71
IV.D	457.2	6.52(-3)	9.40(-3)	0.69
IV.E	457.2	1.70(-3)	2.35(-3)	0.72
IV.F	457.2	3.37(-4)	4.72(-4)	0.71
V.A	501.3	2.68(+0)	3.10(+0)	0.86
V.B	501.3	1.01(+0)	1.10(+0)	0.92
V.C	501.3	5.20(-1)	5.86(-1)	0.89
V.D	501.3	2.82(-1)	2.92(-1)	0.97
V.E	501.3	1.01(-1)	9.90(-2)	1.02
V.F	501.3	4.85(-2)	4.94(-2)	0.98
V.G	501.3	2.63(-2)	2.55(-2)	1.03
V.H	501.3	4.00(-2)	3.81(-2)	1.05
V.I	501.3	1.98(-2)	1.79(-2)	1.11
V.J	501.3	1.13(-2)	9.50(-3)	1.19
VI.A(3-5)	304.8	3.65(+1)	4.81(+1)	0.76
VI.B	304.8	1.68(+1)	2.15(+1)	0.78
VI.C	304.8	6.61(+0)	8.65(+0)	0.76
VI.D	304.8	2.39(+0)	2.93(+0)	0.82
VI.E	304.8	8.08(-1)	1.00(+0)	0.81
VI.F(3-5)	304.8	2.61(-1)	3.18(-1)	0.82
VII.A	304.8	2.55(+1)	3.50(+1)	0.73
VII.B	304.8	8.23(+0)	1.25(+1)	0.66
VII.C	304.8	2.83(-1)	4.16(-1)	0.68
VII.D	304.8	1.65(-1)	2.05(-1)	0.80

[a]Calculation-to-experiment ratio.
[b]Read as $2.36 \times 10^{+2}$.
[c]Calculated result obtained using 51 groups.
[d]Calculated result obtained using 61 groups.

Table 15. Comparison of Calculated and Measured 10-in. Bonner Ball Count Rates ($s^{-1} \cdot W^{-1}$) Behind Configurations at Large Distances from the TSR-II Core Center

Configuration	Distance (cm) behind configuration	Calculated	Measured	C/E[a]
I.A	304.8	1.17(+2)[b]	1.32(+2)	0.89
I.A	457.2	3.29(+1)	4.08(+1)	0.81
II.A[c]	304.8	3.53(+1)	4.39(+1)	0.80
II.A[d]	304.8	3.64(+1)	4.39(+1)	0.83
II.B	304.8	1.70(+0)	2.44(+0)	0.70
II.C	304.8	1.09(-1)	1.81(-1)	0.60
II.D(3-5)	304.8	9.07(-3)	1.65(-2)	0.55
II.E	304.8	4.96(-3)	6.88(-3)	0.72
III.A	304.8	5.71(+1)	6.91(+1)	0.83
III.B	304.8	2.15(+1)	2.69(+1)	0.80
III.C	304.8	2.69(+1)	3.63(+1)	0.74
III.D	304.8	1.04(+1)	1.44(+1)	0.72
III.E	304.8	3.59(+0)	5.27(+0)	0.68
IV.A	304.8	8.18(+0)	1.05(+1)	0.78
IV.B	304.8	1.49(+0)	1.97(+0)	0.76
IV.C(3-5)	304.8	3.79(-2)	4.35(-2)	0.87
IV.C(3-5)	457.2	6.45(-3)	9.12(-3)	0.71
IV.D	457.2	3.41(-3)	4.94(-3)	0.69
IV.E	457.2	7.82(-4)	1.05(-3)	0.74
IV.F	457.2	1.48(-4)	1.94(-4)	0.76
V.A	501.3	1.05(+0)	1.18(+0)	0.89
V.B	501.3	4.14(-1)	4.42(-1)	0.94
V.C	501.3	2.08(-1)	2.29(-1)	0.91
V.D	501.3	1.11(-1)	1.17(-1)	0.95
V.E	501.3	5.23(-2)	4.99(-2)	1.05
V.F	501.3	2.30(-2)	2.28(-2)	1.01
V.G	501.3	1.16(-2)	1.10(-2)	1.05
V.H	501.3	2.23(-2)	2.08(-2)	1.07
V.I	501.3	9.90(-3)	8.85(-3)	1.12
V.J	501.3	5.17(-3)	4.33(-3)	1.19
VI.A(3-5)	304.8	1.59(+1)	2.09(+1)	0.76
VI.B	304.8	6.89(+0)	8.92(+0)	0.77
VI.C	304.8	2.67(+0)	3.49(+0)	0.77
VI.D	304.8	9.67(-1)	1.17(+0)	0.83
VI.E	304.8	3.31(-1)	4.02(-1)	0.82
VI.F(3-5)	304.8	1.10(-1)	1.34(-1)	0.82
VII.A	304.8	1.19(+1)	1.61(+1)	0.74
VII.B	304.8	3.74(+0)	5.63(+0)	0.66
VII.C	304.8	1.31(-1)	1.98(-1)	0.66
VII.D	304.8	7.14(-2)	9.03(-2)	0.79

[a]Calculation-to-experiment ratio.
[b]Read as $1.17 \times 10^{+2}$.
[c]Calculated result obtained using 51 groups.
[d]Calculated result obtained using 61 groups.

Table 16. Comparison of Calculated and Measured Bonner Ball Count Rates ($s^{-1} \cdot W^{-1}$) in the Shielded Void Region of Several Configurations IV

	Configuration				
Detector	IV.IA	IV.J	IV.K	IV.L	IV.M
Bare BF 3					
Calculated	3.28(-5)	1.59(-2)	6.84(-6)	2.90(-6)	1.24(-6)
Measured	6.54(-5)	2.92(-5)	1.38(-5)	6.18(-6)	3.00(-6)
C/E	0.50	0.54	0.50	0.47	0.41
Cd-cov. BF 3					
Calculated	1.95(-5)	8.54(-6)	3.56(-6)	1.45(-6)	6.07(-7)
Measured	2.85(-5)	1.12(-5)	4.85(-6)	1.92(-6)	7.34(-7)
C/E	0.68	0.76	0.73	0.76	0.83
3-in. BB					
Calculated	2.50(-4)	1.02(-4)	4.02(-5)	1.54(-5)	6.08(-6)
Measured	3.12(-4)	1.14(-4)	4.83(-5)	1.76(-5)	6.60(-6)
C/E	0.80	0.89	0.83	0.88	0.92
5-in. BB					
Calculated	4.24(-4)	1.59(-4)	5.85(-5)	2.12(-5)	7.88(-6)
Measured	5.40(-4)	1.82(-4)	7.04(-5)	2.51(-5)	8.50(-6)
C/E	0.79	0.87	0.83	0.84	0.93
8-in. BB					
Calculated	1.71(-4)	5.98(-5)	2.08(-5)	7.21(-6)	2.59(-6)
Measured	2.11(-4)	6.60(-5)	2.40(-5)	8.20(-6)	2.66(-6)
C/E	0.81	0.91	0.87	0.88	0.97
10-in. BB					
Calculated	6.93(-5)	2.35(-5)	8.01(-6)	2.75(-6)	9.83(-7)
Measured	8.82(-5)	2.48(-5)	9.34(-6)	3.12(-6)	1.04(-6)
C/E	0.79	0.95	0.86	0.88	0.95

[a]Read as 3.28×10^{-5}.
[b]Calculation-to-experiment ratio.
[c]Bonner ball.

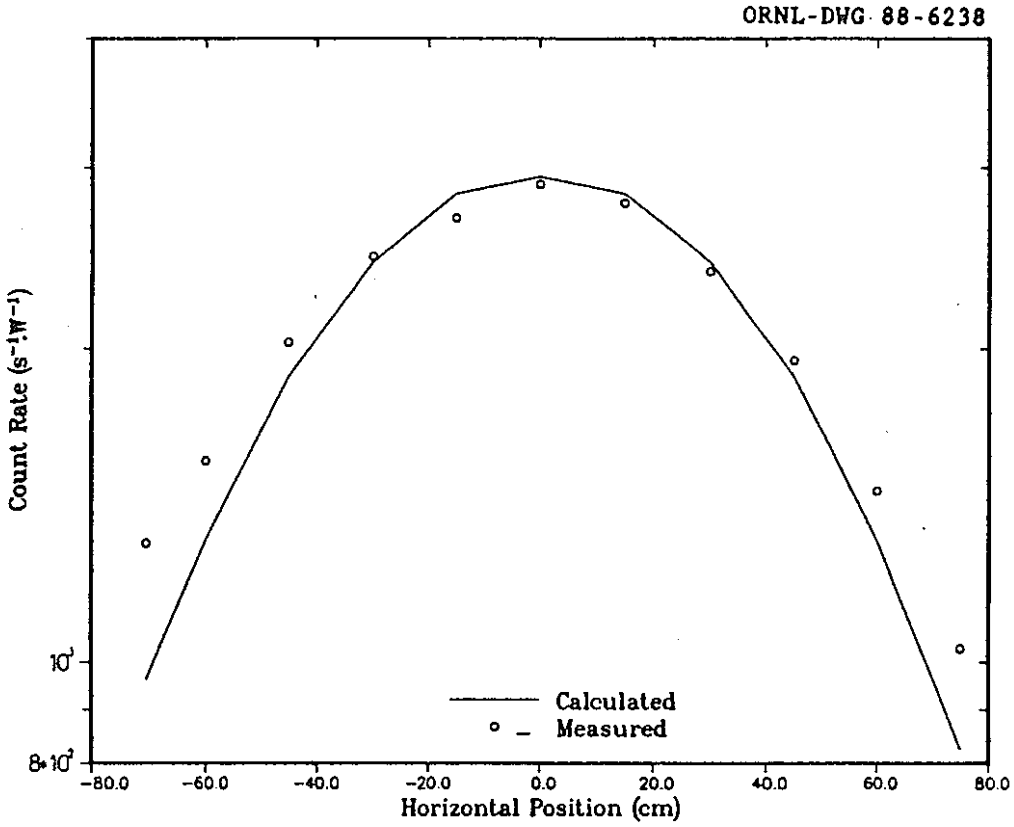

Figure 9. Comparison of calculated and measured 5-in. Bonner ball count rates for a horizontal traverse 30 cm behind Configuration I.A (C/E range: 0.74-1.06).

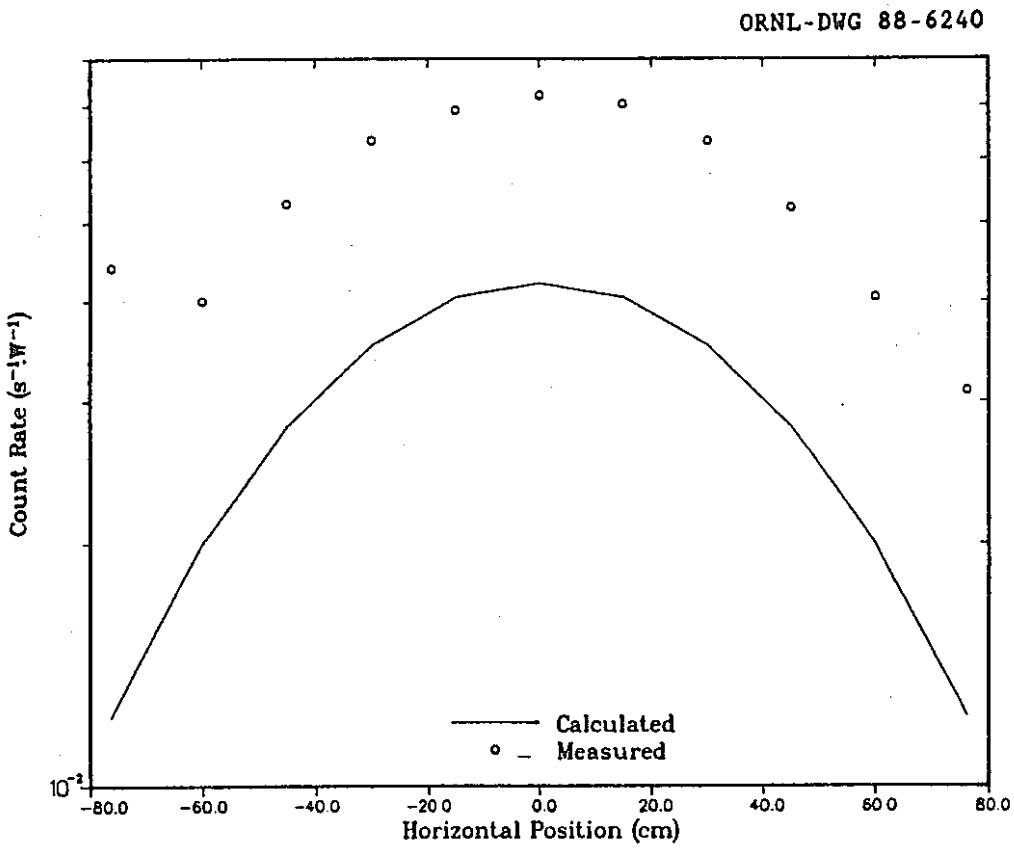

Figure 11. Comparison of calculated and measured 5-in. Bonner ball count rates for a horizontal traverse 30 cm behind Configuration II.D (C/E range: 0.28-0.58).

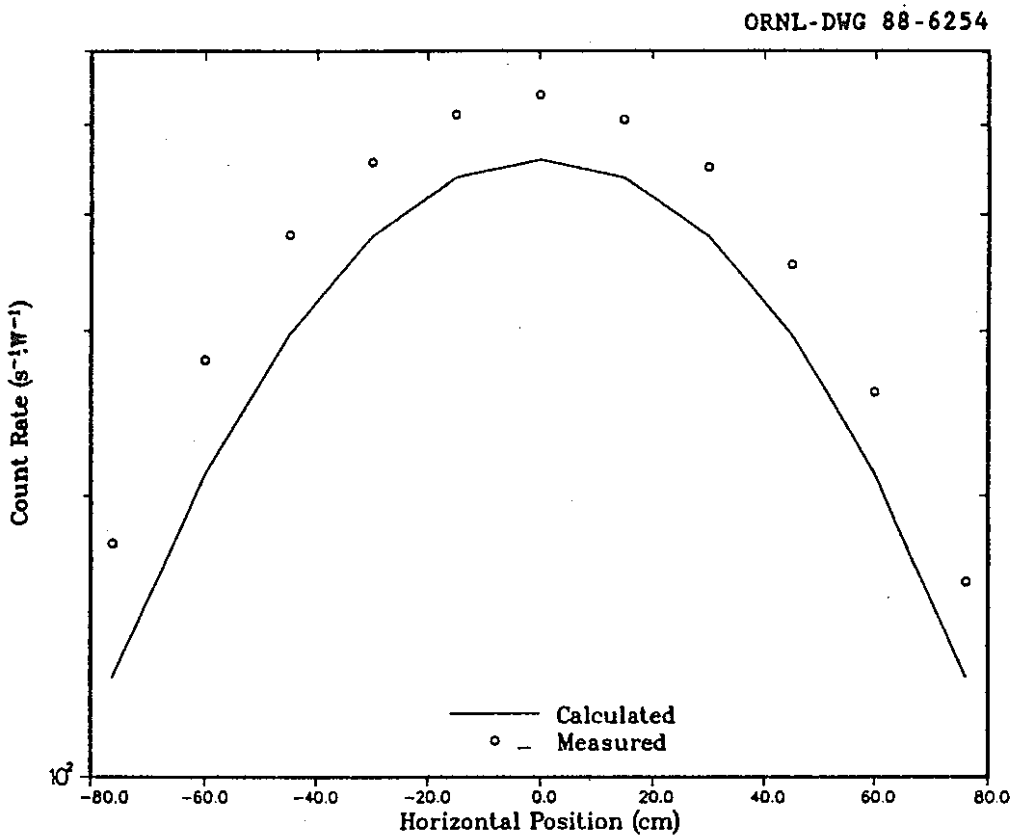

Figure 25. Comparison of calculated and measured 5-in. Bonner ball count rates for a horizontal traverse 30 cm behind Configuration VI.A (C/E range: 0.72-0.87).

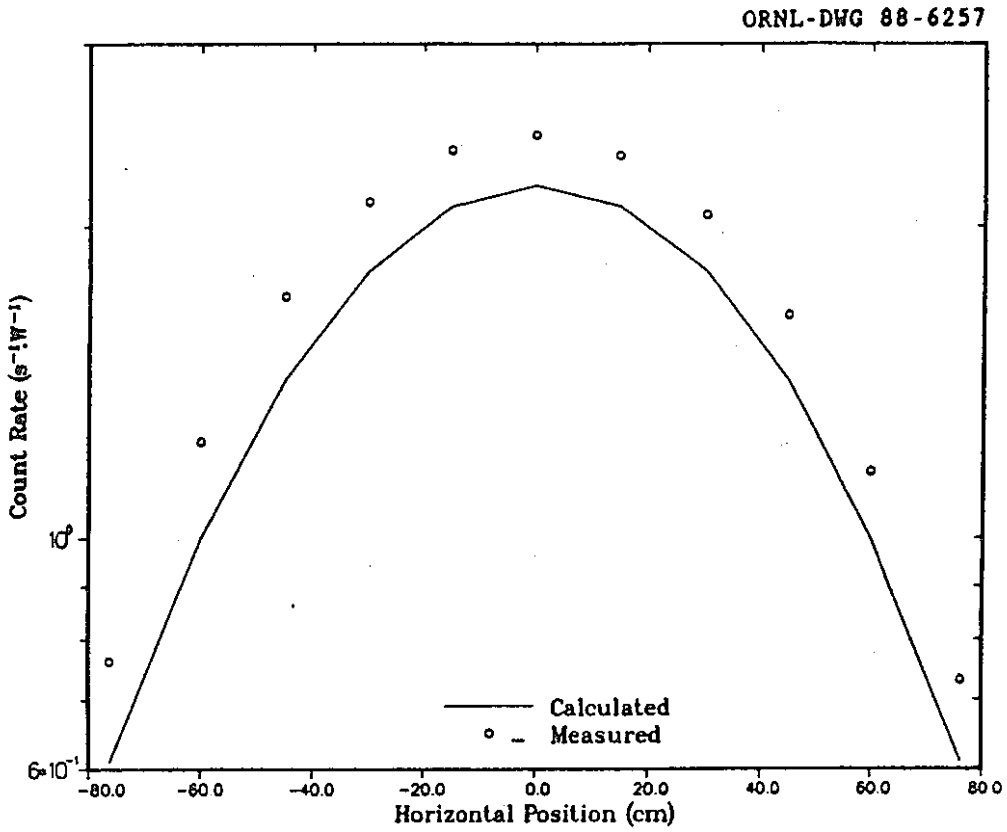

Figure 28. Comparison of calculated and measured 5-in. Bonner ball count rates for a horizontal traverse 30 cm behind Configuration VI.F (C/E range: 0.80-0.89).

4.0 CONCLUSIONS

Measured data from the Radial Shield Attenuation Experiment have been analyzed. Calculations were performed with the DOT-IV two-dimensional discrete ordinates radiation transport code for each of the experimental configurations of the Radial Shield Attenuation Experiment and calculated results were compared with measured results. In general, the calculated results were in good agreement with the measured results. Some cases of disagreement were attributed to a high background contribution to the measured results. However, in other cases, the data appeared to be lacking. Configurations containing large amounts of B_4C gave low calculated results because of over-attenuation by the ENDF/B versions IV and V ^{11}B data set. A LENDL set, which differed from the ENDF set mainly at high energies, gave much improved results but substantially overpredicted portions of the neutron spectra and substantially underpredicted others. It is preferable to the ENDF set, but the need for better high-energy cross-section definition for this set is indicated by the results obtained even with a fine-group structure. The broad-group structure was found to be partially responsible for the underprediction of radiation transmission through graphite. The integrated fast-neutron spectrum obtained using a fine- group structure indicated much better agreement with the measured spectrum for a configuration with much graphite. Detector responses for configurations having B_4C preceding sodium tended to be overpredicted. Finally, detector responses for Configurations VII (with 30 to 45 cm stainless steel) were slightly underpredicted. Larger differences than those seen here were noted between fine-group and broad-group results when the 61-group library was tested using 1-D mockups containing slabs of steel and sodium[7]. Thus, this slight underprediction is attributed to the broad-group structure.

The results of this analysis have a few implications for shield design analyses.

(1) Analyses using the ENDF ^{11}B cross section set will probably underpredict neutron transmission through B4C shields. Though not perfect, the LENDL ^{11}B set is preferableto the ENDF set.

(2) Analyses of B_4C shields in deep sodium are likely to overpredict neutron transmission through the B_4C and the sodium that follows.

(3) Fine group calculations may be required for accurate calculation of neutron transmission through thick steel or graphite shields.

ORNL/TM-10681
Dist. Category UC-535T

Engineering Physics and Mathematics

Liquid Metal Reactor Program

JASPER
USDOE/PNC Shielding Research Program – Analysis of the JASPER Fission Gas Plenum Experiment

C. O. Slater

DATE PUBLISHED — May 1990

Prepared for the
U.S. DOE Office of
Liquid Metal Converter Reactor

Prepared by the
OAK RIDGE NATIONAL LABORATORY
Oak Ridge, Tennessee 37831
operated by
MARTIN MARIETTA ENERGY SYSTEMS, INC.
for the
U.S. DEPARTMENT OF ENERGY
under contract DE-AC05-84OR21400

ABSTRACT

The results of the analysis of the Fission Gas Plenum Experiment are presented. This experiment is the second in a series of several experiments comprising a joint U.S. DOE-Japan PNC Shielding Research Program (JASPER). The four Fission Gas Plenum Experiment configurations, designed for the measurement of neutron streaming through the fission gas plenum region, were analyzed using Monte Carlo and two-dimensional discrete ordinates methods. Calculated results compared well with measured results in many cases, although results were consistently underpredicted for the shorter plenum configurations. Like the measured data, the calculated results indicated no significant streaming when results from the heterogeneous mockups were compared to those from the homogeneous mockups. An explanation is given as to why little streaming was observed. The Hornyak button dose rates were overpredicted because of a normalization problem with the response function but yielded horizontal traverse curves whose shapes agreed well with the measured shapes to the same extent as did those for the other integral detectors.

Table 2. Calculated vs. Measured Detector Responses 30 cm Behind Fission Gas Plenum Experiment Configurations

Detector	Configuration [a] II	III	IV [b]	V [b]	IV [c]	V [c]
3-in. Bonner ball						
Calc.	4.73(+2) [d]	3.25(+2)	4.73(+2)	3.25(+2)	4.81(+2)	3.35(+2)
Meas.	5.85(+2)	3.07(+2)	5.89(+2)	3.10(+2)	5.89(+2)	3.10(+2)
C/E [e]	0.81	1.06	0.80	1.05	0.82	1.08
5-in. Bonner ball						
Calc.	1.97(+3)	1.14(+3)	1.97(+3)	1.14(+3)	2.00(+3)	1.18(+3)
Meas.	2.21(+3)	1.09(+3)	2.19(+3)	1.09(+3)	2.19(+3)	1.09(+3)
C/E	0.89	1.05	0.90	1.05	0.90	1.08
8-in. Bonner ball						
Calc.	1.34(+3)	7.49(+3)	1.34(+3)	7.47(+2)	1.36(+3)	7.73(+3)
Meas.	1.41(+3)	6.98(+2)	1.50(+3)	7.12(+2)	1.50(+3)	7.12(+2)
C/E	0.95	1.07	0.89	1.05	0.91	1.09
10-in. Bonner ball						
Calc.	6.83(+2)	3.78(+2)	6.82(+2)	3.77(+2)	6.90(+2)	3.90(+2)
Meas.	7.23(+2)	3.53(+2)	7.33(+2)	3.61(+2)	7.33(+2)	3.61(+2)
C/E	0.94	1.07	0.93	1.04	0.94	1.08
12-in. Bonner ball						
Calc.	3.22(+2)	1.78(+2)	3.21(+2)	1.77(+2)	3.24(+2)	1.82(+2)
Meas.	3.58(+2)	1.74(+2)	3.49(+2)	1.73(+2)	3.49(+2)	1.73(+2)
C/E	0.90	1.02	0.92	1.02	0.93	1.05
Hornyak Button (270 keV cutoff)						
Calc.	2.40(-1)	1.31(-1)	2.49(-1)	1.30(-1)	2.50(-1)	1.34(-1)
Meas.	1.50(-1)	7.36(-2)	1.46(-1)	6.88(-2)	1.46(-1)	6.88(-2)
C/E	1.60	1.78	1.71	1.89	1.71	1.95

[a] Configurations:
II – 8-cm-thick homogeneous plenum mockup.
III – 20-cm-thick homogeneous plenum mockup.
IV – 8-cm-thick heterogeneous plenum mockup.
V – 20-cm-thick heterogeneous plenum mockup.

[b] Comparisons with DORT-calculated results (no streaming correction).

[c] Comparisons with streaming-corrected DORT-calculated results.

[d] Read as 4.73×10^2.

[e] Ratio of calculated result to measure result.

Table 3. Calculated vs. Measured Bonner Ball Count Rates Behind Fission Gas Plenum Experiment Configurations at 304.8 cm from the TSR-II Core Center

Detector	Configuration II	III	IV	V
3-in. Bonner ball				
Calc.	6.86(+1)[a]	4.75(+1)	6.86(+1)	4.75(+1)
Meas.	9.14(+1)	3.87(+1)	8.64(+1)	4.06(+1)
C/E[b]	0.75	1.23	0.79	1.17
5-in. Bonner ball				
Calc.	2.36(+2)	1.32(+2)	2.36(+2)	1.32(+2)
Meas.	2.82(+2)	1.24(+2)	2.83(+2)	1.29(+2)
C/E	0.84	1.06	0.83	1.02
8-in. Bonner ball				
Calc.	1.49(+2)	7.97(+1)	1.49(+2)	7.96(+1)
Meas.	1.70(+2)	8.15(+1)	1.77(+2)	8.22(+1)
C/E	0.88	0.98	0.84	0.97
10-in. Bonner ball				
Calc.	7.46(+1)	4.00(+1)	7.46(+1)	3.99(+1)
Meas.	8.82(+1)	4.18(+1)	8.53(+1)	4.33(+1)
C/E	0.85	0.96	0.87	0.92
12-in. Bonner ball				
Calc.	3.51(+1)	1.90(+1)	3.51(+1)	1.90(+1)
Meas.	4.30(+1)	2.10(+1)	4.19(+1)	2.13(+1)
C/E	0.82	0.90	0.84	0.89

[a] Read as 6.86×10^{1}.

[b] Ratio of calculated result to measured result.

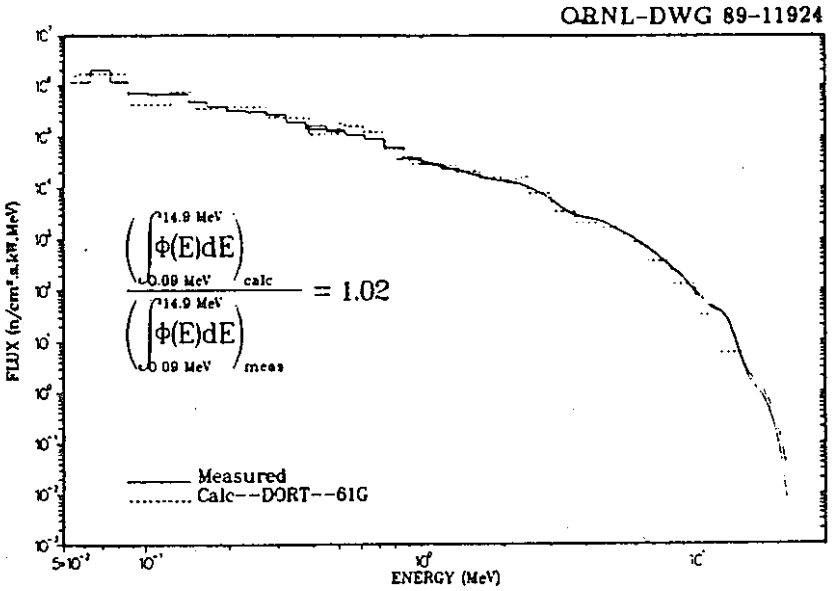

Fig. 6. Calculated versus measured E > 0.05 MeV neutron spectrum behind Configuration III.

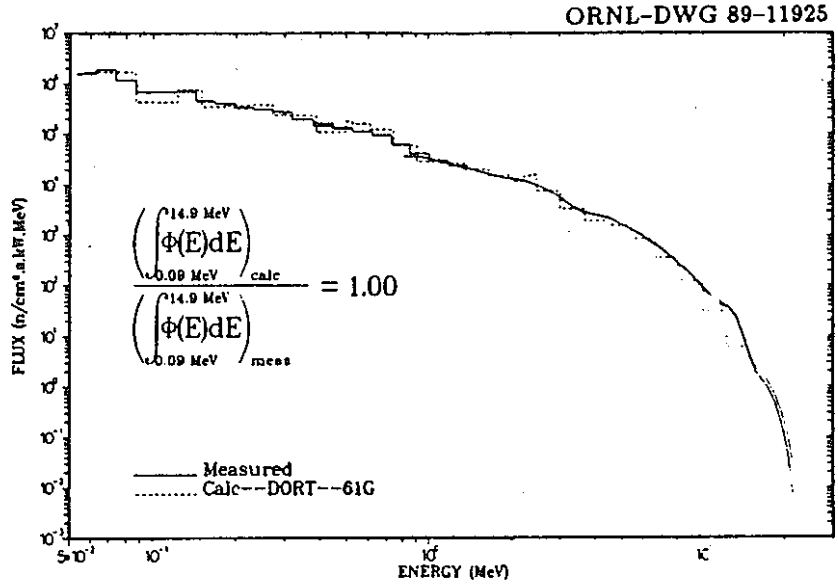

Fig. 7. Calculated versus measured E > 0.05 MeV neutron spectrum behind Configuration V (no streaming correction).

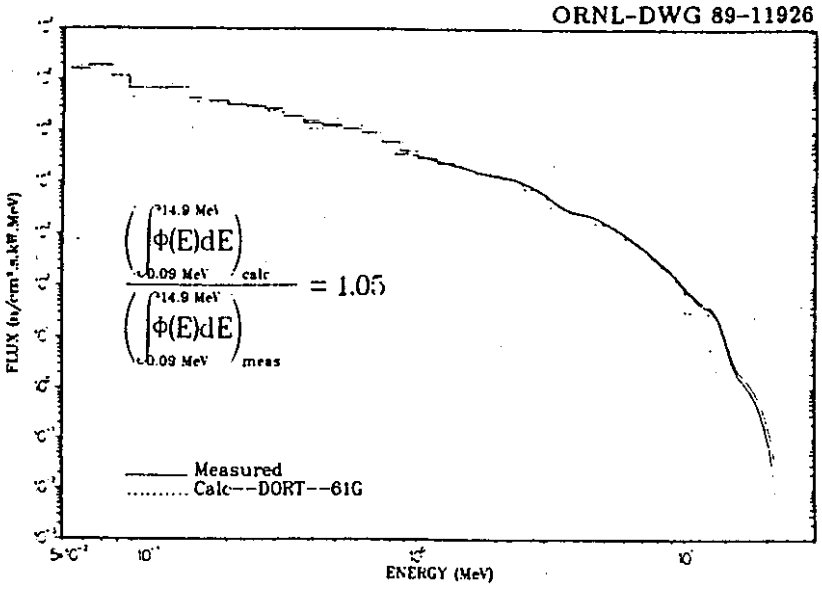

Fig. 8. Calculated versus measured E > 0.05 MeV neutron spectrum behind Configuration V (with streaming correction).

3.4.6 Hornyak Button Dose Rate Horizontal Traverse

Hornyak button horizontal traverse measurements were made as close as feasible behind the configurations in order to try to detect significant changes in the response across the empty tubes with the heterogeneous cases and to establish baseline responses with the homogeneous cases. Since earlier results showed a large overprediction of the Hornyak button response, the cutoff for the response function was adjusted until there was agreement between the calculated and measured results on centerline for Configuration V. This was achieved by retaining the response function values for groups 1-16 of the 61-group structure and 0.535 times the response function for group 17 (see Table A6). Assuming a 1/E distribution of the flux in group 17, this effectively represents a 0.82 MeV cutoff of the response function compared to the 0.27 MeV cutoff used to obtain the results in Table 2. In reality, the response function for each group should be reduced in proportion to the proton-recoil-generated pulse heights with energies below the instrument bias setting. The conversion from count rate to dose rate introduces additional complications. The horizontal traverses obtained with the modified response function are shown in Figs. 13-16 for Configurations II-V, respectively. The calculated and measured curve shapes are in excellent agreement. The C/E ratio ranges are 0.84-0.94, 0.94-1.13, 0.86-0.96, and 1.00-1.19 for Configurations II-V, respectively. These ratios are comparable to the 5-in. Bonner ball count rate ratios for horizontal traverses.

Table 4. Comparison of Calculated and Measured Bonner Ball Count Rates at the Spectrum Measurement Locations Behind Configurations III and V

Detector	Count Rate (S^{-1} W^{-1}) Calculated	Measured	Ratio: Calculated (C/E) / Measured
	Configuration III		
3-in.	2.43+2[a]	2.34+2	1.04
5-in.	8.06+2	7.92+2	1.02
10-in.	2.65+2	2.58+2	1.03
	Configuration V (Homogeneous Calculational Model)		
3-in.	2.43+2	2.40+2	1.01
5-in.	8.05+2	8.23+2	0.98
10-in.	2.64+2	2.57+2	1.03
	Configuration V (Heterogeneous Calculational Model)		
3-in.	2.52+2	2.40+2	1.05
5-in.	8.38+2	8.23+2	1.02
10-in.	2.74+2	2.57+2	1.07

[a] Read as 2.43×10^2.

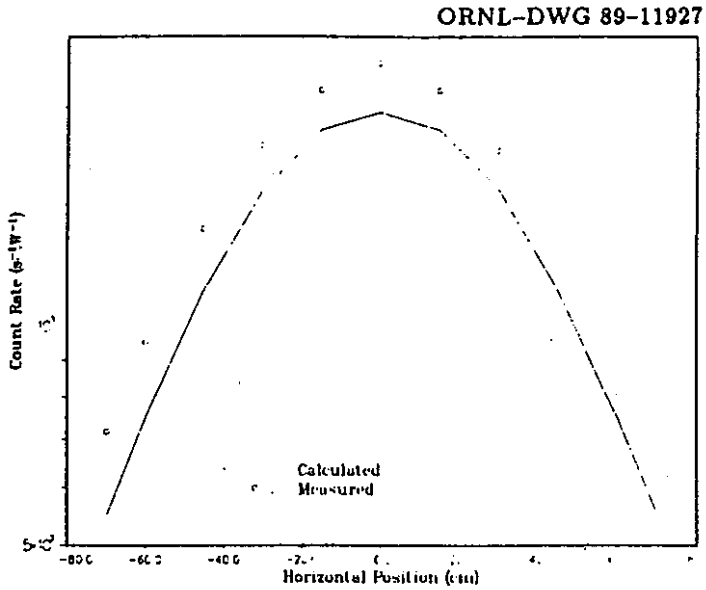

Fig. 9. Calculated versus measured 5-in. Bonner ball count rates ($s^{-1}.W^{-1}$) for a horizontal traverse 30 cm behind Configuration II.

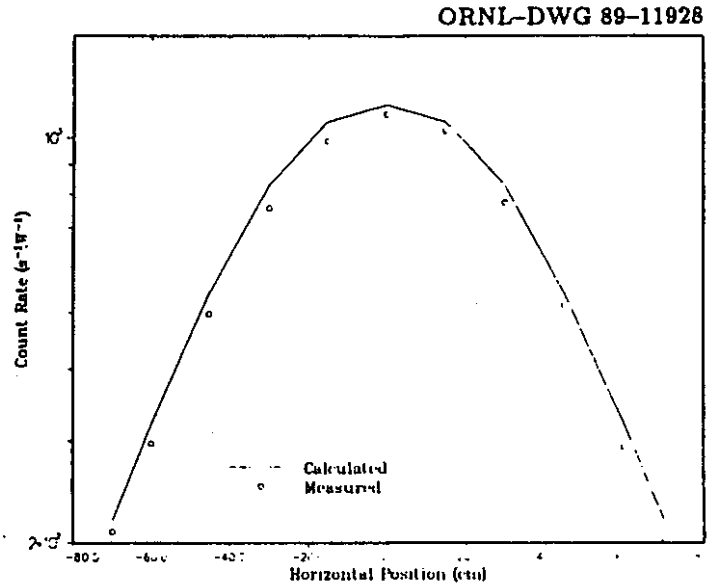

Fig. 10. Calculated versus measured 5-in. Bonner ball count rates ($s^{-1}.W^{-1}$) for a horizontal traverse 30 cm behind Configuration III.

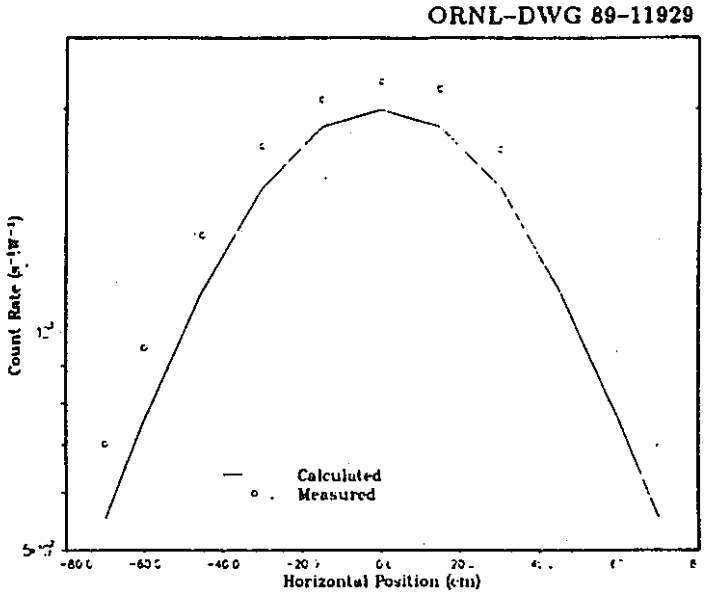

Fig. 11. Calculated versus measured 5-in. Bonner ball count rates ($s^{-1}.W^{-1}$) for a horizontal traverse 30 cm behind Configuration IV.

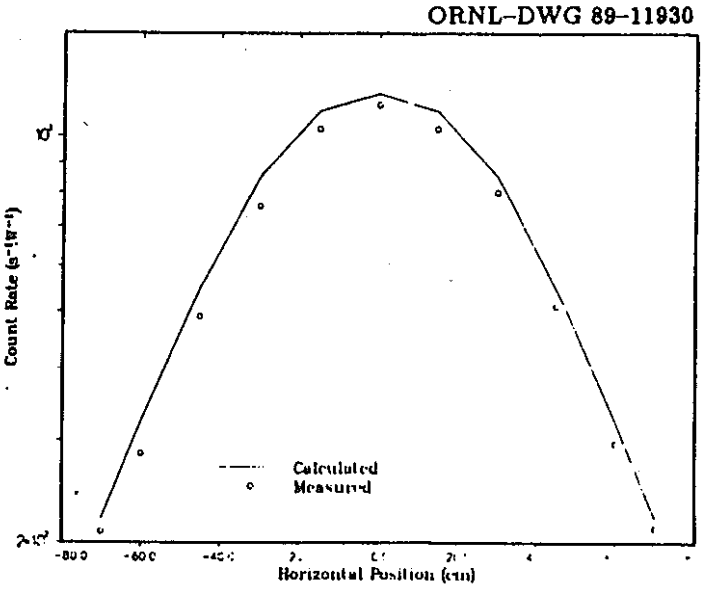

Fig. 12. Calculated versus measured 5-in. Bonner ball count rates ($s^{-1}.W^{-1}$) for a horizontal traverse 30 cm behind Configuration V.

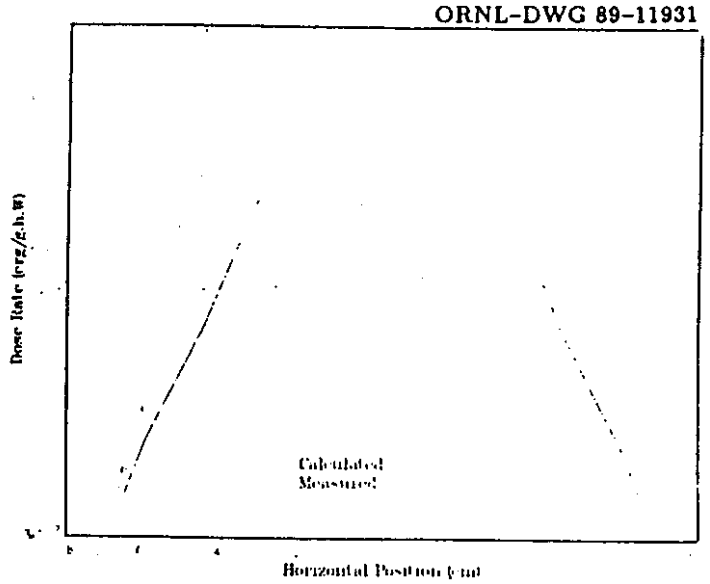

Fig. 13. Calculated versus measured dose rates (erg/g.h.W) for a horizontal traverse 1.6 cm behind Configuration II.

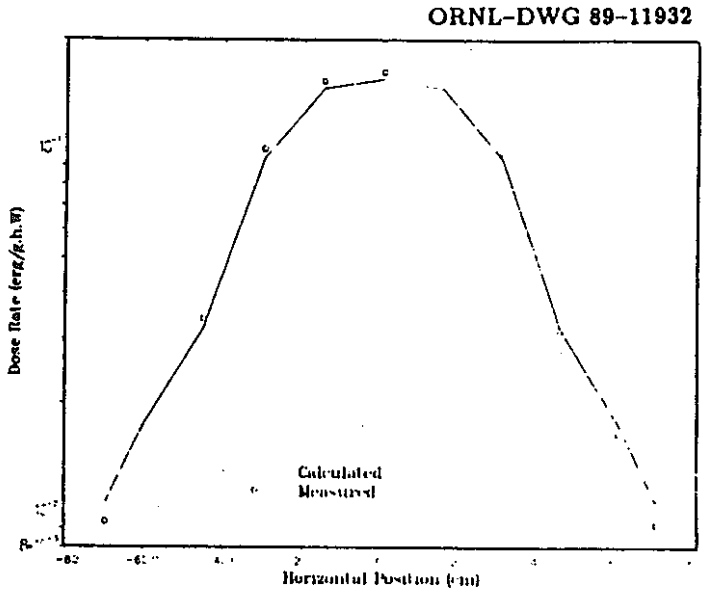

Fig. 14. Calculated versus measured dose rates (erg/g.h.W) for a horizontal traverse 1.6 cm behind Configuration III.

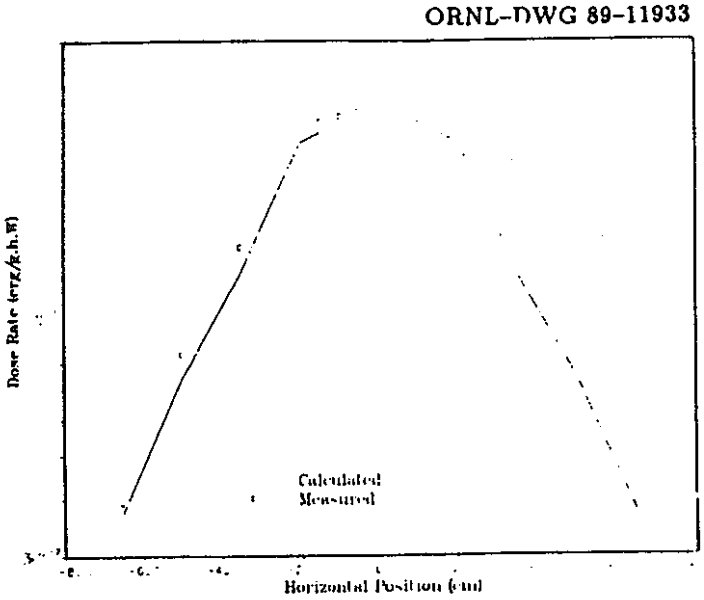

Fig. 15. Calculated versus measured dose rates (erg/g.h.W) for a horizontal traverse 1.6 cm behind Configuration IV.

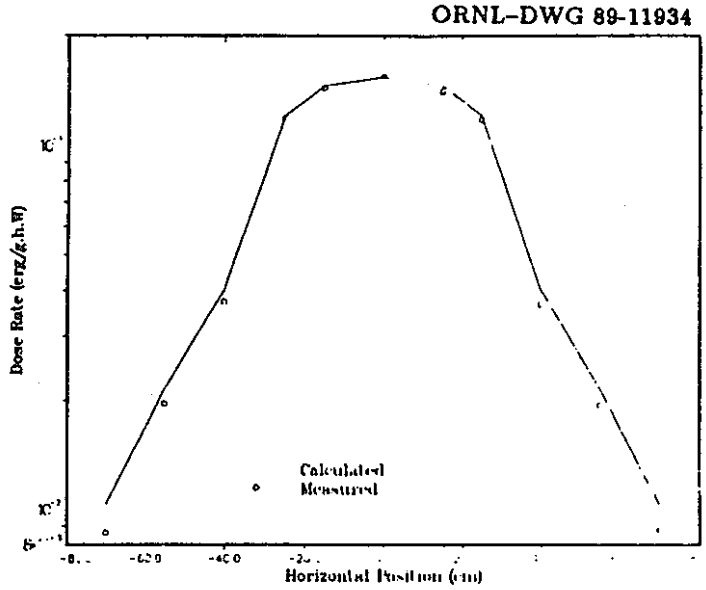

Fig. 16. Calculated versus measured dose rates (erg/g.h.W) for a horizontal traverse 1.6 cm behind Configuration V.

4. SUMMARY

The Fission Gas Plenum Experiment was analyzed using Monte Carlo and two-dimensional discrete ordinates methods. Calculated results were in reasonably good agreement with the measured results in most instances. The calculated results, like the measured results, showed very small streaming effects for the plenum mockups. The streaming issue was analyzed and a possible explanation was given for the insignificant streaming observed from the measurements. The results of both the analysis and the experiment reinforce Boulette's conclusion that the fission gas plenum region can be treated as homogeneous and calculated results can be used without streaming correction provided the fuel rods are small enough and the material fractions are nearly the same as those for the reference design.

Results of the Analysis of the Axial Shield Experiment

C. O. Slater
Oak Ridge National Laboratory†

April 23-24, 1992

† Managed by Martin Marietta Energy Systems, Inc. under Contract No. DE-AC05-84OR21400 for the U. S. Department of Energy.

Bonner Ball Count Rates on Centerline Behind Axial Shield Experiment Configuration I.A

At 30 cm

		Calculated			
Detector	Meas.	Self-Shielded UO_2	C/E	Std. Wtd. UO_2	C/E
3" BB	6.00+2[a]	6.70+2	1.12	5.69+2	0.95
4" BB	2.09+3	2.27+3	1.09	2.12+3	1.01
5" BB	3.03+3	3.21+3	1.06	3.12+3	1.03
8" BB	2.17+3	2.29+3	1.06	2.34+3	1.08
10" BB	1.14+3	1.18+3	1.04	1.23+3	1.08
12" BB	5.45+2	5.65+2	1.04	5.95+2	1.09

At 150 cm

		Calculated			
Detector	Meas.	Self-Shielded UO_2	C/E	Std. Wtd. UO_2	C/E
3" BB	8.92+1	1.01+2	1.13	8.65+1	1.03
4" BB	3.11+2	3.35+2	1.08	3.14+2	1.01
5" BB	4.55+2	4.70+2	1.03	4.58+2	1.01
8" BB	3.28+2	3.35+2	1.02	3.45+2	1.05
10" BB	1.72+2	1.75+2	1.02	1.83+2	1.06
12" BB	8.29+1	8.47+1	1.02	9.00+1	1.09

[a]Read as 6.02×10^2.

Bonner Ball Count Rates and Fluxes at Spectrum Measurement Location Behind JASPER Axial Shield Experiment Configuration I.A

		Calculated			
Detector	Meas.	Self-Shielded UO_2	C/E	Std. Wtd. UO_2	C/E
3" BB	6.49+1[a]	7.39+1	1.14	6.33+1	0.98
5" BB	3.37+2	3.45+2	1.02	3.36+2	1.00
10" BB	1.27+2	1.28+2	1.01	1.34+2	1.06
E > 0.0865 MeV flux	1.325+5	1.283+5	0.97	1.405+5	1.06
E > 0.0525 MeV flux	1.585+5	1.560+5	0.98	1.712+5	1.08

[a]Read as 6.49×10^1.

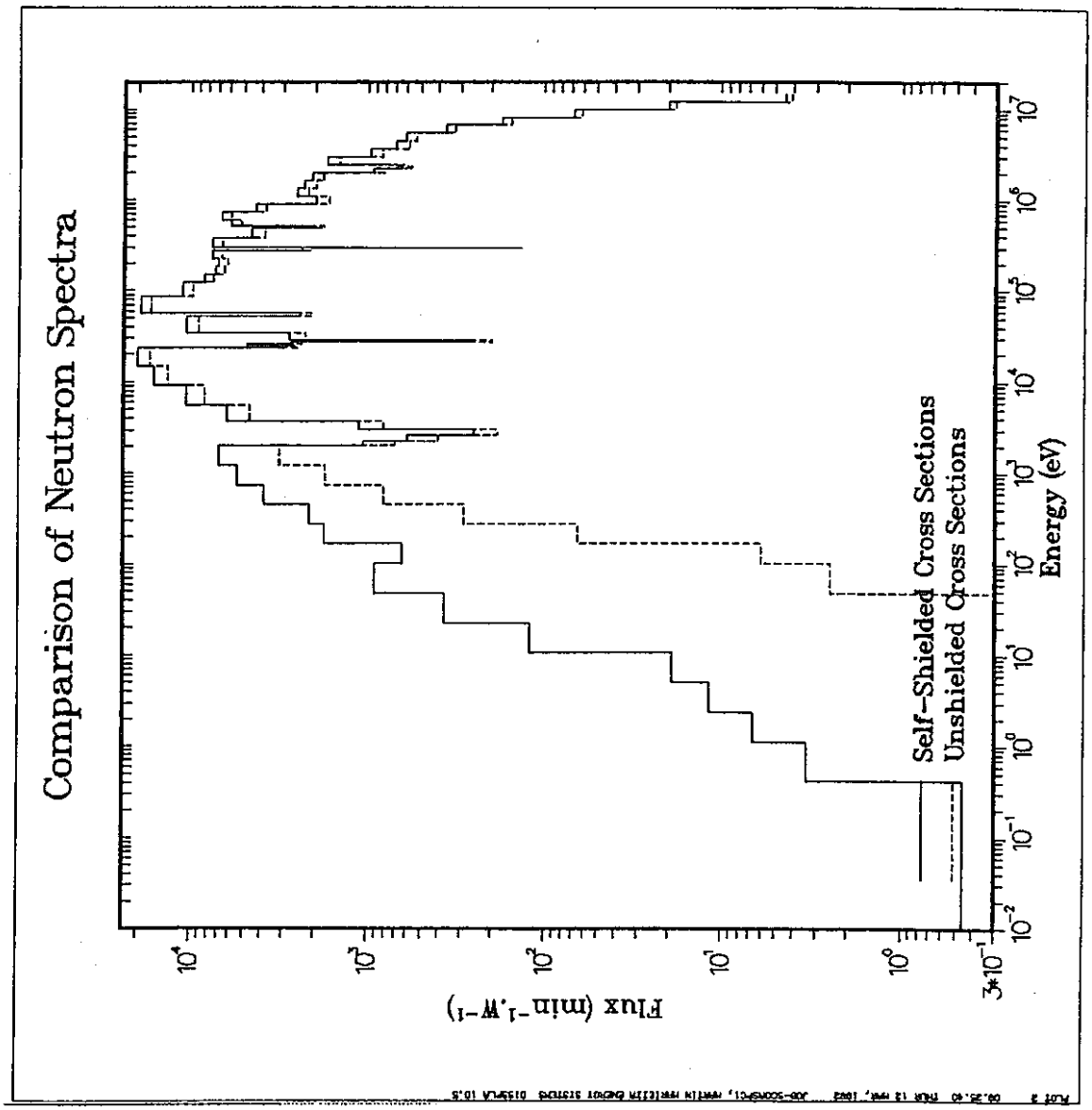
Comparison of Neutron Spectra
Self-Shielded Cross Sections
Unshielded Cross Sections
Energy (eV)
Flux (min^{-1},W^{-1})

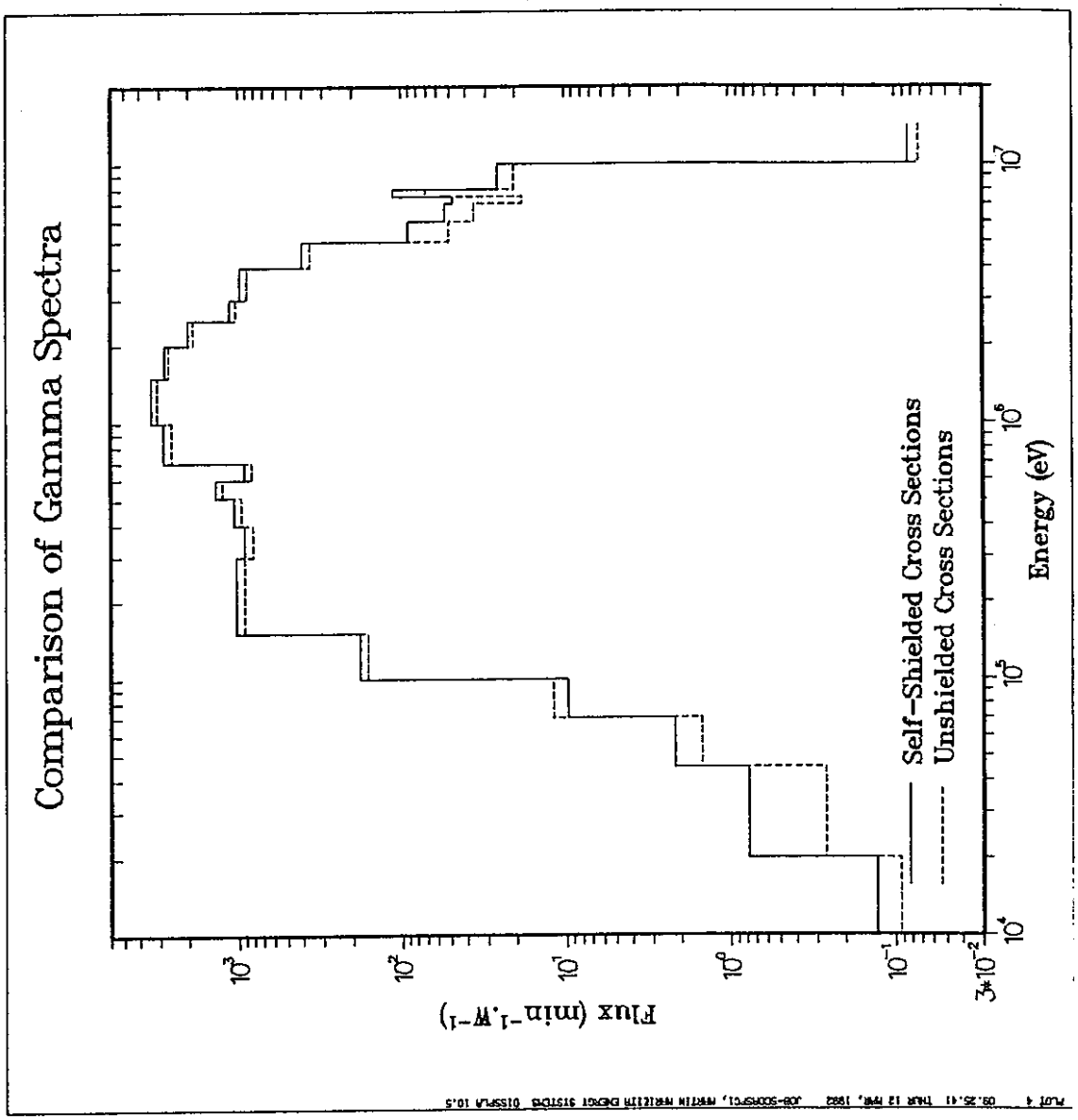
Comparison of Gamma Spectra
Self-Shielded Cross Sections
Unshielded Cross Sections
Energy (eV)
Flux (min⁻¹,W⁻¹)
10⁻²
10⁻¹
10⁰
10¹
10²
10³
10⁴
10⁵
10⁶
10⁷

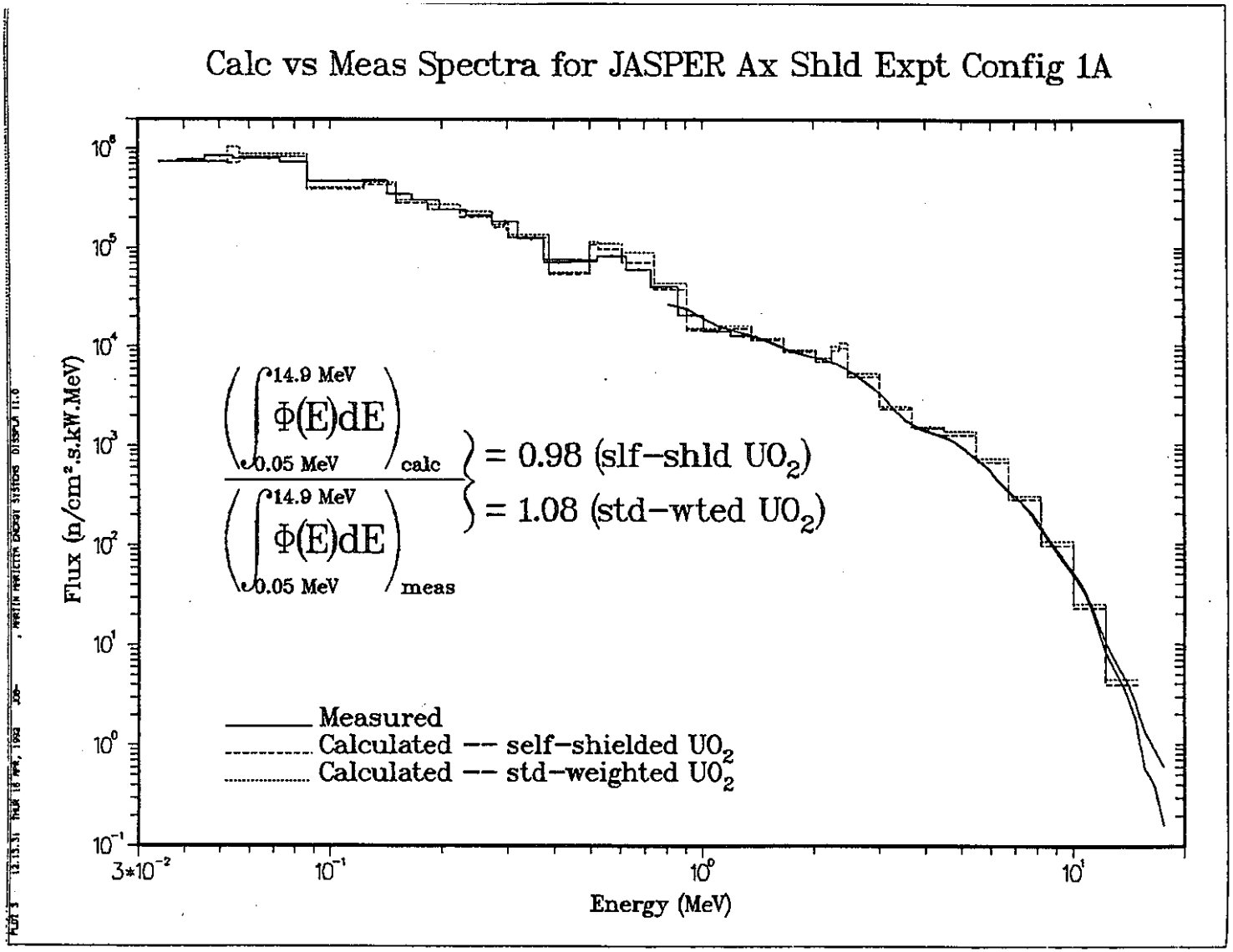
Calc vs Meas Spectra for JASPER Ax Shld Expt Config 1A
Flux (n/cm².s.kW.MeV)
Energy (MeV)
$\left(\int_{0.05\ MeV}^{14.9\ MeV} \Phi(E)dE\right)_{calc}$ = 0.98 (slf-shld UO_2)
$\left(\int_{0.05\ MeV}^{14.9\ MeV} \Phi(E)dE\right)_{meas}$ = 1.08 (std-wted UO_2)
Measured
Calculated -- self-shielded UO_2
Calculated -- std-weighted UO_2

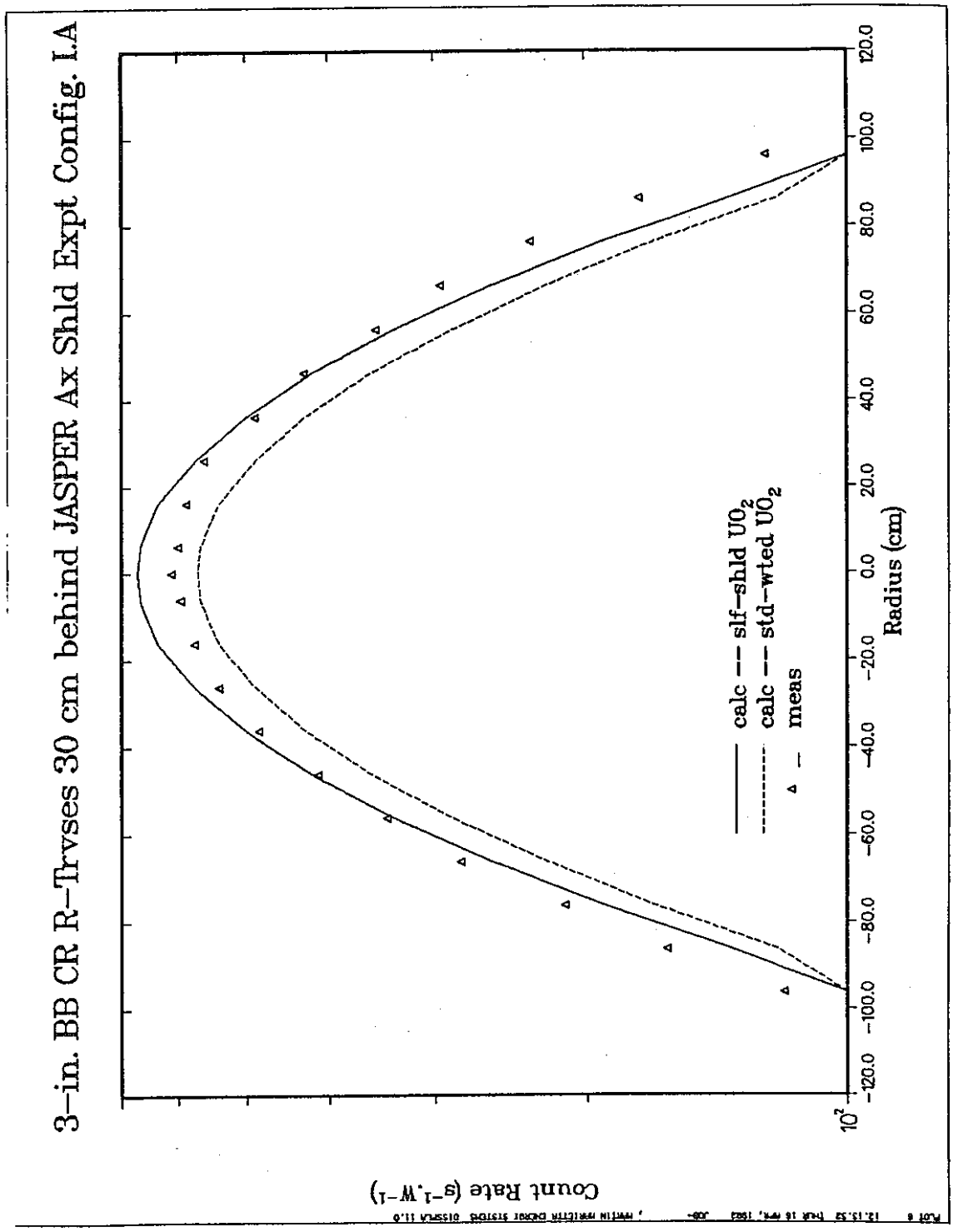
3-in. BB CR R-Trvses 30 cm behind JASPER Ax Shld Expt Config. I.A
Count Rate (s⁻¹.W⁻¹)
Radius (cm)
calc — slf-shld UO2
calc -- std-wted UO2
meas
10²
120.0
100.0
80.0
60.0
40.0
20.0
0.0
-20.0
-40.0
-60.0
-80.0
-100.0
-120.0

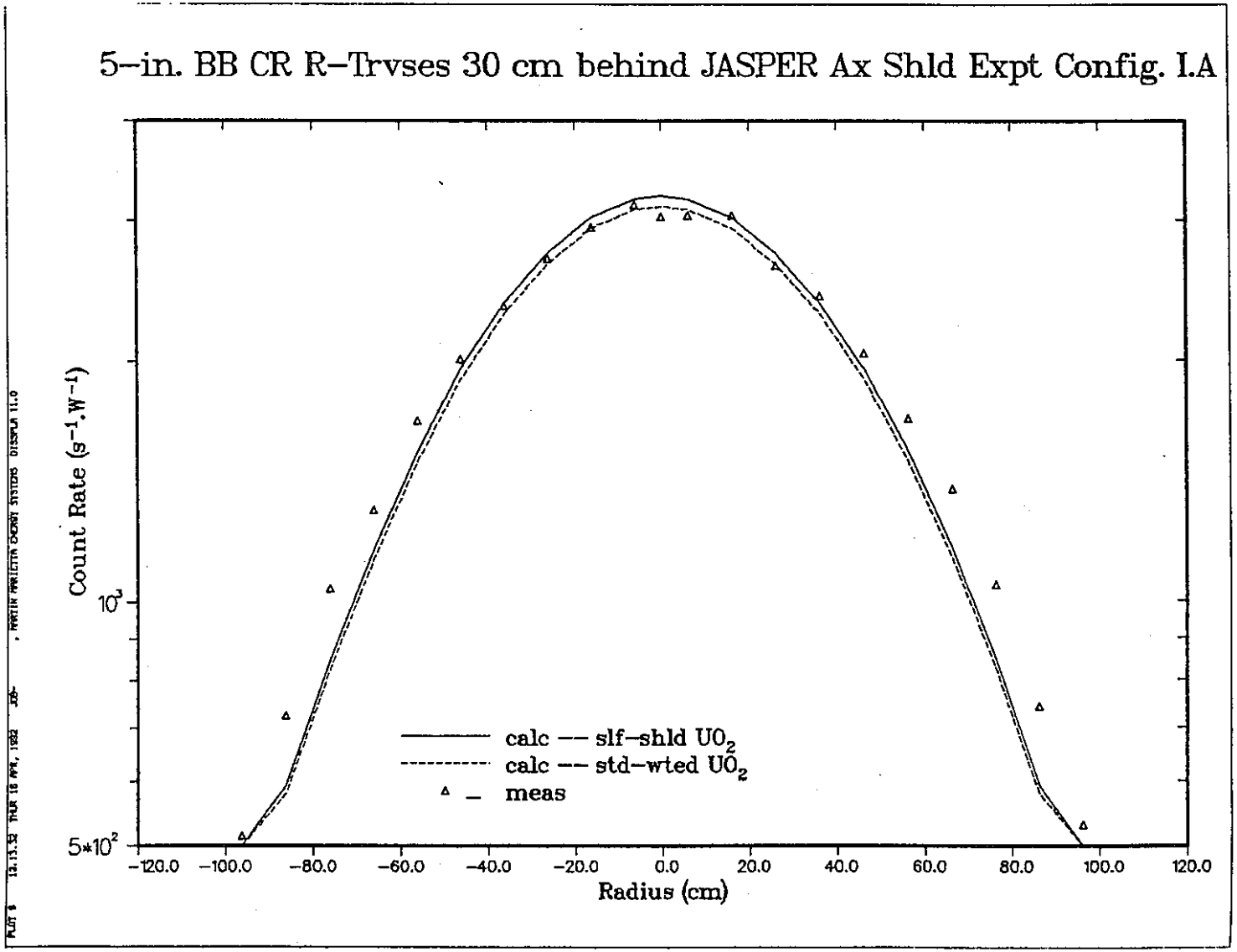
5–in. BB CR R–Trvses 30 cm behind JASPER Ax Shld Expt Config. I.A
Count Rate (s⁻¹.W⁻¹)
10³
5*10²
calc — slf–shld UO₂
calc — std–wted UO₂
meas
–120.0
–100.0
–80.0
–60.0
–40.0
–20.0
0.0
20.0
40.0
60.0
80.0
100.0
120.0
Radius (cm)

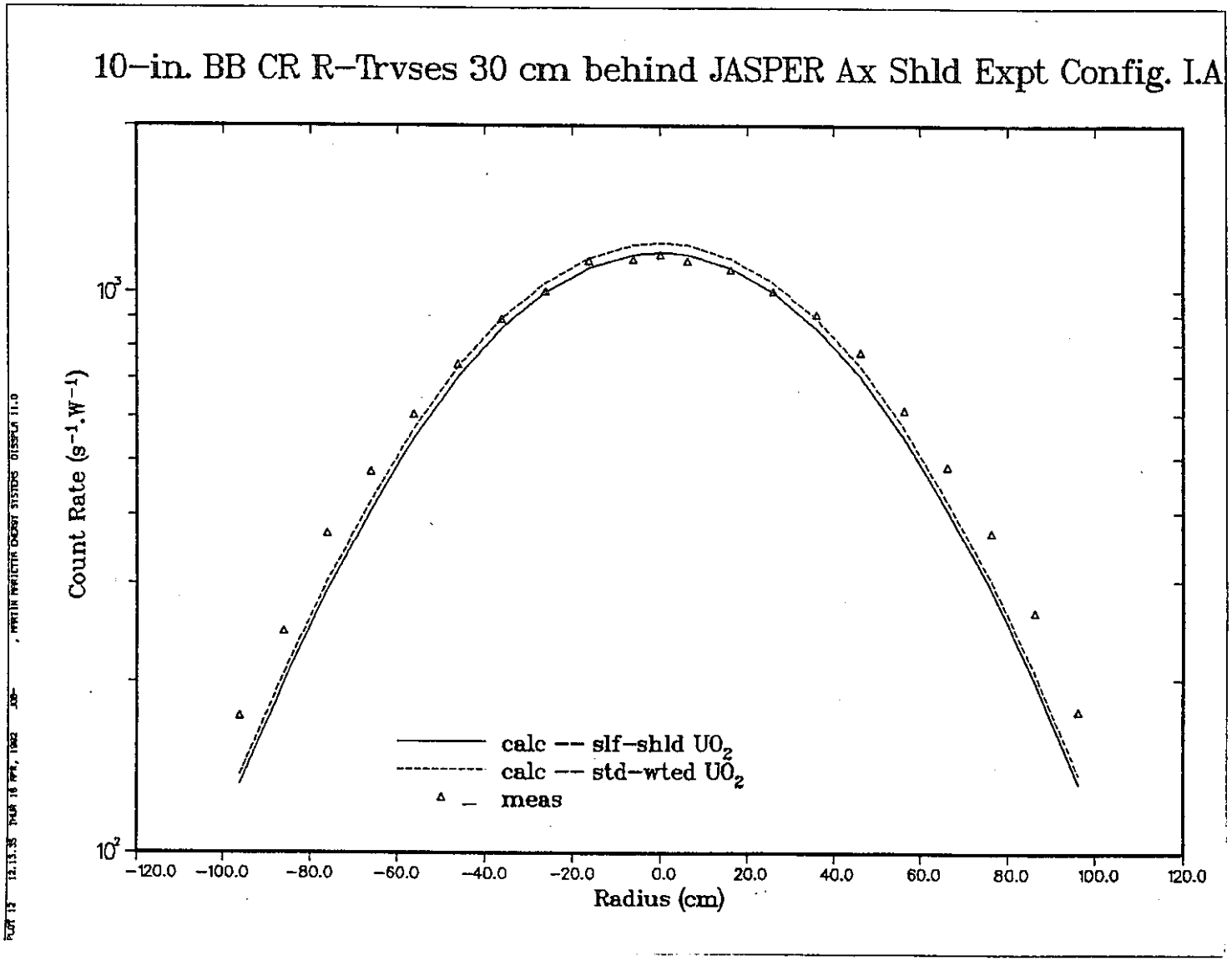
10-in. BB CR R-Trvses 30 cm behind JASPER Ax Shld Expt Config. I.A
Count Rate ($s^{-1}.W^{-1}$)
10^3
10^2
calc --- slf-shld UO_2
calc --- std-wted UO_2
meas
-120.0 -100.0 -80.0 -60.0 -40.0 -20.0 0.0 20.0 40.0 60.0 80.0 100.0 120.0
Radius (cm)

MEASUREMENT OF WT% H_2O IN AXIAL SHIELDS AND FISSION GAS PLENUM CONCRETE SLABS

R. R. Spencer
J. V. Pace III
Oak Ridge National Laboratory*

Paper to Presented at the
US-JAPAN Informal JASPER Meeting
ORNL, Oak Ridge, TN
April 23-24, 1992

---

*Managed by Martin Marietta Energy Systems, Inc. under Contract No. DE-AC05-84OR21400 for the U.S. Department of Energy.

Measurement of Wt% H_2O in Axial Shields and Fission Gas Plenum Concrete Slabs

Chemical analyses of concrete samples for hydrogen content usually assume that this element is bound as water and typically the weight percent of H_2O determined in the analysis (2-3%) is too low to account for the observed neutron slowing down properties of the concrete. As a result, a nuclear technique for hydrogen (water) content has been suggested.[1] This method consists of placement of a strong neutron source at the center of the large concrete sample and detection of the relative intensities of the 2.223 MeV hydrogen capture gamma ray and 1.942 MeV Ca capture gamma ray with an NaI detector. It is assumed that the neutron captures take place primarily at thermal energies and therefore the known[2,3] spectral intensities of Ca gamma rays and the ratio of thermal capture cross sections of hydrogen and Ca can be used in the analysis. Justification for this assumption will be given (see Appendix 1).

In the present measurements, 1-in-diameter holes were drilled in the concrete slabs so that insertion of a 4-in-long x 1-in-diameter lead shadow shield would allow the 2.1×10^7 n/s ^{252}Cf source to be positioned next to the lead and approximately at the center of the slab. A 5-in x 5-in NaI detector was then positioned some distance away with a 5-ft x 5-ft boral sheet placed between it and the concrete slab. This geometry is shown schematically in Figure 1 for the Axial Shield slab. The boral sheet reduced the neutron activation of the iodine in the detector and improved the measurement significantly. In addition to the NaI, the detection system consisted of a Tennelec TC-145 pre-amp and Nuclear Data ND-581 ADC interfaced to an IBM PS/2 Model 80 computer through a National Instruments MC-D10-32 I/O board. The linearity of this system was checked with a pulser and with gamma rays of 0.511 MeV, 1.17 MeV, 1.275 MeV, 1.33 MeV, and 4.43 MeV in addition to the Ca and hydrogen capture gammas and was found to be quite linear. Energy calibration of the system for the measurements was carried out with the 0.511 and 1.275 MeV gamma rays from a Na-22 source.

Figure 2 shows the NaI spectrum obtained for the Axial Shield slab. The no-source background was negligible in this region. The peaks correspond to the 1.942 MeV Ca and 2.223 MeV hydrogen capture gamma rays. However, neither peak is totally monochromatic. From references 2 and 3, which are the result of high resolution Ge(Li) detector studies of thermal neutron capture on many targets, it may be seen that for Ca capture

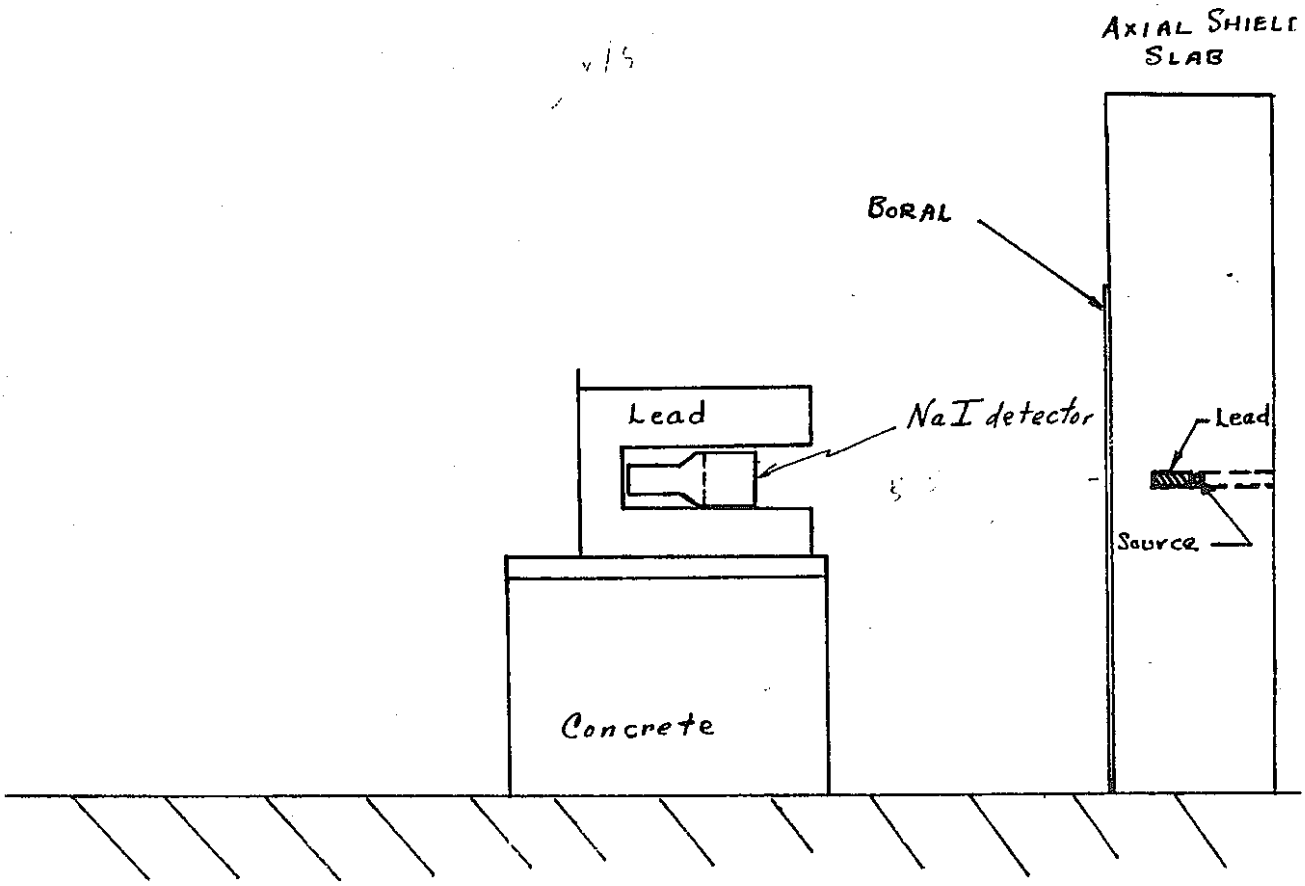
Cf
AXIAL SHIELD SLAB
BORAL
Lead
NaI detector
Lead
Source
Concrete

FIG. 1

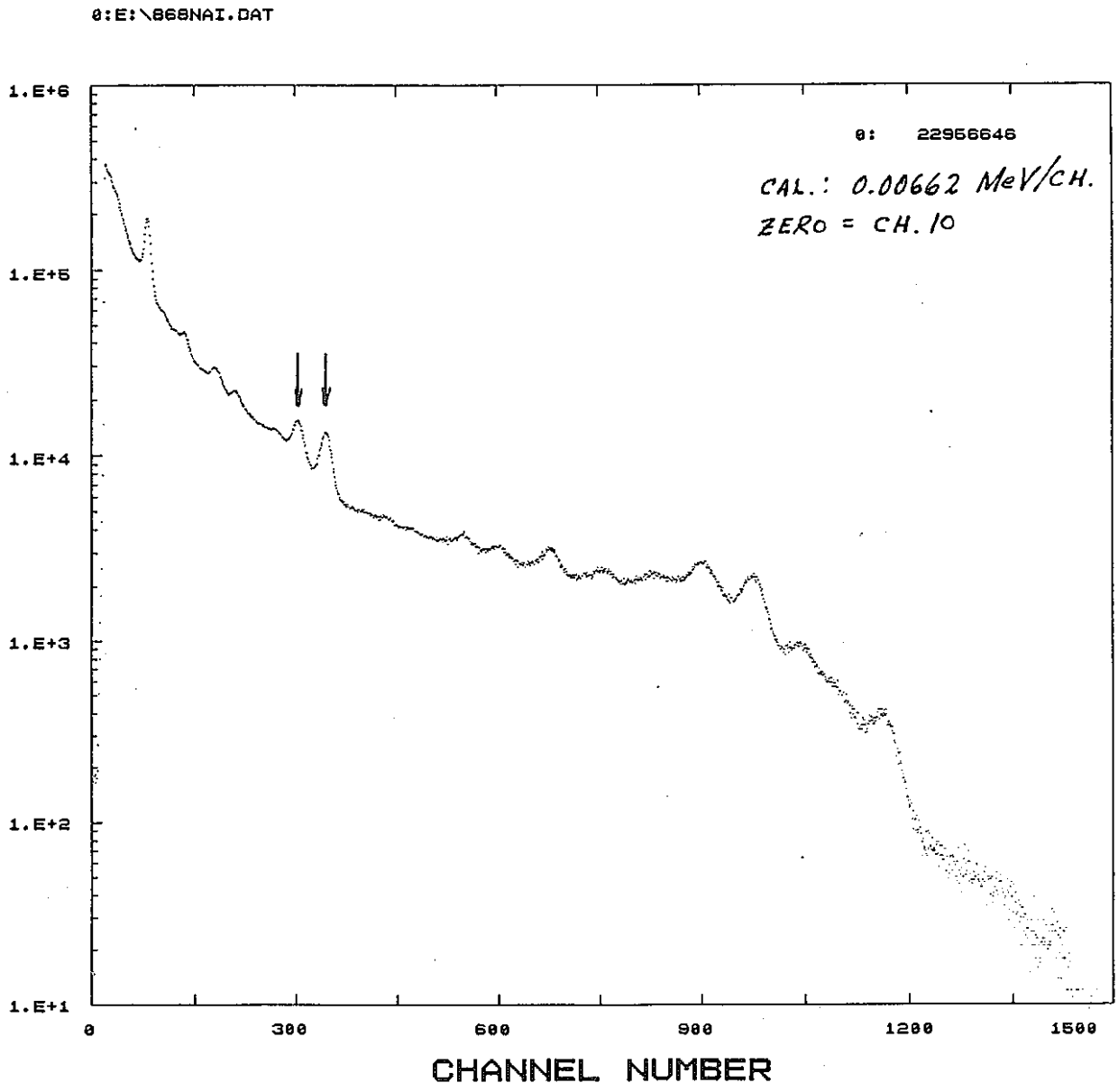
0:E:\868NAI.DAT
1.E+6
1.E+5
1.E+4
1.E+3
1.E+2
1.E+1
0: 22956646
CAL.: 0.00662 MeV/CH.
ZERO = CH. 10
0
300
600
900
1200
1500
CHANNEL NUMBER

FIG. 2

there are several less intense lines in the neighborhood of the strong 1.942 MeV gamma ray and also there are several Ca lines in the vicinity of the 2.223 hydrogen gamma ray. The NaI peaks of Figure 3 are approximately 100 keV wide (FWHM). If one chooses to integrate over a region of approximately ±100 keV from each peak, which covers the wings well, then reference 3 gives a total strength for Ca gamma rays of approximately 93.32/100 captures in this region around 1.942 MeV and 14.17/100 captures in the ±100 keV region around the 2.223 MeV line. Thus one must correct the integral under the 2.223 peak in the NaI spectrum by subtracting approximately 14.17/93.32 or 0.1518 of the area under the 1.942 MeV peak. An average background was subtracted from each channel under both peaks by simply using a straight line across the wings of each peak as indicated in Figure 3. In this way, the ratio of strength of the hydrogen capture gamma to the Ca capture gammas was found to be

$$\frac{108630 - 0.1518 \times 85860}{85860} = 1.1134$$

and the neutron capture rate ratio $= R_c = 1.134 \times \frac{93.93}{100} = 1.0458$

i.e. the hydrogen capture gamma has a strength of 100/100 captures.

These estimates neglect the relatively small effects of any difference in NaI efficiency and any difference in gamma-ray attenuation by concrete for the two energies.

Also if

$$R_\gamma = \text{Avg. Capture Cross Section Ratio} = \frac{\bar{\sigma}_c(Ca)}{\bar{\sigma}_c(H)} \sim 1.3$$

Then,

$$\frac{n_H\,(\text{atoms/barn})}{n_{Ca}\,(\text{atoms/barn})} \cong R_c \cdot R_\gamma$$

and,

$$\text{(1)} \qquad \frac{Wt\%\ H_2O}{Wt\%\ Ca} = \frac{(Mol.\ Wt\,H_2O)}{(Mol.\ Wt\,Ca)\ 2} R_c \cdot R_\gamma$$

$$= 0.22474\ R_c \cdot R_\gamma$$

From Table 14 in ORNL/TM-11839:

$$\text{(2)} \qquad Wt\%\ Ca = \frac{40.08}{56.079} \cdot 36.96 \cdot \frac{(100 - Wt\%\ H_2O)}{95.085}$$

$$= 0.2782\,(100 - Wt\%\ H_2O)$$

Solving Eqs. (1) and (2):

$$Wt\%\ H_2O = \frac{(.2782)(.22474)(100)\ R_c \cdot R_\gamma}{1 + (.2782)(.22474)\ R_c \cdot R_\gamma}$$

Axial Shield:

$$R_c = 1.0458 \Rightarrow Wt\%\ H_2O = 7.83$$

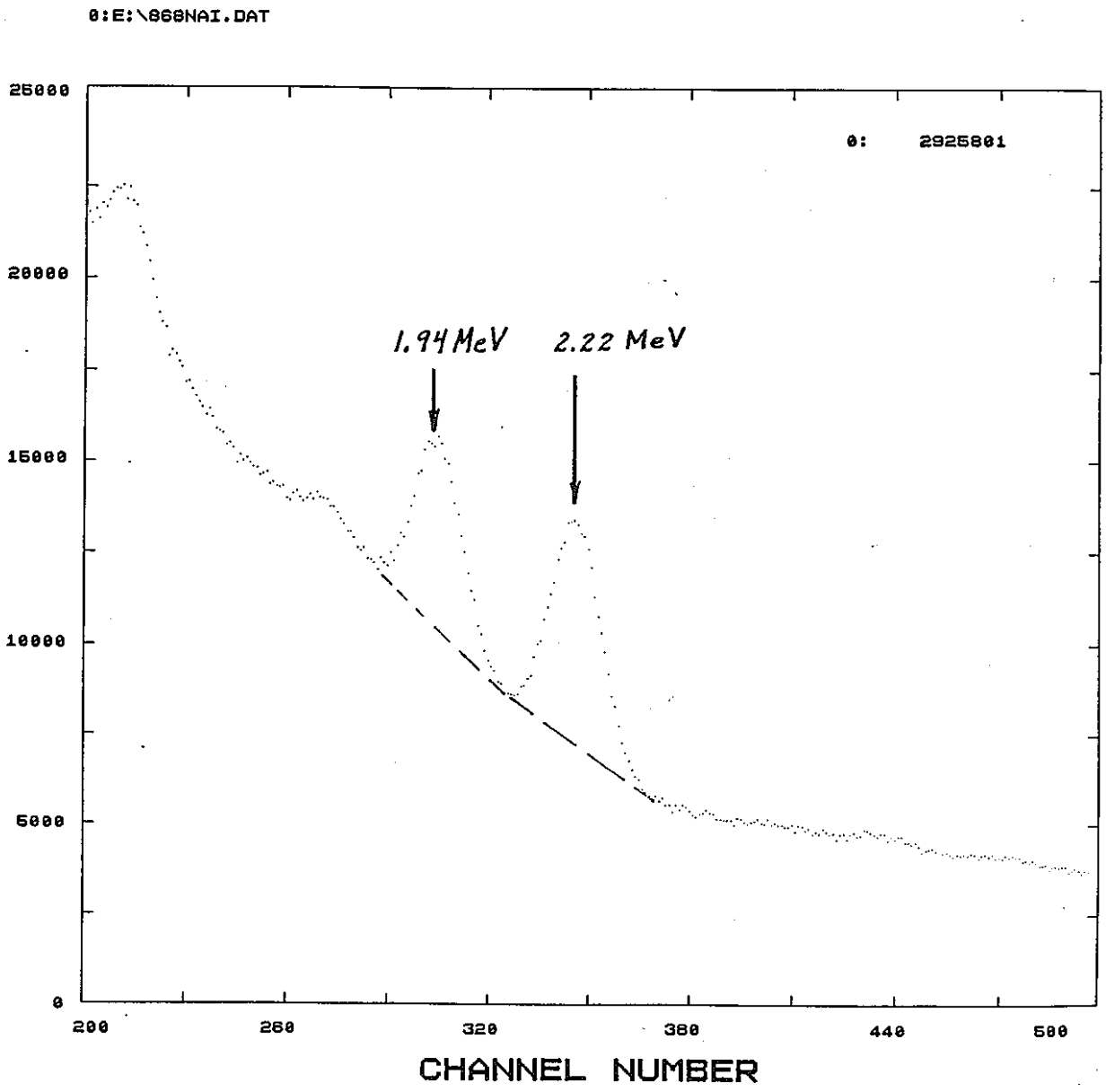
0:E:\868NAI.DAT
0: 2925801
1.94 MeV
2.22 MeV
25000
20000
15000
10000
5000
0
200
260
320
380
440
500
CHANNEL NUMBER

FIG. 3

APPENDIX 1

The average capture cross-section for Ca and H was determined as follows. A spherical concrete model, 18 inches in radius, was set up with the I-D ANISN code. Two concrete compositions were used, as shown in Table 1. Additionally there were two H cross-section sets on the VELM Library which was used in the codes. The source was a ^{252}Cf neutron spectrum, which was placed at the center of the sphere. Runs were made using both H sets and the number densities as shown in Table 2. The H & Ca capture cross sections were used in the 1-D calculations to calculate the average capture cross sections as follows:

$$\sigma_c = \frac{\int\int \phi \, \sigma_c \, dE \, dV}{\int\int \phi \, dE \, dV}$$

where Φ = the energy-spatial dependent flux
σ_c = the energy-spatial dependent capture cross sections
E = the energy variable
V = the volume variable

Table 1 shows the results from the calculations. Although the capture cross section changes depending on the H_2O content, the ratio is nearly the same. Only the different H Mat numbers produce different ratios.

Table 1. Averaged Capture Cross Sections Calculated from 1-D ANISN Runs

% H_2O in Cell	H Mat Number	σ_c(H)	σ_c(Ca)	σ_c(Ca)/σ_c(H)
3.462	9301	1.0838-1	1.5027-1	1.3870+0
3.462	930101	1.1396-1	1.4824-1	1.3061+0
9.0	9301	1.58072-1	2.18484-1	1.3822+0
9.0	930101	1.65848-1	2.15606-1	1.3000+0

For comparison, the thermal neutron capture cross section ratio is

$$\sigma_c(\mathrm{Ca})/\sigma_c(\mathrm{H}) = \frac{0.430}{0.332} = 1.295$$

In addition it was found in the ANISN runs that over 99% of the captures occurred below 100 eV neutron energy. Thus use of the thermal cross section ratio and the thermal capture gamma ray strengths for Ca are justified.

References

[1]Lorraine S. Abbott, *Analysis of a TSF Experiment on Secondary Gamma-Ray Production in Reinforced Concrete Shields*, ORNL-5272 (9/80).

[2]N. C. Rasmussen, Y. Hukai, T. Inouye, and V. J. Orphan, *Thermal Neutron Capture Gamma-Ray Spectra of the Elements*, Massachusetts Institute of Technology, MITNE-85 (approximately 1970).

[3]M. A. Lone, R. A. Leavitt, and D. A. Harrison, *Prompt Gamma Rays from Thermal-Neutron Capture*, RSIC Data Library, DLC-140 (10/88).

Calculational Results of Re-Configurations of the JASPER Axial Shield

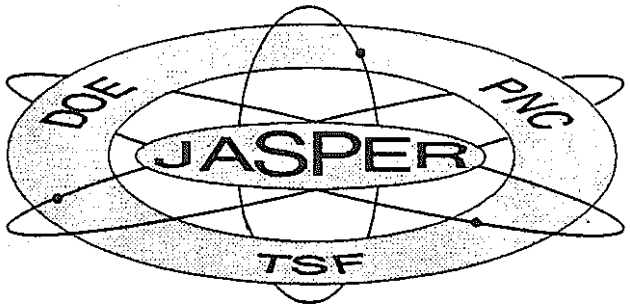

C.O. Slater, J.V. Pace III

ornl

US-JAPAN INFORMAL JASPER MEETING
ORNL, Oak Ridge, TN
April 23-24, 1992

CONFIGURATION DESCRIPTIONS

(1) The modified axial shield configuration with no B_4C around the axial shield assemblies. The calculational geometry for this configuration is shown in Fig. 1.

(2) The modified axial shield configuration with a 10-cm-thick layer of B_4C around the axial shield assemblies. The calculational geometry for this configuration is shown in Fig. 2.

(3) The modified axial shield configuration with a 20-cm-thick layer of B_4C around the axial shield assemblies. The calculational geometry for this configuration is shown in Fig. 3.

(4) The modified axial shield configuration with no B_4C around the axial shield assemblies and with a 10.16-cm-thick lithiated paraffin layer preceding the axial shield concrete. The calculational geometry for this configuration is shown in Fig. 4.

(5) The modified axial shield configuration with no B_4C around the axial shield assemblies and with a 10.16-cm-thick borated polyethylene layer preceding the axial shield concrete. The calculational geometry for this configuration is shown in Fig. 4.

(6) The modified axial shield configuration with no B_4C around the axial shield assemblies and with a 10.16-cm-thick lithiated paraffin layer following the axial shield concrete. The calculational geometry for this configuration is shown in Fig. 5.

(7) The modified axial shield configuration with no B_4C around the axial shield assemblies and with a 10.16-cm-thick borated polyethylene layer following the axial shield concrete. The calculational geometry for this configuration is shown in Fig. 5.

(8) The modified axial shield configuration with no B_4C around the axial shield assemblies, with a pure absorber (Σ_a=10.0 cm^{-1}) replacing the axial shield concrete, and with a 10.16-cm-thick lithiated paraffin layer following the pure absorber region. The calculational geometry for this configuration is shown in Fig. 5.

(9) The modified axial shield configuration with no B_4C around the axial shield assemblies, with a pure absorber (Σ_a=10.0 cm^{-1}) replacing the axial shield concrete, and with a 10.16-cm-thick borated polyethylene layer following the pure absorber region. The calculational geometry for this configuration is shown in Fig. 5.

(14) The modified axial shield configuration with a 20-cm-thick B_4C layer around the axial shield assemblies and with a 10.16-cm-thick lithiated paraffin layer preceding the axial shield concrete. The calculational geometry for this configuration is shown in Fig. 6.

(15) The modified axial shield configuration with a 20-cm-thick B_4C layer around the axial shield assemblies and with a 10.16-cm-thick lithiated paraffin layer following the axial shield concrete. The calculational geometry for this configuration is shown in Fig. 7.

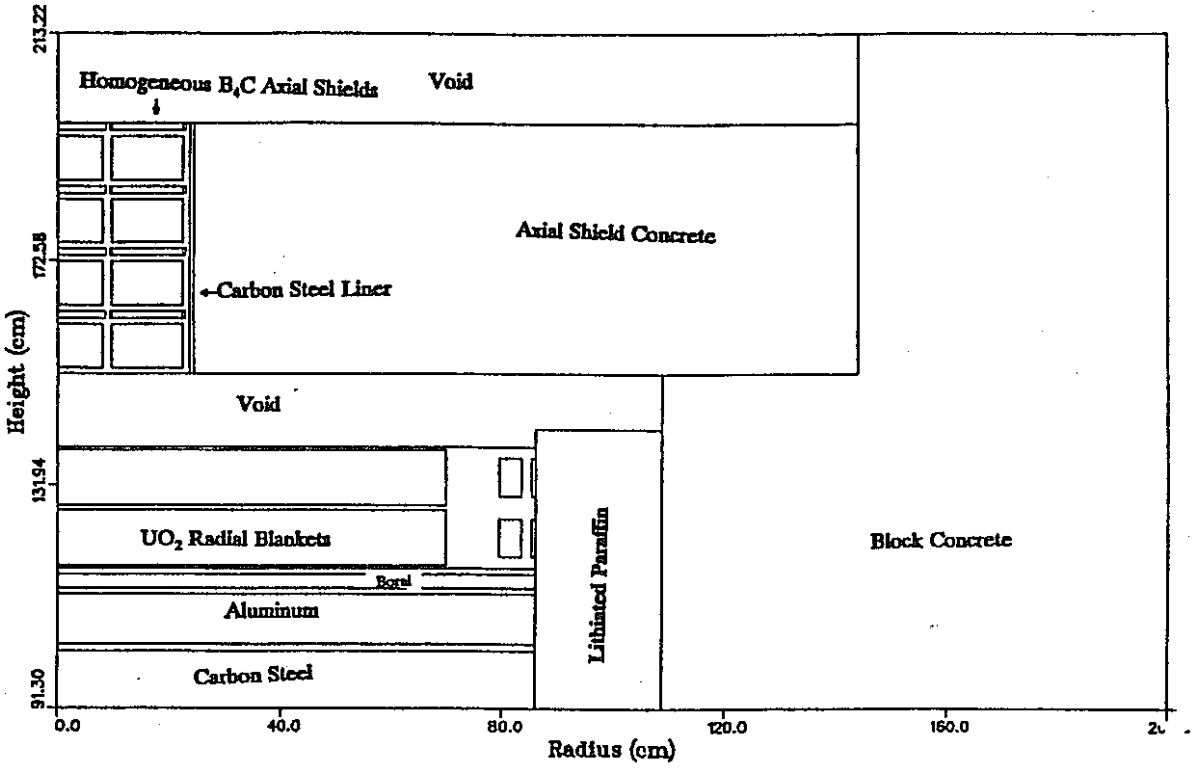

Fig. 1. Axial Shield Experiment 2-D Calculational Geometry Model for Case 1.

(16) The modified axial shield configuration with a 5-cm-thick layer of B_4C around the axial shield assemblies. The calculational geometry for this configuration is shown in Fig. 8.

(17) The modified axial shield configuration with a 5-cm-thick B_4C layer around the axial shield assemblies and with a 10.16-cm-thick lithiated paraffin layer preceding the axial shield concrete. The calculational geometry for this configuration is shown in Fig. 9.

(18) The modified axial shield configuration with a 5-cm-thick B_4C layer around the axial shield assemblies and with a 10.16-cm-thick lithiated paraffin layer preceding the axial shield concrete. The calculational geometry for this configuration is shown in Fig. 10.

following

Note that in all configurations, the axial shield concrete has been offset 10.16 cm axially in order to accomodate th[PNC TN9600 92-004]te and to avoid the introduction of effects due to differences in t[PNC TN9600 92-004]ld components. Also, all configurations contain the homogeneous B_4C axial shield assembly mockup. In addition, it should be noted that the cases skip from 9 to 14 due to four intervening cases dealing with the Gap Streaming Experiment (i.e. I still have most of my marbles).

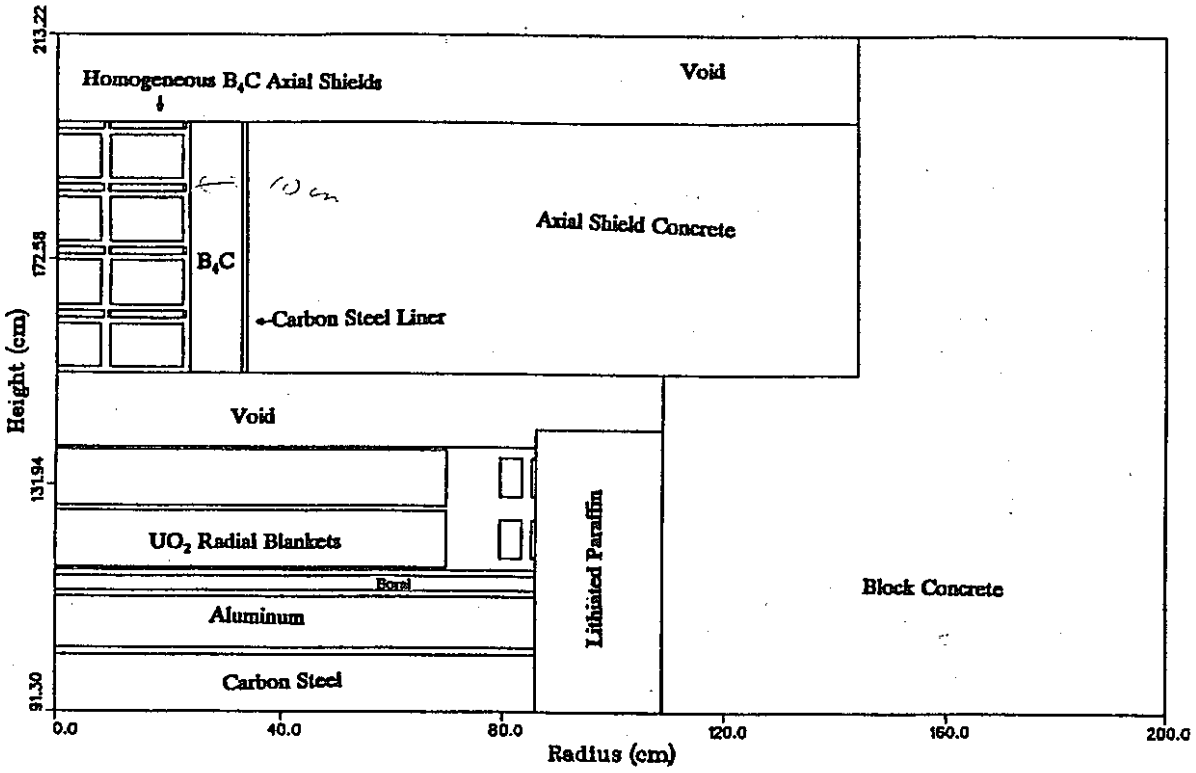

Fig. 2. Axial Shield Experiment 2-D Calculational Geometry Model for Case 2.

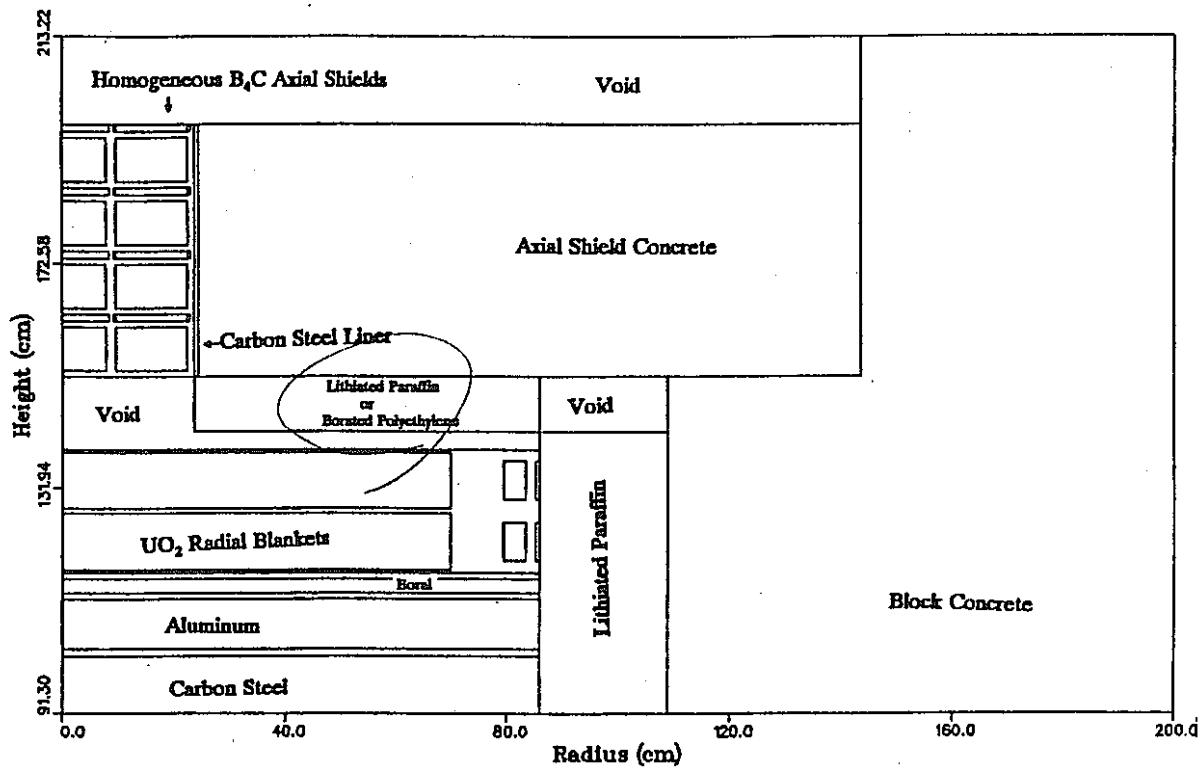

Fig. 4. Axial Shield Experiment 2-D Calculational Geometry Model for Cases 4 and 5.

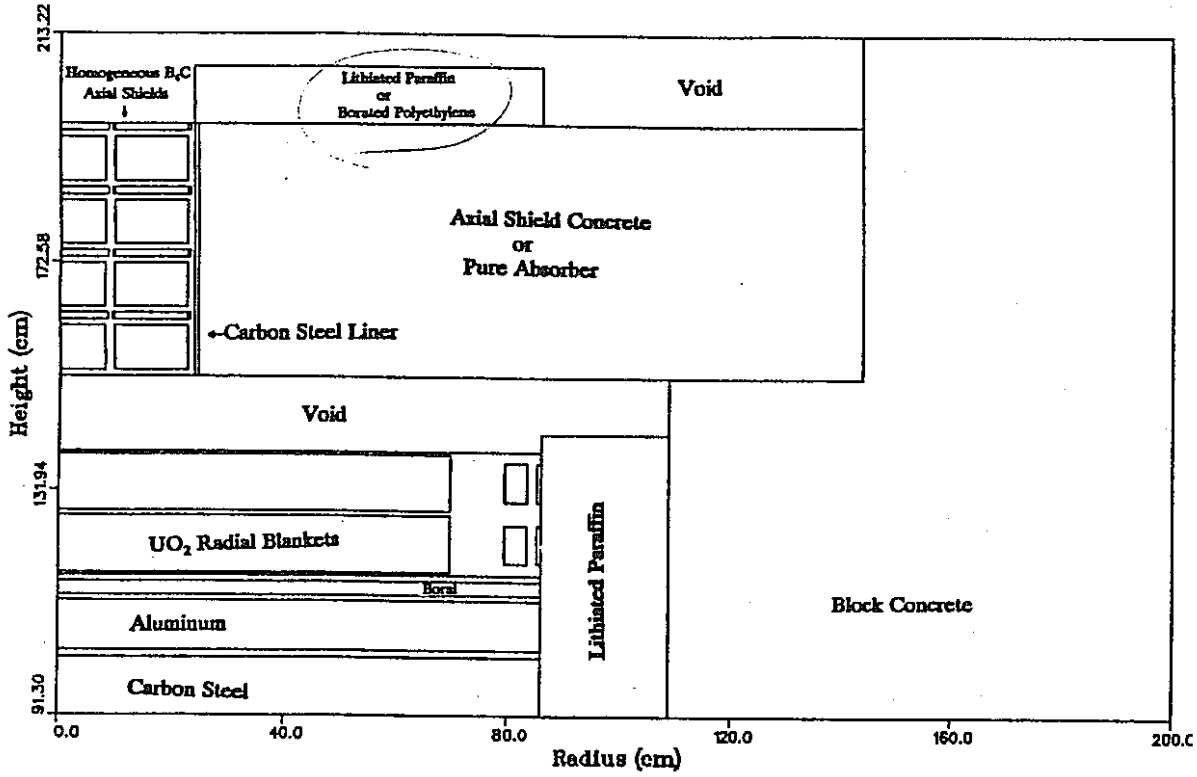

Fig. 5. Axial Shield Experiment 2-D Calculational Geometry Model for Cases 6 through 9.

Table 1. Bare and Cd-Covered BF_3 Detector Count Rates ($min^{-1} \cdot W^{-1}$) Behind the Axial Shielding Experiment Configuration Having All Homogeneous B_4C Assemblies.

Case	Distance (cm) From the End of the Configuration		
	0	30	150
Bare BF_3 Detector			
1	4.174+1[a]	1.064+3	3.557+2
2	9.899+0	5.593+2	1.772+2
3	4.051+0	2.925+2	1.585+2
4	7.266+0	1.250+2	3.987+1
5	6.640+0	1.111+2	3.552+1
6	3.623+1	6.307+1	2.953+1
7	2.232+1	5.102+1	2.820+1
8	2.005+0	9.453−1	1.755−1
9	1.489+0	5.912−1	9.708−2
14	1.057+0	1.574+1	8.531+0
15	7.922+0	1.757+1	2.381+1
16	1.709+1	7.679+2	2.293+2
17	2.444+0	6.308+1	1.539+1
18	7.975+0	1.881+1	2.579+1
Cd-Covered BF_3 Detector			
1	2.612+0	2.044+1	7.420+0
2	1.565+0	1.008+1	2.110+0
3	1.420+0	5.541+0	1.881+0
4	1.288+0	4.715+0	1.859+0
5	1.236+0	4.429+0	1.755+0
6	5.932+0	4.957+0	7.581−1
7	5.073+0	4.237+0	6.402−1
8	1.228+0	4.303−1	7.205−2
9	1.175+0	3.907−1	5.843−2
14	9.140−1	7.486−1	1.569−1
15	3.881+0	2.110+0	5.114−1
16	1.731+0	1.383+1	3.712+0
17	9.784−1	2.471+0	5.797−1
18	3.927+0	2.068+0	5.129−1

[a]Read as 4.174×10^1.

Table 2. 5- and 6-in. Bonner Ball Count Rates ($min^{-1} \cdot W^{-1}$) Behind the Axial Shielding Experiment Configuration Having All Homogeneous B_4C Assemblies.

Case	Distance (cm) From the End of the Configuration		
	0	30	150
5-in. Bonner Ball			
1	1.590+3[a]	7.356+2	1.689+2
2	1.549+3	6.159+2	1.112+2
3	1.513+3	5.757+2	1.119+2
4	1.018+3	3.280+2	6.004+1
5	9.785+2	3.128+2	5.691+1
6	1.706+3	5.104+2	3.412+1
7	1.686+3	4.979+2	3.184+1
8	8.328+2	1.545+2	5.406+0
9	8.299+2	1.536+2	5.153+0
14	1.011+3	2.804+2	3.934+1
15	1.635+3	4.679+2	3.197+1
16	1.561+3	6.510+2	1.275+2
17	1.008+3	2.962+2	4.462+1
18	1.670+3	4.615+2	3.024+1
6-in. Bonner Ball			
1	1.771+3	7.375+2	1.568+2
2	1.736+3	6.609+2	1.233+2
3	1.697+3	6.399+2	1.275+2
4	1.136+3	3.445+2	5.691+1
5	1.091+3	3.287+2	5.391+1
6	1.876+3	5.447+2	3.451+1
7	1.857+3	5.333+2	3.238+1
8	9.300+2	1.739+2	5.440+0
9	9.269+2	1.729+2	5.215+0
14	1.136+3	3.198+2	4.688+1
15	1.812+3	5.230+2	3.471+1
16	1.748+3	6.801+2	1.303+2
17	1.130+3	3.245+2	4.804+1
18	1.850+3	5.120+2	3.207+1

[a]Read as 1.590×10^3.

Table 3. 10-in. Bonner Ball Count Rates ($min^{-1} \cdot W^{-1}$) Behind the Axial Shielding Experiment Configuration Having All Homogeneous B_4C Assemblies.

Case	Distance (cm) From the End of the Configuration		
	0	30	150
1	8.437+2[a]	3.255+2	6.494+1
2	8.369+2	3.274+2	7.137+1
3	8.188+2	3.347+2	7.931+1
4	5.424+2	1.606+2	2.310+1
5	5.210+2	1.533+2	2.181+1
6	8.757+2	2.591+2	1.658+1
7	8.688+2	2.551+2	1.568+1
8	4.487+2	9.127+1	2.264+0
9	4.475+2	9.083+1	2.186+0
14	5.517+2	1.717+2	3.004+1
15	8.576+2	2.734+2	2.047+1
16	8.402+2	3.223+2	6.415+1
17	5.451+2	1.626+2	2.475+1
18	8.731+2	2.600+2	1.713+1

[a]Read as 8.437×10^2.

Table 4. Fractions of Bonner Ball Count Rates Due to Neutron Leakage From the Axial Shield Mockup (Region 1) and the Surrounding Shielding (Region 2).

Bonner Ball	30 cm From Configuration		150 cm From Configuration	
	Reg. 1 Fraction	Reg. 2 Fraction	Reg. 1 Fraction	Reg. 2 Fraction
Case 4				
3-in.	0.963	0.037	0.247	0.753
5-in.	0.987	0.013	0.433	0.567
10-in.	0.999	0.001	0.522	0.478
Case 6				
3-in.	0.984	0.016	0.530	0.470
5-in.	0.992	0.008	0.700	0.300
10-in.	0.997	0.003	0.700	0.300
Case 16				
3-in.	0.856	0.144	0.067	0.933
5-in.	0.954	0.046	0.208	0.792
10-in.	0.996	0.004	0.313	0.687
Case 17				
3-in.	0.948	0.052	0.197	0.803
5-in.	0.986	0.014	0.418	0.582
10-in.	0.999	0.001	0.520	0.480
Case 18				
3-in.	0.977	0.023	0.438	0.562
5-in.	0.991	0.009	0.679	0.321
10-in.	0.997	0.003	0.709	0.291

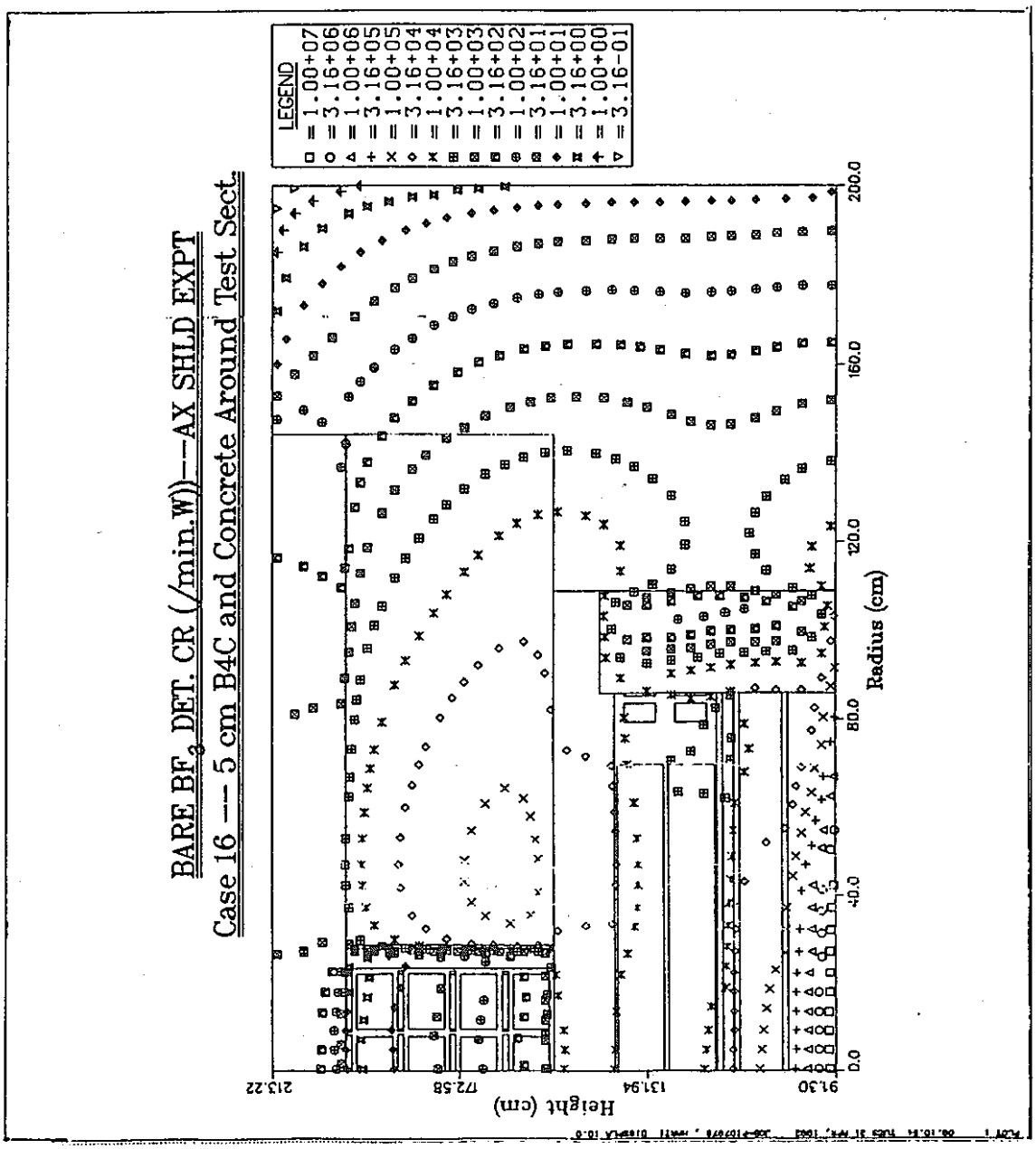
BARE BF3 DET. CR (/min.W))--AX SHLD EXPT
Case 16 -- 5 cm B4C and Concrete Around Test Sect.
LEGEND
□ = 1.00+07
○ = 3.16+06
△ = 1.00+06
+ = 3.16+05
× = 1.00+05
◇ = 3.16+04
× = 1.00+04
⊞ = 3.16+03
⊠ = 1.00+03
⊡ = 3.16+02
⊕ = 1.00+02
⊠ = 3.16+01
◆ = 1.00+01
⊠ = 3.16+00
← = 1.00+00
▽ = 3.16-01
Height (cm)
91.30
131.94
172.58
213.22
Radius (cm)
0.0
40.0
80.0
120.0
160.0
200.0

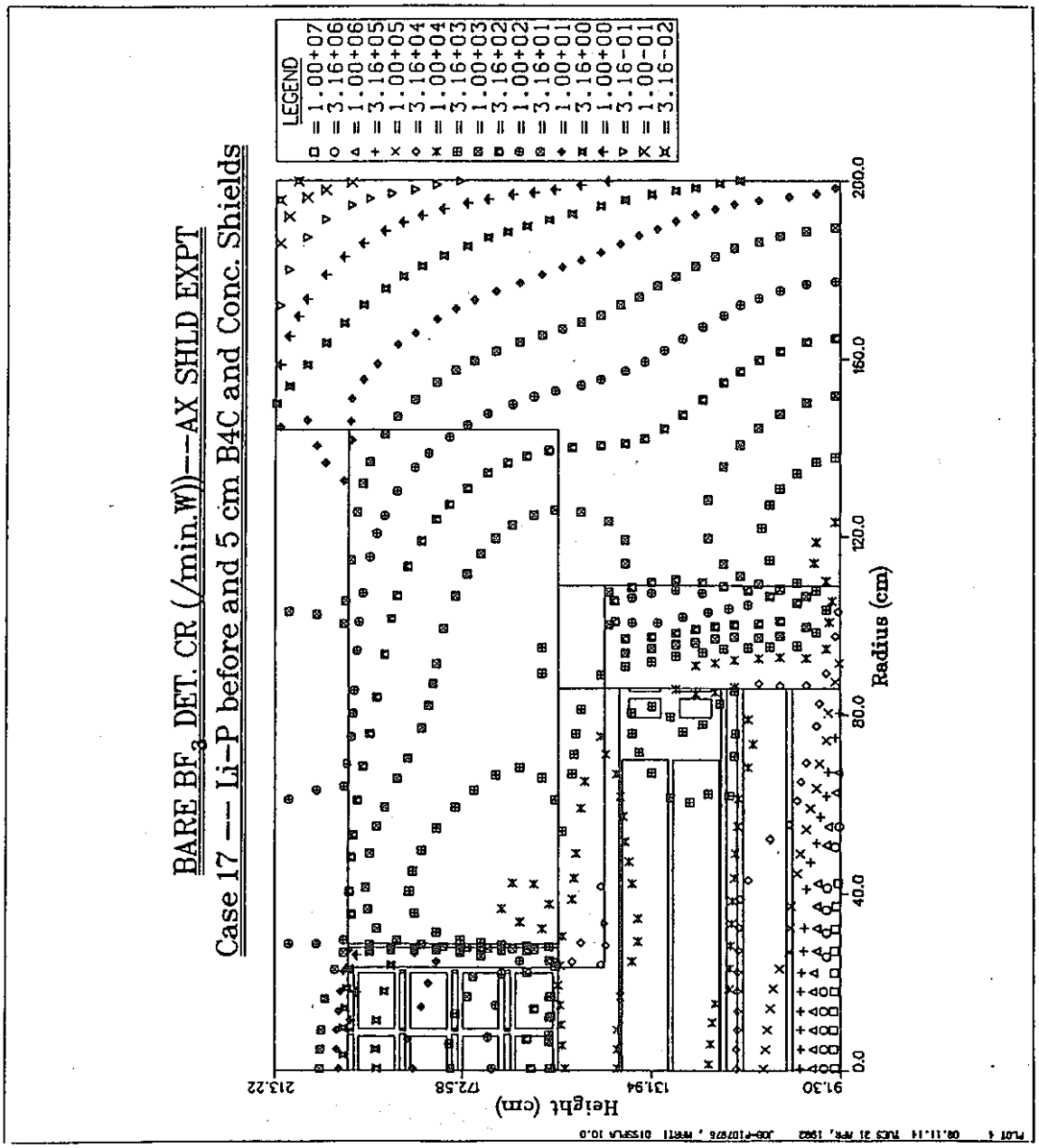
BARE BF_3 DET. CR (/min.W))--AX SHLD EXPT
Case 17 -- Li-P before and 5 cm B4C and Conc. Shields
LEGEND
□ = 1.00+07
○ = 3.16+06
△ = 1.00+06
+ = 3.16+05
× = 1.00+05
◇ = 3.16+04
⊠ = 1.00+04
⊞ = 3.16+03
⊠ = 1.00+03
⊡ = 3.16+02
⊕ = 1.00+02
⊗ = 3.16+01
◆ = 1.00+01
⋈ = 3.16+00
+ = 1.00+00
▽ = 3.16-01
⋉ = 1.00-01
⋊ = 3.16-02
Height (cm)
213.22
72.58
131.94
91.30
Radius (cm)
0.0
40.0
80.0
120.0
160.0
200.0

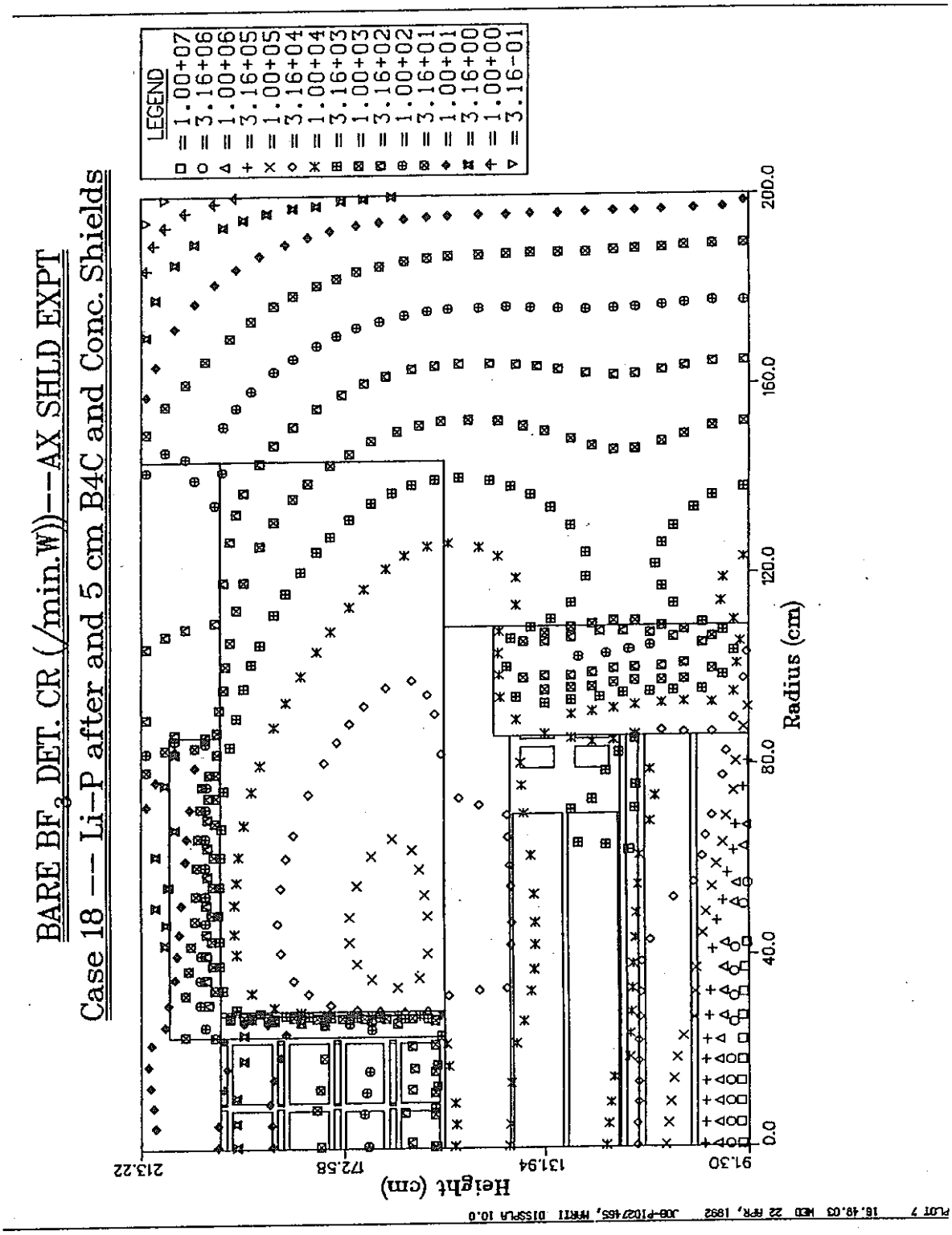
BARE BF_3 DET. CR (/min.W))--AX SHLD EXPT
Case 18 -- Li-P after and 5 cm B4C and Conc. Shields
LEGEND
□ = 1.00+07
○ = 3.16+06
△ = 1.00+06
+ = 3.16+05
× = 1.00+05
◇ = 3.16+04
* = 1.00+04
⊞ = 3.16+03
⊠ = 1.00+03
⊡ = 3.16+02
⊕ = 1.00+02
⊗ = 3.16+01
◆ = 1.00+01
⋈ = 3.16+00
◁ = 1.00+00
▷ = 3.16-01
Height (cm)
91.30
131.94
172.58
213.22
Radius (cm)
0.0
40.0
80.0
120.0
160.0
200.0
PLOT 7 16.49.03 MED 22 APR, 1992 JOB-P102/455, MERIT DISSPLA 10.0

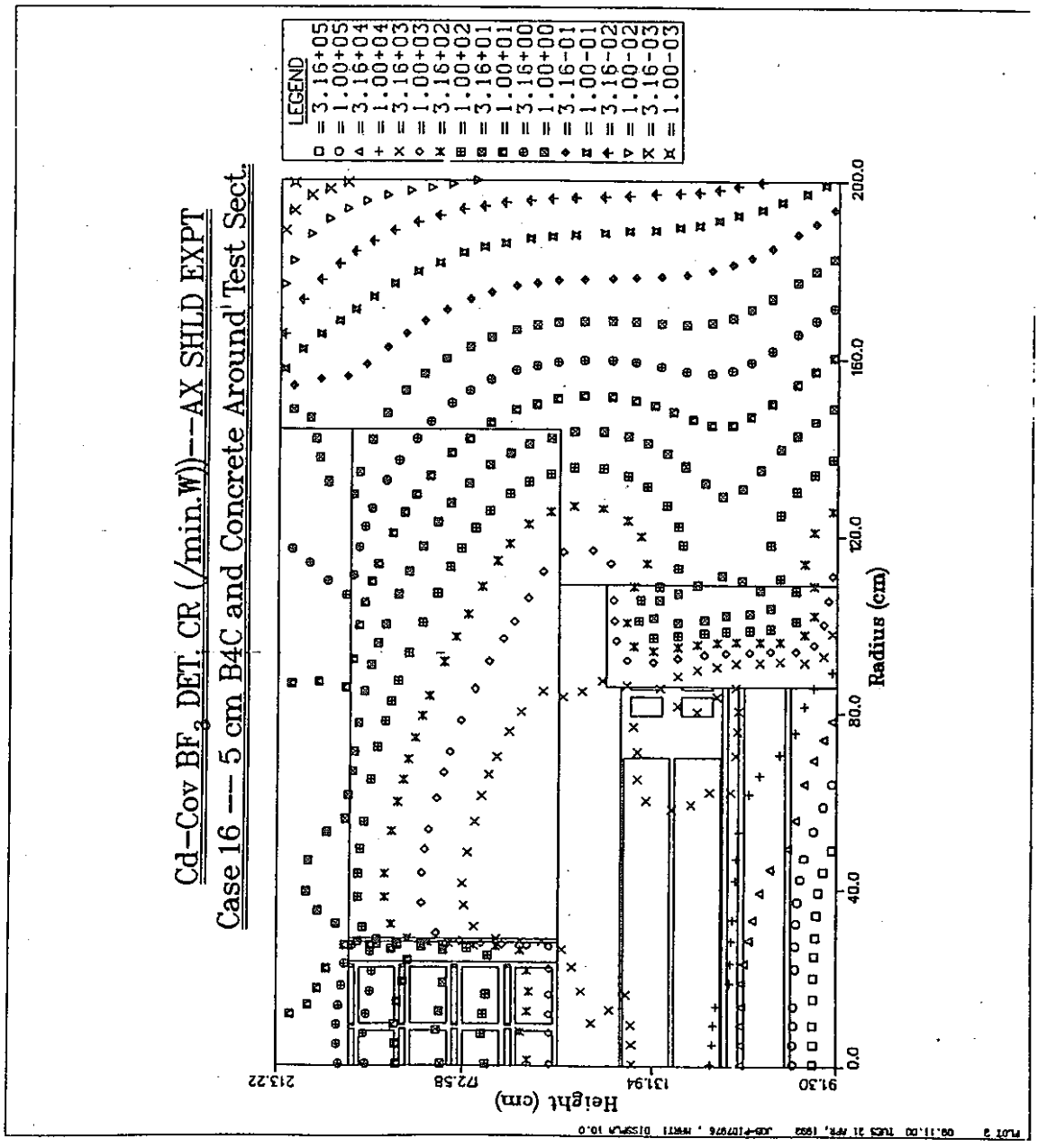
Cd-Cov BF3 DET. CR (/min.W)--AX SHLD EXPT
Case 16 --- 5 cm B4C and Concrete Around Test Sect.
LEGEND
= 3.16+05
= 1.00+05
= 3.16+04
= 1.00+04
= 3.16+03
= 1.00+03
= 3.16+02
= 1.00+02
= 3.16+01
= 1.00+01
= 3.16+00
= 1.00+00
= 3.16-01
= 1.00-01
= 3.16-02
= 1.00-02
= 3.16-03
= 1.00-03
Height (cm)
91.30
131.94
172.58
213.22
Radius (cm)
0.0
40.0
80.0
120.0
160.0
200.0

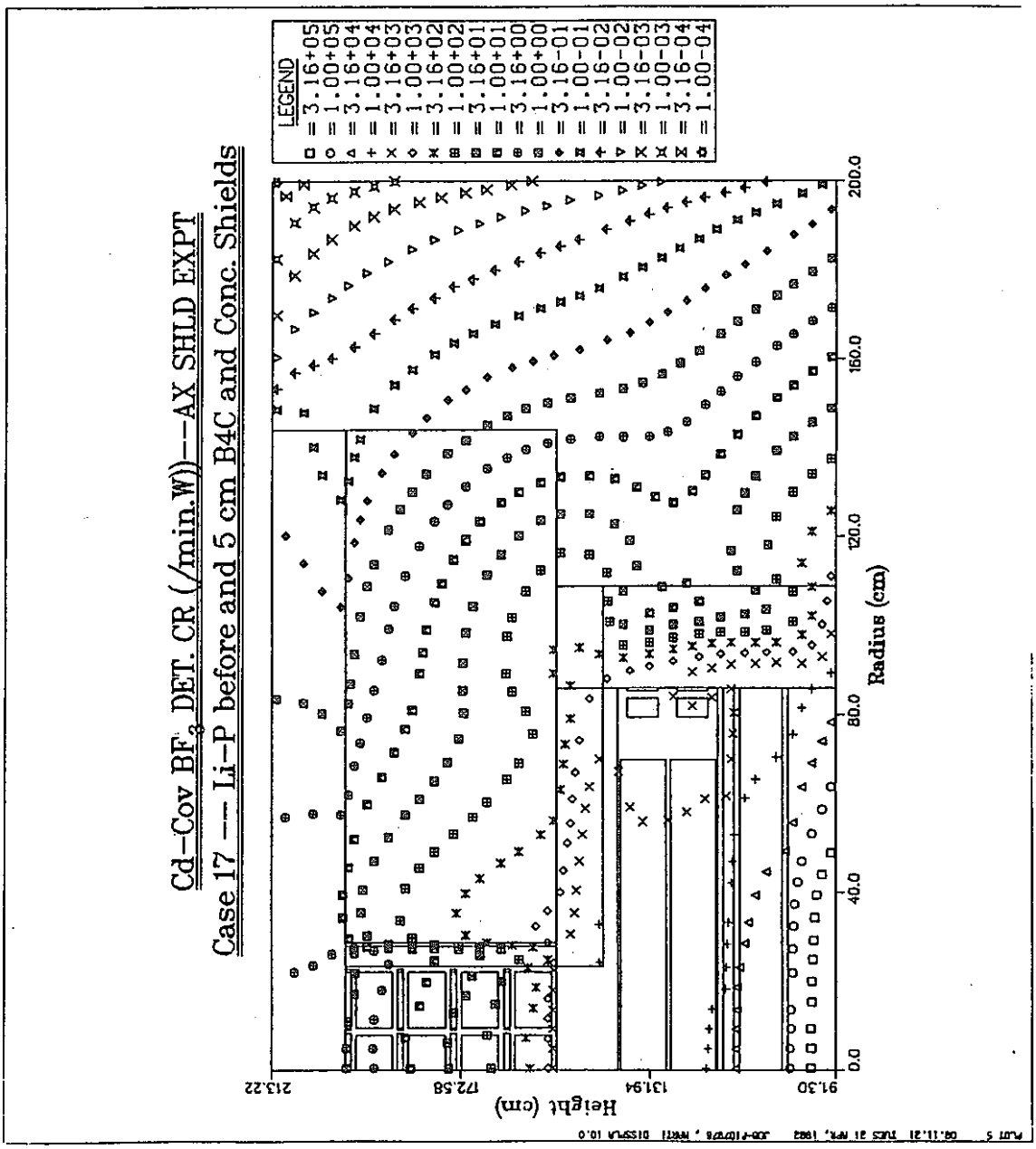
Cd-Cov BF_3 DET. CR (/min.W))--AX SHLD EXPT
Case 17 --- Li-P before and 5 cm B4C and Conc. Shields
LEGEND
□ = 3.16+05
○ = 1.00+05
△ = 3.16+04
+ = 1.00+04
× = 3.16+03
◇ = 1.00+03
⊠ = 3.16+02
■ = 1.00+02
⊞ = 3.16+01
▣ = 1.00+01
⊕ = 3.16+00
◆ = 1.00+00
+ = 3.16-01
▷ = 1.00-01
⋈ = 3.16-02
⋈ = 1.00-02
⋈ = 3.16-03
⋈ = 1.00-03
⋈ = 3.16-04
✪ = 1.00-04
Height (cm)
91.30
131.94
172.58
213.22
Radius (cm)
0.0
40.0
80.0
120.0
160.0
200.0

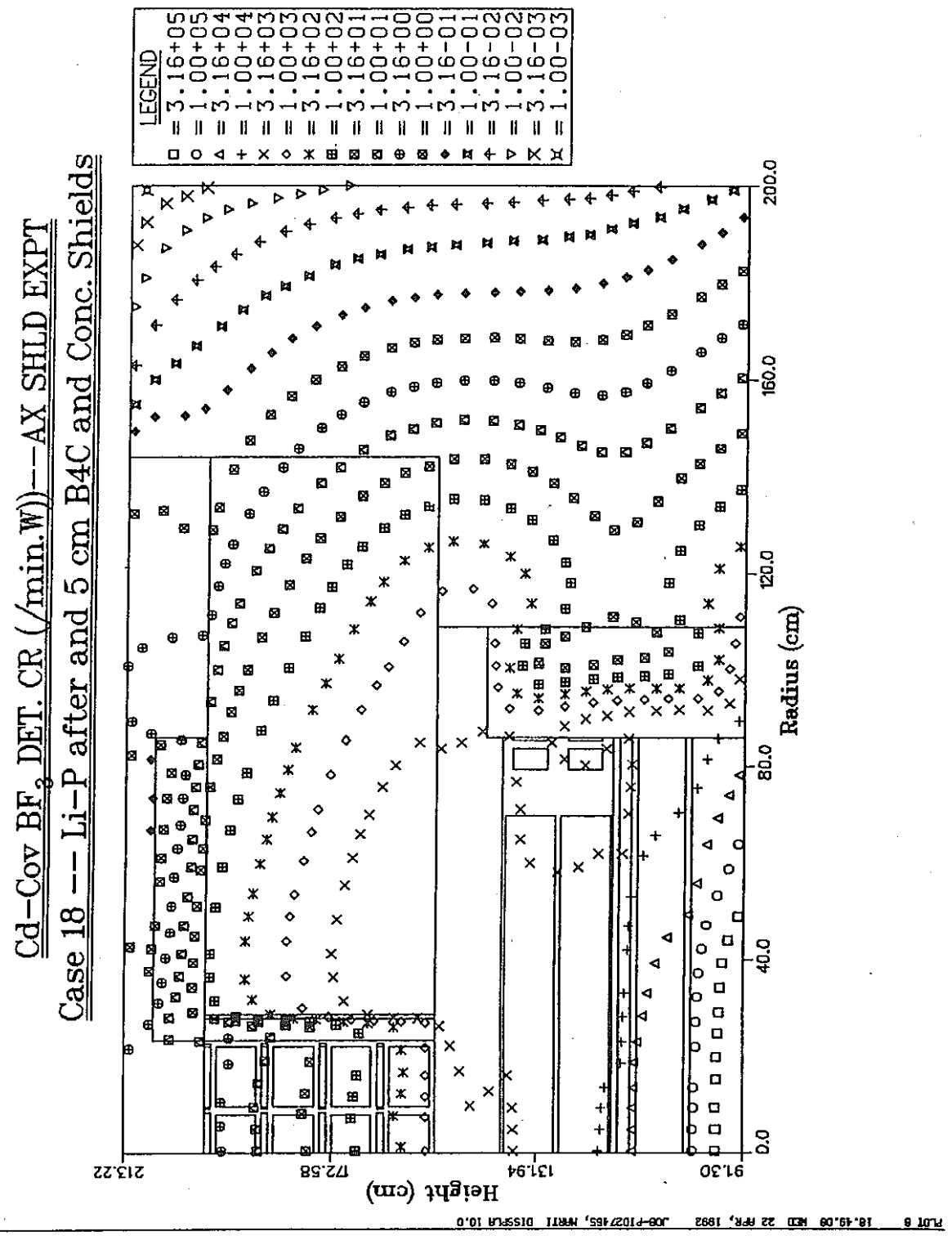
Cd-Cov BF_3 DET. CR (/min.W))--AX SHLD EXPT
Case 18 -- Li-P after and 5 cm B4C and Conc. Shields
LEGEND
= 3.16+05
= 1.00+05
= 3.16+04
= 1.00+04
= 3.16+03
= 1.00+03
= 3.16+02
= 1.00+02
= 3.16+01
= 1.00+01
= 3.16+00
= 1.00+00
= 3.16-01
= 1.00-01
= 3.16-02
= 1.00-02
= 3.16-03
= 1.00-03
Height (cm)
91.30
131.94
172.58
213.22
Radius (cm)
0.0
40.0
80.0
120.0
160.0
200.0
PLOT 8 18.49.08 MON 22 APR, 1992 JOB-P10274S5, NRTI DISSPLA 10.0

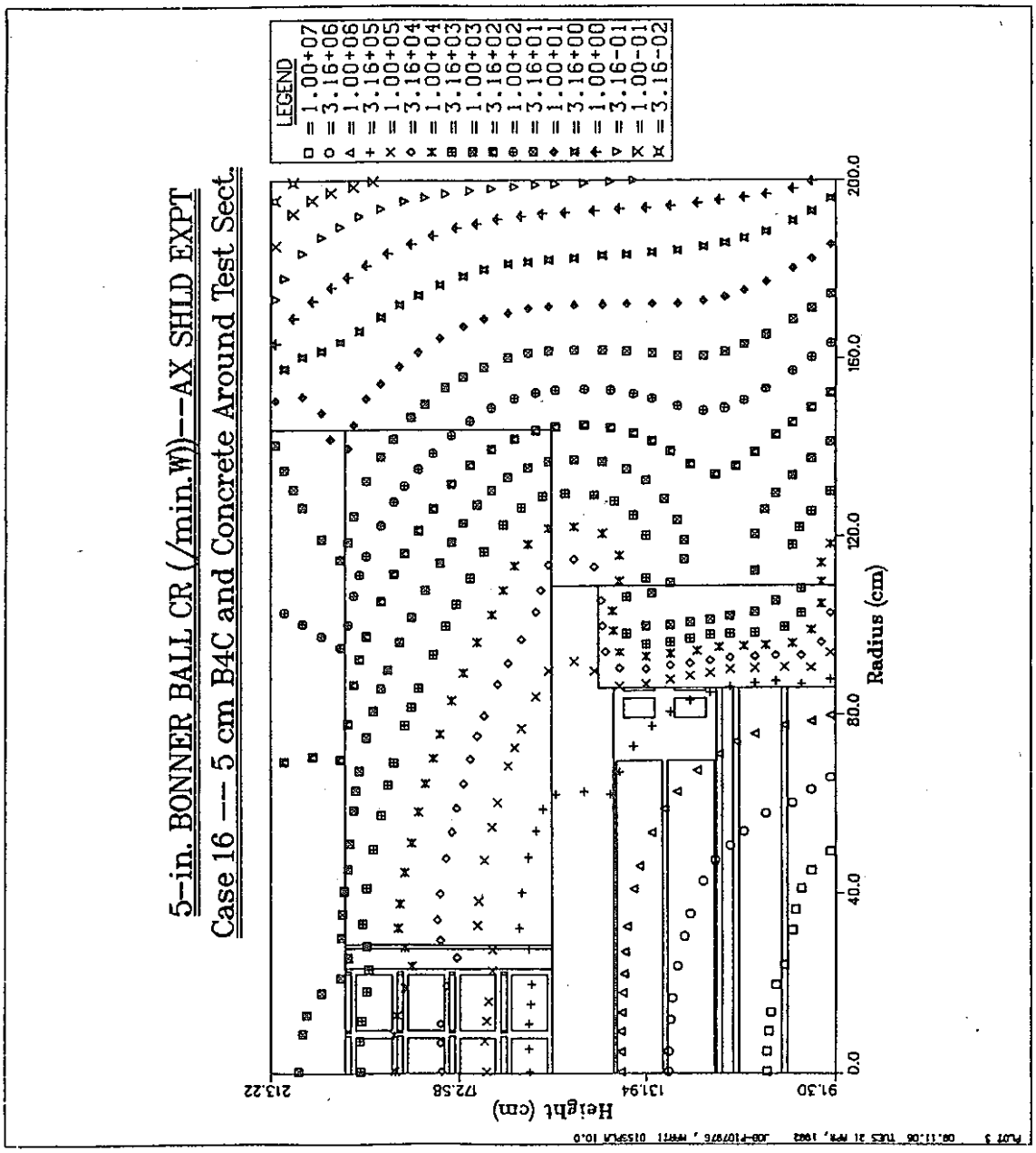
5-in. BONNER BALL CR (/min.W)--AX SHLD EXPT
Case 16 -- 5 cm B4C and Concrete Around Test Sect.
LEGEND
□ = 1.00+07
○ = 3.16+06
△ = 1.00+06
+ = 3.16+05
× = 1.00+05
◇ = 3.16+04
✕ = 1.00+04
⊞ = 3.16+03
⊠ = 1.00+03
⊕ = 3.16+02
⊠ = 1.00+02
◆ = 3.16+01
⊠ = 1.00+01
✕ = 3.16+00
◆ = 1.00+00
▷ = 3.16-01
✕ = 1.00-01
✕ = 3.16-02
Height (cm)
213.22
172.58
131.94
91.30
Radius (cm)
0.0
40.0
80.0
120.0
160.0
200.0

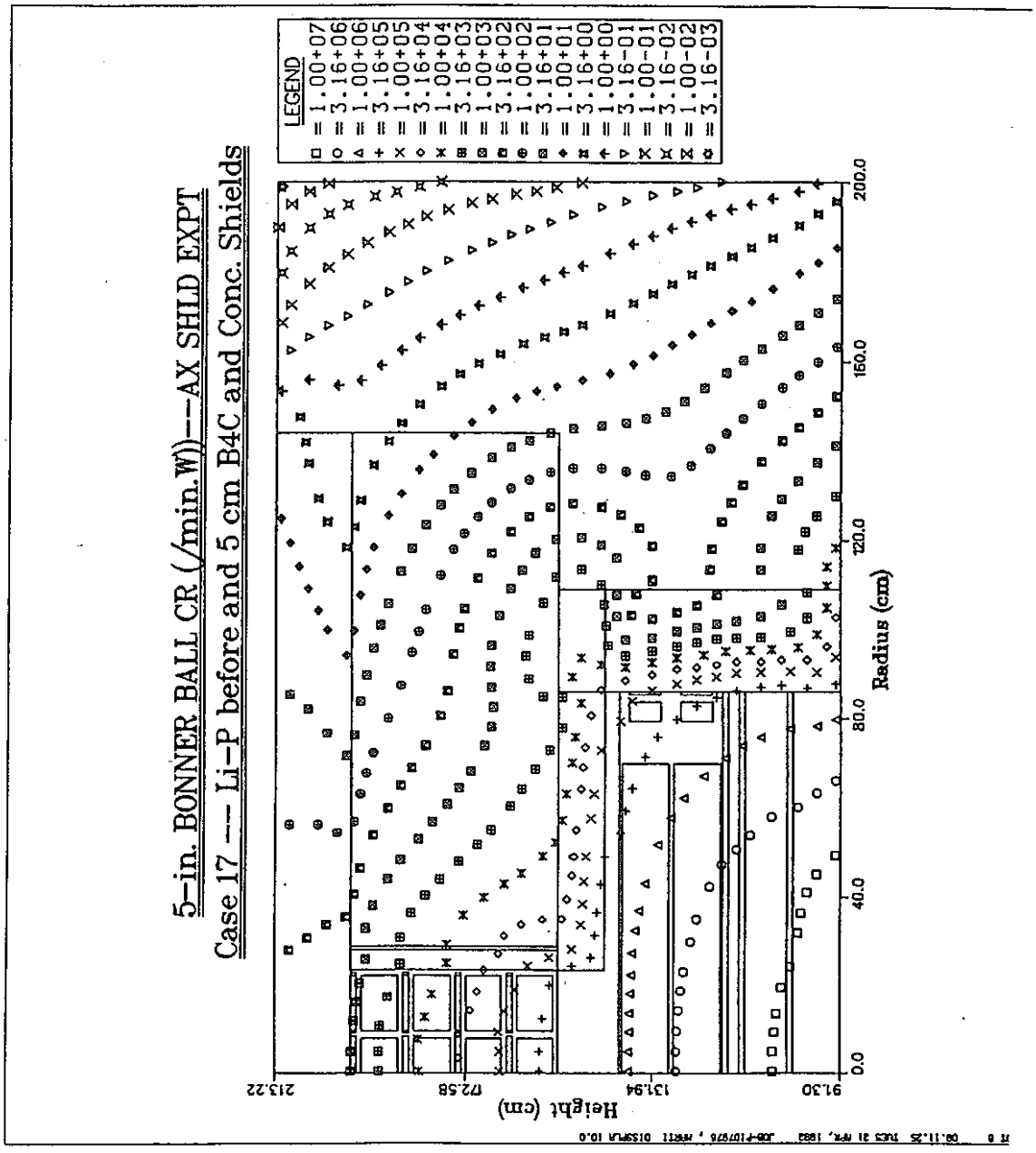
5-in. BONNER BALL CR (/min.W))--AX SHLD EXPT
Case 17 -- Li-P before and 5 cm B4C and Conc. Shields
LEGEND
□ = 1.00+07
○ = 3.16+06
△ = 1.00+06
+ = 3.16+05
× = 1.00+05
◇ = 3.16+04
⊠ = 1.00+04
⊞ = 3.16+03
⊡ = 1.00+03
⊟ = 3.16+02
⊕ = 1.00+02
⊠ = 3.16+01
◆ = 1.00+01
⋈ = 3.16+00
← = 1.00+00
▷ = 3.16-01
▽ = 1.00-01
⋈ = 3.16-02
⋈ = 1.00-02
✡ = 3.16-03
Height (cm)
213.22
172.58
131.94
91.30
Radius (cm)
0.0
40.0
80.0
120.0
160.0
200.0

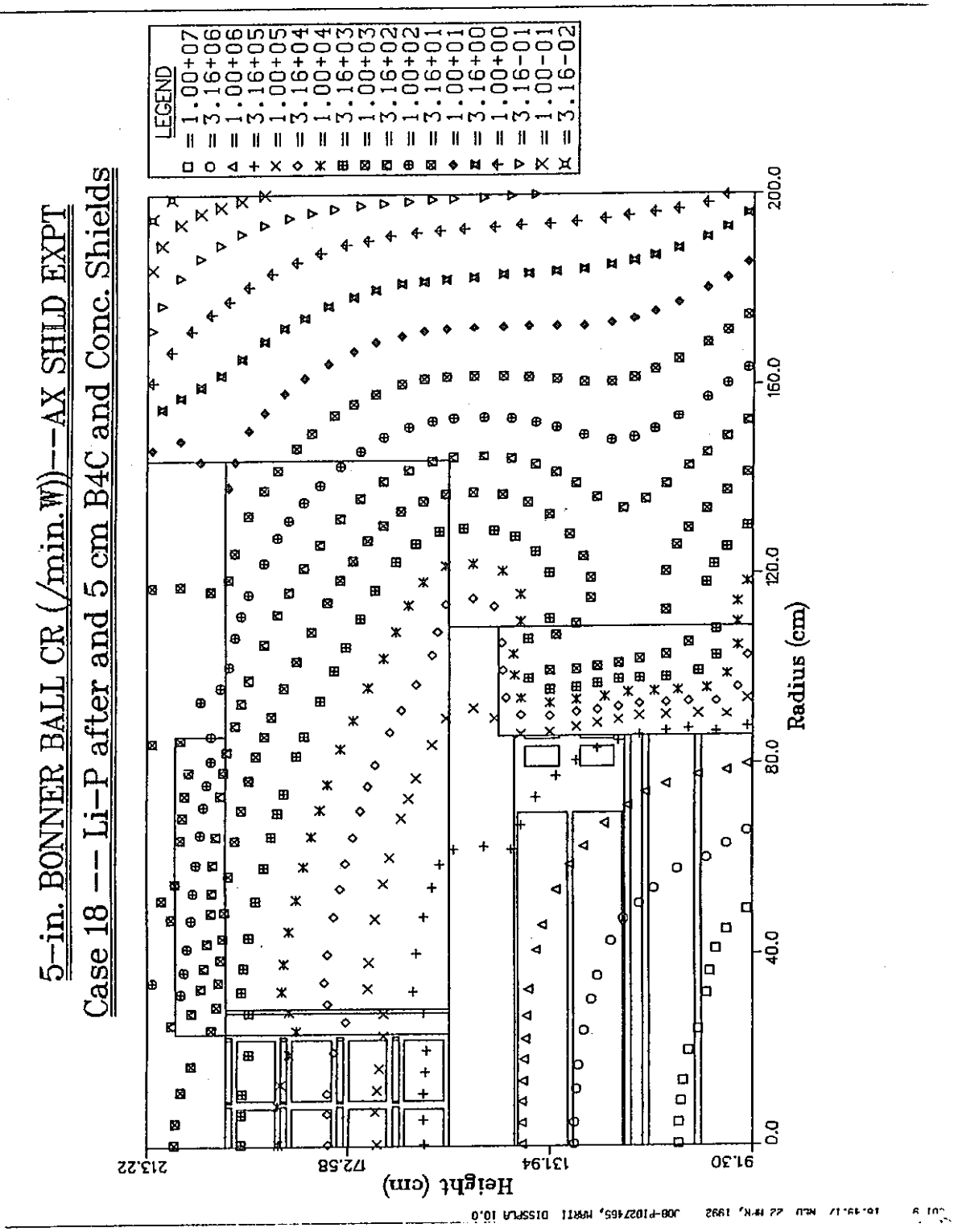
5-in. BONNER BALL CR (/min.W))--AX SHLD EXP'T
Case 18 -- Li-P after and 5 cm B4C and Conc. Shields
LEGEND
□ = 1.00+07
○ = 3.16+06
△ = 1.00+06
+ = 3.16+05
× = 1.00+05
◇ = 3.16+04
✳ = 1.00+04
⊞ = 3.16+03
⊠ = 1.00+03
⊡ = 3.16+02
⊕ = 1.00+02
⊠ = 3.16+01
◆ = 1.00+01
⊠ = 3.16+00
✚ = 1.00+00
▷ = 3.16-01
✕ = 1.00-01
⌘ = 3.16-02
Height (cm)
91.30
131.94
172.58
213.22
Radius (cm)
0.0
40.0
80.0
120.0
160.0
200.0

THE JASPER IN-VESSEL FUEL STORAGE (IVFS) EXPERIMENTS

by

J. A. Bucholz

OAK RIDGE NATIONAL LABORATORY

4-24-92

PARTIAL LIST OF HANDOUTS TAKEN FROM IVFS REPORT, ORNL/TM-11989:

Pages 31-40: IVFS program plan, describing all experiments

Page 104: Spectral modifier Config I.A
Page 105: Spectral modifier Config I.B
Page 107: Spectral modifier Config I.C

Page 110: thick IVFS mockup (Japanese experiments only)
Page 111: heterogeneous IVFS mockup (for US experiments)
Page 112: homogeneous IVFS mockup (for US experiments)

Pages showing the removable radial shield configurations used only for the Japanese experiments:

119 120 123 126 127 128 131 134 135 136
137 138 139 140 143 146 147 148 149

Page 150: Config III.A (for US experiments)
Page 151: Config III.B (for US experiments)
Page 152: Config III.C (for US experiments)
Page 153: Config III.D (for US experiments)
Page 154: Config III.E (for US experiments)
Page 155: Config III.F (for US experiments)

PARTIAL LIST OF HANDOUTS TAKEN FROM VELM61 REPORT, ORNL/TM-10302:

Fig 13 from page 21: flux thru sodium when x-sects not weighted
Fig 15 from page 25: flux thru sodium when x-sects properly weighted

Table 5 from page 35: materials in VELM61 library that have been specially weighted for use in LMFBR Na-Fe shielding calculations

TENTATIVE TIMETABLE FOR IVFS ANALYSES (U.S. EXPERIMENTS ONLY):

Preliminary Work ..... March and April 1992

- Port VELM x-sects to workstation
- Port BSPREP & DISKTRAN to workstation
- Establish number densities for all materials
- Run GIP to get reference macro x-sects
- Finish scoping out all 2-D models & fix dimensions
- Run BSPREP to get boundary source

Complete first cut at 2-D analyses
for Configs I.A, I.B, and I.C ..... late Apr --> mid/late May 92

Complete first cut at 2-D analyses
for Configs III.B, C, D, E & F;
run DISKTRAN; and compare against
experiments ..... mid-May --> end of June 92

Convert DOTTOR code to workstation
and run it to get 3-D boundary flux;
also: start setting up 3-D TORT model
for Config III.A (and maybe III.B) ..... by end of July 1992

Finish up 3-D TORT analyses for US
experiments (Config III.A) ..... by end of Aug 1992

Complete first draft of report ..... by end of Sept 1992

INTERESTING EXPERIMENTAL OBSERVATIONS:

(1) Results for Config III.D (with B4C slab downstream of IVFS) can be compared with results for Config III.B (with nothing downstream of IVFS) to see how much attenuation is afforded by the B4C slab

	Bonner Balls				Fission Chambers	
	3"	5"	10"	12"	Bare	Cd-cov
III.B	5.72-0	1.96+1	9.83-0	5.54-0	1.71-2	1.42-2
III.D	8.18-1	6.43-0	4.29-0	2.50-0	1.23-3	1.08-3

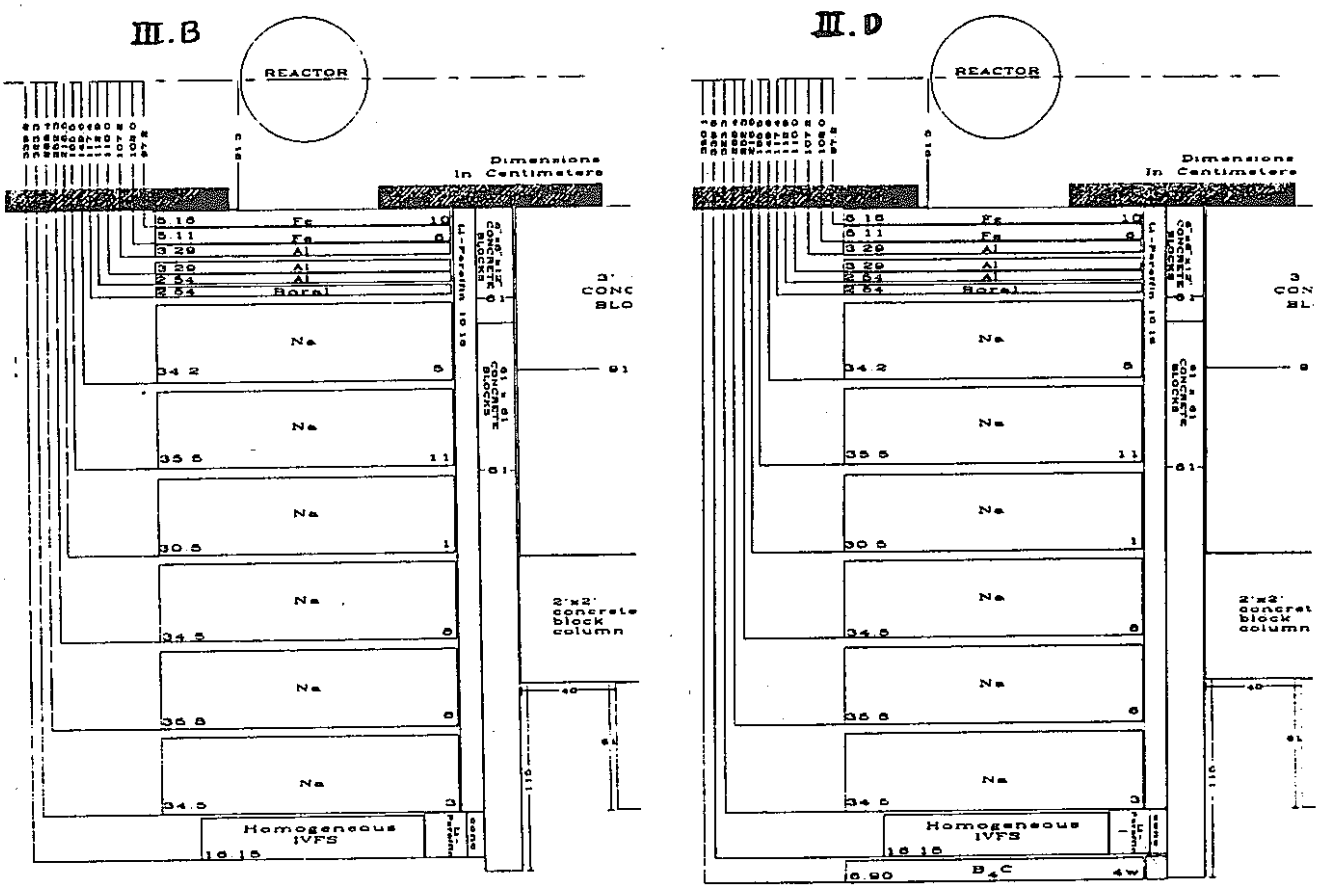

INTERESTING EXPERIMENTAL OBSERVATIONS (CONT):

(2) Config III.E (with B4C slab upstream of IVFS) should be, and is, a more effective shield than Config III.D (where the B4C slab is downstream of the IVFS)

	Bonner Balls				Fission Chambers	
	3"	5"	10"	12"	Bare	Cd-cov
III.D	8.18-1	6.43-0	4.29-0	2.50-0	1.23-3	1.08-3
III.E	1.28-1	5.34-1	1.88-1	9.94-2	2.45-4	1.63-4

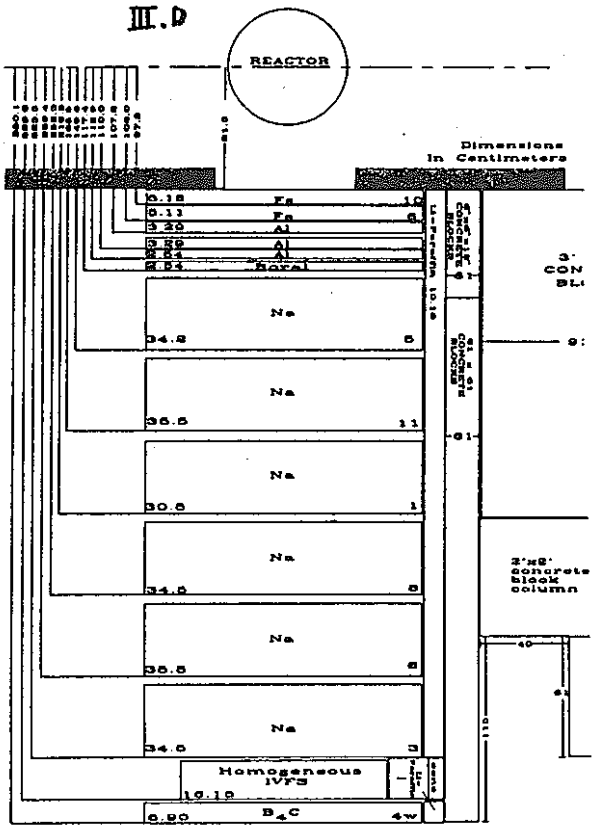

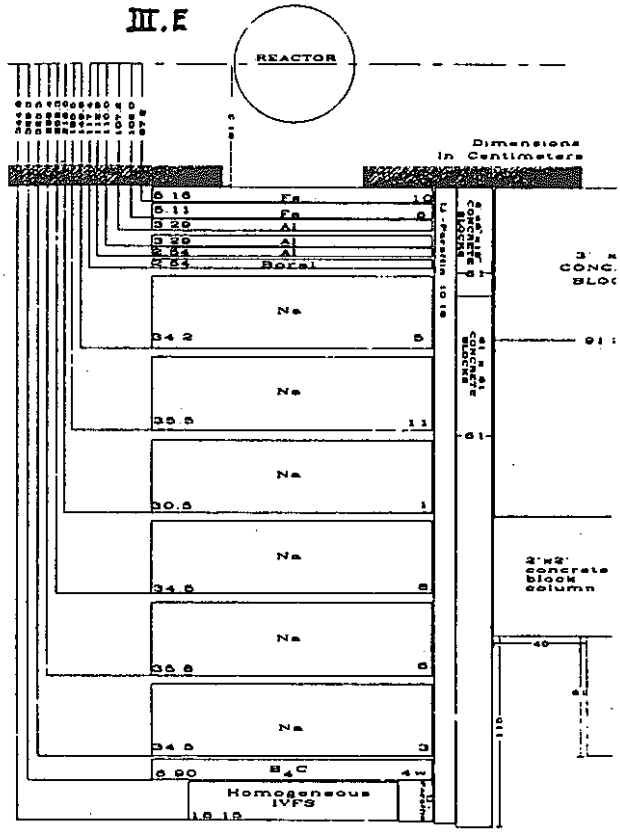

INTERESTING EXPERIMENTAL OBSERVATIONS (CONT):

(3) Results for Config III.F next to IVFS (with B4C slab further downstream) can be compared with results for Config III.B next to IVFS (with nothing downstream) to see how much the backscatter & reflection from the B4C slab will increase the flux next to IVFS

	Fission Chambers 0.7 cm past IVFS	
	Bare	Cd-cov
III.B	1.71-2	1.42-2
III.F	3.68-2	2.25-2

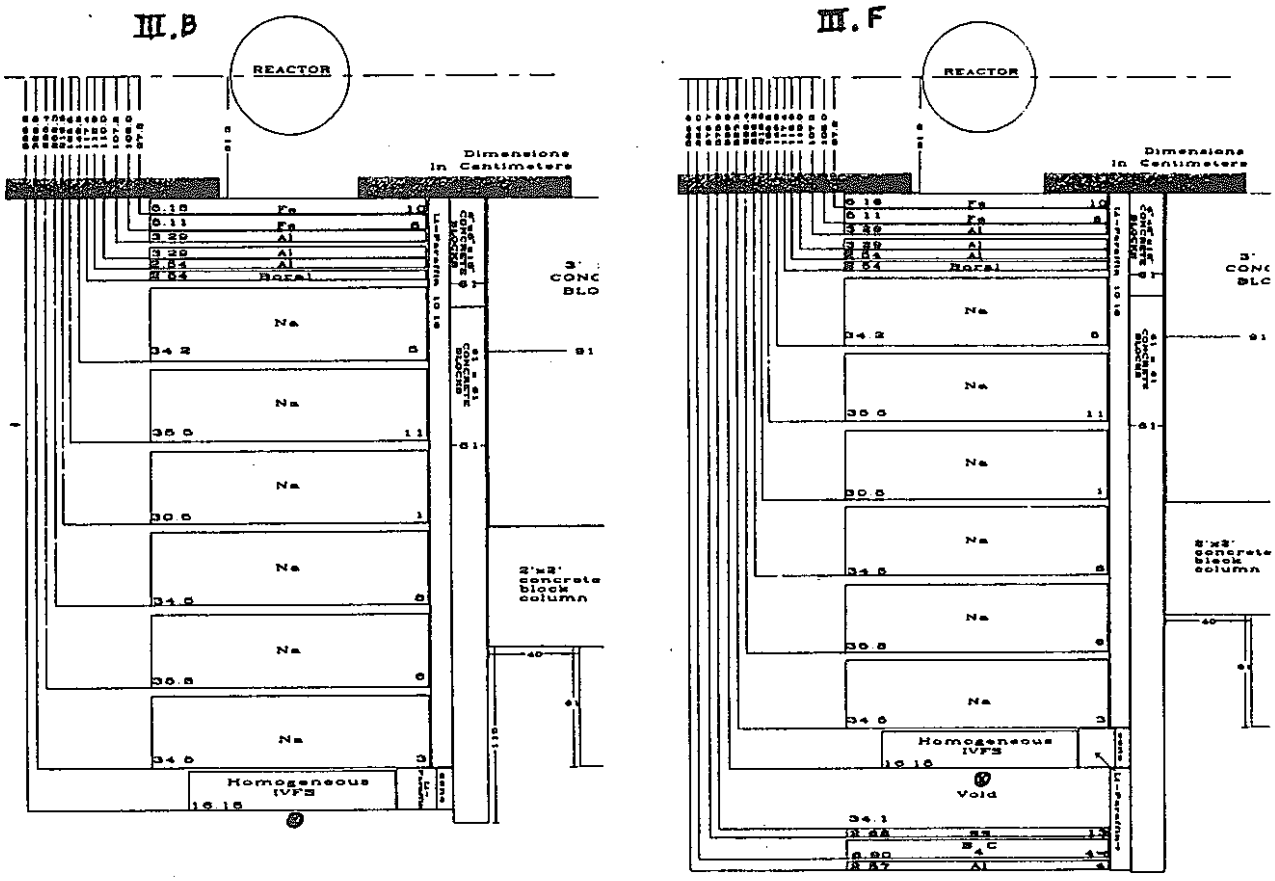

INTERESTING EXPERIMENTAL OBSERVATIONS (CONT):

(4) Results for Config III.A (with 3-region, heterogeneous IVFS) may be compared with results for Config III.B (with homogeneous IVFS) to see effect on fluxes downstream of the IVFS

	Bonner Balls 30 cm downstream				Bonner Balls 150 cm downstream			
	3"	5"	10"	12"	3"	5"	10"	12"
III.B (hom)	5.72-0	1.96+1	9.83-0	5.54-0	9.91-1	2.87-0	1.32-0	7.30-1
III.A (het)	8.86-0	2.28+1	8.71+0	4.78+0	1.47-0	3.44-0	1.19-0	6.24-1

Homog mockup yields thermal fluxes that are 1.55 times lower than heterog mockup
Homog mockup yields fast fluxes that are 1.16 times higher than heterog mockup

Suggests that credible results can probably be obtained with far simpler and less costly (homogeneous) 2-D analytic models if one is willing to apply these reasonable modest streaming correction factors.

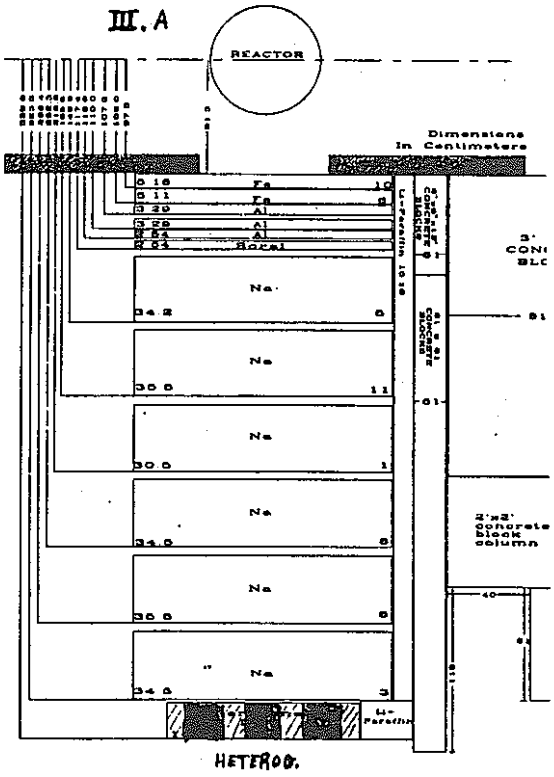

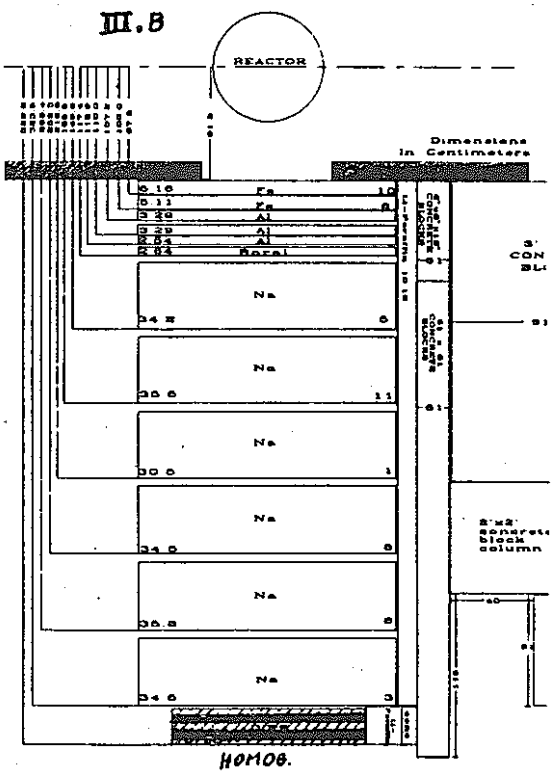

TECHNICAL CONCERNS/CONSIDERATIONS IN MODELING THESE EXPERIMENTS:

- III.A (heterogeneous IVFS) will require 3-D TORT analysis;
  III.B (homogeneous IVFS) may require 3-D TORT analysis

  -- These are needed to get flux traverses across face

  -- We will get boundary source from 2-D DORT analysis of III.B

  -- We may use DOTTOR code to translate boundary source or may have to write new DORT/TORT coupling code

- There is some concern about the modeling of streaming thru the 9 to 10 cm long fission gas plenum in the top of the SPERT fuel rods. This concern applies to all IVFS calcs.

- There is some concern over resonance self-shielding in the fuel rods. We have decided not to worry about this for now, and to simply use the VELM61 library "as is" to see how well that LMFBR shielding library does with no additional resonance self-shielding. (After all, that is one of the US objectives.)

- Attenuation through the 2 meters of sodium may require use of specially weighted Na cross sections in the VELM61 library. We plan to use these. (Pre-experimental analyses without any special weighting of the Na cross sections overestimated the flux downstream of the thick sodium spectral modifier by a factor of 3 according to Slater.)

- Bulging of the Na tanks (and the large 4 to 7 cm void between Na in adjacent tanks near the edges of the tanks) may significantly increase the transverse leakage of neutrons from the spectral modifier to the surrounding lithiated paraffin. To avoid overestimating the flux downstream of the spectral modifier, this transverse leakage must be represented correctly.

- Analytic results 150 cm downstream of the experimental configuration:

  -- should be calculated using the DISKTRAN code to integrate the boundary flux, thereby avoiding ray effects that might otherwise be present in the DORT results this far downstream in a void

  -- should only be compared against experimentally measured fluxes where the background radiation has been adequately shielded out; this may be difficult to do

CONCEPTUAL DRAWING OF SPERT FUEL PINS IN IVFS SLABS

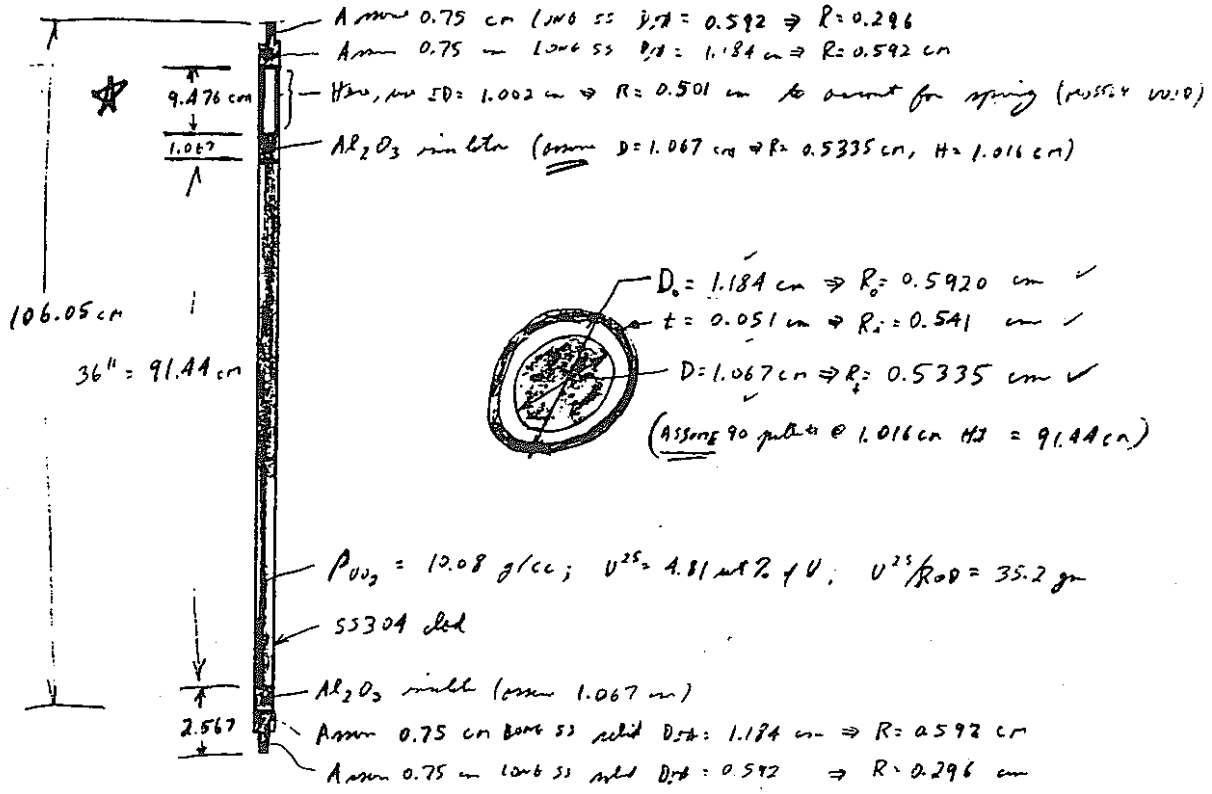

3-D TORT XYZ MODEL OF HOMOGENEOUS IVFS SLAB

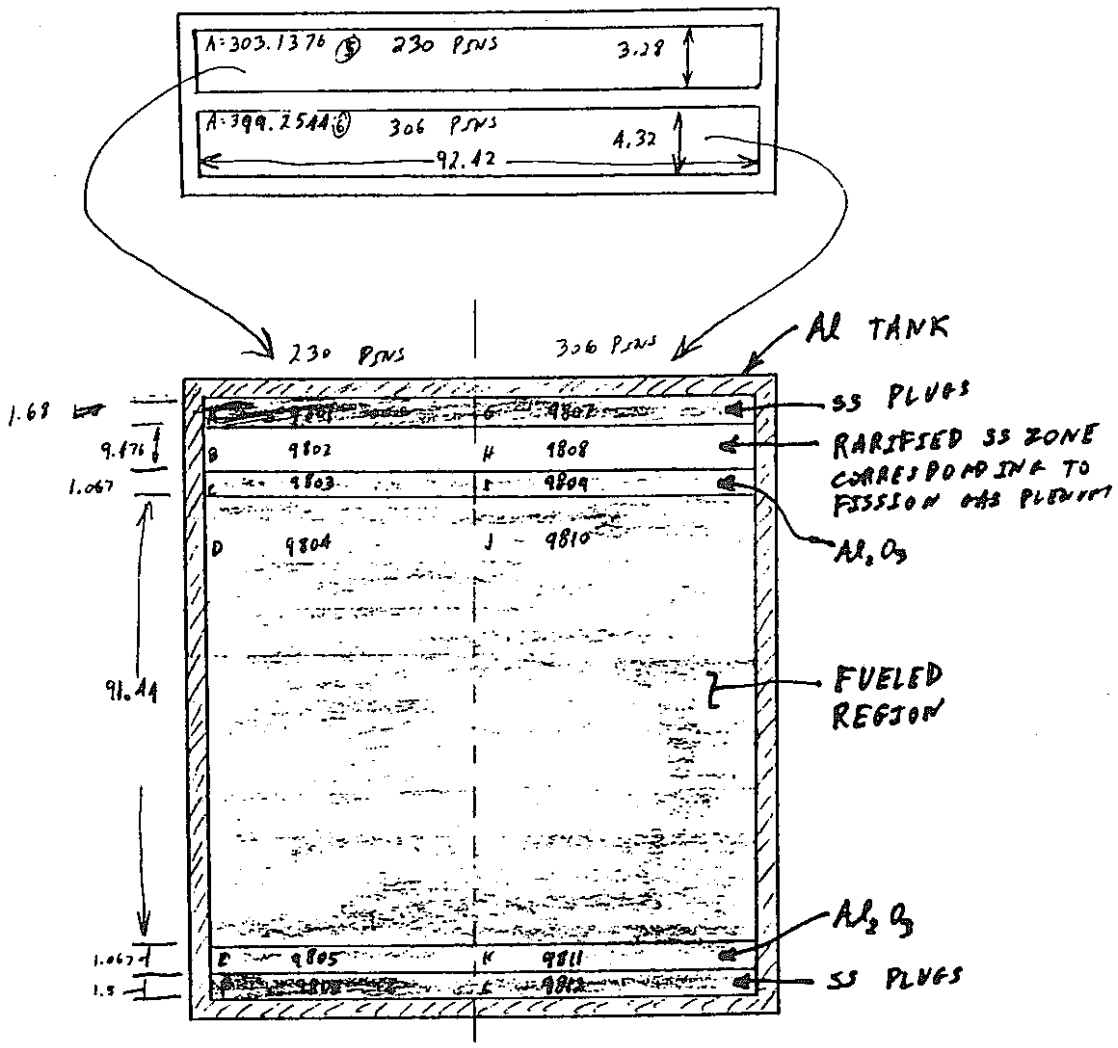

2-D RZ MODEL OF HOMOGENEOUS IVFS SLAB

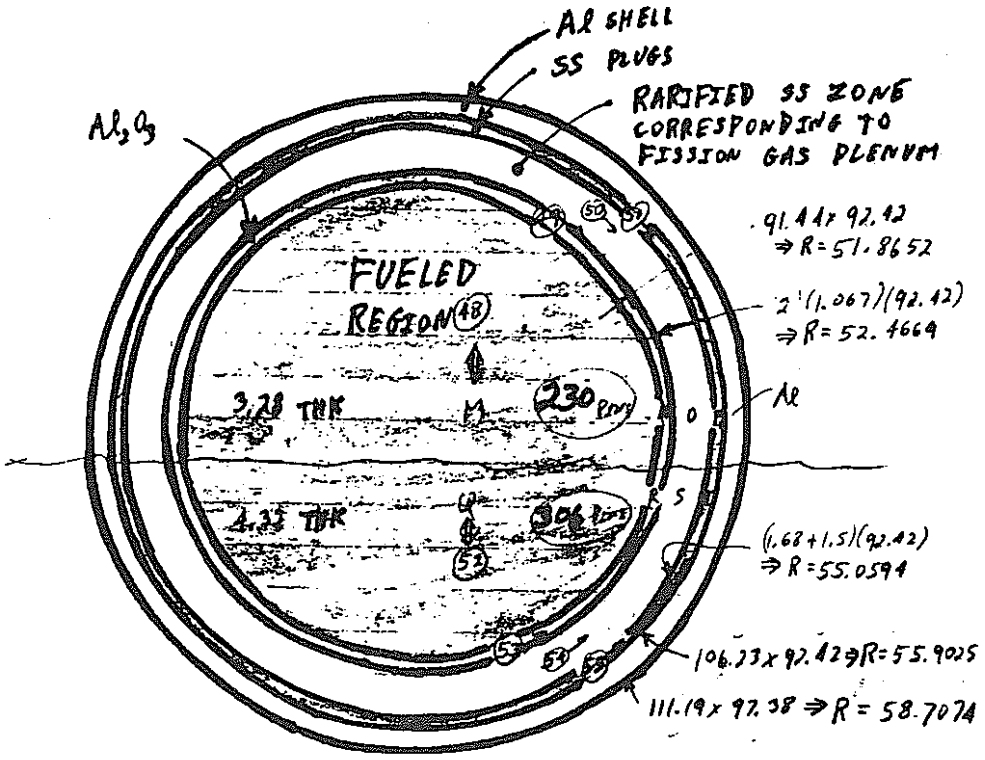

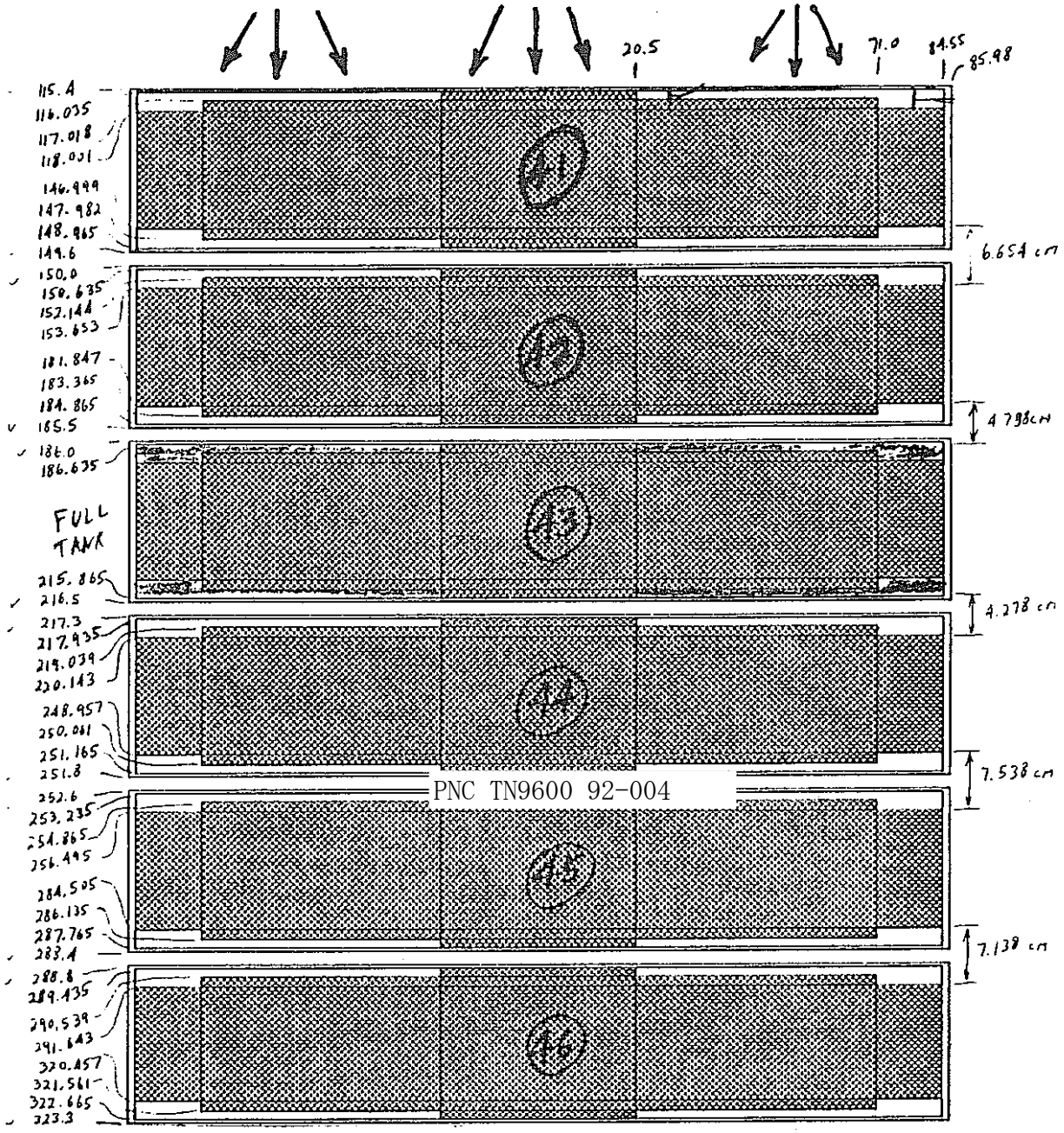

ASSUMED DISTRIBUTION OF SODIUM IN THE BULGED SODIUM TANKS. MODEL CONSERVES KNOWN (ORIGINAL) VOLUME AND PRESENT DIMENSIONS ALONG THE CENTERLINE.

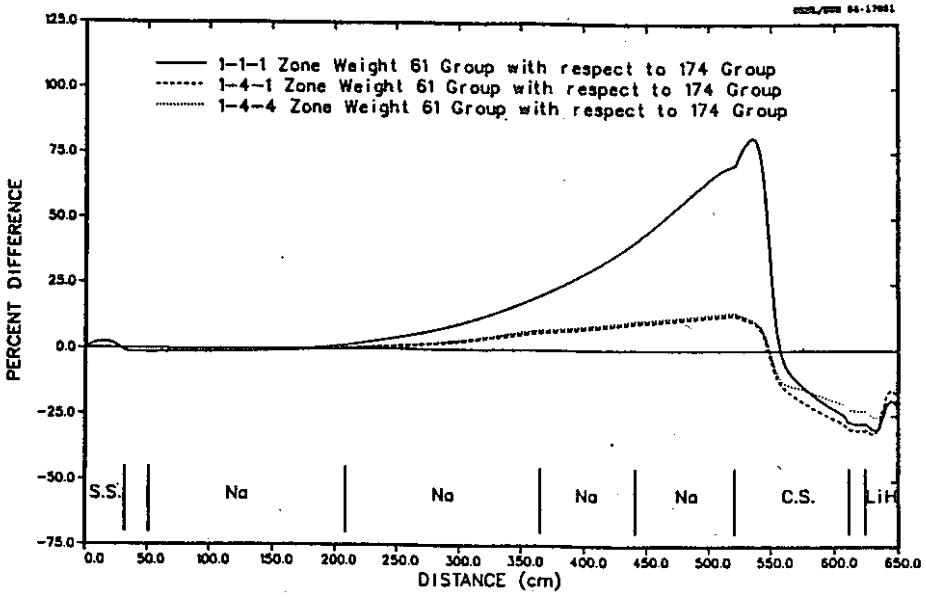

Fig. 13. Comparison of 4-in. Bonner ball responses calculated using fine-group cross sections and 61-group neutron cross sections collapsed using three different zone-averaged weighting functions.

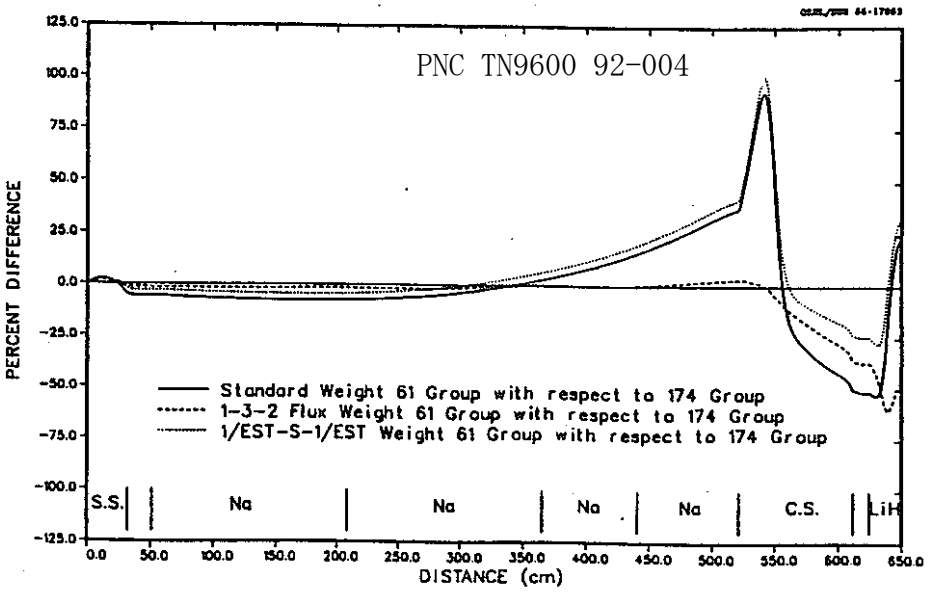

Fig. 15. Comparison of 4-in. Bonner ball responses calculated using fine-group cross sections and 61-group neutron cross sections collapsed using three final weighting functions.

Table 5. Materials in the VELM61 and VELM22 Libraries used in the Na-Fe Calculations

Material	ID (AMPX)	ID (ANISN)	Description
		(Standard Weighting, Self-Shielded)	
Fe	132611	501-506	
Cr	132411	507-512	Constituents of SS-304
Ni	132811	513-518	
Mn-55	132511	519-524	
Fe	132612	525-530	Constituents of Al
Al-27	131311	531-536	
H-1	9311	537-542	
O-16	127611	543-548	
Na-23	131111	549-554	Constituents of Na
Ca	132011	555-560	
K	115011	561-566	
Fe	132613	567-572	
Mn-55	132512	573-578	Constituents of Carbon Steel
C	130611	579-584	
H-1	9312	585-590	
Li-6	130311	591-596	Constituents of LiH
Li-7	139711	597-602	
		(Na-Fe Interval-Flux Weighting)[a]	
Fe	132621	603-608	
Cr	132421	609-614	Flux 3.8-cm into SS-304
Ni	132821	615-620	
Mn-55	132521	621-626	
Mo	132121	627-632	
Na	131121	633-638	Flux 76.2-cm into Na
Na	131122	639-644	Flux 228.6-cm into Na
Na	131123	645-650	Flux 381.0-cm into Na
Fe	132622	651-656	Flux 15.2-cm into Carbon Steel
Fe	132623	657-662	Flux 45.7-cm into Carbon Steel
		($1/E\Sigma_t$ Weighting)	
Fe	132631	663-668	
Cr	132431	669-674	
Ni	132831	675-680	$1/E\Sigma_t$(SS-304)
Mn-55	132531	681-686	
Mo	132131	687-692	
Fe	132632	693-698	$1/E\Sigma_t$ (Carbon Steel)

[a]Designated as the 1-3-2 flux weighting in Section II.4.

PARTIAL LIST OF HANDOUTS TAKEN FROM IVFS REPORT, ORNL/TM-11989:

Pages 31-40: IVFS program plan, describing all experiments

Page 104: Spectral modifier Config I.A
Page 105: Spectral modifier Config I.B
Page 107: Spectral modifier Config I.C

Page 110: thick IVFS mockup (Japanese experiments only)
Page 111: heterogeneous IVFS mockup (for US experiments)
Page 112: homogeneous IVFS mockup (for US experiments)

Pages showing the removable radial shield configurations used only for the Japanese experiments:

119 120 123 126 127 128 131 134 135 136
137 138 139 140 143 146 147 148 149

Page 150: Config III.A (for US experiments)
Page 151: Config III.B (for US experiments)
Page 152: Config III.C (for US experiments)
Page 153: Config III.D (for US experiments)
Page 154: Config III.E (for US experiments)
Page 155: Config III.F (for US experiments)

PARTIAL LIST OF HANDOUTS TAKEN FROM VELM61 REPORT, ORNL/TM-10302:

Fig 13 from page 21: flux thru sodium when x-sects not weighted
Fig 15 from page 25: flux thru sodium when x-sects properly weighted

Table 5 from page 35: materials in VELM61 library that have been specially weighted for use in LMFBR Na-Fe shielding calculations

APPENDIX A

EXPERIMENTAL PROGRAM PLAN FOR THE JASPER IN-VESSEL FUEL STORAGE (IVFS) EXPERIMENT

I. Spectrum Modifier (SM-0)
- A. SM-0 (10 cm Fe + 9 cm Al + 2.54 cm boral).
  1. NE 213 and hydrogen counter spectral measurements on centerline as close as feasible behind shield mockup
  2. 3-, 5-, and 10-in Bonner ball measurements on centerline at location of NE 213 measurements
  3. 3-, 4-, 5-, 8-, 10-, and 12-in Bonner ball measurements on centerline:
     a. 30 cm behind shield mockup
     b. 150 cm behind shield mockup (foreground and background)
  4. ^{235}U fission chamber (bare and Cd-covered) on centerline:
     a. 30 cm behind shield mockup
     b. 150 cm behind shield mockup (foreground and background)
- B. SM-1 (10 cm Fe + 9 cm Al + 2.54 cm boral + 20 cm radial blanket slabs)
  1. NE 213 and hydrogen counter spectral measurements on centerline as close as feasible behind shield mockup
  2. 3-, 5-, and 10-in Bonner ball measurements on centerline at location of NE 213 measurements
  3. 3-, 4-, 5-, 8-, 10-, and 12-in Bonner ball measurements on centerline:
     a. 30 cm behind shield mockup
     b. 150 cm behind shield mockup (foreground and background)
  4. ^{235}U fission chamber (bare and Cd-covered) on centerline:
     a. 30 cm behind shield mockup
     b. 150 cm behind shield mockup (foreground and background)
- C. SM-2 (10 cm Fe + 9 cm Al + 2.54 cm boral + 180 cm Na)
  1. NE 213 and hydrogen counter spectral measurements on centerline as close as feasible behind shield mockup
  2. 3-, 5-, and 10-in Bonner ball measurements on centerline at location of NE 213 measurements
  3. 3-, 4-, 5-, 8-, 10-, and 12-in Bonner ball measurements on centerline:
     a. 30 cm behind shield mockup
     b. 150 cm behind shield mockup (foreground and background)
  4. ^{235}U fission chamber on centerline:
     a. 0.7, 30, and 150 cm behind shield mockup (bare and Cd-covered detector)
     b. bare detector at 30 and 150 cm, cadmium over face of shield mockup
     c. bare detector with cadmium hut, 0.7 and 30 cm

II. Removable Radial Shield
- A. SM-1 + 1.3 cm Al + 15 cm SS + 1.3 cm Al + 10 cm C + 5 cm SS
  1. 3-, 4-, 5-, 8-, 10-, and 12-in Bonner ball measurements on centerline:
     a. 30 cm behind shield mockup

b. 150 cm behind shield mockup (foreground and background)

2. ^{235}U fission chamber on centerline:
   a. 30 cm behind shield mockup (bare and Cd-covered detector)
   b. 150 cm behind shield mockup (foreground and background), (bare and Cd-covered detector)
   c. bare detector at 150 cm, cadmium over face of shield mockup

B. SM-1 + 1.3 cm Al + 15 cm SS + 1.3 cm Al + 10 cm C + 5 cm SS + 1.3 cm Al + 10 cm C + 5 cm SS + 1.3 cm Al + 2.5 cm SS
   1. NE 213 and hydrogen counter spectrum measurements on centerline as close as feasible behind shield mockup (also background if necessary)
   2. 3-, 5-, and 10-in Bonner ball measurements on centerline at location of NE 213 measurements
   3. 3- and 10-in Bonner ball horizontal traverses at 30 cm behind shield mockup
   4. ^{235}U fission chamber horizontal traverses at 30 cm behind shield mockup
      a. bare detector
      b. Cd-covered detector
      c. bare detector, cadmium over face of shield mockup
   5. 3-, 4-, 5-, 8-, 10-, and 12-in Bonner ball measurements on centerline:
      a. 30 cm behind shield mockup
      b. 150 cm behind shield mockup (foreground and background)
   6. ^{235}U fission chamber measurements on centerline:
      a. 30 and 150 cm behind shield mockup (bare and Cd-covered detector)
      b. bare detector at 30 and 150 cm, cadmium over face of shield mockup

C. SM-1 + 1.3 cm Al + 15 cm SS + 1.3 cm Al + 10 cm C + 5 cm SS + 1.3 cm Al + 10 cm C + 5 cm SS + 1.3 cm Al + 2.5 cm SS + 18.3 cm thick IVFS vessel
   1. NE 213 and hydrogen counter spectrum measurements on centerline as close as feasible behind shield mockup (also background if necessary)
   2. 3-, 5-, and 10-in Bonner ball measurements on centerline at location of NE 213 measurements (also background if necessary)
   3. 3- and 10-in Bonner ball horizontal traverses at 30 cm behind shield mockup
   4. ^{235}U fission chamber horizontal traverses at 30 cm behind shield mockup
      a. bare detector
      b. Cd-covered detector
      c. bare detector, cadmium over face of shield mockup
   5. 3-, 4-, 5-, 8-, 10-, and 12-in Bonner ball measurements on centerline:
      a. 30 cm behind shield mockup
      b. 150 cm behind shield mockup (foreground and background)
   6. ^{235}U fission chamber measurements on centerline:
      a. 30 and 150 cm behind shield mockup (bare and Cd-covered

detector)
   b. bare detector at 30 and 150 cm, cadmium over face of shield mockup

D. SM-1 + 1.3 cm Al + 15 cm SS + 1.3 cm Al + 10 cm C + 5 cm SS + 1.3 cm Al + 10 cm C + 5 cm SS + 1.3 cm Al + 2.5 cm SS + 16.8 cm heterogeneous IVFS slab
   1. 3- and 10-in Bonner ball horizontal traverses at 30 cm behind shield mockup
   2. ^{235}U fission chamber horizontal traverses at 30 cm behind shield mockup
      a. bare detector
      b. Cd-covered detector
      c. bare detector, cadmium over face of shield mockup
   3. 3-, 4-, 5-, 8-, 10-, and 12-in Bonner ball measurements on centerline:
      a. 30 cm behind shield mockup
      b. 150 cm behind shield mockup (foreground and background)
   4. ^{235}U fission chamber measurements on centerline:
      a. 0.7, 30, and 150 cm behind shield mockup (bare and Cd-covered detector)
      b. bare detector at 30 and 150 cm, cadmium over face of shield mockup
      c. bare detector inside cadmium hut, 0.7 and 30 cm
      d. 0.7 cm, bare detector with cadmium wrapped around cylinder housing the detector

E. SM-1 + 1.3 cm Al + 15 cm SS + 1.3 cm Al + 10 cm C + 5 cm SS + 1.3 cm Al + 10 cm C + 5 cm SS + 1.3 cm Al + 2.5 cm SS + 16.15 cm homogeneous IVFS slab
   1. 3- and 10-in Bonner ball horizontal traverses at 30 cm behind shield mockup
   2. ^{235}U fission chamber horizontal traverses at 30 cm behind shield mockup
      a. bare detector
      b. Cd-covered detector
      c. bare detector, cadmium over face of shield mockup
   3. 3-, 4-, 5-, 8-, 10-, and 12-in Bonner ball measurements on centerline:
      a. 30 cm behind shield mockup
      b. 150 cm behind shield mockup (foreground and background)
   4. ^{235}U fission chamber measurements on centerline:
      a. 0.7, 30, and 150 cm behind shield mockup (bare and Cd-covered detector)
      b. bare detector at 30 and 150 cm, cadmium over face of shield mockup
      c. bare detector inside cadmium hut, 0.7 and 30 cm

F. SM-1 + 1.3 cm Al + 15 cm SS + 1.3 cm Al + 10 cm C + 5 cm SS + 1.3 cm Al + 10 cm C + 5 cm SS + 1.3 cm Al + 5 cm B_4C + 2.5 cm SS
   1. NE 213 and hydrogen counter spectrum measurements on centerline as close as feasible behind shield mockup
   2. 3-, 5-, and 10-in Bonner ball measurements on centerline at location

of NE 213 measurements

3. 3-, 4-, 5-, 8-, 10-, and 12-in Bonner ball measurements on centerline:
   a. 30 cm behind shield mockup
   b. 150 cm behind shield mockup (foreground and background)
4. ^{235}U fission chamber measurements on centerline:
   a. 30 and 150 cm behind shield mockup (bare and Cd-covered detector)
   b. bare detector at 30 and 150 cm, cadmium over face of shield mockup

G. SM-1 + 1.3 cm Al + 15 cm SS + 1.3 cm Al + 10 cm C + 5 cm SS + 1.3 cm Al + 10 cm C + 5 cm SS + 1.3 cm Al + 5 cm B_4C + 2.5 cm SS + 18.3 cm thick IVFS slab

1. NE 213 and hydrogen counter spectrum measurements on centerline as close as feasible behind shield mockup
2. 3-, 5-, and 10-in Bonner ball measurements on centerline at location of NE 213 measurements
3. 3-, 4-, 5-, 8-, 10-, and 12-in Bonner ball measurements on centerline:
   a. 30 cm behind shield mockup
   b. 150 cm behind shield mockup (foreground and background)]
4. ^{235}U fission chamber measurements on centerline:
   a. 30 and 150 cm behind shield mockup (bare and Cd-covered detector)
   b. bare detector at 30 and 150 cm, cadmium over face of shield mockup

H. SM-1 + 1.3 cm Al + 15 cm SS + 1.3 cm Al + 10 cm C + 5 cm SS + 1.3 cm Al + 10 cm C + 5 cm SS + 1.3 cm Al + 15 cm B_4C + 2.5 cm SS

1. 3- and 10-in Bonner ball horizontal traverses at 30 cm behind shield mockup
2. ^{235}U fission chamber horizontal traverses at 30 cm behind shield mockup
   a. bare detector
   b. Cd-covered detector
   c. bare detector, cadmium over face of shield mockup
3. 3-, 4-, 5-, 8-, 10-, and 12-in Bonner ball measurements on centerline:
   a. 30 cm behind shield mockup
   b. 150 cm behind shield mockup (foreground and background)
4. ^{235}U fission chamber measurements on centerline:
   a. 0.7, 30, and 150 cm behind shield mockup (bare and Cd-covered detector)
   b. bare detector at 30 and 150 cm, cadmium over face of shield mockup
   c. 0.7 and 30 cm, bare detector with cadmium wrapped around cylinder housing the detector

I. SM-1 + 1.3 cm Al + 15 cm SS + 1.3 cm Al + 10 cm C + 5 cm SS + 1.3 cm Al + 10 cm C + 5 cm SS + 1.3 cm Al + 15 cm B_4C + 2.5 cm SS + 18.3 cm thick IVFS slab

1. 3- and 10-in Bonner ball horizontal traverses at 30 cm behind shield mockup

2. ^{235}U fission chamber horizontal traverses at 30 cm behind shield mockup
   a. bare detector
   b. Cd-covered detector
   c. bare detector, cadmium over face of shield mockup
3. 3-, 4-, 5-, 8-, 10-, and 12-in Bonner ball measurements on centerline:
   a. 30 cm behind shield mockup
   b. 150 cm behind shield mockup (foreground and background)
4. ^{235}U fission chamber measurements on centerline:
   a. 0.7, 30, and 150 cm behind shield mockup (bare and Cd-covered detector)
   b. bare detector at 30 and 150 cm, cadmium over face of shield mockup
   c. 0.7 cm, bare detector with cadmium wrapped around cylinder housing the detector
   d. 0.7 and 30 cm, bare detector inside cadmium hut
5. Remove lithiated paraffin blocks from around fuel pins
   a. Repeat 3 and 4 above

J. SM-1 + 1.3 cm Al + 15 cm SS + 1.3 cm Al + 10 cm C + 5 cm SS + 1.3 cm Al + 10 cm C + 5 cm SS + 1.3 cm Al + 15 cm B_4C + 2.5 cm SS + 16.8 cm heterogeneous IVFS slab
1. 3- and 10-in Bonner ball horizontal traverses at 30 cm behind shield mockup
2. ^{235}U fission chamber horizontal traverses at 30 cm behind shield mockup
   a. bare detector
   b. Cd-covered detector
   c. bare detector, cadmium over face of shield mockup
3. 3-, 4-, 5-, 8-, 10-, and 12-in Bonner ball measurements on centerline:
   a. 30 cm behind shield mockup
   b. 150 cm behind shield mockup (foreground and background)
4. ^{235}U fission chamber measurements on centerline:
   a. 0.7, 30, and 150 cm behind shield mockup (bare and Cd-covered detector)
   b. bare detector at 30 and 150 cm, cadmium over face of shield mockup
   c. 0.7 and 30 cm, bare detector inside cadmium hut

K. SM-1 + 1.3 cm Al + 15 cm SS + 1.3 cm Al + 10 cm C + 5 cm SS + 1.3 cm Al + 10 cm C + 5 cm SS + 1.3 cm Al + 15 cm B_4C + 2.5 cm SS + 16.15 cm homogeneous IVFS slab
1. 3- and 10-in Bonner ball horizontal traverses at 30 cm behind shield mockup
2. ^{235}U fission chamber horizontal traverses at 30 cm behind shield mockup
   a. bare detector
   b. Cd-covered detector
   c. bare detector, cadmium over face of shield mockup
3. 3-, 4-, 5-, 8-, 10-, and 12-in Bonner ball measurements on centerline:

a. 30 cm behind shield mockup
b. 150 cm behind shield mockup (foreground and background)

4. ^{235}U fission chamber measurements on centerline:
   a. 0.7, 30, and 150 cm behind shield mockup (bare and Cd-covered detector)
   b. bare detector at 30 and 150 cm, cadmium over face of shield mockup
   c. 0.7 and 30 cm, bare detector inside cadmium hut

L. SM-1 + 1.3 cm Al + 15 cm SS + 1.3 cm Al + 10 cm C + 5 cm SS + 1.3 cm Al + 10 cm C + 5 cm SS + 1.3 cm Al + 15 cm B_4C + 2.5 cm SS + 10 cm radial blanket

1. 3- and 10-in Bonner ball horizontal traverses at 30 cm behind shield mockup
2. ^{235}U fission chamber horizontal traverses at 30 cm behind shield mockup
   a. bare detector
   b. Cd-covered detector
   c. bare detector, cadmium over face of shield mockup
3. 3-, 4-, 5-, 8-, 10-, and 12-in Bonner ball measurements on centerline:
   a. 30 cm behind shield mockup
   b. 150 cm behind shield mockup (foreground and background)
4. ^{235}U fission chamber measurements on centerline:
   a. 0.7, 30, and 150 cm behind shield mockup (bare and Cd-covered detector)
   b. bare detector at 30 and 150 cm, cadmium over face of shield mockup
   c. 0.7 cm, bare detector with cadmium wrapped around cylinder housing the detector
   d. 0.7 and 30 cm, bare detector inside cadmium hut

M. SM-1 + 1.3 cm Al + 15 cm SS + 1.3 cm Al + 15 cm B_4C + 2.5 cm SS + 1.3 cm Al + 15 cm B_4C + 1.3 cm Al + 15 cm B_4C (Loop-type mockup)

1. ^{235}U fission chamber horizontal traverses at 30 cm behind shield mockup
   a. bare detector
   b. Cd-covered detector
   c. bare detector, cadmium over face of shield mockup
2. 3-, 4-, 5-, 8-, 10-, and 12-in Bonner ball measurements on centerline:
   a. 30 cm behind shield mockup
   b. 150 cm behind shield mockup (foreground and background)
3. ^{235}U fission chamber measurements on centerline:
   a. 0.7, 30, and 150 cm behind shield mockup (bare and Cd-covered detector)
   b. bare detector at 30 and 150 cm, cadmium over face of shield mockup
   c. 0.7 cm, bare detector with cadmium wrapped around cylinder housing the detector
   d. 0.7 and 30 cm, bare detector inside cadmium hut

N. SM-1 + 1.3 cm Al + 15 cm SS + 1.3 cm Al + 15 cm B_4C + 2.54 cm SS +

1.3 cm Al + 15 cm B_4C + 1.3 cm Al + 15 cm B_4C + 18.3-cm-thick IVFS slab (Loop-type mockup)

1. NE 213 and hydrogen counter spectrum measurements on centerline as close as feasible behind shield mockup (also background if necessary)
2. 3-, 5-, and 10-in Bonner ball measurements on centerline at location of NE 213 measurements.
3. 3- and 10-in Bonner ball horizontal traverses at 30 cm behind shield mockup.
4. ^{235}U fission chamber horizontal traverses at 30 cm behind shield mockup
   a. bare detector
   b. Cd-covered detector
   c. bare detector, cadmium over face of shield mockup
5. 3-, 4-, 5-, 8-, 10-, and 12-in Bonner ball measurements on centerline:
   a. 30 cm behind shield mockup
   b. 150 cm behind shield mockup (foreground and background)
6. ^{235}U fission chamber measurements on centerline:
   a. 0.7, 30, and 150 cm behind shield mockup (bare and Cd-covered detector)
   b. bare detector at 30 and 150 cm, cadmium over face of shield mockup
   c. 0.7 cm, bare detector with cadmium wrapped around cylinder housing the detector
   d. 0.7 and 30 cm, bare detector inside cadmium hut

O. SM-1 + 1.3 cm Al + 15 cm SS + 1.3 cm Al + 15 cm B_4C + 2.54 cm SS + 1.3 cm Al + 15 cm B_4C + 1.3 cm Al + 15 cm B_4C + 16.8 cm heterogeneous IVFS slab (Loop-type mockup)

1. NE 213 and hydrogen counter spectrum measurements on centerline as close as feasible behind shield mockup (also background if necessary)
2. 3-, 5-, and 10-in Bonner ball measurements on centerline at location of NE 213 measurements.
3. 3- and 10-in Bonner ball horizontal traverses at 30 cm behind shield mockup.
4. ^{235}U fission chamber horizontal traverses at 30 cm behind shield mockup
   a. bare detector
   b. Cd-covered detector
   c. bare detector, cadmium over face of shield mockup
5. 3-, 4-, 5-, 8-, 10-, and 12-in Bonner ball measurements on centerline:
   a. 30 cm behind shield mockup
   b. 150 cm behind shield mockup (foreground and background)
6. ^{235}U fission chamber measurements on centerline:
   a. 0.7, 30, and 150 cm behind shield mockup (bare and Cd-covered detector)
   b. bare detector at 30 and 150 cm, cadmium over face of shield mockup

c. 0.7 cm, bare detector with cadmium wrapped around cylinder housing the detector
d. 0.7 and 30 cm, bare detector inside cadmium hut

P. SM-1 + 1.3 cm Al + 15 cm SS + 1.3 cm Al + 10 cm C + 5 cm SS + 1.3 cm Al + 10 cm C + 5 cm SS + 1.3 cm Al + 15 cm B_4C + 2.5 cm SS + 18.3-cm-thick IVFS slab + void + 2.5 cm Al + 5 cm SS + 20 cm B_4C

1. 3-, 4-, 5-, 8-, 10-, and 12-in Bonner ball measurements on centerline:
   a. 30 cm behind shield mockup
   b. 150 cm behind shield mockup (foreground and background)
2. ^{235}U fission chamber measurements on centerline:
   a. 0.7, 30, and 150 cm behind shield mockup (bare and Cd-covered detector)
   b. bare detector at 30 and 150 cm, cadmium over face of shield mockup
   c. 0.7 cm, bare detector with cadmium wrapped around cylinder housing the detector
   d. 0.7 and 30 cm, bare detector inside cadmium hut
3. ^{235}U fission chamber measurements on centerline in the void:
   a. bare detector
   b. Cd-covered detector
   c. bare detector with cadmium wrapped around the detector's cylindrical housing

Q. SM-1 + 1.3 cm Al + 15 cm SS + 1.3 cm Al + 10 cm C + 5 cm SS + 1.3 cm Al + 10 cm C + 5 cm SS + 1.3 cm Al + 15 cm B_4C + 2.5 cm SS + 18.3-cm-thick IVFS slab + void + 2.5 cm Al + 5 cm SS + 1.3 cm Al + 10 cm C + 5 cm SS + 1.3 cm Al + 10 cm C + 5 cm SS + 1.3 cm Al + 10 cm C + 5 cm SS

1. 3-, 4-, 5-, 8-, 10-, and 12-in Bonner ball measurements on centerline:
   a. 30 cm behind shield mockup
   b. 150 cm behind shield mockup (foreground and background)
2. ^{235}U fission chamber measurements on centerline:
   a. 0.7, 30, and 150 cm behind shield mockup (bare and Cd-covered detector)
   b. bare detector at 30 and 150 cm, cadmium over face of shield mockup
   c. 0.7 cm, bare detector with cadmium wrapped around cylinder housing the detector
   d. 0.7 and 30 cm, bare detector inside cadmium hut
3. ^{235}U fission chamber measurements on centerline in the void:
   a. bare detector
   b. Cd-covered detector
   c. bare detector, with cadmium wrapped around the detector's cylindrical housing

III. Above-Core (ALMR)

A. SM-2 + 16.8 cm heterogeneous IVFS slab

1. 3-, 4-, 5-, 8-, 10-, and 12-in Bonner ball measurements on centerline:
   a. 30 cm behind shield mockup

b. 150 cm behind shield mockup (foreground and background)

2. 3- and 10-in Bonner ball horizontal traverses at 30 cm behind shield mockup
3. ^{235}U fission chamber measurements on centerline:
   a. 0.7, 30, and 150 cm behind shield mockup (bare and Cd-covered detector)
   b. bare detector at 30 and 150 cm, cadmium over face of shield mockup
   c. 0.7 and 30 cm, bare detector inside Cd hut
4. ^{235}U fission chamber horizontal traverses at 30 cm behind shield mockup:
   a. bare detector
   b. Cd-covered detector
   c. bare detector, cadmium over face of shield mockup

B. SM-2 + 16.15 cm homogeneous IVFS slab
1. 3-, 4-, 5-, 8-, 10-, and 12-in Bonner ball measurements on centerline:
   a. 30 cm behind shield mockup
   b. 150 cm behind shield mockup (foreground and background)
2. 3- and 10-in Bonner ball horizontal traverses at 30 cm behind shield mockups
3. ^{235}U fission chamber measurements on centerline:
   a. 0.7, 30, and 150 cm behind shield mockup (bare and Cd-covered detector)
   b. bare detector at 30 and 150 cm, cadmium over face of shield mockup
   c. 0.7 and 30 cm, bare detector inside Cd hut
4. ^{235}U fission chamber horizontal traverses at 30 cm behind shield mockup:
   a. bare detector
   b. Cd-covered detector
   c. bare detector, cadmium over face of shield mockup

C. SM-2 + 10 cm radial blanket
1. 3-, 4-, 5-, 8-, 10, and 12-in Bonner ball measurements on centerline:
   a. 30 cm behind shield mockup
   b. 150 cm behind shield mockup (foreground and background)
2. ^{235}U fission chamber measurements on centerline:
   a. 0.7, 30, and 150 cm behind shield mockup (bare and Cd-covered detector)
   b. bare detector at 30 and 150 cm, cadmium over face of shield mockup
   c. 0.7 and 30 cm, bare detector inside Cd hut

D. SM-2 + 16.15 cm homogeneous IVFS slab + 5 cm B_4C
1. 3-, 4-, 5-, 8-, 10, and 12-in Bonner ball measurements on centerline:
   a. 30 cm behind shield mockup
   b. 150 cm behind shield mockup (foreground and background)
2. ^{235}U fission chamber measurements on centerline:
   a. 0.7, 30, and 150 cm behind shield mockup (bare and Cd-covered detector)

b. bare detector at 30 and 150 cm, cadmium over face of shield mockup
c. 0.7 and 30 cm, bare detector inside Cd hut

E. SM-2 + 5 cm B_4C + 16.15 cm homogeneous IVFS slab
1. 3-, 4-, 5-, 8-, 10, and 12-in Bonner ball measurements on centerline:
a. 30 cm behind shield mockup
b. 150 cm behind shield mockup (foreground and background)
2. ^{235}U fission chamber measurements on centerline:
a. 0.7, 30, and 150 cm behind shield mockup (bare and Cd-covered detector)
b. bare detector at 30 and 150 cm, cadmium over face of shield mockup
c. 0.7 and 30 cm, bare detector inside Cd hut

F. SM-2 + 16.15 cm homogeneous IVFS slab + void + 2.5 cm SS + 5.15 cm B_4C + 2.5 cm Al
1. 3-, 4-, 5-, 8-, 10-, and 12-in Bonner ball measurements on centerline:
a. 30 cm behind shield mockup
b. 150 cm behind shield mockup (foreground and background)
2. ^{235}U fission chamber measurements on centerline:
a. 0.7, 30, and 150 cm behind shield mockup (bare and Cd-covered detector)
b. bare detector at 30 and 150 cm, cadmium over face of shield mockup
c. 0.7 and 30 cm, bare detector inside Cd hut
3. ^{235}U fission chamber measurements on centerline in the void:
a. bare detector
b. Cd-covered detector

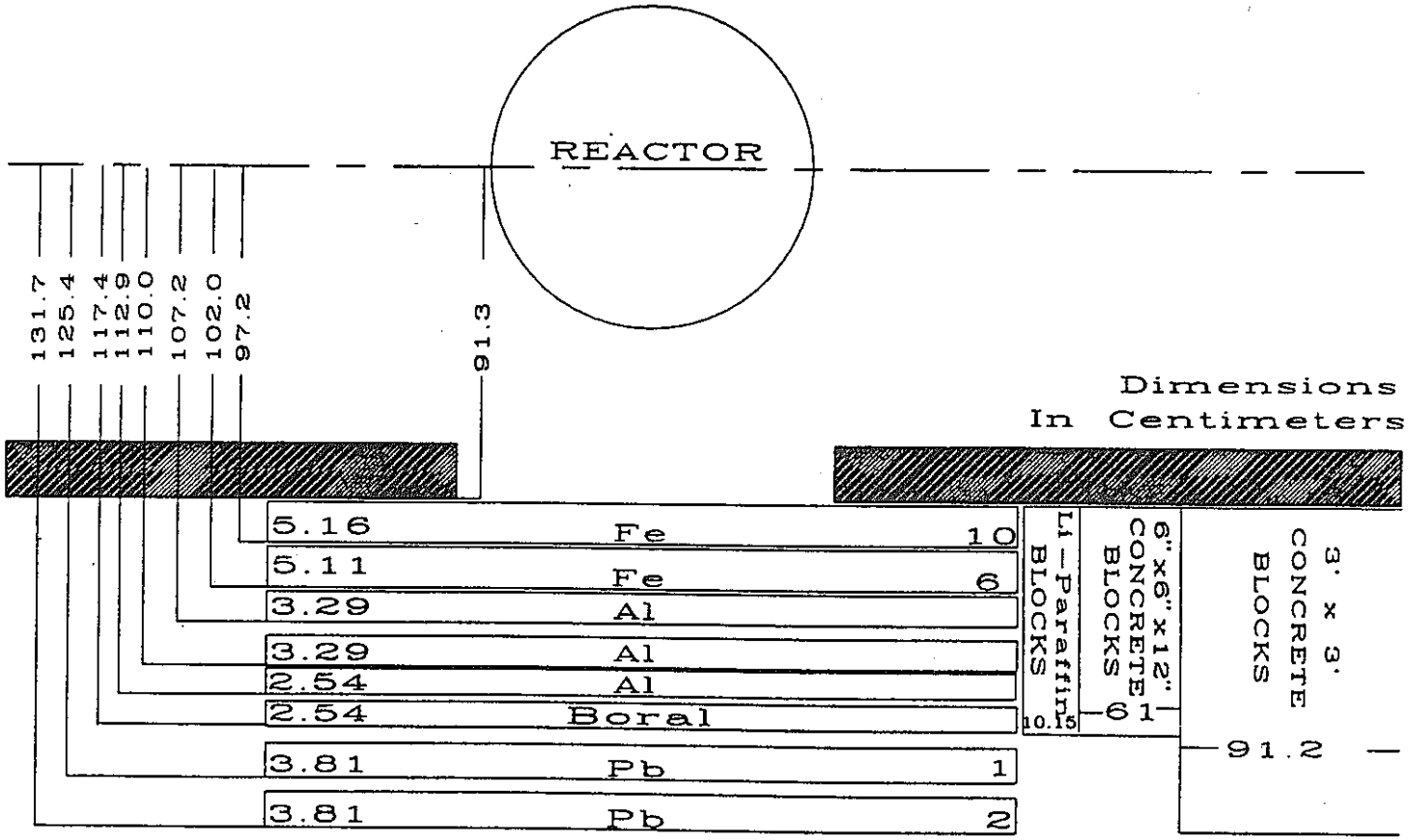

Figure 2. Schematic of SM-0 (Fe + Al + Boral) Item IA plus lead.

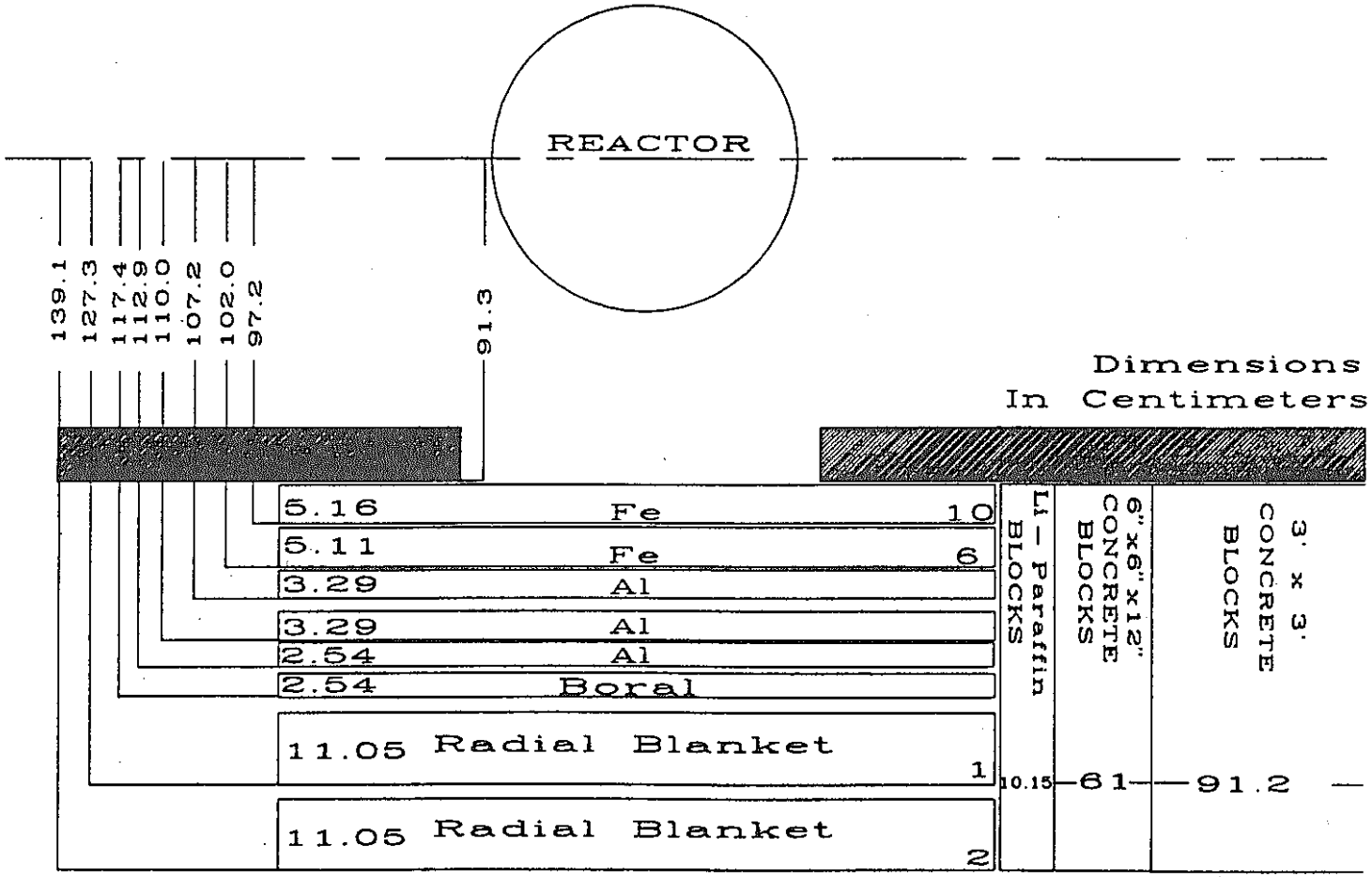

Figure 3. Schematic of SM-1 (Fe + Al + Boral + radial blankets) Item IB.

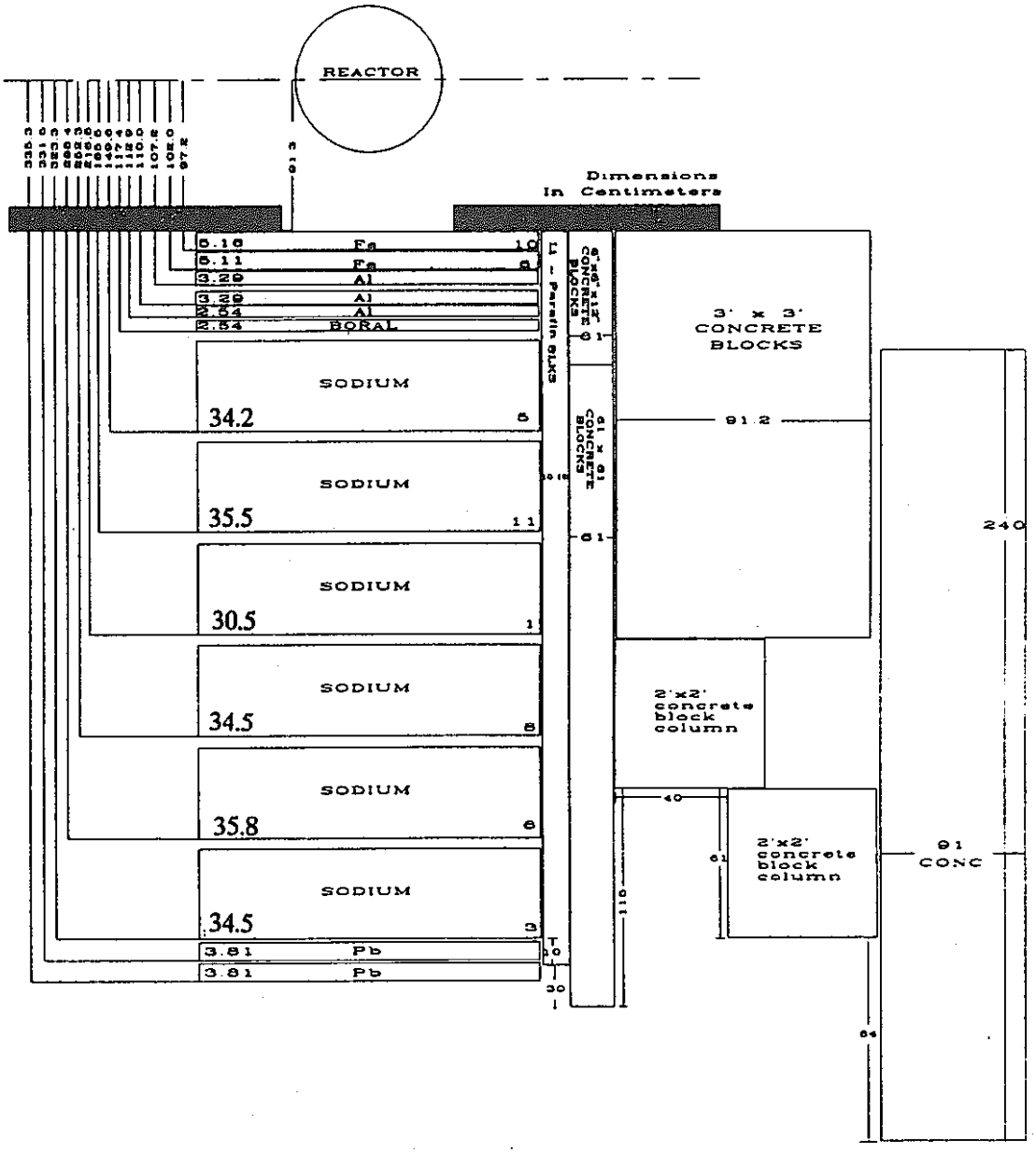

Figure 5. Schematic of SM-2 (Fe + Al + Boral + sodium) plus lead.

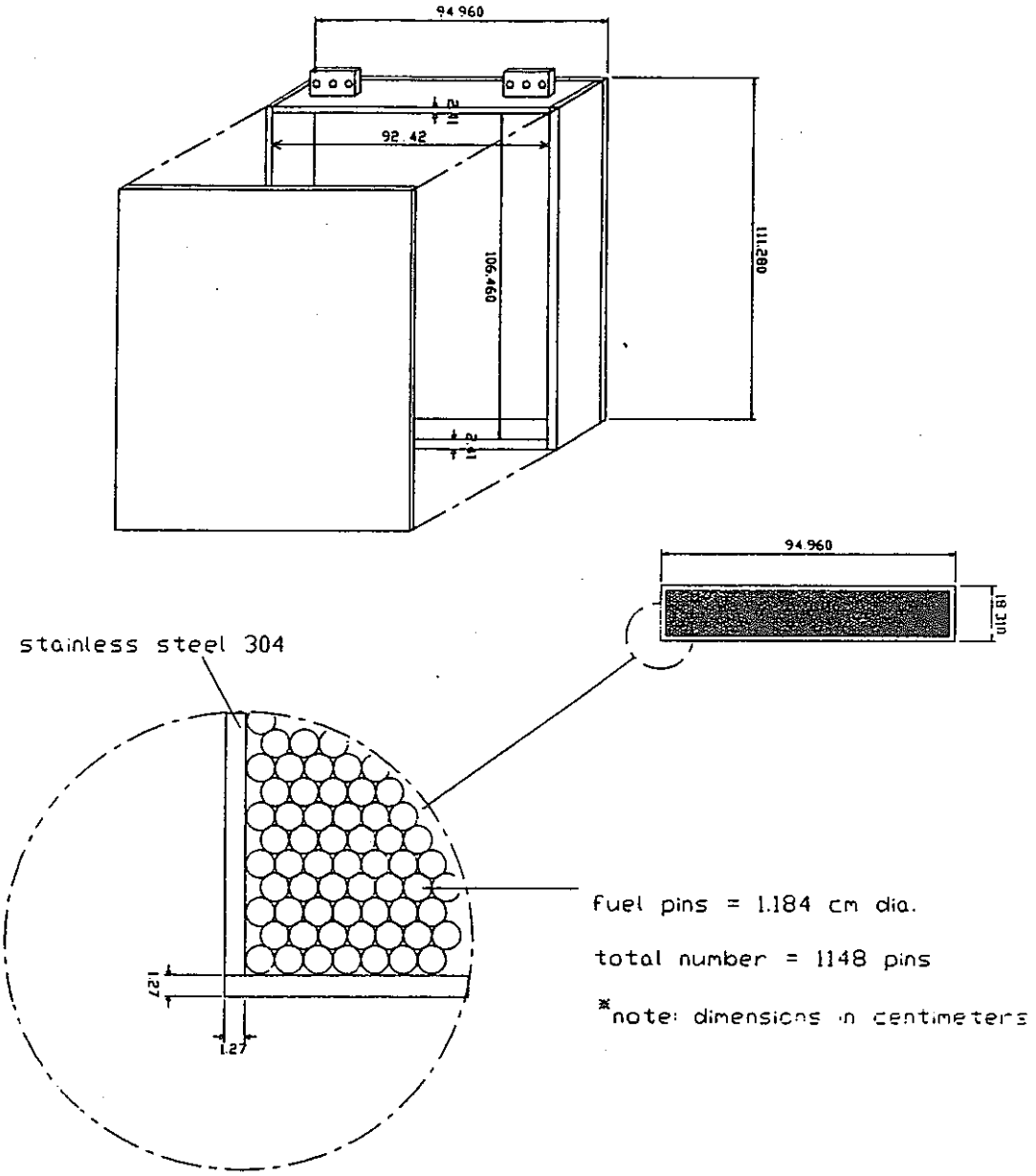

Figure 8. Schematic of thick IVFS mockup (slab #1).

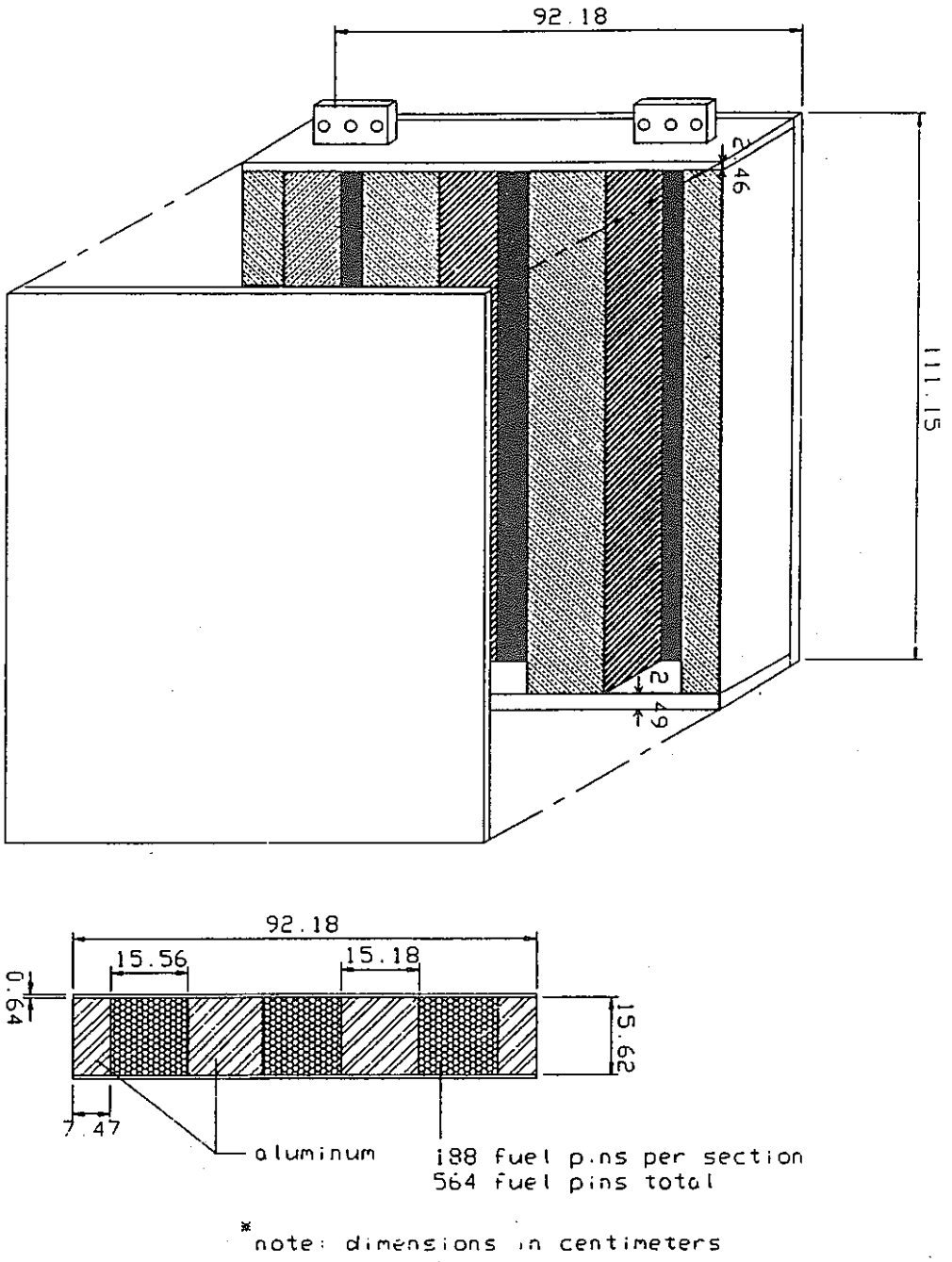

Figure 9. Schematic of heterogeneous IVFS mockup (slab #2).

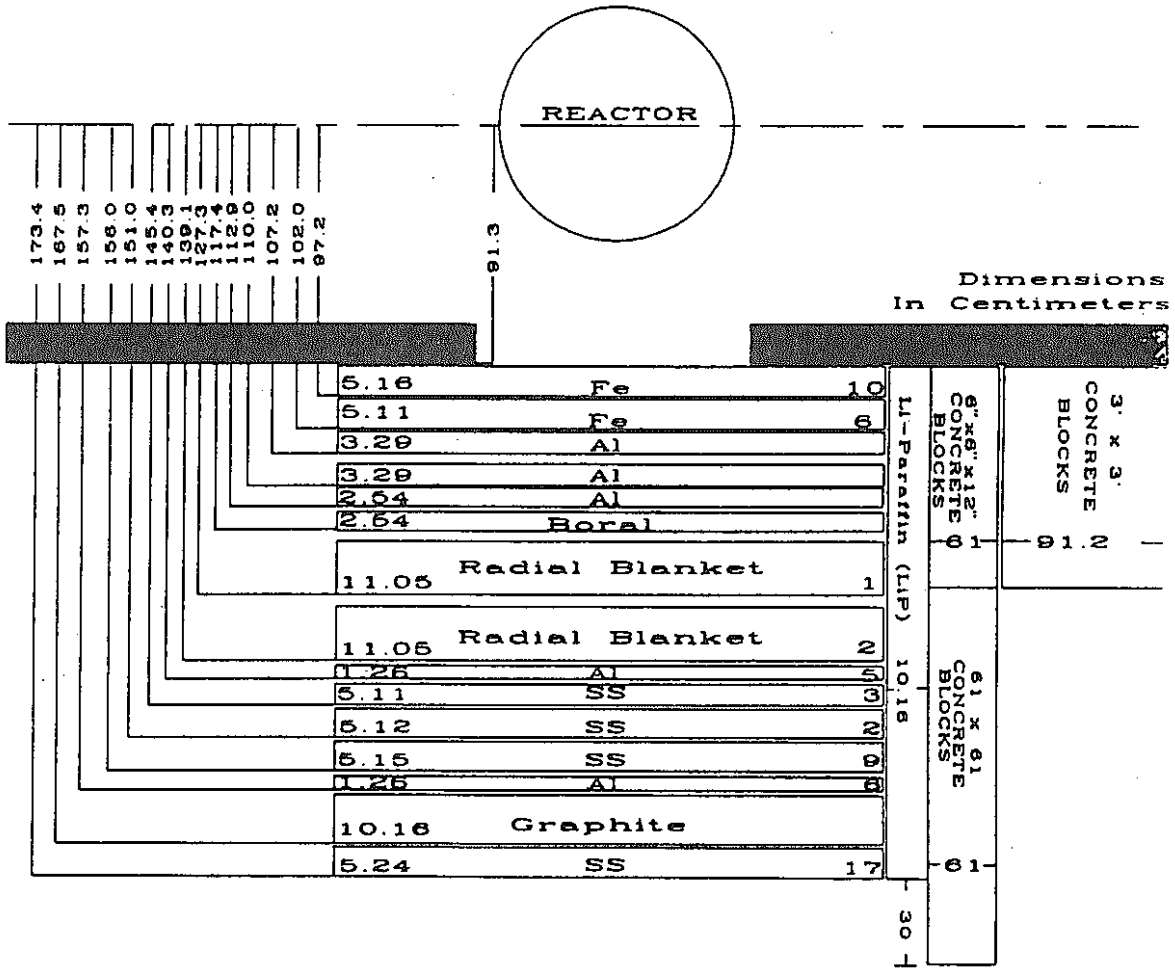

Figure 17. Schematic of SM-1 plus shield configuration for Item IIA.

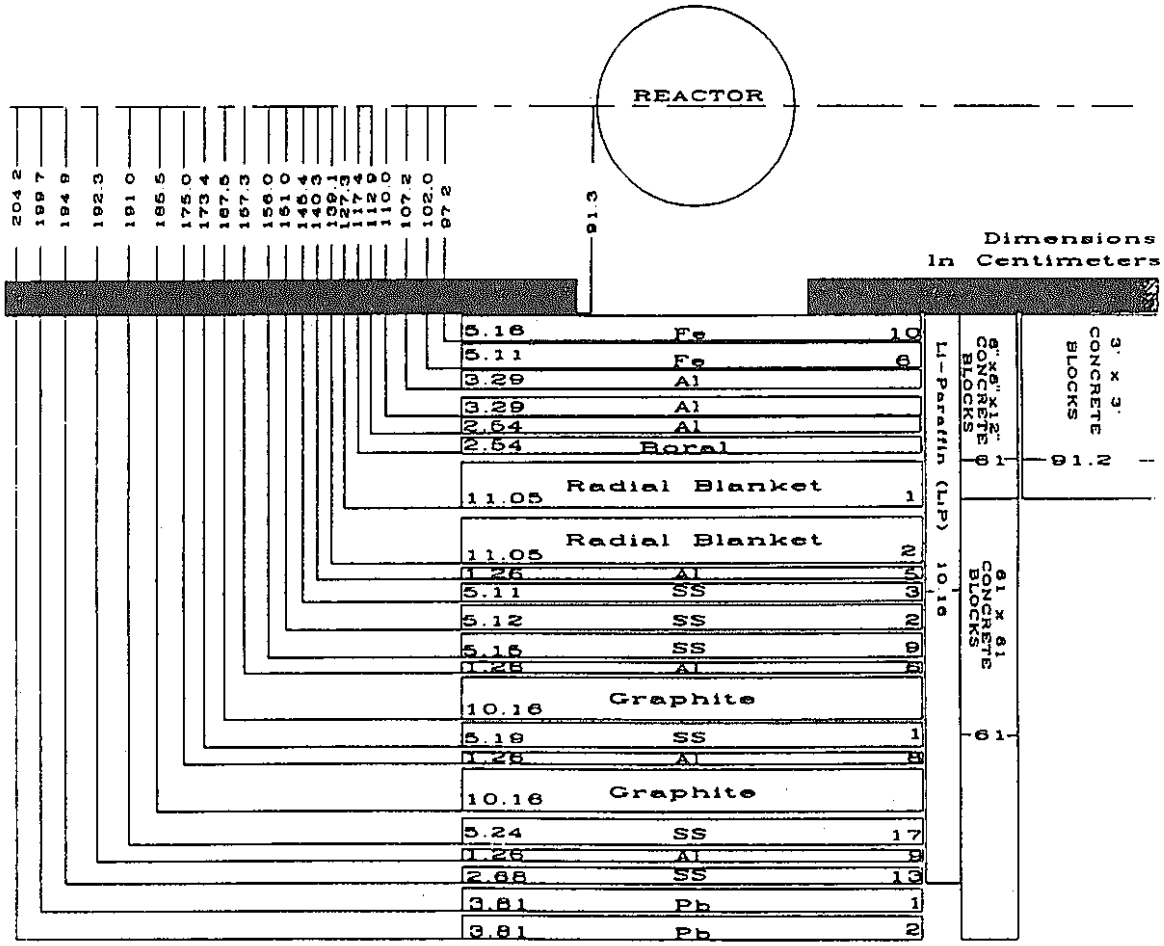

Figure 18. Schematic of SM-1 plus shield configuration for Item IIB plus lead.

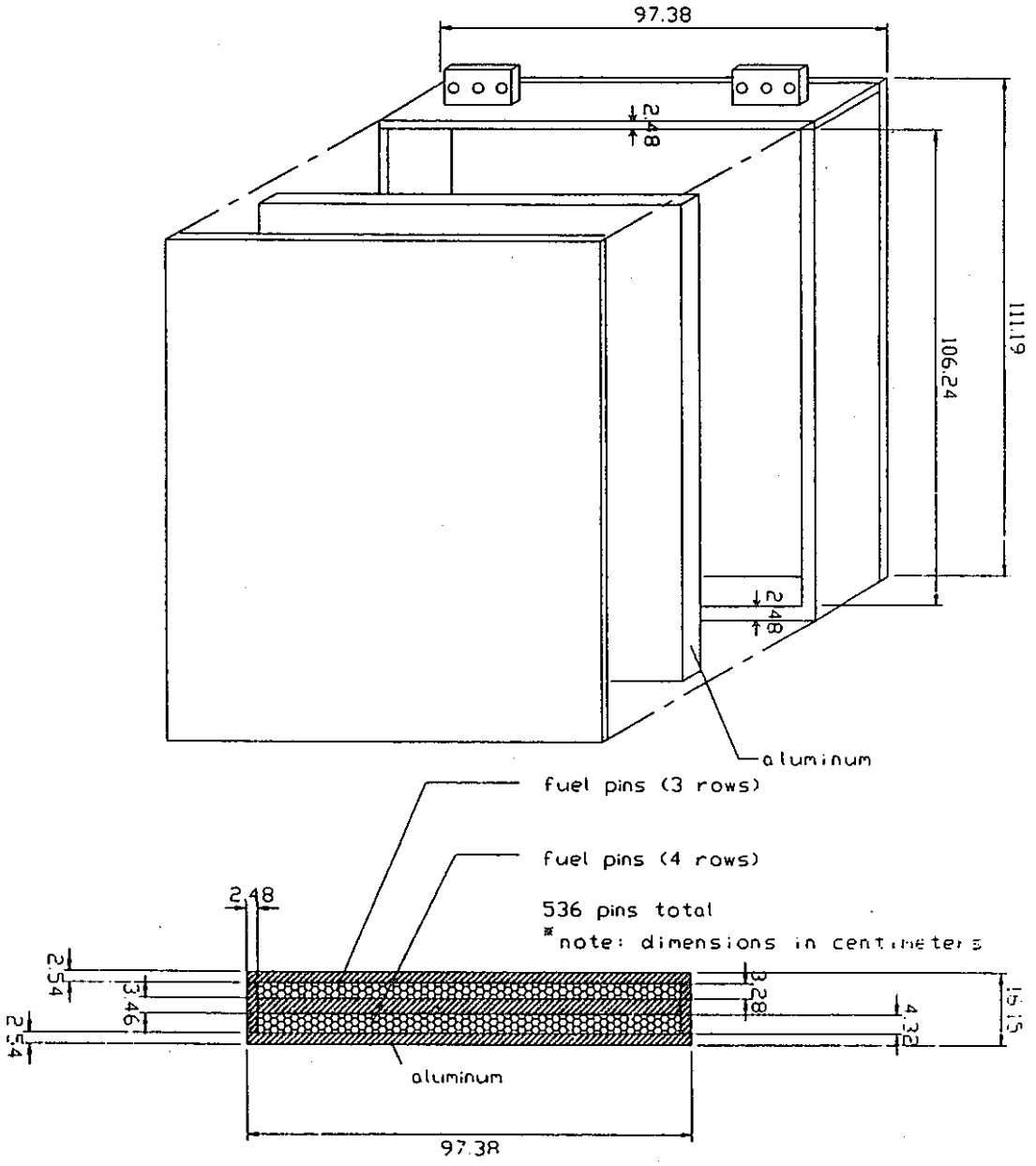

Figure 10. Schematic of homogeneous IVFS mockup (slab #3).

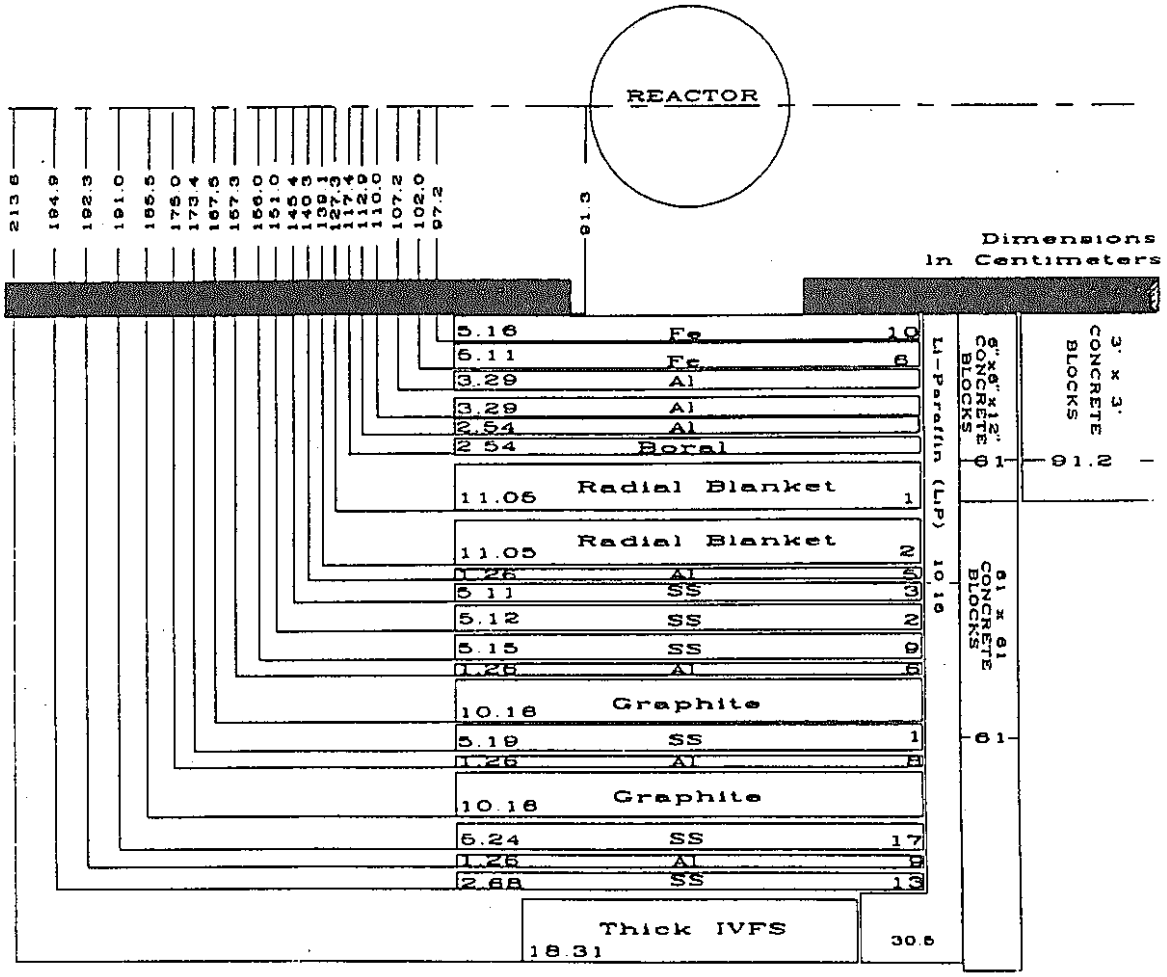

Figure 21. Schematic of SM-1 plus shield configuration for Item IIC.

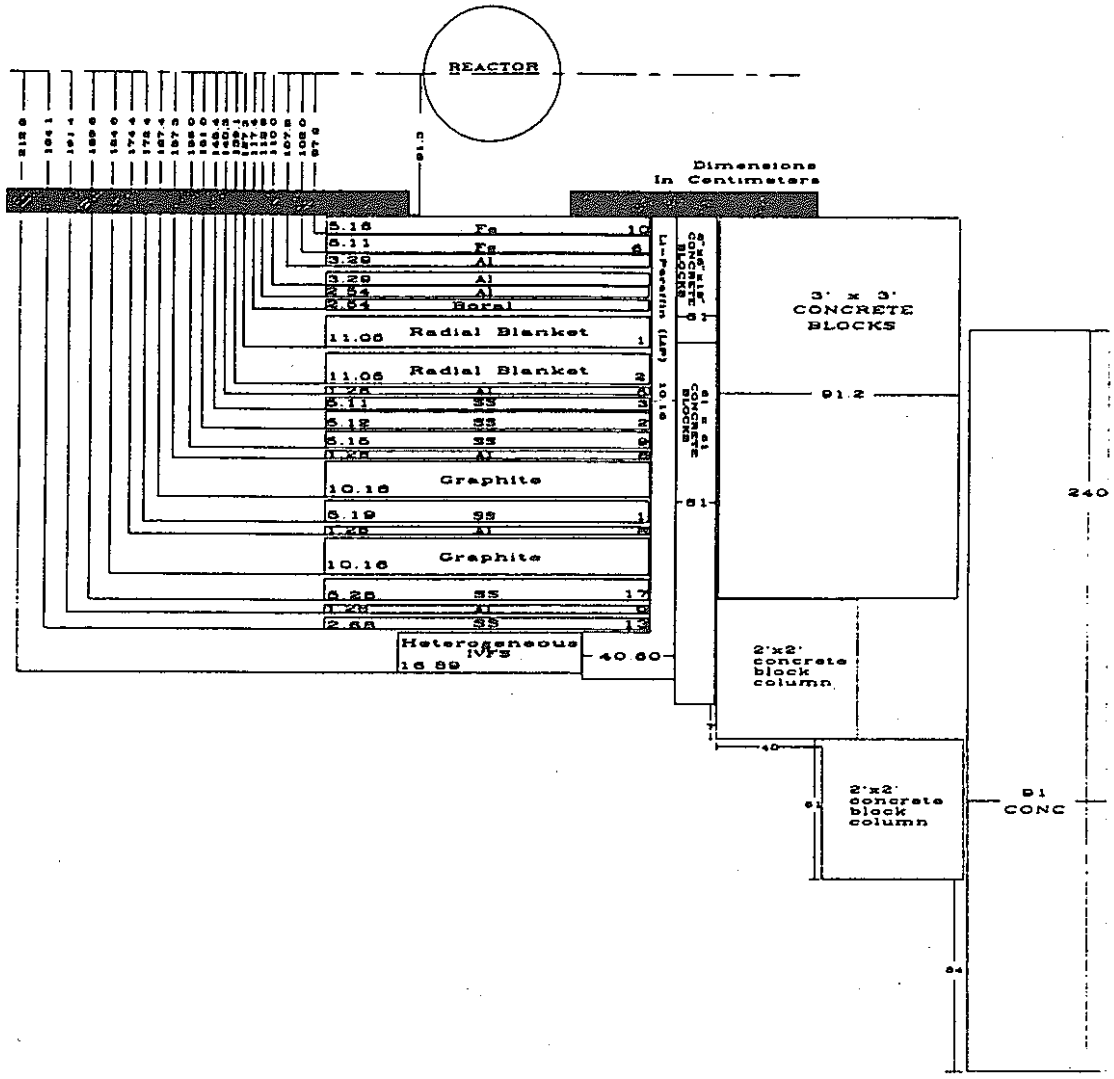

Figure 24. Schematic of SM-1 plus shield configuration for Item IID.

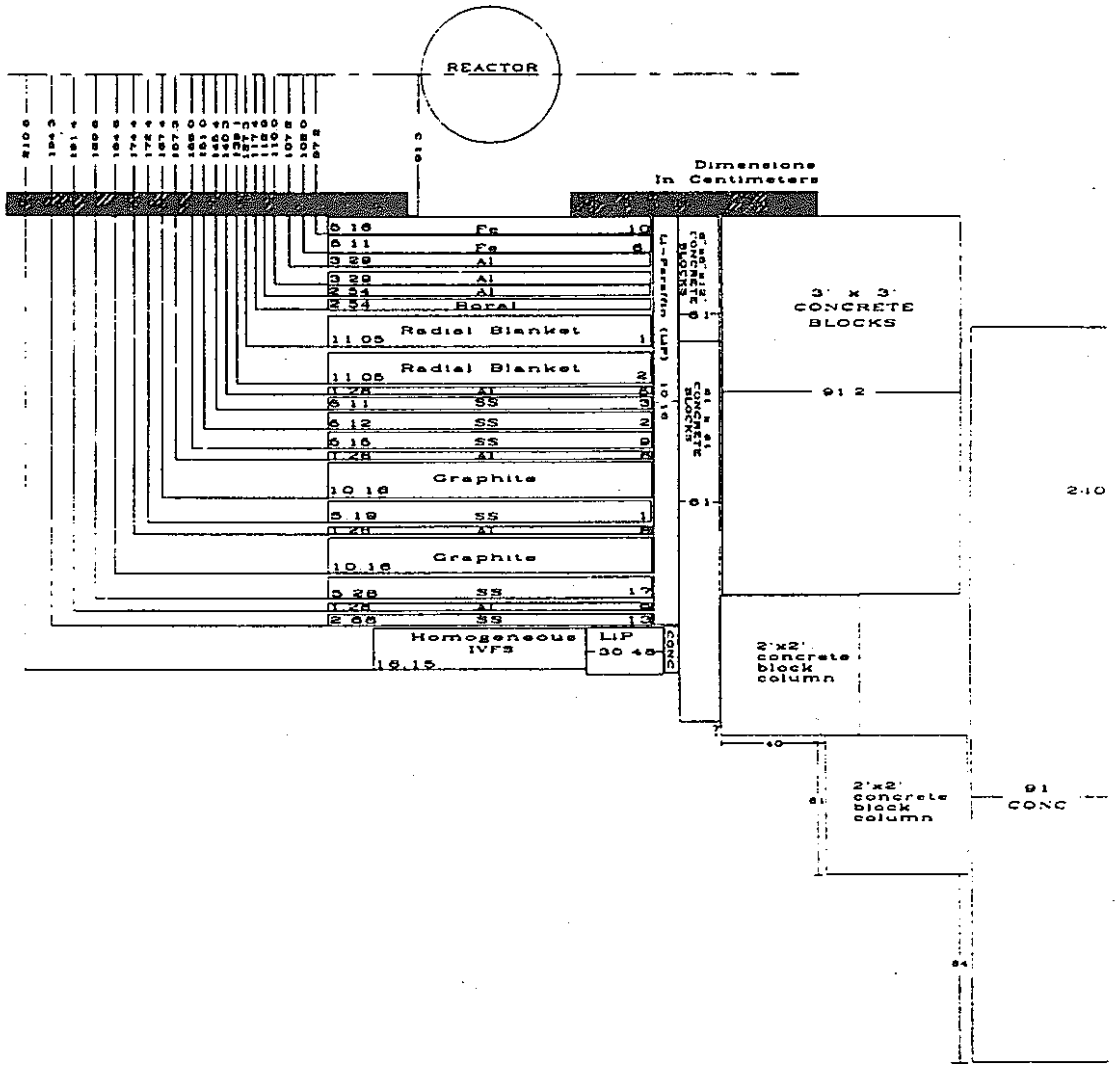

Figure 25. Schematic of SM-1 plus shield configuration for Item IIE.

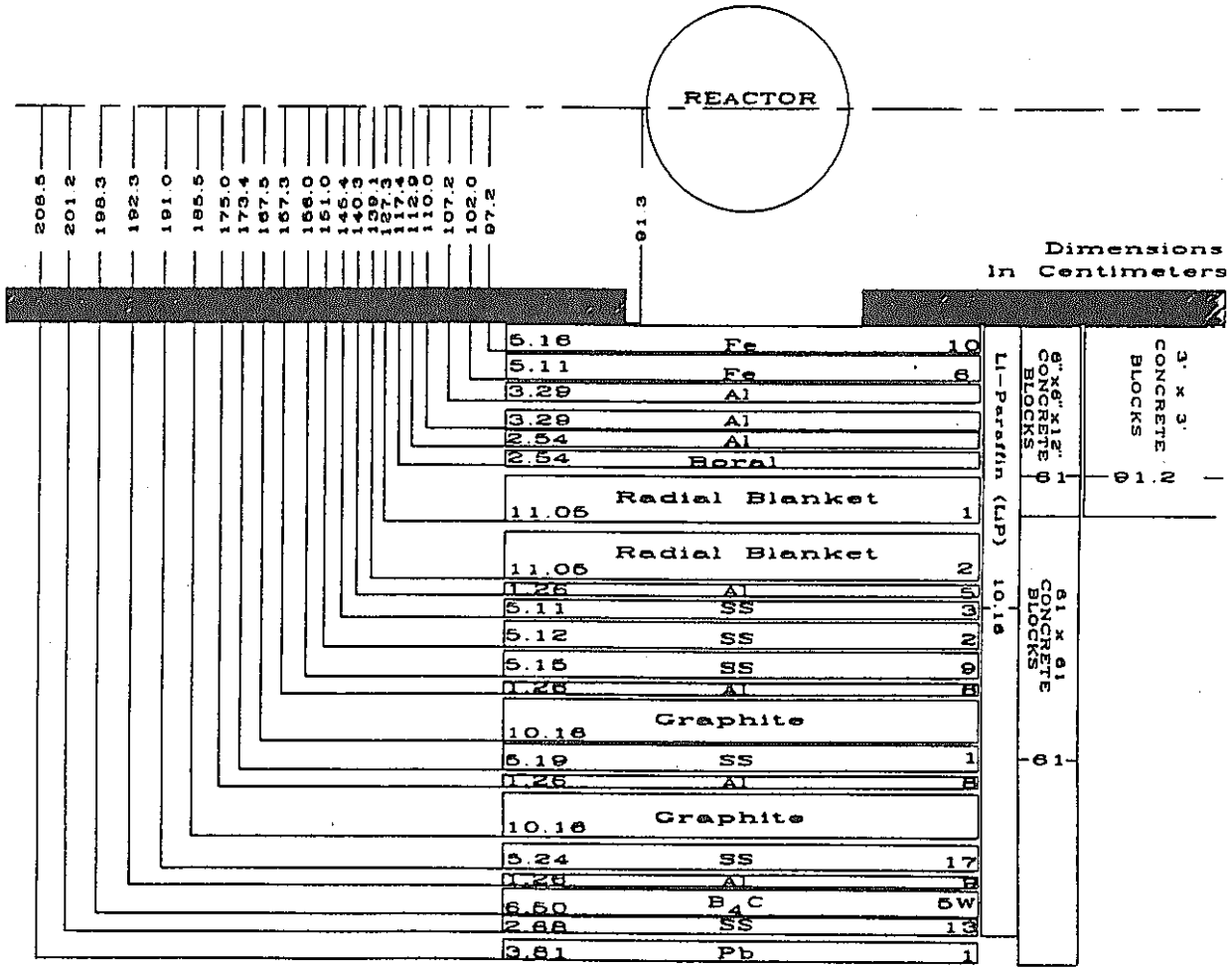

Figure 26. Schematic of SM-1 plus shield configuration for Item IIF plus lead.

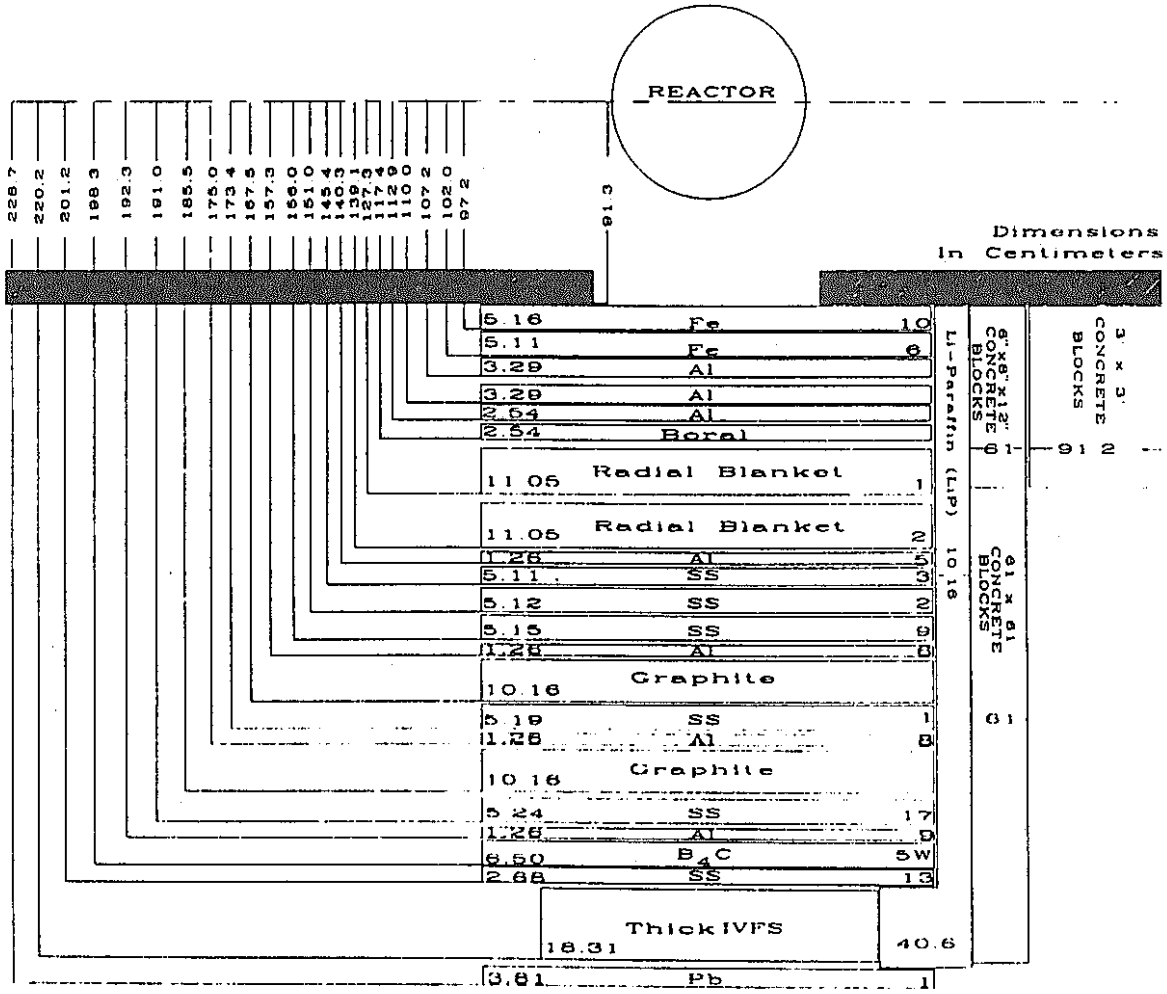

Figure 29. Schematic of SM-1 plus shield configuration for Item IIG plus lead.

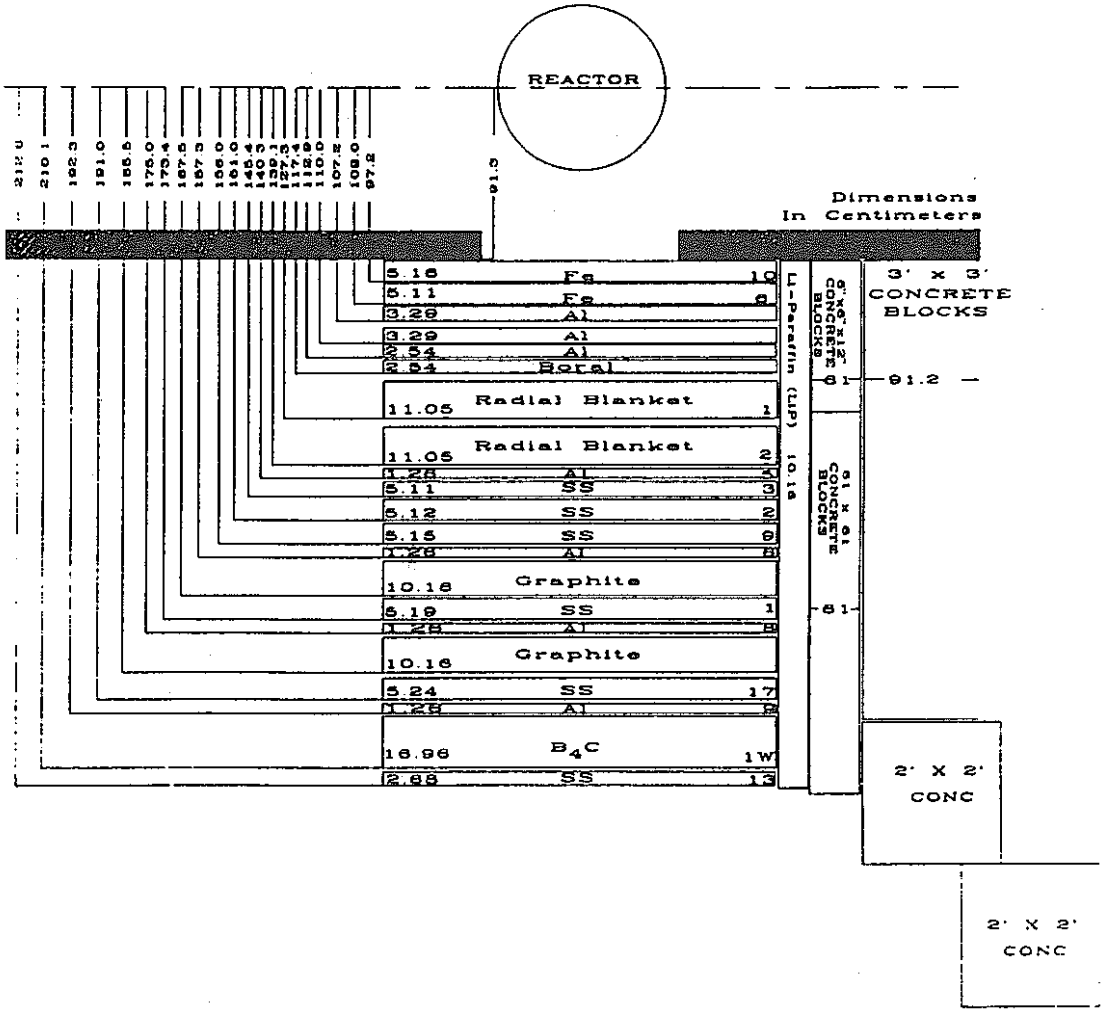

Figure 32. Schematic of SM-1 plus shield configuration for Item IIH.

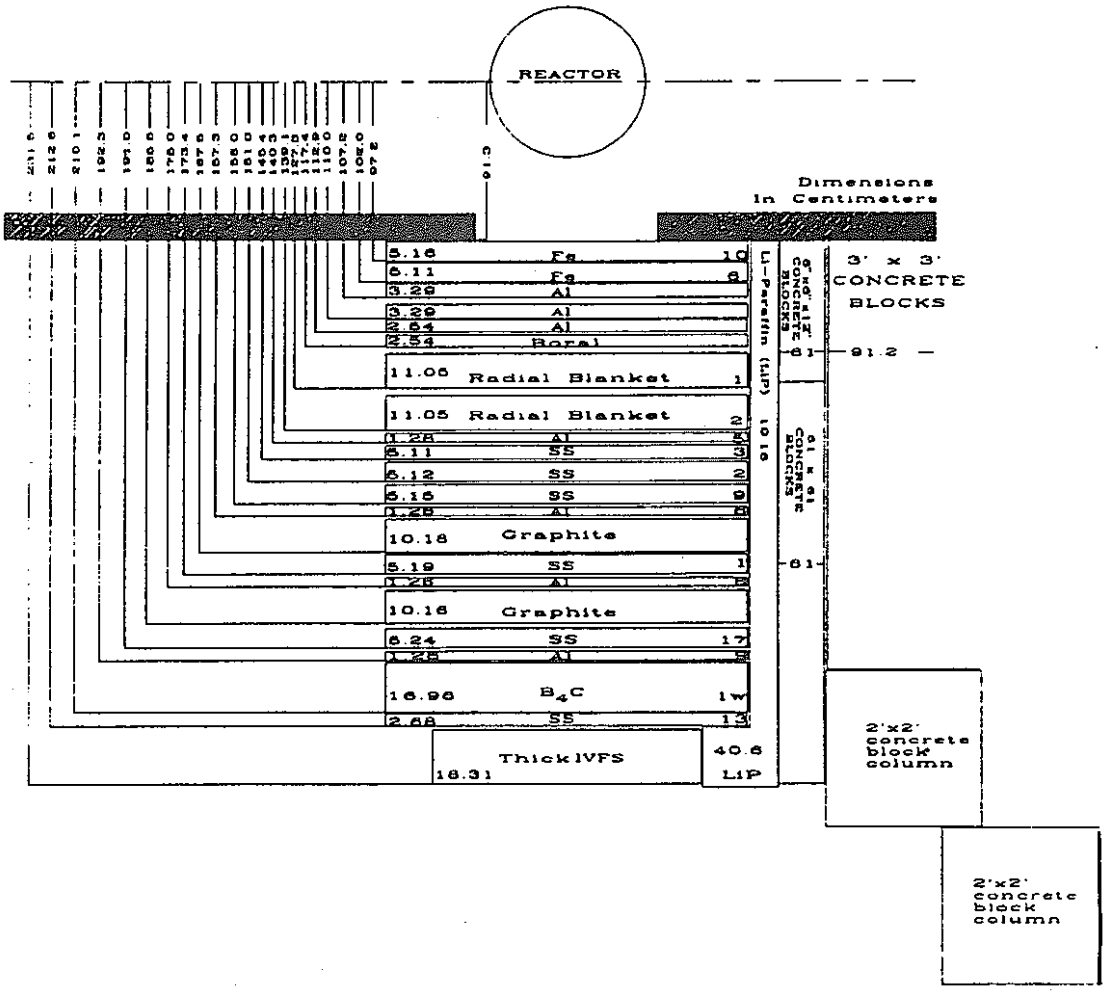

Figure 33. Schematic of SM-1 plus shield configuration for Item II I.

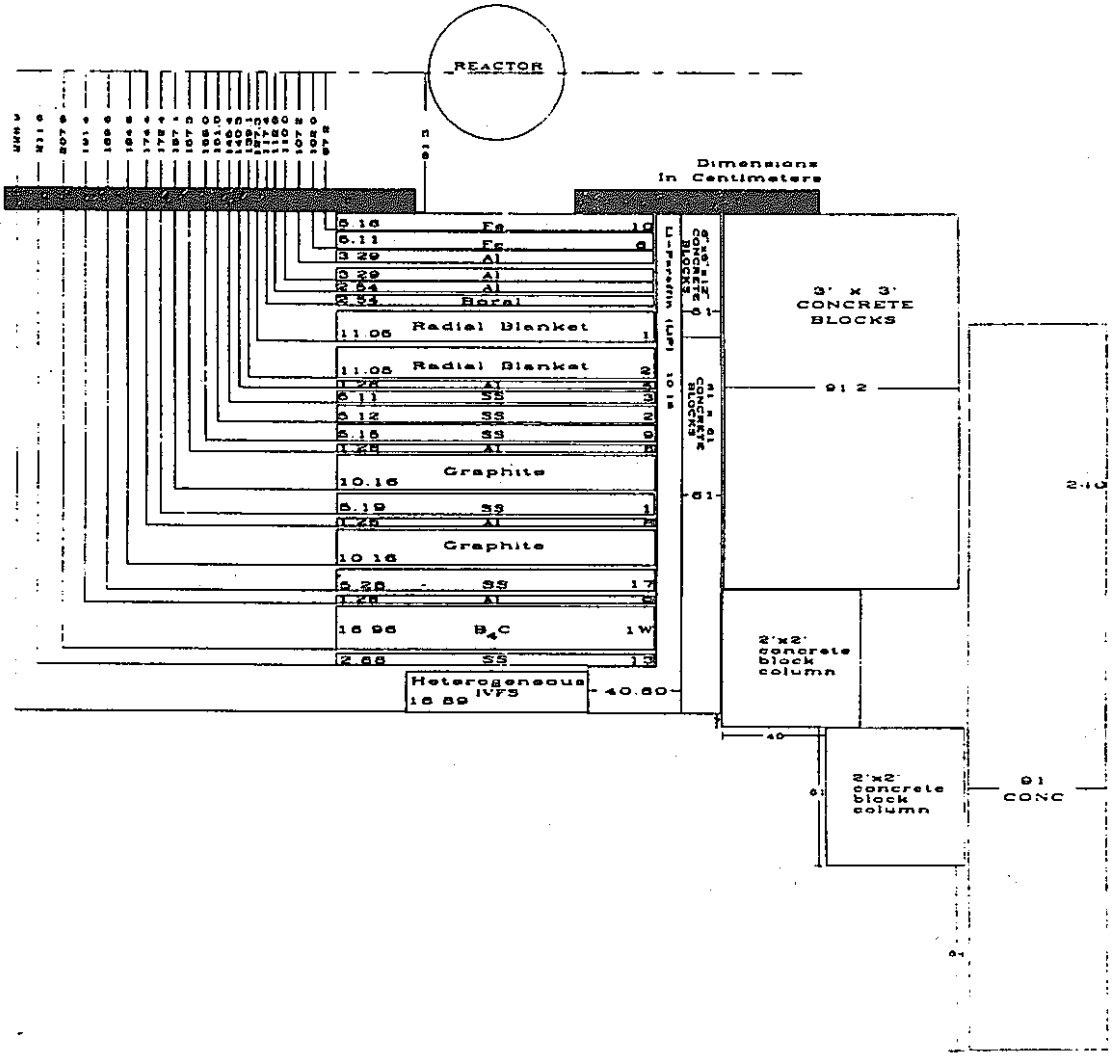

Figure 34. Schematic of SM-1 plus shield configuration for Item III.

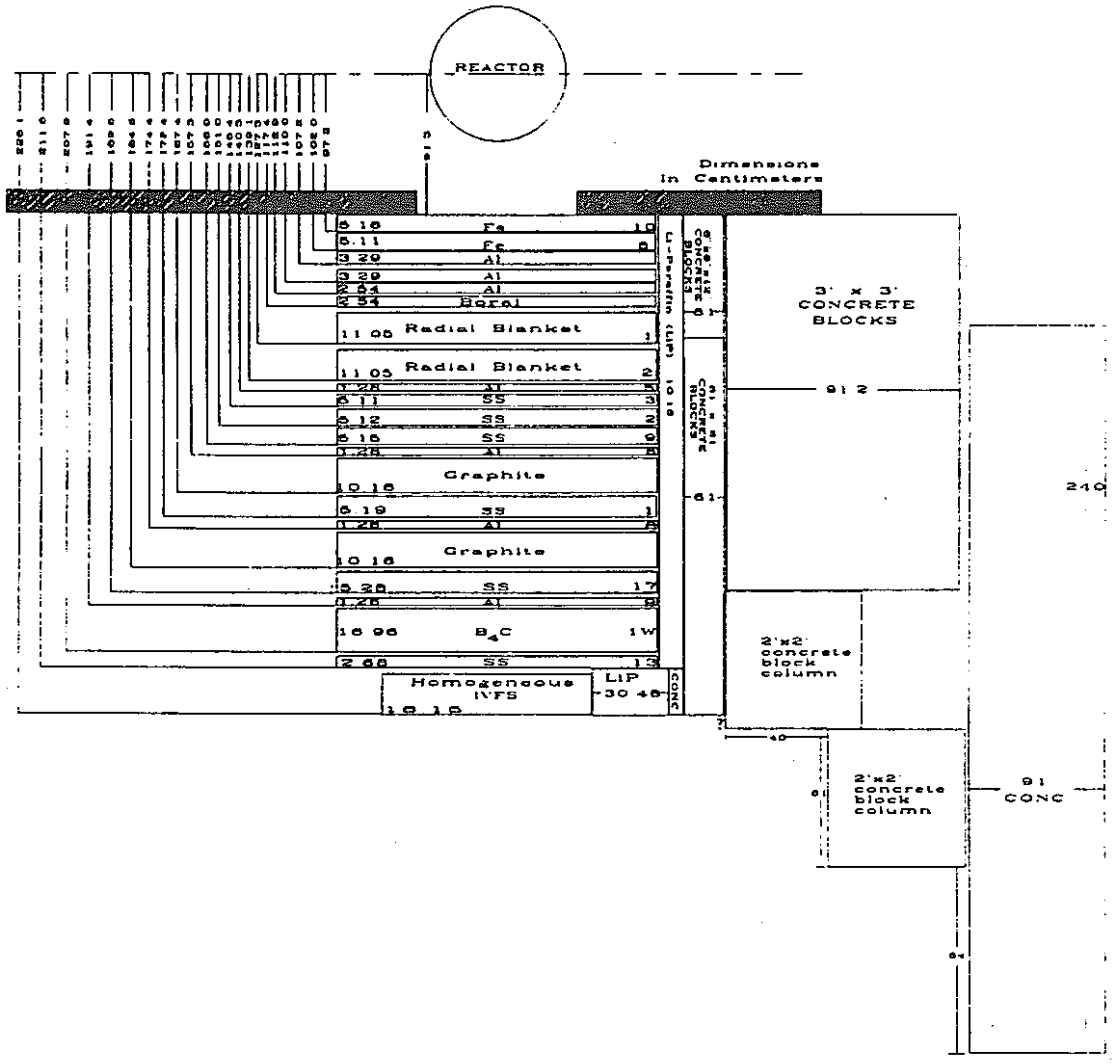

Figure 35. Schematic of SM-1 plus shield configuration for Item IIK.

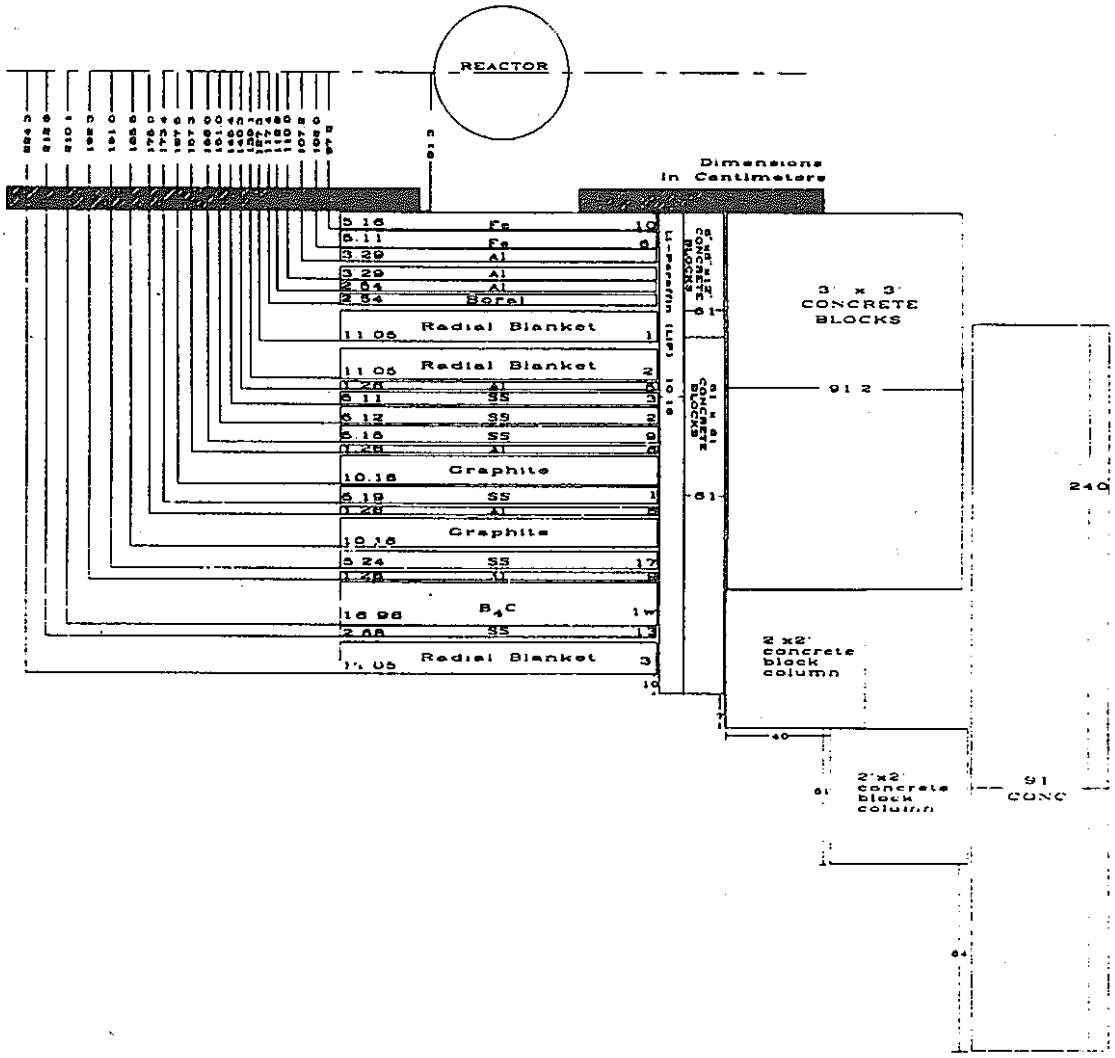

Figure 36. Schematic of SM-1 plus shield configuration for Item IIL.

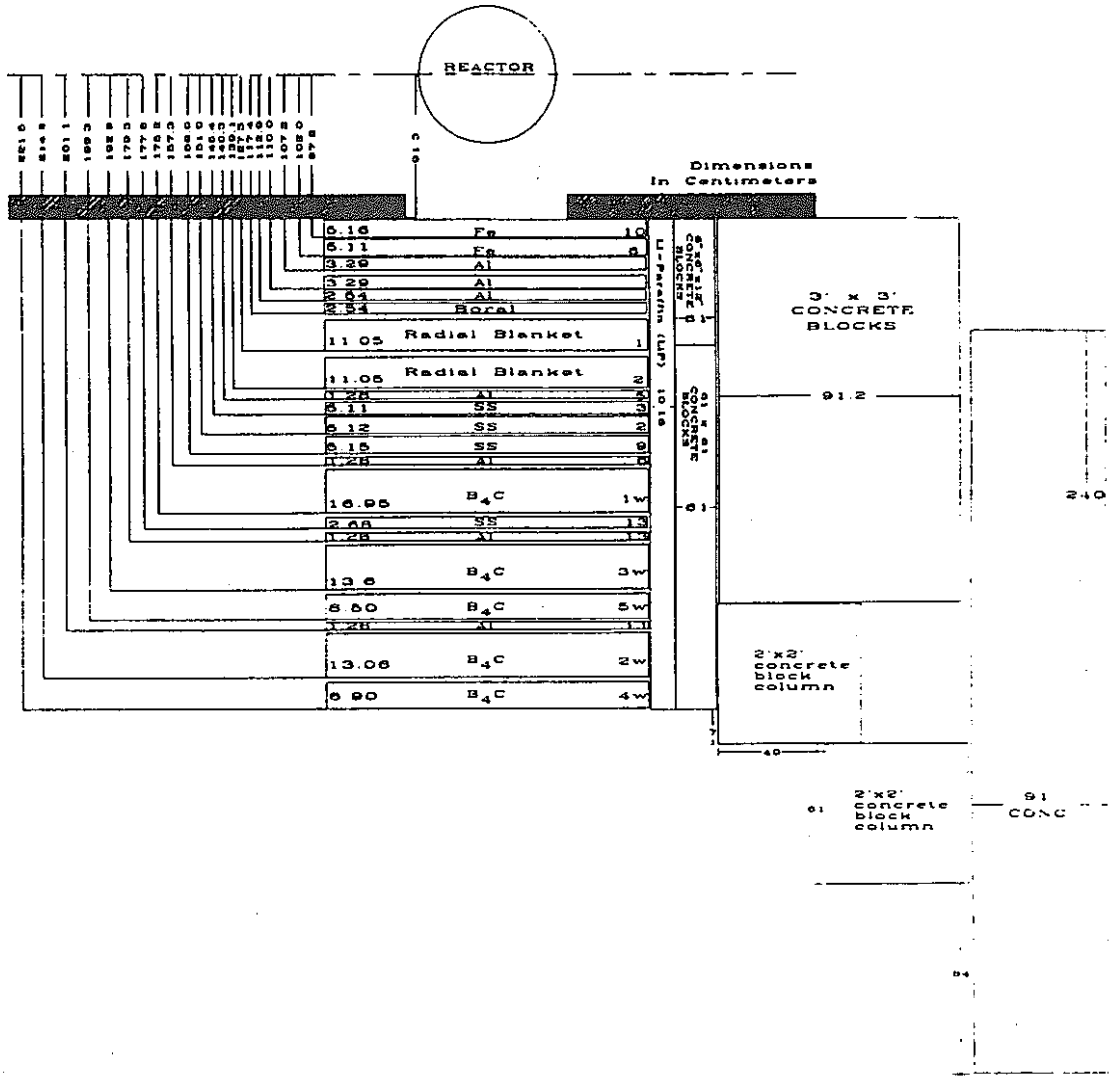

Figure 37. Schematic of SM-1 plus shield configuration for Item IIM.

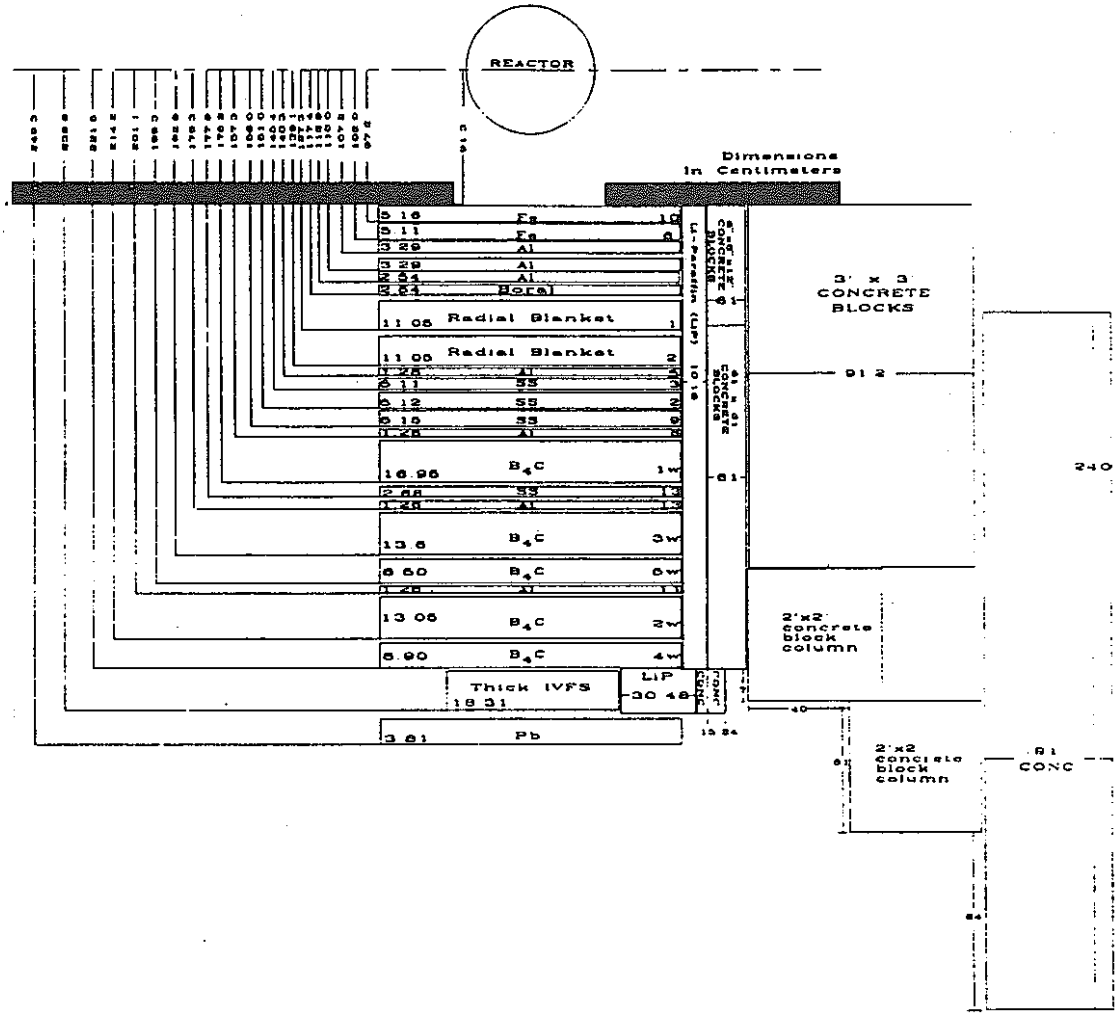

Figure 38. Schematic of SM-1 plus shield configuration for Item IIN plus lead.

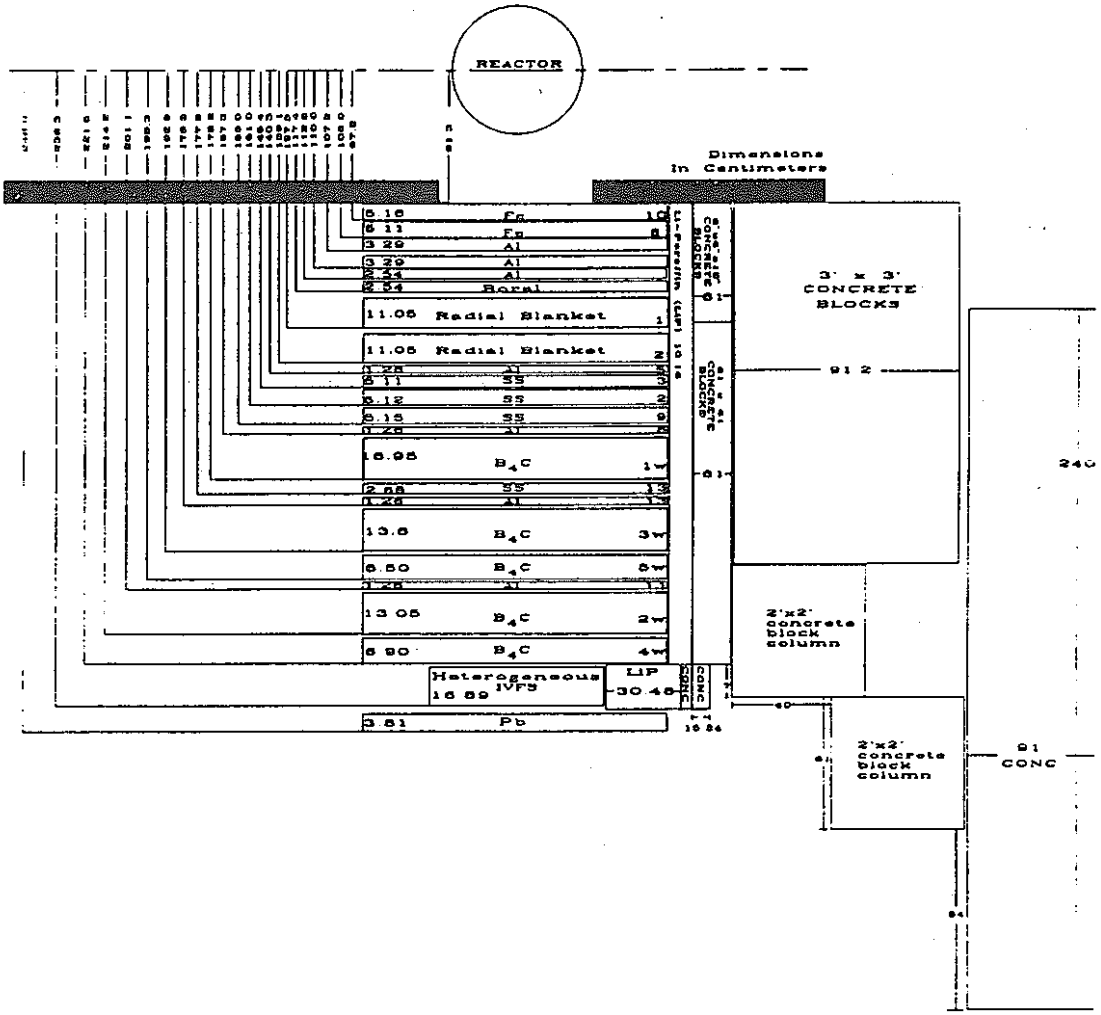

Figure 41. Schematic of SM-1 plus shield configuration for Item IIO plus lead.

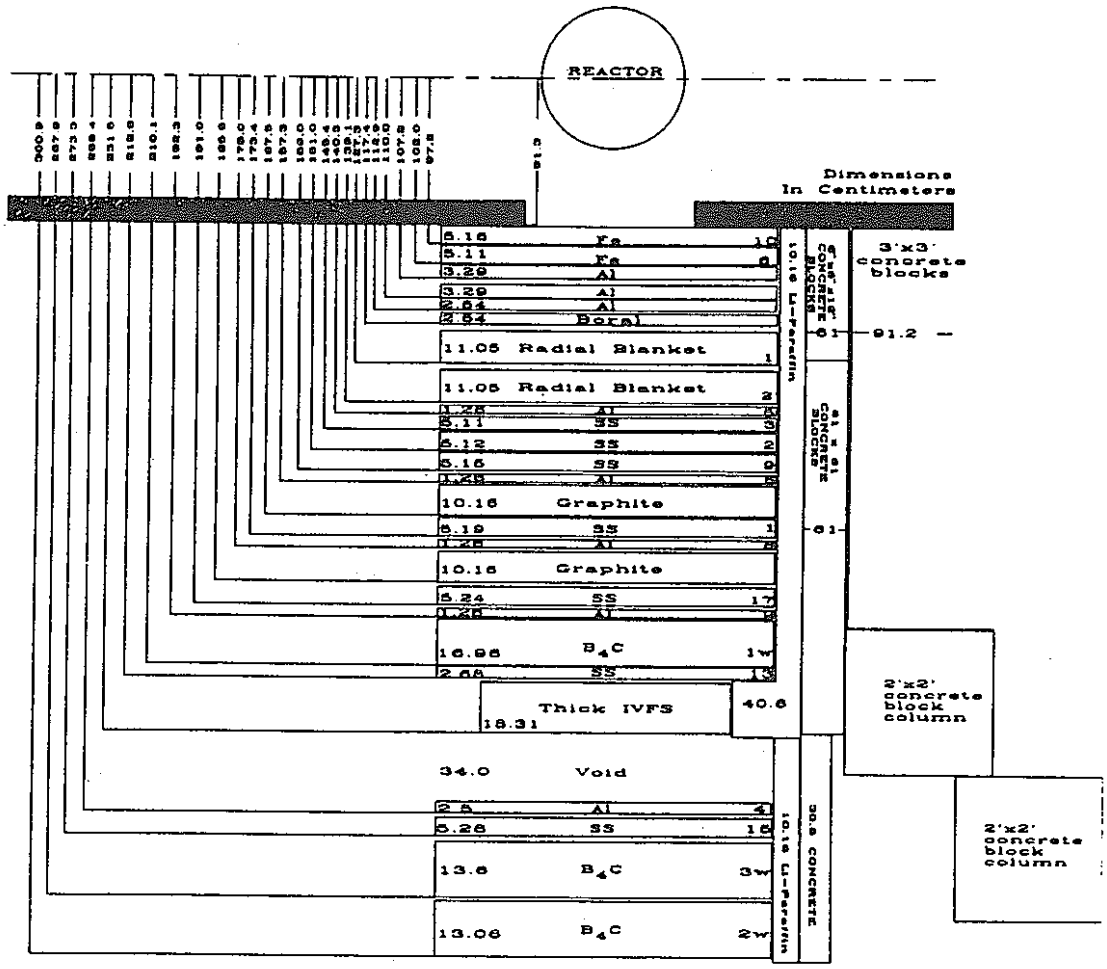

Figure 44A. Schematic of SM-1 plus shield mockup for Item IIP (Note: This mockup was used for measurements with the fission chamber in the void and at 0.7 and 30 cm behind mockup).

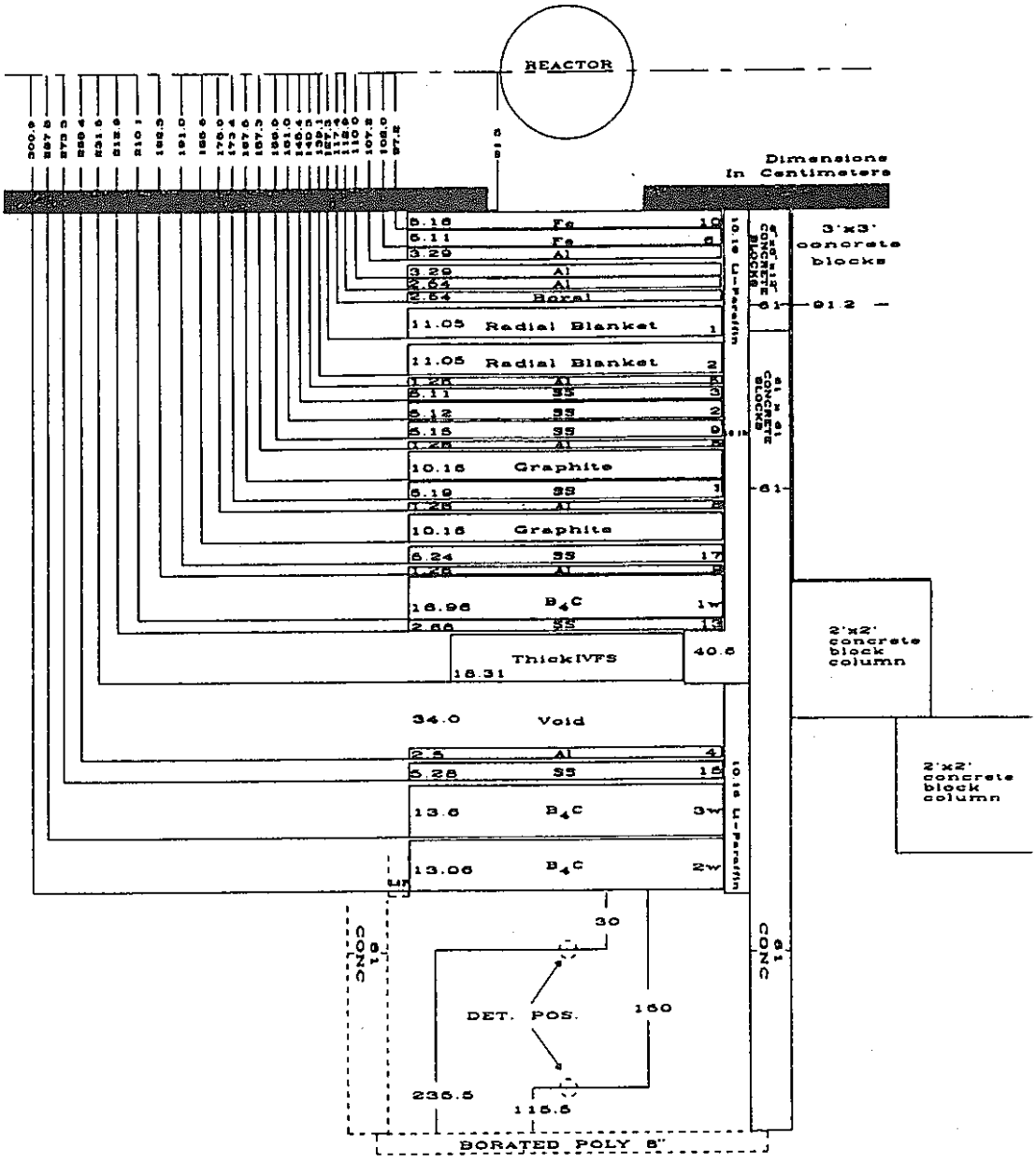

Figure 44B. Schematic of SM-1 plus shield configuration for Item IIP (Note: This mockup was used for measurements behind B_4C slab 2W only).

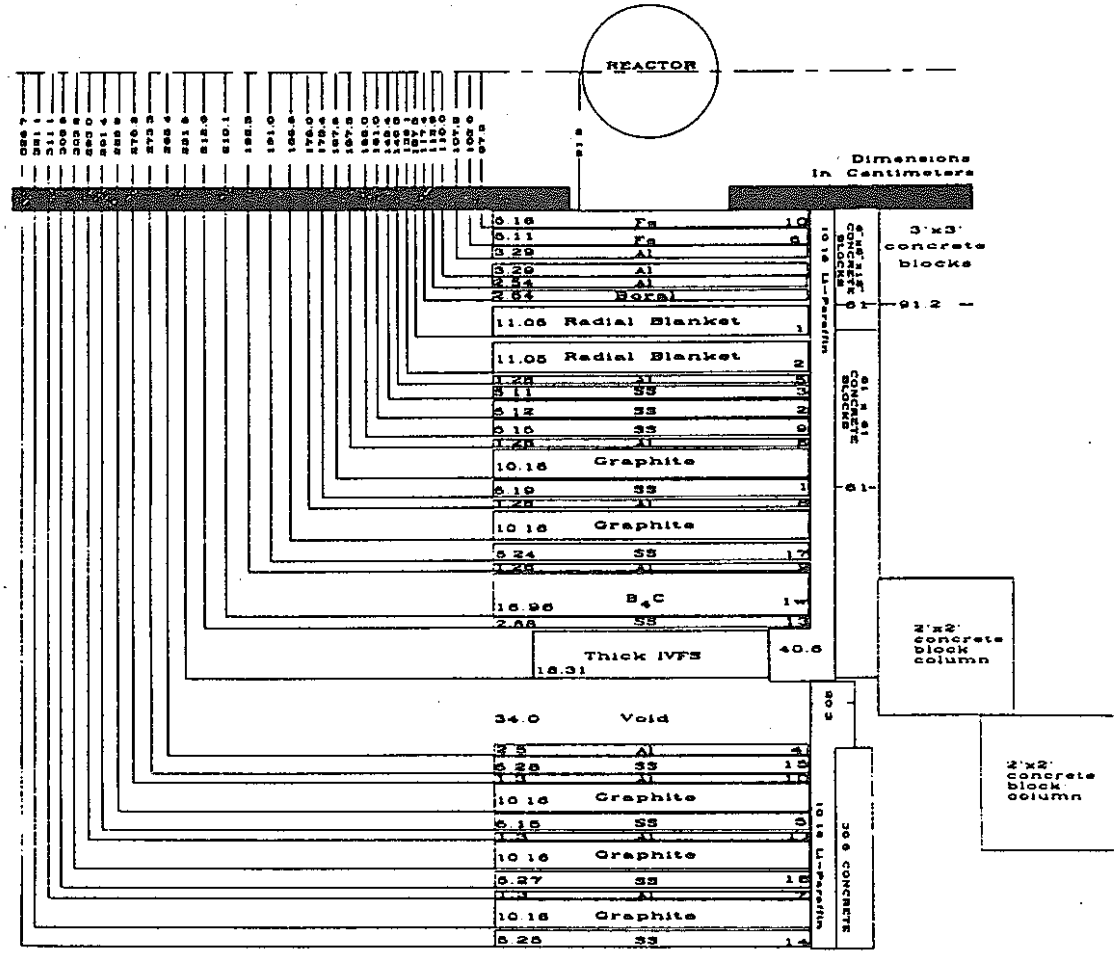

Figure 45A. Schematic of SM-1 plus shield configuration for Item IIQ (Note: Measurements in the void only).

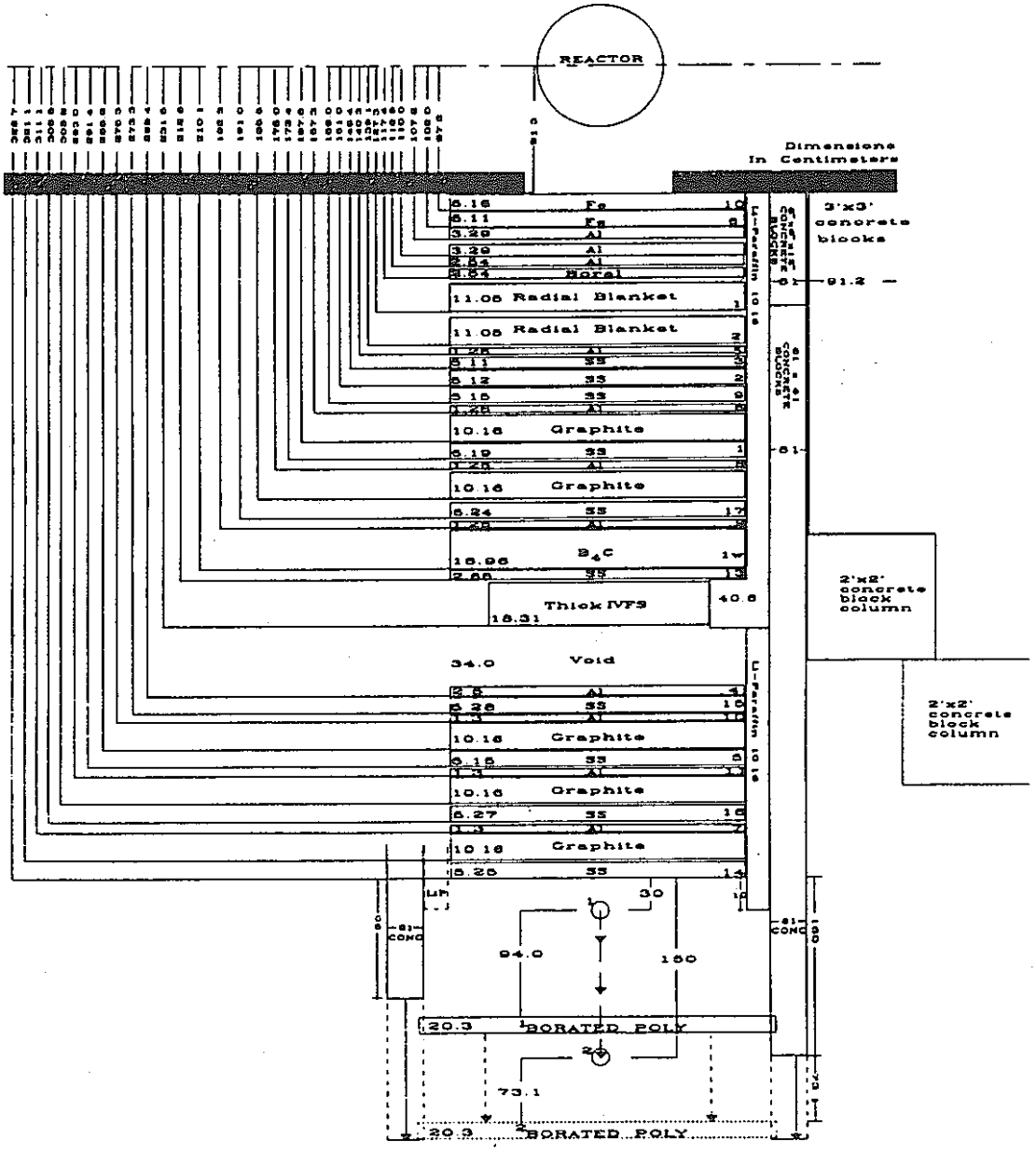

Figure 45B. Schematic of SM-1 plus shield configuration for Item IIQ (Note: Measurements behind mockup only).

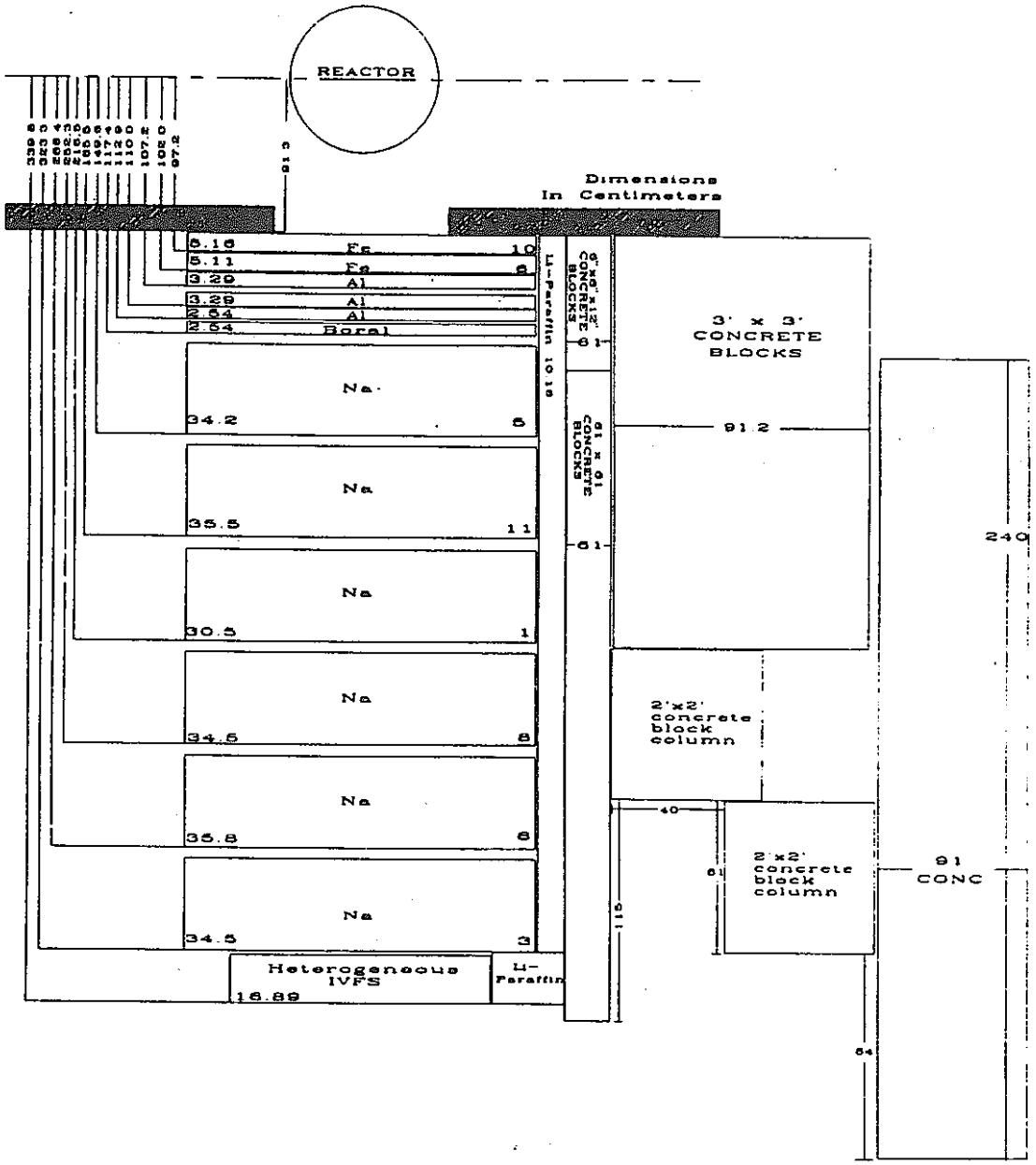

Figure 46. Schematic of SM-2 plus shield configuration for Item IIIA.

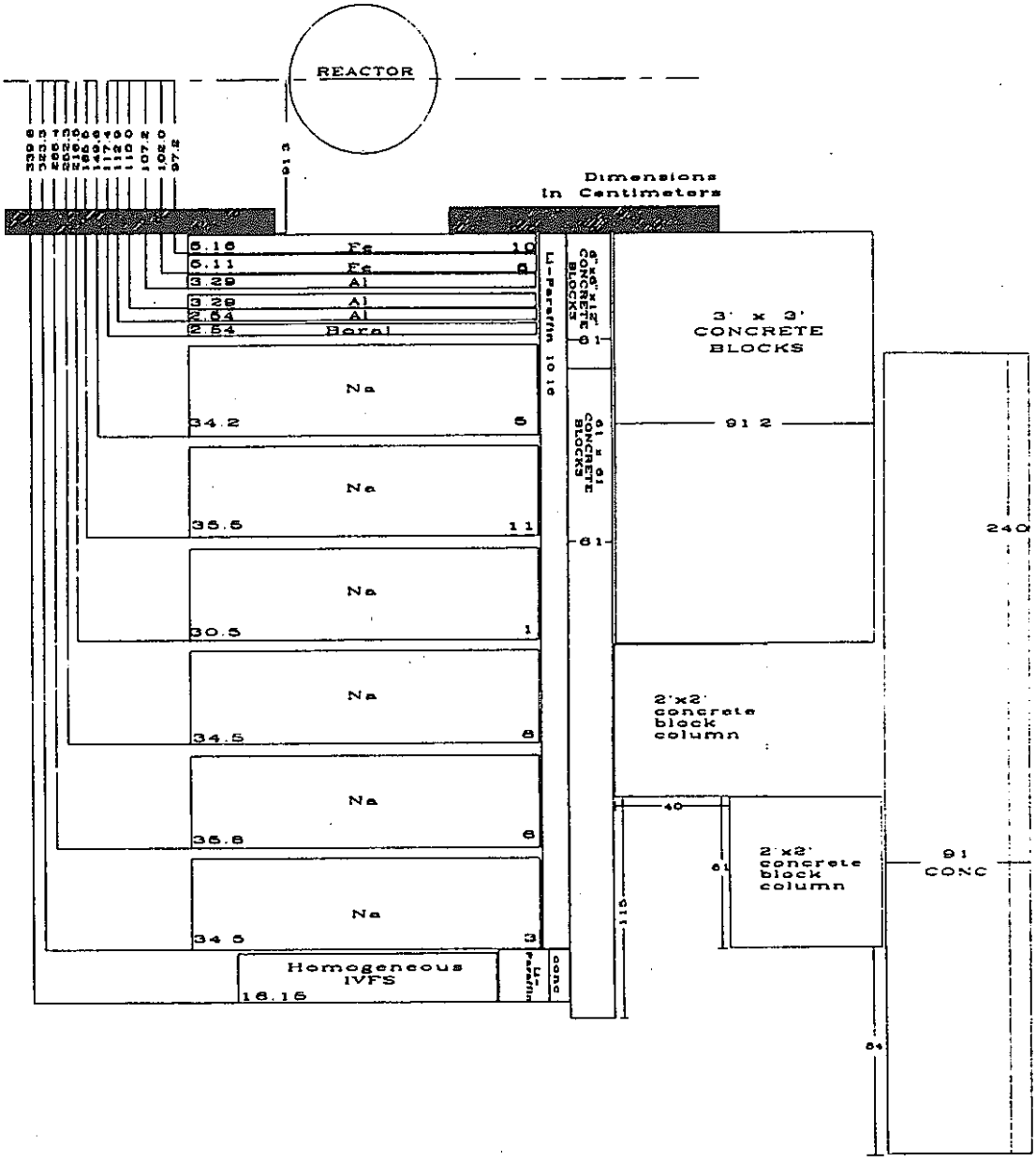

Figure 47. Schematic of SM-2 plus shield configuration for Item IIIB.

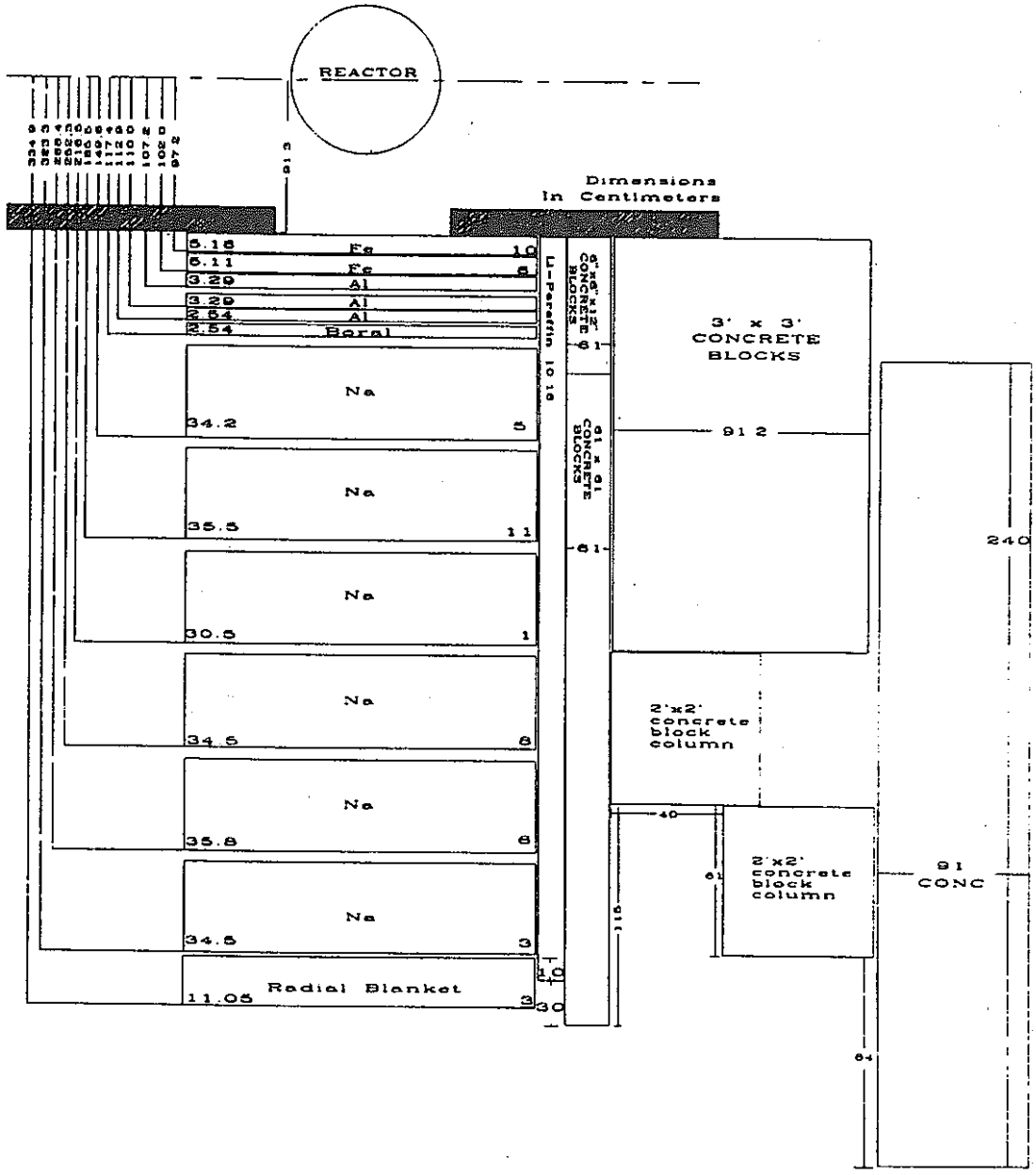

Figure 48. Schematic of SM-2 plus shield configuration for Item IIIC.

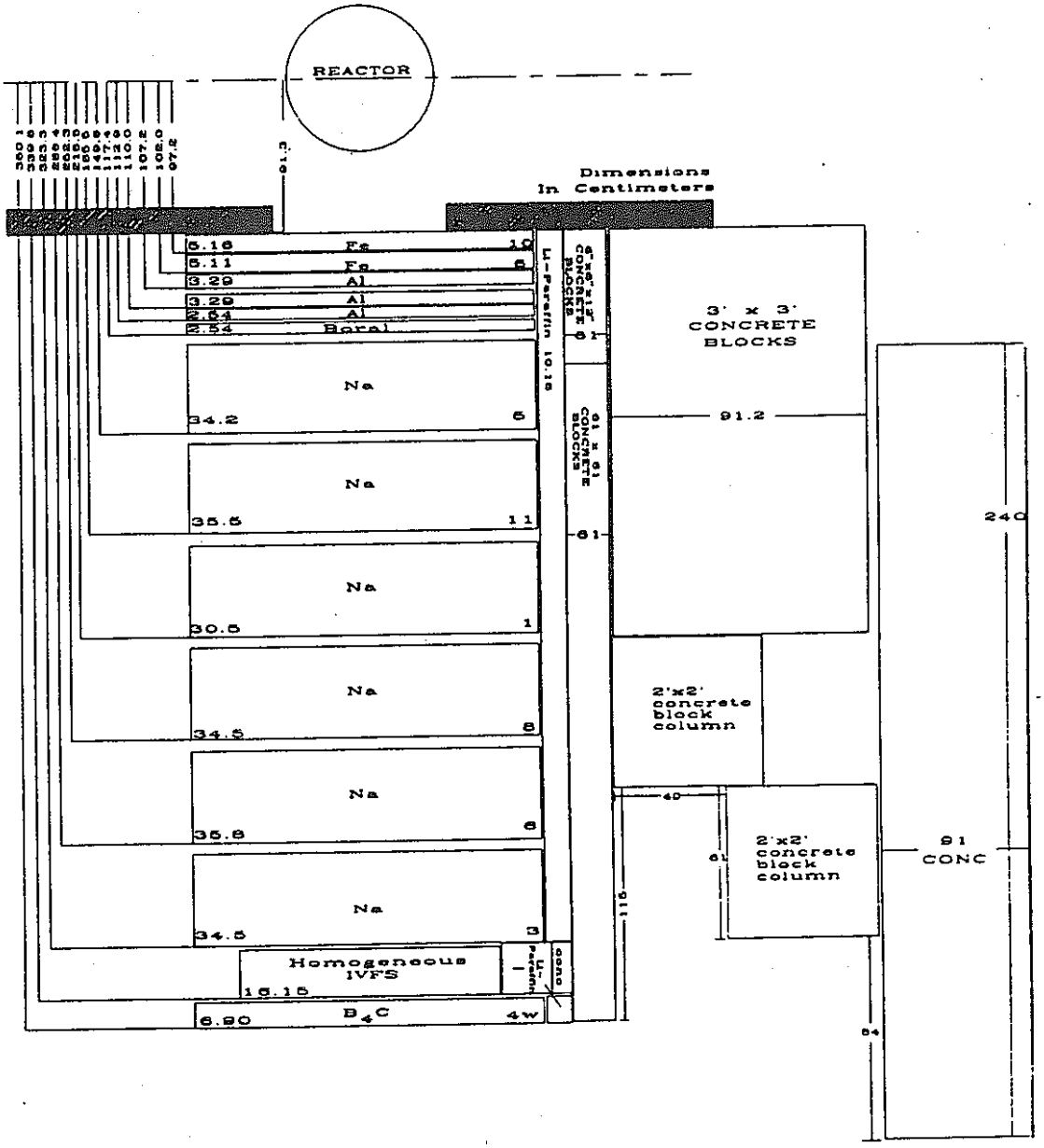

Figure 49. Schematic of SM-2 plus shield configuration for Item IIID.

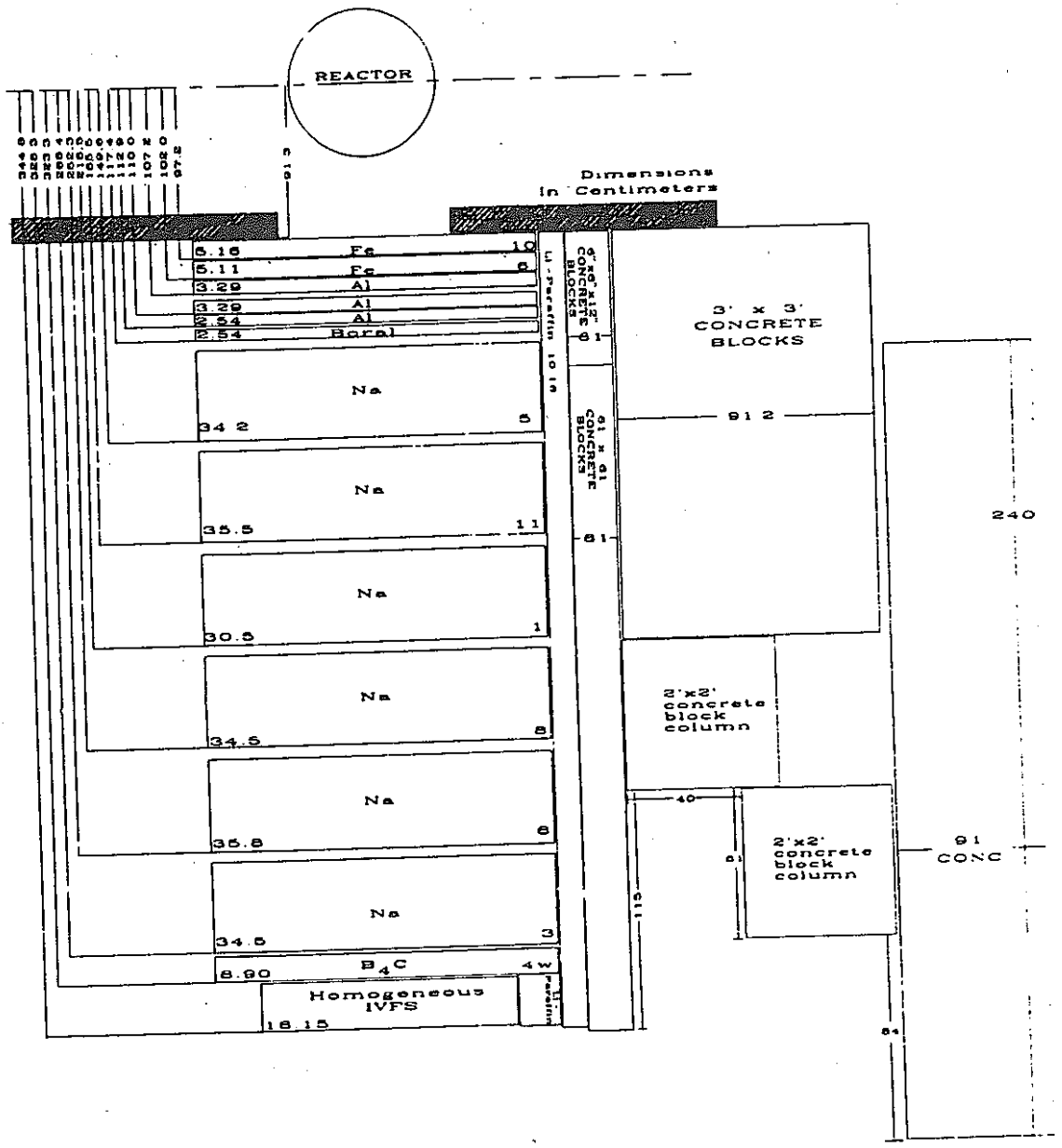

Figure 50. Schematic of SM-2 plus shield configuration for Item IIIE.

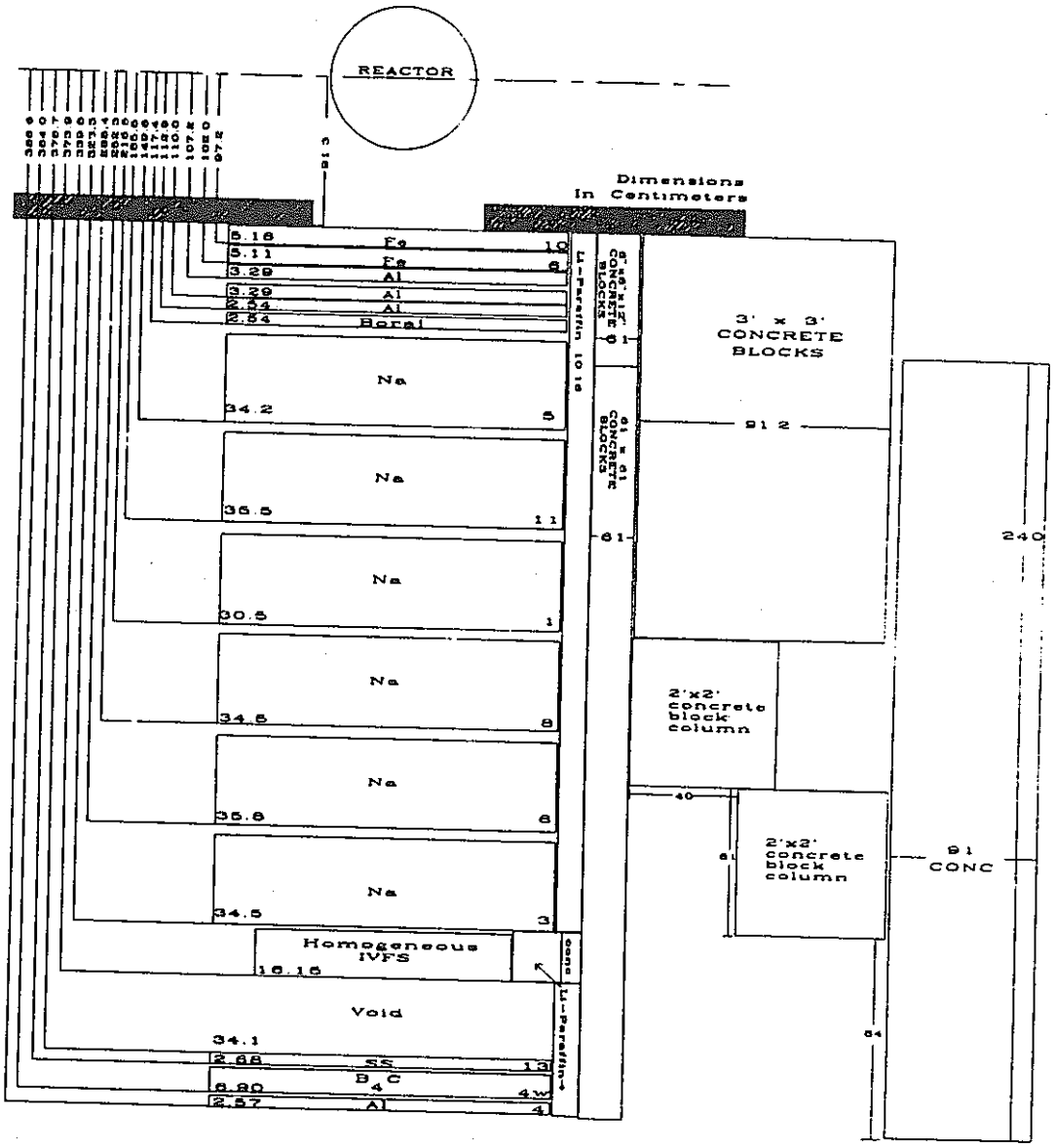

Figure 51. Schematic of SM-2 plus shield configuration for Item IIIF.

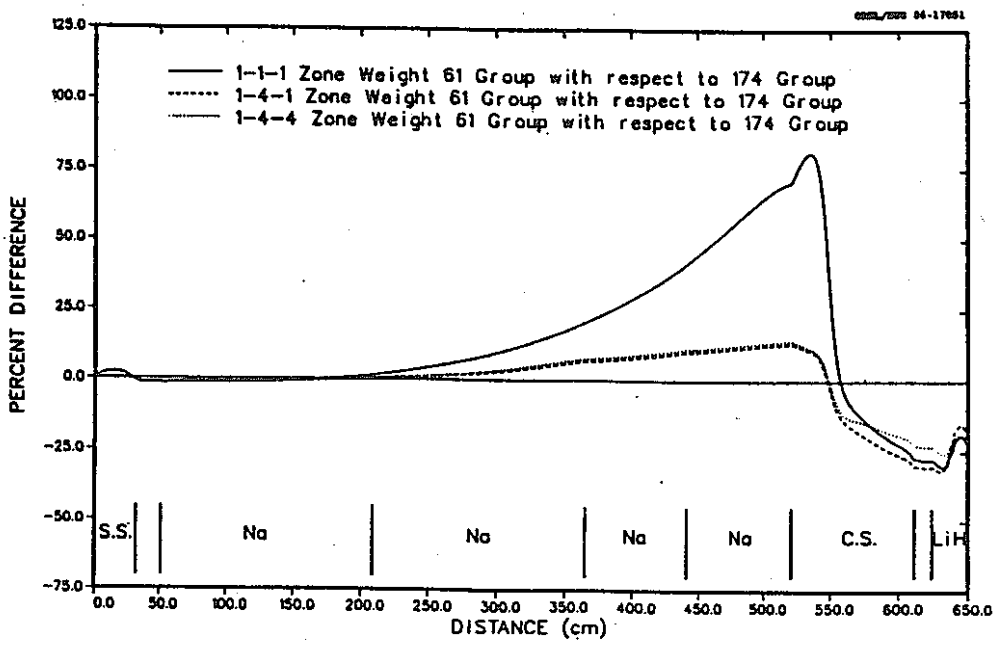

Fig. 13. Comparison of 4-in. Bonner ball responses calculated using fine-group cross sections and 61-group neutron cross sections collapsed using three different zone-averaged weighting functions.

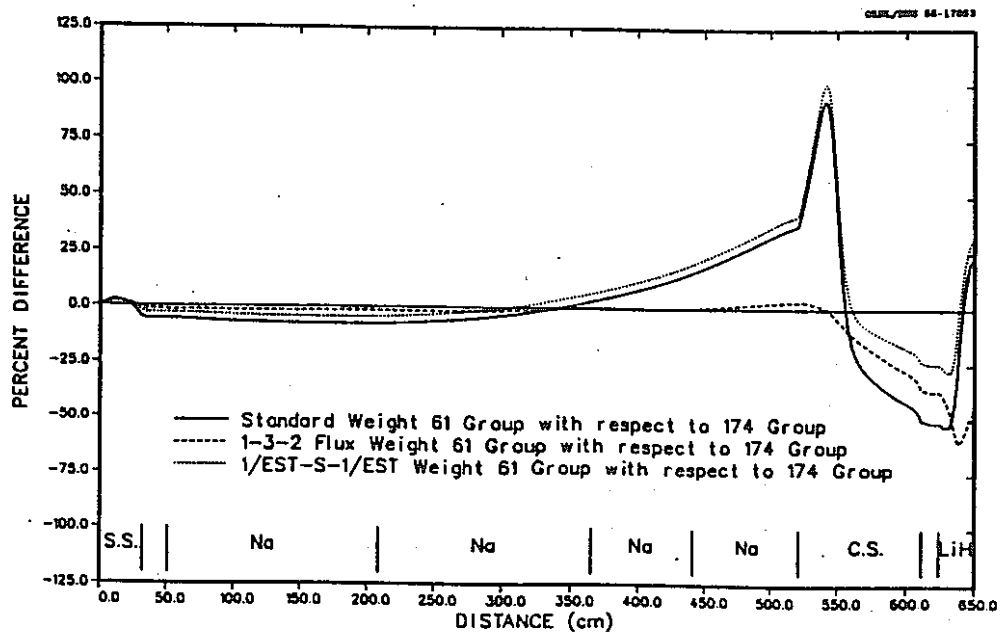

Fig. 15. Comparison of 4-in. Bonner ball responses calculated using fine-group cross sections and 61-group neutron cross sections collapsed using three final weighting functions.

Table 5. Materials in the VELM61 and VELM22 Libraries used in the Na-Fe Calculations

Material	ID (AMPX)	ID (ANISN)	Description
		(Standard Weighting, Self-Shielded)	
Fe	132611	501-506	
Cr	132411	507-512	Constituents of SS-304
Ni	132811	513-518	
Mn-55	132511	519-524	
Fe	132612	525-530	Constituents of Al
Al-27	131311	531-536	
H-1	9311	537-542	
O-16	127611	543-548	
Na-23	131111	549-554	Constituents of Na
Ca	132011	555-560	
K	115011	561-566	
Fe	132613	567-572	
Mn-55	132512	573-578	Constituents of Carbon Steel
C	130611	579-584	
H-1	9312	585-590	
Li-6	130311	591-596	Constituents of LiH
Li-7	139711	597-602	
		(Na-Fe Interval-Flux Weighting)[a]	
Fe	132621	603-608	
Cr	132421	609-614	Flux 3.8-cm into SS-304
Ni	132821	615-620	
Mn-55	132521	621-626	
Mo	132121	627-632	
Na	131121	633-638	Flux 76.2-cm into Na
Na	131122	639-644	Flux 228.6-cm into Na
Na	131123	645-650	Flux 381.0-cm into Na
Fe	132622	651-656	Flux 15.2-cm into Carbon Steel
Fe	132623	657-662	Flux 45.7-cm into Carbon Steel
		($1/E\Sigma_t$ Weighting)	
Fe	132631	663-668	
Cr	132431	669-674	
Ni	132831	675-680	$1/E\Sigma_t$(SS-304)
Mn-55	132531	681-686	
Mo	132131	687-692	
Fe	132632	693-698	$1/E\Sigma_t$ (Carbon Steel)

[a]Designated as the 1-3-2 flux weighting in Section II.4.

5-22-87

Concrete surrounding Reactor Plenum Mockups ($\rho = 2.44\ g/cm^3$)

Component	wt %	Element #1	wt %	Element #2	wt %
Al_2O_3	2.43	Al	1.286	O	1.144
CaO	36.78	Ca	26.286	O	10.494
CO_2	32.5	C	8.870	O	23.630
Fe_2O_3	0.92	Fe	0.6435	O	0.2765
H_2O	3.79	H	0.424	O	3.366
K_2O	0.57	K	0.4732	O	0.0968
MgO	13.78	Mg	8.310	O	5.470
Na_2O	0.13	Na	0.0964	O	0.0356
P_2O_5	0.0285(0.03)	P	0.0131	O	0.0169
SiO_2	8.54	Si	3.992	O	4.548
SO_3	0.53	S	0.212	O	0.318
					49.3958

Element	wt %	concrete atom density	With Fe in 3" slab	with Fe in 8" slab
H	0.424	6.182-3	6.152-3	6.160-3
C	8.87	1.085-2	1.080-2	1.081-2
O	49.3958	4.537-2	4.515-2	4.521-2
Na	0.0964	8.310-5	8.270-5	8.280-5
Mg	8.31	5.025-3	5.000-3	5.006-3
Al	1.286	7.004-4	6.971-4	6.979-4
Si	3.992	2.089-3	2.079-3	2.081-3
* P	0.0131	6.216-6	6.185-6	6.193-6
* S	0.212	9.716-5	9.669-5	9.681-5
K	0.4732	1.779-4	1.770-4	1.772-4
Ca	26.286	9.639-3	9.592-3	9.604-3
Fe	0.6435	1.693-4	5.789-4	4.755-4

5-26-87

Average composition for Plenum Concrete

Element	atomdensity average
H	6.16-3
C	1.08-2
O	4.52-2
Na	8.28-5
Mg	5.01-3
Al	6.98-4
Si	2.08-3
P	6.19-6
S	9.68-5
K	1.77-4
Ca	9.60-3
Fe	5.27-4

PNC's request about the
Data Plan for future Experiments April 24, 1992.

1. PNC would like to add 3 configurations for re-measurement of the Axial Shield Experiment. The specification of those 3 configurations are shown in Table 1 presented by Mr. Pace. (page 7)
PNC prefers to put Li-Par bricks both preceding and following the Axial Shield Mockup. (10cm thick)
If the arrangement is very difficult, the second choice is to put Li-Par bricks preceding the Axial Shield Mockup.
The third choice might be to put the Li-Par bricks following the Axial Shield Mockup.

2. PNC would like to request ORNL to put Li-Par bricks preceding the Axial Shield Mockup to be used in the NIS Experiment. If the arrangement is acceptable for ORNL, PNC could eliminate all measurements

planned in the Configuration II shown in Table 1 (Rev. 1).
(page 3)

And, PNC would like to add Bonner Ball measurements in void on IIIB, IIIC, IIIE & IIIF, which are shown in Table 1 (Rev. 1).
(page 4)

3. If the request described in the last paragrah is not acceptable for ORNL, PNC would like to remain the Configuration IIA, IIB, IID & IIE shown in Table 1 (Rev. 1)
(page 3)
with lower priority than other configurations.
Hornyak Button measurements would be replaced with Bonner Ball measurements in those 4 configurations.

4. PNC would like ORNL to perform the Special Material Experiment according to the Data Plan shown in Table 1.
(page 6)

3．2　米国遮蔽専門家会議資料

Ⅰ　ＰＮＣ発表論文

Ⅱ　ＰＮＣ発表論文

Ⅲ　出席者リスト

Ⅳ　発表論文リスト

B4C SHIELDING DESIGN STUDY FOR THE JOYO REACTOR

A. Yoshida, K. Chatani, S. Suzuki and K.Kinjo

O-arai Engineering Center,
Power Reactor and Nuclear Fuel Development Corporation,
4002, O-arai-machi, Ibaraki-ken, 311-13, JAPAN
3-011-81-0292-67-4141

ABSTRACT

In Experimental Fast Reactor "JOYO", an In-Vessel Storage (IVS) system using cooling pots is applied to remove the decay heat of the spent fuel subassemblies(S/A) during one duty cycle operation. Thus, the fuel handling procedure in the reactor vessel is complicated. To simplify the fuel handling procedure and save refueling time, it is necessary to enhance the radial shield performance in order to reduce heat generation in the spent fuel of the IVS rack caused by fission from core-leakage neutrons. To achieve the above objectives, a shielding design study of a system using boron carbide (B4C) as a removable radial shield was performed. The result of this study showed that simplification of refueling could be achieved by replacing the outer two layers of stainless steel(SS) reflectors with B4C shields. Also, a detailed shielding analysis of the JOYO shielding design was conducted and the adequacy of the shielding design for the new higher-power core, which is called Mk-III, is assured.

1 INTRODUCTION

Experimental Fast Reactor "JOYO" Is the first sodium cooled fast reactor constructed in Japan, and it achieved its initial criticality in April 1977 as a breeder core(Mk-I core). Next, the first core was replaced and JOYO became an irradiation bed core(Mk-II core) in March 1983 to perform irradiation tests for FBR fuels and materials development. The Mk-II core consists of 67 uranium-plutonium mixed oxide(MOX) fuel S/As, 6 control rods, and 239 SS reflectors, including some material irradiation reflectors surrounding the core.

In JOYO, a spent fuel S/A is stuffed in a cooling pot and stored in the IVS rack during one duty cycle(70 days) operation to remove decay heat. As a spent fuel S/A in the IVS rack also generates heat by fission due to neutrons leaking from the core during high power operation, the cooling pot has a coolant entrance hole to cool down the spent fuel. When a fuel S/A is moved to the outside of the reactor vessel, it must be transferred from a cooling pot to a sodium-filled transfer pot that has no coolant entrance hole. Therefore, this fuel handling procedure is complicated and extends the refueling periods. To simplify the function of the IVS and thus shorten the refueling period, the heat generation of spent fuel S/A's in the IVS rack should be decreased to a level less than that for which the heat can be removed by natural convection of coolant in a transfer pot. For this purpose, the replacement of the outer SS reflectors by B_4C shields, which are considered as in-vessel shields in the demonstration FBR(DFBR) in Japan, is now under investigation.This paper summarizes the results of shielding analysis around JOYO core. Furthermore, this study has been carried out as a part of a series of design efforts for the Mk-III program. The main core parameters of the Mk-III core and the core matrix are shown in Table 1 and Fig.1, respectively.

Table 1. Main Core Parameters of MK-III Core

Reactor Output	MWt	140
PRIMARY Coolant Flow Rate	t/h	2,700
Reactor Inlet Temperature	℃	350
Reactor Outlet Temperature	℃	500
Number of fuel S/A		85
Number of control Rods		6
Core Stack Length	cm	50
Core Diameter	cm	82
Core Volume(max.)	ℓ	250
Fuel Pin Diameter	mm	5.5
$PuO_2/(PuO_2+UO_2)$	w/o	~ 30
^{235}U Enrichment	w/o	~ 10(Inner Core) ~ 16(Outer Core)
Neutron Flux(max.)	$n/cm^2 \cdot sec$	5.5×10^{15}

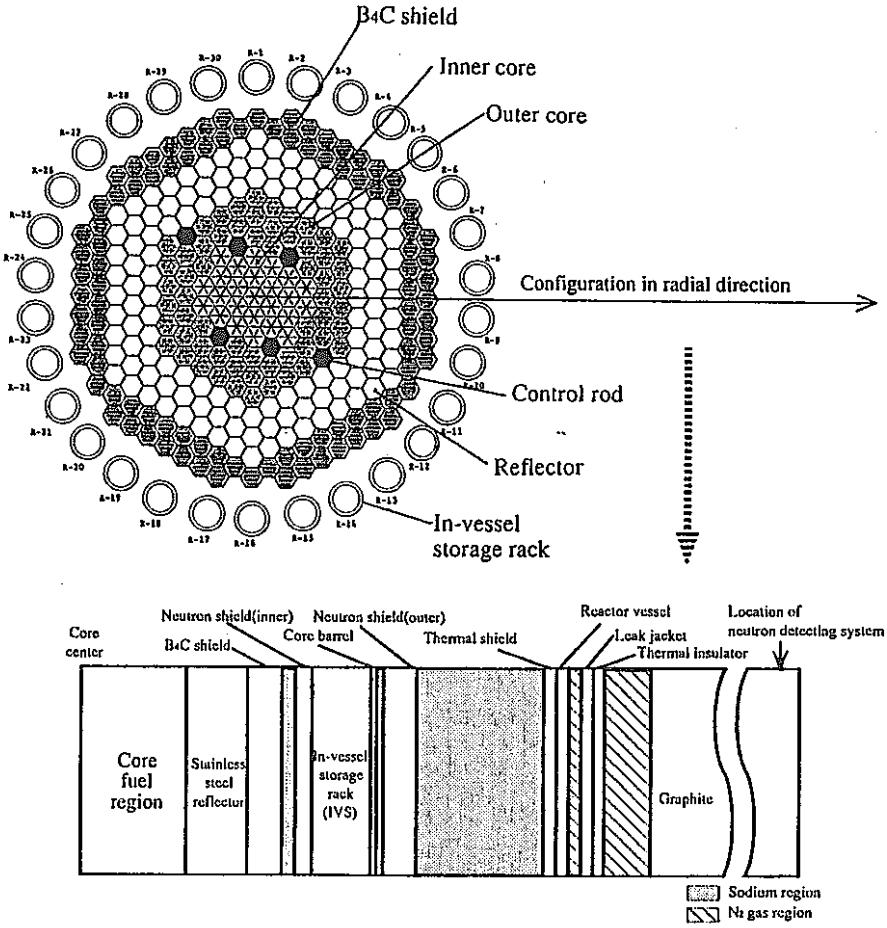

Fig. 1. Core configuration of JOYO

2. METHOD OF SHIELDING ANALYSIS

(1) Design Goal

The first step in the analysis was the determination of the maximum allowable thermal power level of a fuel S/A in the IVS rack. A fuel S/A generates heat not only by fission due to neutrons leaking from the core, but also by gamma-heat and decay heat. From the results of the evaluation of the clad temperature of IVS fuel, it was shown that the maximum clad temperature reaches the design limit when a fuel S/A has a thermal power level of 65kW. Taking into account the design margin and uncertainties in the heat generation, the limit on heating in the IVS fuel was conservatively set at 50kW.

(2) Calculational Method

The calculational scheme involved several computer codes. First, the "RADHEAT-V3"[1] code system was used to prepare a coupled 100-neutron and 20-gamma-ray group cross section library. The basic cross section data were obtained from the shielding nuclear data library JSDJ2/JFTJ2,which is based on the Japanese Evaluated Nuclear Data Library Version 2 (JENDL-2)[2], "New POPOP4" (gamma production cross sections), and "GAMLEG-N" (gamma transport cross sections). Second, as the first stage of the design, the neutron flux distributions in the radial direction were calculated parametrically with the one-dimensional(1-D) discrete ordinates (Sn) code "ANISN-W"[3] to investigate basic specifications of B_4C shield (such as radial thickness or B_4C volume content in the S/A) which satisfy the design goal.

According to the decided basic specifications of the B_4C shields, the 1-D calculations were carried out from the core center to the biological shield in the radial direction and from the bottom of the core support to the rotating pump in the axial direction using multi-group cross sections. The multi-group cross sections were collapsed to a region-dependent broad-group structure consisting of 21 neutron and 7 gamma-ray groups using the spectra obtained from ANISN-W.

In addition, the neutron source distribution that was used for both the 1-D calculation and two-dimensional(2-D) calculations was obtained from the 7 neutron energy groups, 2-D R-Z calculation performed with the diffusion theory code "CITATION"[4] using the fission spectrum of ^{239}Pu.

Lastly, the 2-D Sn code "DOT3.5"[5] was used in an R-Z geometry, to perform detailed design analyses and obtain results such as (1) the thermal power of a spent fuel S/A, (2) the response of the ex-vessel neutron instrumentation system(NIS). In addition, the shielding design was totally evaluated.

The schematic flow diagram of shielding analyses employed in this study is shown in Fig 2. The calculational conditions are shown in Table.2. The analytic accuracy using the system has been evaluated and verified through the analyses of experimental results from the Japanese-American shielding Program of Experimental Research (JASPER program[6]) being performed at the Oak Ridge National Laboratory(ORNL). The system has been utilized in the design analyses of the prototype FBR, "MONJU", and DFBR.

Table 2. Parameters of Calculation by DOT 3.5

	2-D R-Z		2-D X-Y
	Step 1	Step 2	
Geometry	Cylinder R: 2.5 Meters from Core Center to Graphite Shild Z: 7.3 Meters from Bottom of Core Support to Rotating Plug	Cylinder R: 2.8 Meters from Graphite Shield to Biologocal Shield Z: 7.3 Meters from Bottom of Core Support to Rotating Plug	Plane X: 3.25 Meters from Core Center to Biological Shield Y: 3.25 Meters from Core Center to Biological Shield
Number of Mesh Intervals	R: 96 Z: 200	R: 69 Z: 200	X: 107 Y: 107
Order of Scattering	P_3	P_3	P_3
Number of Angles	S_{30}	S_{96}	S_{30}
Number of Energy Groups	Neutron 21Groups, Gamma-ray 7Groups		
Boumdary Conditions	Left : Reflection Bottom&Right&Top : Vacum	Left : Boundary Source(STEP1) Bottom&Right&Top : Vacum	Left&Bottom : Reflection Right&Top : Vacum
Acceleration Technique	Space Dependent Scaling(MWESOL) $\varepsilon < 0.01$		
Flux Calculation Model	Weighted Difference		

3. BASIC SPECIFICATIONS OF THE B_4C SHIELD S/A

Considering the shielding characteristics of B_4C, we chose a radial shielding arrangement with the SS reflectors loaded outside of the core and the B_4C shields loaded in the outermost region. To decide the basic specifications of the B_4C shield, a survey calculation of the thermal power level of an IVS fuel was carried out by using ANISN-W. The design parameters were the number of B_4C shield S/As, the B_4C volume content in the S/A, and the ^{10}B enrichment. The thermal power level of a fuel S/A is evaluated from the fission rate calculated by ANISN-W, and to increase reliability, it is corrected by applying the bias factor(C/E) that is evaluated through the analysis of the reaction rate distribution measurement in the JOYO Mk-II core, (the core is surrounded by SS reflectors only).

The relationship between the thermal power level of a fuel S/A and the B_4C volume content in a S/A when SS reflectors are loaded in the 6~8th rows and B_4C shields are loaded in the 9~10th rows is shown in Fig. 3. Also, the relationship between the thermal power of a fuel S/A and the ^{10}B enrichment of the B_4C shields loaded in the 10th row, when the B_4C volume content of all B_4C shields is 40%, is shown in Fig. 4. As a result of this survey, it is shown that increasing the B_4C volume content in a S/A more effectively decreases the thermal power of an IVS fuel S/A than does increasing the ^{10}B enrichment of the B_4C shields loaded in the 10th row. The analysis leads to the following specifications:

- 96 B_4C shield S/A's are loaded in the outermost 2 rows of the core matrix
- the B_4C volume content in a S/A is 45%
- the ^{10}B enrichment is 20% (natural boron).

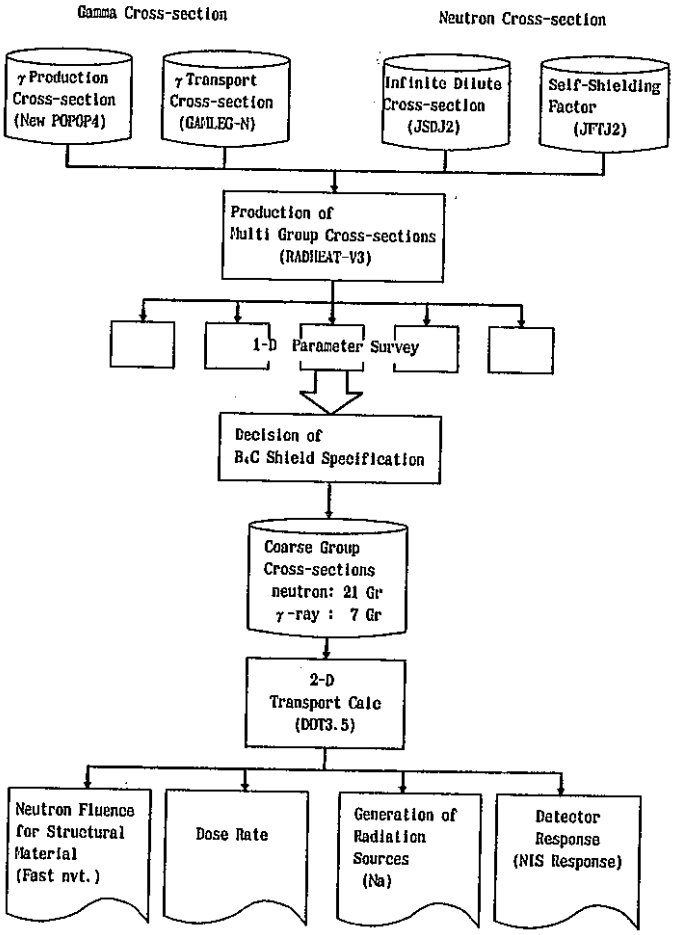

Fig. 2. Schematic Flow Diagram of Shielding Design

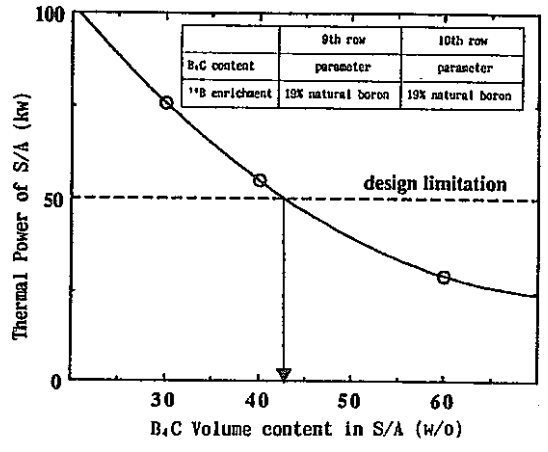

Fig. 3. Relationship between the thermal power of S/A in IVS and the B_4C volume content in B_4C shield S/A

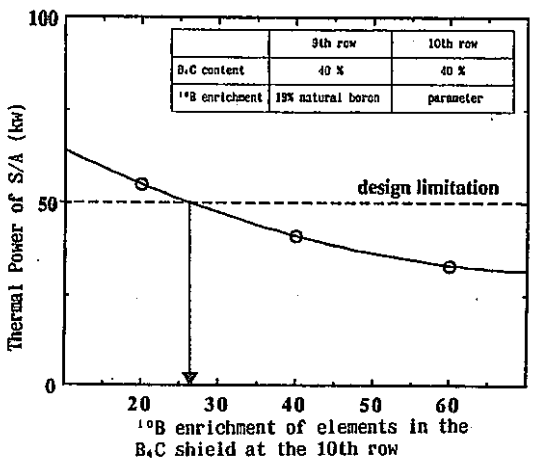

Fig. 4. Relationship between the thermal power of S/A in IVS and the ^{10}B enrichment of B_4C element

4. RESULTS OF THE DETAILED CALCULATION

According to the basic specifications decided in the section 3, detailed design analyses were performed with the 2-D Sn code "DOT3.5" in R-Z geometry. The calculational region is shown in Fig. 5. First , an S30-P3 calculation was performed as Step 1 from the core center to the inside of graphite shield region in the radial direction, and from the bottom of the core support to the rotating plug in the axial direction. Next, by applying the "boot-strapping technique", an S96-P3 calculation was performed as Step 2 from the reactor vessel to the biological shielding concrete region in the radial direction. In the calculation of step 2, the number of angular quadrature directions is increased to 96 in order to take into account the effect of neutron streaming in the nitrogen gas region.

The followings are shielding characteristics that have been evaluated through this work.

(1) The heat generation of an IVS fuel

In JOYO, 30 IVS racks are located at the outside of the reflector-shield region (R=96cm from core center), and each IVS rack is isolated from the others. To evaluate the heat generation of an IVS fuel, it is required that the neutron multiplication effect of the isolated fuel S/A be considered.

First, we calculated the neutron flux at the IVS rack using two R-Z models. One had a fuel region at the location of IVS and the other had a sodium region(no fuel). In the calculation for the former

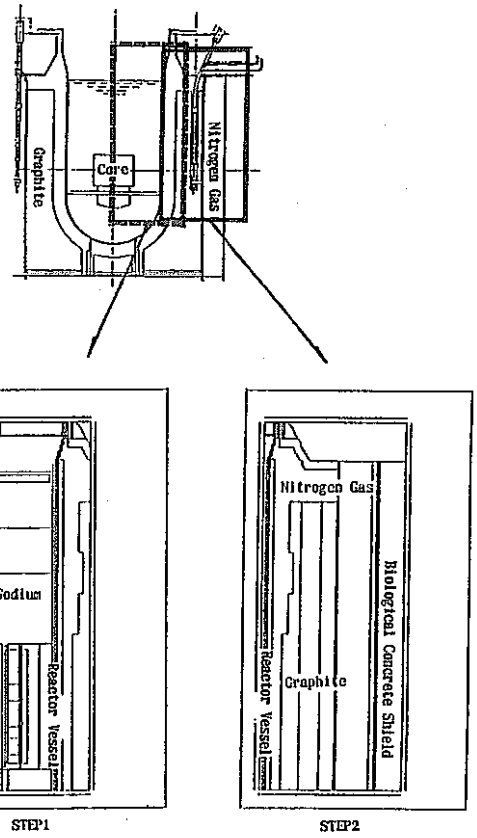

Fig. 5. Geometry modelings for 2-dimensional calculations

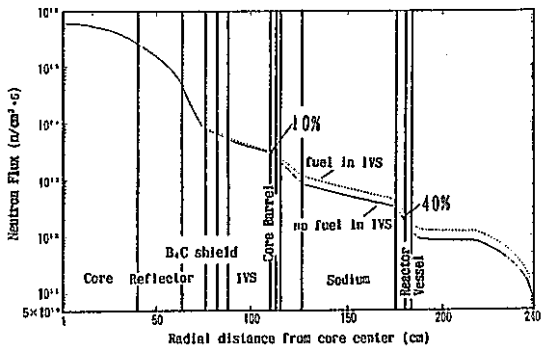

Fig. 6. Radial traverse of fast neutrin flux

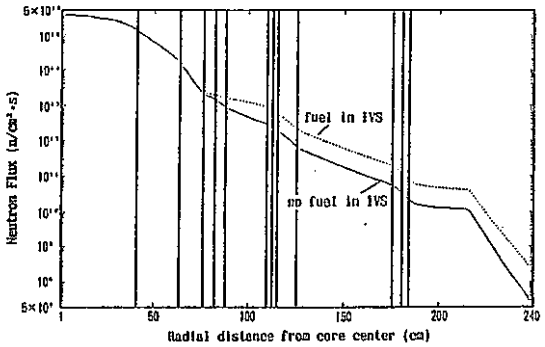

Fig. 7. Radial traverse of fast neutrin flux

case, the neutron source in the core was fixed but outer iterations were required to converge the fission source in the fuel region in the IVS.

The comparisons of total and fast (E>0.1Mev) neutron flux for the two models at the core midplane are shown in Fig.6 and Fig.7, respectively. Taking into account the IVS fuels increases the total neutron flux at the IVS by ~10%, affecting the evaluation of fission rate of IVS fuel. As in the R-Z model, the fuel region at the IVS was homogenized and modeled as a ring, the calculated results might overestimate the neutron multiplication effect . In order to verify the calculated results on neutron multiplication effect of the isolated fuel S/A in the IVS rack precisely, calculations with DOT3.5 in X-Y geometry were also carried out for a quarter of the core with the following 5 models that had IVS fuel in certain patterns (see Fig.8).

Case 0 : Equivalent to the R-Z model (same as the homogenized model of Case 2).

Case 1 : No fuel in IVS.

Case 2 : All IVSs are filled with fuel.

Case 3 : One half of IVSs are filled with fuel.

Case 4 : Alternate IVSs are filled with fuel.

Case 5 : One IVS is filled with fuel.

The thermal powers of the IVS fuel S/A's evaluated from the calculated neutron flux for each case are summarized in Table 3. From the results, the following are made clear:

- The change of thermal power caused by the homogenizing is less than 1%.
- The thermal power decreases with the increase of fuel S/A's in the closer IVS racks.
- The thermal power of a spent fuel S/A loaded alone(Case 5) was higher than that for a fuel S/A loaded as a ring(Case 0 : same as R-Z model) by a factor of 1.09.

Considering the factor 1.09 to the thermal power evaluated from the result of the R-Z calculation, the maximum thermal power of the IVS fuel is expected to be 45kW, which is lower than the design goal (50kW).

Thus, it is recognized that the arrangement of SS reflectors and B_4C shields, decided in section 3, satisfies the design goal.

(2) The response of the NIS

In JOYO, the change of neutron flux or reactivity is monitored by the response of the ex-vessel NIS. As the response of the NIS must be decreased by introducing the B_4C shields, we evaluated the change of the response of the NIS from the results of the shielding analyses.

Two systems utilizing a fission chamber are located in the graphite region(R=290cm) in JOYO. The response of the NIS is evaluated as a fission rate of ^{235}U, which is calculated from the neutron flux at the location of the NIS and the fission cross section of ^{235}U. From the result of the 2-D R-Z calculation, the response of the NIS of the MK-III core with the B_4C shields decreases by half compared with that of MK-II core. Next we evaluated the effect of the fuels in the IVS racks on the response of the NIS from the results of 2-D X-Y calculation. The comparison of the total neutron flux distribution of typical examples, such as Cases 1, 2,and 5, are shown in Fig. 9. It is shown from Fig.9 that the total neutron flux at the location of the NIS increases in proportion to the increase in the number of IVS fuels. Table 4 shows the fission rate of ^{235}U at the location of the NIS for all the calculational cases. As the ratio of response of Case 1 for which fuel S/As are loaded in all IVS racks, to that of Case 2, for which no fuel is loaded in the IVS racks is 0.65, at least 65% of the NIS response for Case 1 is caused by the neutrons leaking from the core region for any case.

As a result, it was made clear that the NIS in JOYO has a high enough response to allow monitoring the core neutronics, even when the B_4C shields are loaded.

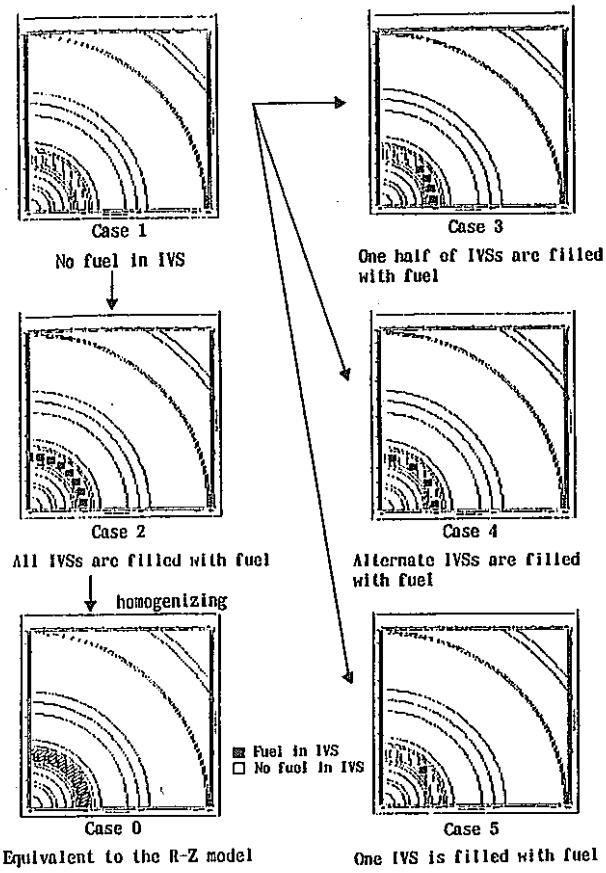

Fig. 8. Models for the 2D X-Y calculations by DOT3.5

Table 3. Thermal Power of Fuel S/A in IVS

	Case 0	Case 2	Case 3	Case 4	Case 5
Thermal Power (kW)	45.2	44.7	43.1 (46.8)*	48.6	49.4
Ratio	1.00	0.99	0.95 (1.04)*	1.08	1.09

* : Value of the S/A that IVS on one side is filled with fuel S/A and another is filled with sodium

Table 4. ^{235}U Fission Rate at the Location of NIS

Case	Reaction Rate(n/cc·s)	Ratio
1	7.17×10^{-11}	1.00
2	1.05×10^{-10}	1.46
3	8.89×10^{-11}	1.24
4	9.10×10^{-11}	1.27
5	7.78×10^{-11}	1.09

5. SUMMARY

The results obtained from the shielding study of the JOYO design with B_4C are summarized as follows:

- The basic specifications and arrangements of B_4C shield S/A's were decided.
- The radiation distribution inside and outside the reactor vessel containing a small FBR core with SS reflectors and B_4C shield S/A's was analyzed in detail.
- With the results of 2-D R-Z and 2-D X-Y calculations, the effects of isolated neutron sources located outside the core could be evaluated quantitatively.
- By considering the effect of an isolated neutron source, it was confirmed that the maximum thermal power of an IVS fuel S/A satisfies the design limitation.
- It was shown that although the response of the NIS decreases by approximately 1/2 with B_4C shields, it is still high enough to monitor the core neutronics from the point of view of safe reactor operation.

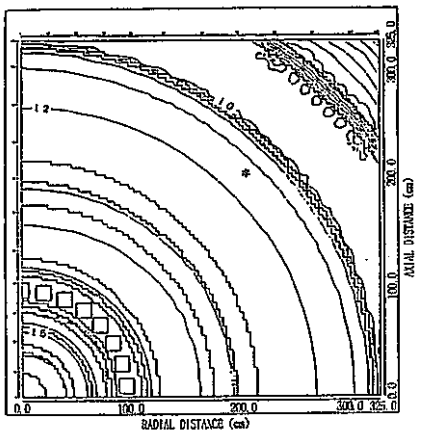

Case 1

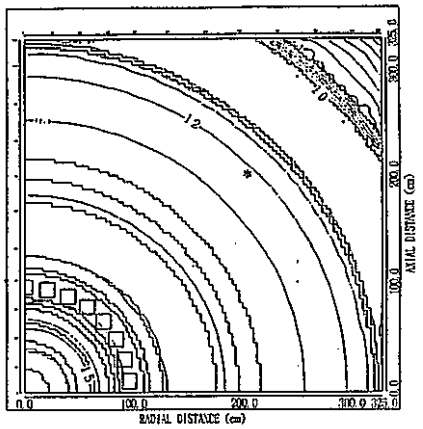

Case 2

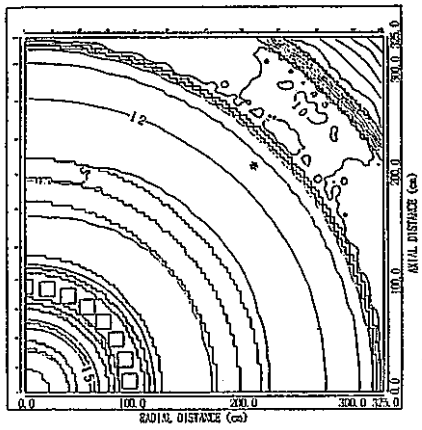

Case 5

* : Location of the NIS

Fig. 9. Total Neutron Flux Distributions calculated for 2D X-Y models

6. CONCLUSIONS

In this study, we investigated a JOYO shielding design having B_4C shields that are expected to be the in-vessel shield of future FBRs. A key result of this study is that when the outermost two layers of SS reflectors are replaced by two layers of B_4C shields, the heat generation in an IVS fuel due to core-leakage neutron-induced fission decreased, and the refueling procedure could be simplified by the elimination of fuel transfer between two types of coolant pots at refueling.

Finally, when the response of ex-vessel NIS and the neutron fluence at the in-vessel structure were evaluated using results from the detailed calculation of radiation distribution, it was shown that on the whole the shielding characteristics of B_4C shield satisfied the design requirements even when the reactor power was increased by 40%.

REFERENCES

1. K. Koyama et al., "RADHEAT-V3, A Code System for Generating Coupled Neutron and Gamma-Ray Group Constants and Analyzing Radiation Transport", JAERI-M7155(1977)
2. T. Nakagawa, et al., "Summary of JENDL-2 General Purpose File", JAERI-M84-103(1984)
3. W. W. Engle Jr., "A Users Manual for ANISN: A One Dimensional Discrete Ordinates Transport Code with Anisotropic Scattering," ORNL-K-1693(1976),WANL-TM1(1967)
4. T. B. Fowler, et al, "Nuclear Reactor Core Analysis Code : CITATION", ORNL-TM-2496, Rev. 2(11971)
5. F. R. Mynatt et al., "The DOT III Two-Dimensional Discrete Ordinates Transport Code," ORNL/TM-4280(1973)
6. N. Ohtani, et al, "Advanced in FBR Shielding - Ten Years in Japan-", Proc. LMR Progress and Promise, ANS Winter Mtg., Washington D.C., USA, Nov. 1990;p89(1990)

Experiment and Analysis of Neutron Streaming through an Axial Shield in an FBR Fuel Subassembly

K.Chatani, H.Tsunoda*, A.Shono,
S.Suzuki and K.Kinjo
O-arai Engineering Center
Power Reactor and Nuclear Fuel
Development Corporation
O-arai, Ibaraki, Japan
3-011-81-0292-67-4141

ABSTRACT

Power Reactor and Nuclear Fuel Development Corporation (PNC) and United States Department of Energy started the cooperative shielding experiments program designated JASPER (Japanese-American Shielding Program for Experimental Research) in 1985. The second and third JASPER experiments, the Fission Gas Plenum Experiment** and the Axial Shield Experiment*** were conducted to improve the prediction accuracy of the shielding analysis for the neutron streaming along the fission gas plenum of the fuel elements and along the sodium channel of fuel subassembly. This is important in order to evaluate the fast neutron fluence on the core support plate and the activation of the secondary sodium contained within the Intermediate Heat Exchanger (IHX).

The Fission Gas Plenum experiment indicated that the neutron streaming was not an important consideration in the fission gas plenum region. The measurement data for axial shields, which consisted of boron carbide or stainless steel, were also provided to evaluate the neutron streaming in the axial shielding region. Comparisons of the experimental results with the two dimensional analytic results obtained using the shielding analysis system for Fast Breeder Reactor (FBR) indicated that streaming can be predicted within five percent accuracy in this case.

1. INTRODUCTION

PNC has developed and verified the shielding analysis system for the FBR through measurements and analyses on experimental fast reactor JOYO in Japan and through the international information exchange. The FBR analysis system has been used for the shielding design of the prototype fast breeder reactor MONJU and demonstration FBR (DFBR) as the standard shielding method of Japan.

The JASPER program [1), 2), 3)] was planned and performed to improve the prediction accuracy, using the shielding analysis system, to study the nuclear characteristics of the boron carbide (B_4C) and graphite and to develop the new shielding materials such as zirconium hydride. The first JASPER experiment provided the neutron attenuation data for the removable radial shield which consisted of the B_4C, graphite and stainless steel (SS). Analysis of this experiment provided the data useful for impovement of the prediction accuracy. This paper summarizes the Fission Gas Plenum Experiment and the Axial Shield Experiment is focused on the analysis of the neutron streaming in an FBR fuel subassembly.

2. DESCRIPTION OF THE EXPERIMENTS

2.1 FISSION GAS PLENUM EXPERIMENT

The Fission Gas Plenum Experiment as the second JASPER experiment was conducted from January through February of 1987 to investigate the neutron streaming in the gas plenum region of DFBR fuel elements. The experimental mockups consisted of a 61 cm in diameter gas plenum region and the concrete surrounding the gas plenum region as shown in Fig. 1.
The gas plenum region was made of SS and aluminum(Al) which was used as a substitute for the sodium(Na). The volume fractions for SS, Al, and air were 15% 18% and 67% respectively. The mockups were either homogeneous or heterogeneous. The heterogeneous mockups consisted of a total of 512 SS tubes with an outer diameter(OD) of 7.93 mm. This

* H. Tsunoda of Mitsubishi Research Institute participated in the calculations and analyses of this work.

** Experiment conducted at the Tower Shielding Facility by F. J. Muckenthaler (chief experimentalist), B. D. Rooney, and J. D. Drischler of Oak Ridge National Laboratory (ORNL) and N. Ohtani of Power Reactor and Nuclear Fuel Development Corporation (PNC).

***Experiment conducted at the Tower Shielding Facility by F. J. Muckenthaler (chief experimentalist), R. R. Spencer, and H. T. Hamilton of ORNL and A. Shono of PNC.

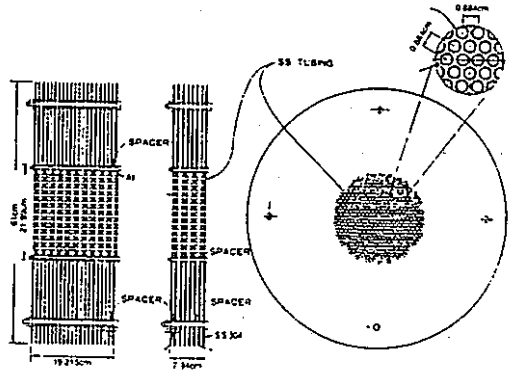

Heterogeneous Gas Plenum Inserts

Schematic of heterogeneous gas plenums

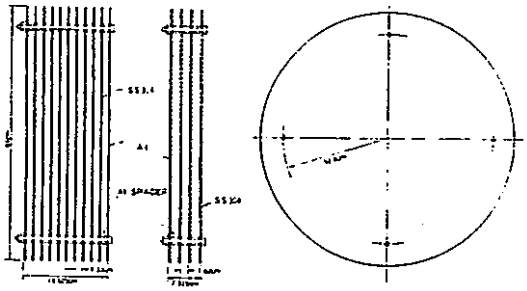

Heterogeneous Gas Plenum Inserts

Schematic of homogeneous fission gas plenums

Fig. 1 Experimental Mockups of the Fission Gas Plenum Experiment

heterogeneous region was 22 cm in diameter. Axial lengths of 20 cm and 8 cm were used. Neutron streaming was determined by measuring the neutron flux with the Bonner ball or the Hornyak button.

Comparisons of the heterogeneous to homogeneous measurement results showed there was no significant streaming for either of axial plenum lengths (20 cm and 8 cm). The neutron source entering the mockups had a nearly isotropic distribution because the mockups were preceded by UO_2 slabs representing the radial blanket. In the actual reactor, the neutron flux entering the gas plenum region is more isotropic than in this experiment. Therefore, it is not necessary to consider neutron streaming.

As a result of the experiment, it was confirmed that the ordinary calculational modeling in the FBR shielding design, in which the calculational region is homogenized according to the volume fraction of each structural material, is adequate.

2.2 AXIAL SHIELD EXPERIMENT

The Axial Shield Experiment was the third JASPER experiment performed from August through December of 1990. The purpose was to evaluate the neutron attenuation characteristic of and the neutron streaming through the different axial shielding designs consisting of the different shielding materials, as well as to improve the analysis accuracy for regions beyond the fission gas plenum region.

The 45-cm-long experimental mockups were fabricated in the form of a central hexagon surrounded by six hexagons measuring 15 cm from flat edge to flat edge. The experimental mockups were surrounded by B_4C and concrete as shown in Fig.2.

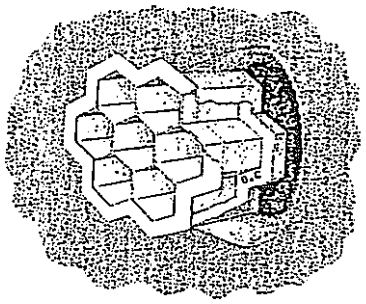

Support Structure for Experimental Assemblies

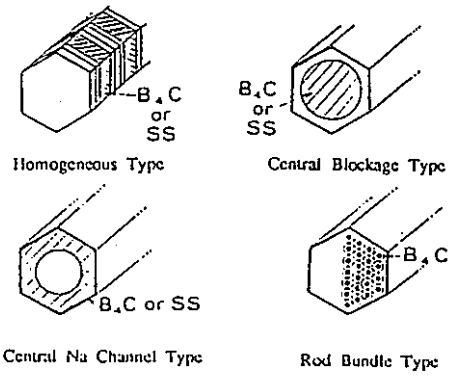

Fig. 2 Experimental Assembly of the Axial Shield Experiment

The shielding materials were B_4C and SS. The mockup designs consisted of a central blockage type, a rod bundle type, a central Na channel type, and their corresponding homogeneous types. The volume fractions for SS, Al, and B_4C were 11%, 29% and 60% for the B_4C hexagon assembly. For the SS hexagon assembly, the volume fractions for SS and Al were 71% and 29 %. Neutron streaming was evaluated by measuring with the

Bonner ball or the Hornyak button detectors. As the evaluation of the fast neutron flux is important in the FBR shielding design, the results of the Hornyak button and the Bonner ball detectors, which are sensitive to fast neutron energy, are rather important.

The streaming factor defined as the Hornyak buttor heterogeneous-to-homogeneous measurement ratio is shown in Fig. 3 for the central Na channel type.

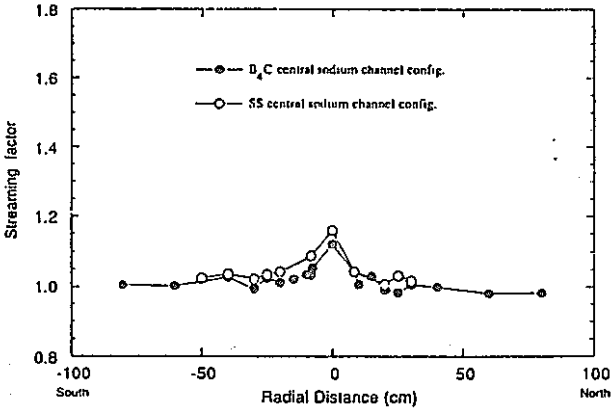

Fig. 3 Radial distribution of streaming factor derived from measured Hornyak button data.

The railial distribution of the measured streaming factors is very similar for the B_4C subassembly and the SS subassembly. As stated the above, the data were used to evaluate the magnitude of neutron streaming which is necessary for analyzing the FBR shielding design.

3. CALCULATIONAL METHOD

The calculations were performed using the shielding analysis system for the FBRs shown in Fig.4. This analysis system, which is based on the calculational method used for the MONJU shielding design, is the standard shielding analysis system in Japan. The 100 nuclear group constants employed in the calculations were prepared from the JENDL-2[4] file, and were changed to effective cross section by the RADHEAT code system[5]. The effective cross sections were collapsed to 21 nuclear group constants using the one-dimensional discrete ordinates radiation transport code ANISN-W[6]. The selection of nuclear group constants were determined from experience with MONJU shielding design. The two dimensional calculations were conducted using the two-dimensional discrete ordinates computer code DOT 3.5[7] and DORT[8]. Bonner ball responses were calculated with the SPACETRAN code[9].

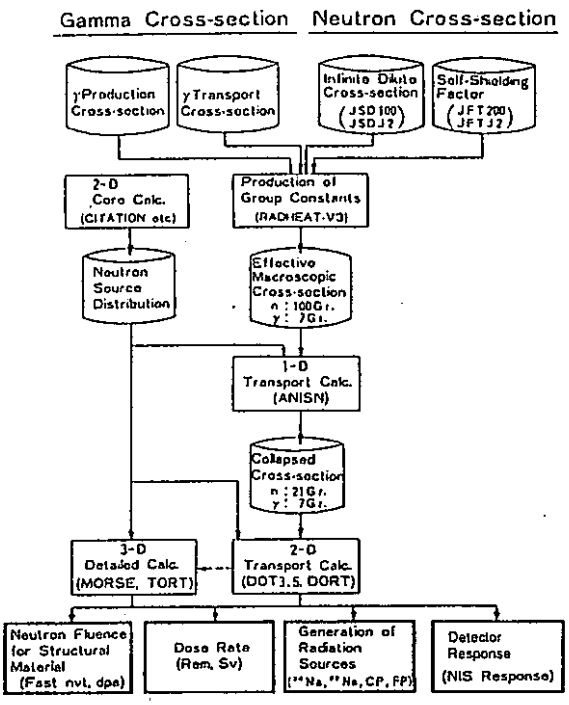

Fig. 4 Schematic Flow Diagram for the Shielding Analysis FBR Design

4. EXPERIMENTAL ANALYSIS

4.1 ANALYSIS OF THE FISSION GAS PLENUM EXPERIMENT

Because measured results indicated no streaming along the gas plenum region, a series of the two-dimensional calculations were performed for the homogeneous configurations only to estimate the accuracy of the calculational system mentioned above.

For the spectrum modifier configuration, calculated Bonner ball responses on centerline axis showed good agreement with the measured responses. Calculated-to-measured ratio (C/E) values were in the range of 1.0 to 1.1 for five types of Bonner ball responses. For the 8 cm length fission gas plenum configuration, C/E values were in the range of 1.1 to 1.2. For the 20 cm length configuration, C/E values were in the range of 1.2 to 1.3. These results indicated that with an increase in the length of the experimental test slab, the C/E values increase also. One of the main reasons of this tendency was the inconsistency between compositions used for the calculation and the real compositions, especially the water content in the concrete region which surrounded the gas plenum.

4.2 ANALYSIS OF THE AXIAL SHIELD EXPERIMENT

One of the main objectives of this experimental analysis is the estimation of the calculational system accuracy employed for the FBR shielding design when it is applied to configurations

where neutron streaming dominates. So, conventional two-demensional Sn calculations were performed and compared to the measured results.

Preliminary results showed uncertain ties in the concrete compositions of the test slab might cause Bonner ball responses for the homogeneous model to be overestimated not only for the B_4C configuration but also for the SS configuration. Since more certain compositions are not yet available, an estimate of the composition was temporarily determined from survey calculations by varying the water content. In the calculation using this determined composition, radial C/E distributions were flat.

For the homogeneous assembly model, C/E values of Bonner ball responses were in the range of 1.1 to 1.3 for the B_4C configuration and 1.0 to 1.1 for the SS configuration. For the heterogeneous assembly model, comparisons with measured and calculated responses were performed for the central sodium channel configurations. Calculated responses using symmetric 96 direction angular quadrature underestimated measured responses about 20 to 30 % for centerline detection points. Thus, the calculations for such configurations where neutrom streaming dominates were performed using biased 100 direction angular quadrature. The results are shown in Table 1 for the B_4C configuration and Table 2 for the SS configuration along with the corresponding homogeneous configuration results.

In this case, a streaming factor was defined as the ratio of heterogeneous to homogeneous Bonner ball responses. Comparisons of these measured and calculated factors are shown in Table 3 for the B_4C and Table 4 for the SS, respectively. Calculated and measured streaming factor agreed with each other within five percent for almost all Bonner ball detectors.

Table 1. Calculated to measured ratios (C/E) for B_4C central sodium channel configuration

	Bonner ball Detectors	Homogeneous Configuration	Heterogeneous Configuration
*1	3-in BB	1.08	1.10
	4-in BB	1.10	1.10
	5-in BB	1.10	1.07
	8-in BB	1.17	1.12
	10-in BB	1.21	1.18
	12-in BB	1.29	1.26
*2	3-in BB	1.69	1.66
	4-in BB	1.36	1.38
	5-in BB	1.26	1.26
	8-in BB	1.32	1.33
	10-in BB	1.48	1.50
	12-in BB	1.58	1.70

*1) 30 cm behind shield mockup
*2) 150 cm behind shield mockup

Table 2. Calculated to measured ratios (C/E) for SS central sodium channel configuration

	Bonner ball Detectors	Homogeneous Configuration	Heterogeneous Configuration
*1	3-in BB	1.06	1.12
	4-in BB	1.00	1.05
	5-in BB	1.00	1.04
	8-in BB	1.03	1.07
	10-in BB	1.07	1.05
	12-in BB	1.10	1.13
*2	3-in BB	1.13	1.10
	4-in BB	0.97	0.98
	5-in BB	0.93	0.94
	8-in BB	0.97	0.98
	10-in BB	1.09	1.06
	12-in BB	1.27	1.24

*1) 30 cm behind shield mockup
*2) 150 cm behind shield mockup

Table 3. Measured and calculated streaming factors (Sf) derived from Bonner rsponse for B_4C central sodium channel configuration

	Bonner ball Detectors	Measured Sf's (E)	Caluculated Sf's (C)	(C-E)/E
*1	3-in BB	1.28	1.30	0.01
	4-in BB	1.29	1.30	0.00
	5-in BB	1.26	1.22	-0.03
	8-in BB	1.14	1.09	-0.04
	10-in BB	1.07	1.04	-0.03
	12-in BB	1.05	1.02	-0.03
*2	3-in BB	1.19	1.17	-0.02
	4-in BB	1.19	1.21	0.02
	5-in BB	1.20	1.21	0.01
	8-in BB	1.13	1.14	0.01
	10-in BB	1.09	1.10	0.01
	12-in BB	1.01	1.08	0.07

*1) 30 cm behind shield mockup
*2) 150 cm behind shield mockup

Table 4. Measured and calculated streaming factors (Sf) derived from Bonner ball response for SS central sodium channel configuration

	Bonner ball Detectors	Measured Sf's (E)	Caluculated Sf's (C)	(C-E)/E
*1	3-in BB	1.37	1.44	0.05
	4-in BB	1.32	1.38	0.05
	5-in BB	1.28	1.34	0.04
	8-in BB	1.17	1.21	0.04
	10-in BB	1.18	1.16	-0.01
	12-in BB	1.10	1.13	0.03
*2	3-in BB	1.35	1.31	-0.02
	4-in BB	1.29	1.31	0.01
	5-in BB	1.27	1.28	0.01
	8-in BB	1.19	1.20	0.01
	10-in BB	1.18	1.15	-0.03
	12-in BB	1.14	1.12	-0.02

*1) 30 cm behind shield mockup
*2) 150 cm behind shield mockup

From the analyses, the accuracy of the calculational system to predict the neutron streaming factors along the assembly axial direction was estimated to be about five percent for the energy integrated flux.

5. CONCLUSIONS

To estimate the accuracy of prediction of neutron leakage from the FBR fuel assembly, analyses of the JASPER experiments were performed using the standard shielding analysis system used in Japan. Major conclusions from the analyses are the following:

1) The Fission Gas Plenum Experiment showed that it is not necessary to consider neutron streaming along the gas plenum region. Thus, it is assured that the conventional treatment of homogenizing the region based on the volume fraction of each material is adequate for calculating neutron transport through the region.

2) From the Axial Shield Experiment, various streaming factors were obtained from measured detector responses. These factors may be used to calculae C/E correction factors by considering the differences between the design and experimental configurations.

3) From the analyses of Axial Shield Experiment, the accuracy of the calculational system to predict a neutron streaming effect along the fuel subassembly was estimated to be about five percent for the energy integrated flux.

4) Analyses of the Fission Gas Plenum Experiment and the Axial Shield Experiment produced calculated detector responses that were in good agreement with measured detector responses. Information about accuracy of the shielding analysis system will be reflected in the large FBR shielding design.

REFERENCES

1. D.T.Ingersoll and N.Ohtani," JASPER: A Joint U.S.-Japan Program of Experimental Shielding Research,." ANS Topical Conference on Theory and Practices in Radiation Protection and Shielding, Knoxville, USA, April 1987; Proc. Vol. 2, p.346(1987)

2. N.Ohtani et al., " Benchmark Experiment and Analysis of Neutron Penetration through FBR Radial Shield Mockups," Proc.7th Int. Conf. on Radiatiion Shielding, Bournemouth, UK, p433(1988)

3. N.Ohtani and S.Suzuki, " Advancement in FBR Shielding-Ten Years in Japan-," Proc. LMR: A Decade of LMR Progress and Promise, ANS Winter Mtg., Washington D.C., USA, Nov. 1990; P89(1990)

4. T.Nakagawa et al.," Summary of JENDL-2 General Purpose File," JAERI-M84-103(1984)

5. K.Koyama et al., " RADHEAT-V3, A Code System for Generating Coupled Neutron and Gamma-Ray Groups Constants and Analyzing Radiation Transport," JAERI-M 7155 (1977)

6. W.W.Engle Jr., " A Useres Manual for ANISN: A One Dimensional Discrete Ordinates Transport Code with Anisotropic Scattering, " ORNL-K-1693(1967), WANL-TM1 (1967)

7. F.R.Mynatt et al., " The DOT III Two-Dimensional Discrete Ordinates Transport Code, " ORNL/TM-4280(1973)

8. W.A.Rhoades et al., " The DORT Two-Dimensional Discrete Ordinates Transport Code, " Nucl, Sci. & Engr. 99.1, P88 (1988)

9. S.N.Cramer and M.Solomito, " SPACETRAN: A Code to Calculation Dose at Detectors at Various Distances fom the Surface of a Cylinder," ORNL-TM-2592

Ⅲ 日本側資料リスト

B_4C Shielding Design Study for the JOYO Core

Akihiro Yoshida

O-arai Enginnering Center
Power Reactor and Nuclear Fuel Development Corporation
JAPAN

Table Key Parameters of JOYO Core

Items \ Core		MK-II	MK-III
Reactor Output	MWt	100	140
Primary Coolant Flow Rate	t/h	2,200	2,700
Reactor Inlet Temperature	°C	370	350
Reactor Outlet Temperature	°C	500	500
Fuel Stack Length	cm	55	50
Core Volume (max.)	ℓ	230	260
Fuel		MOX	MOX
Fast Neutron Flux (max.) (>0.1MeV)	$n/cm^2 \cdot sec$	3.0×10^{15}	4.1×10^{15}
Max. Burn-up(pin av.)	MWd/t	75,000	~90,000
Plant availability factor		~40%	~60%

OBJECTIVE

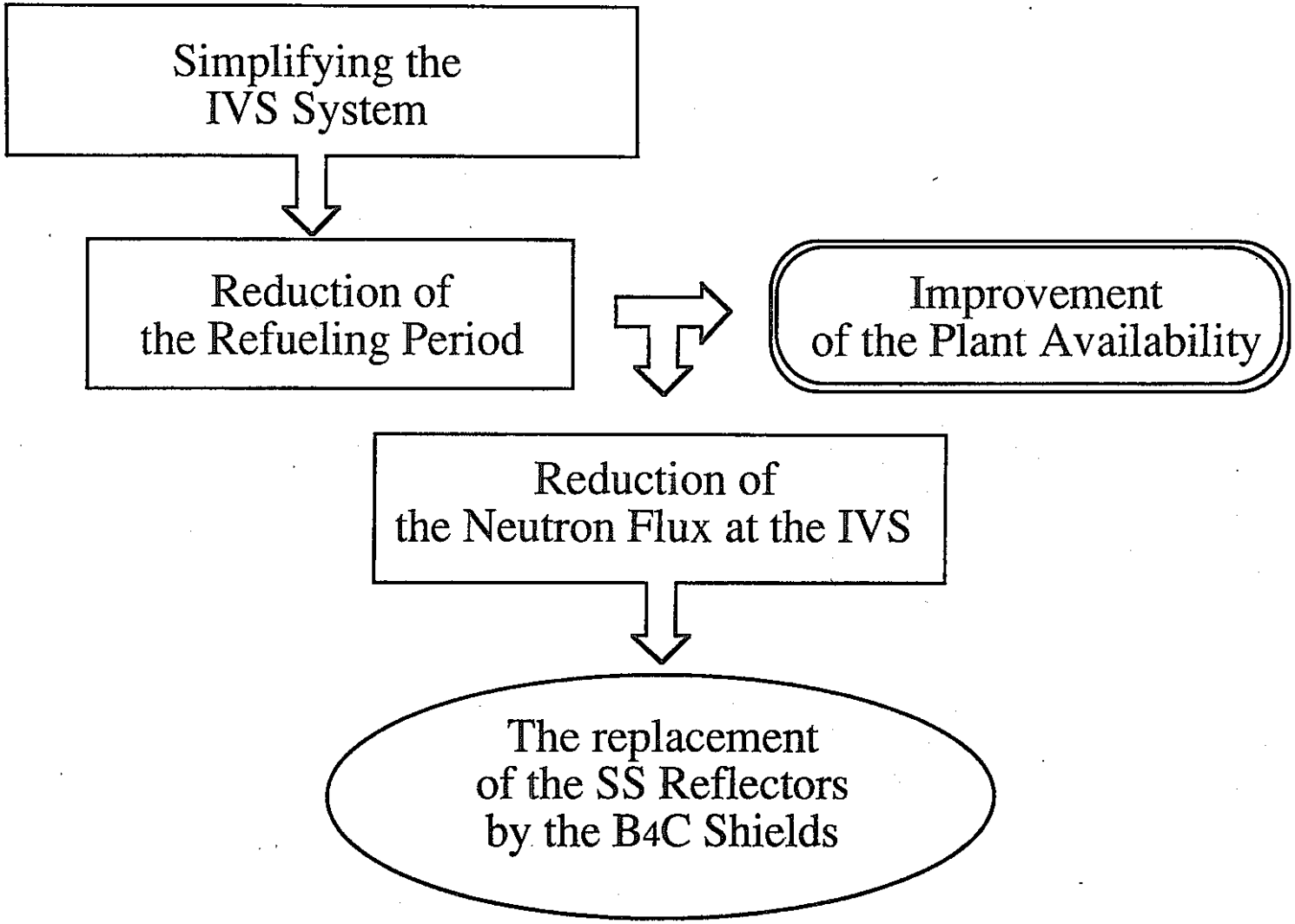
Simplifying the
IVS System
Reduction of
the Refueling Period
Improvement
of the Plant Availability
Reduction of
the Neutron Flux at the IVS
The replacement
of the SS Reflectors
by the B4C Shields

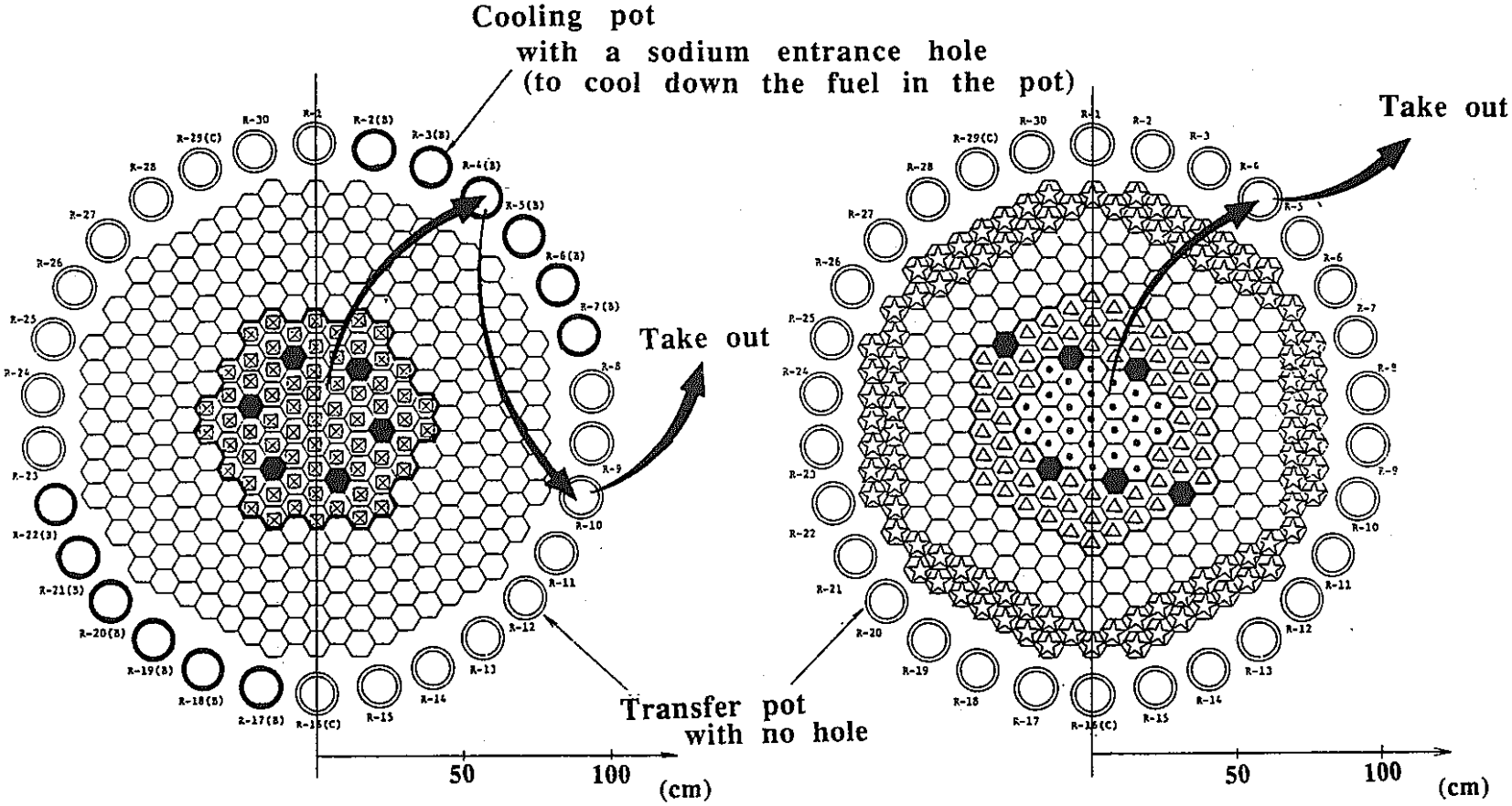

Fig. Refueling Procedure

Design of the B_4C Shields

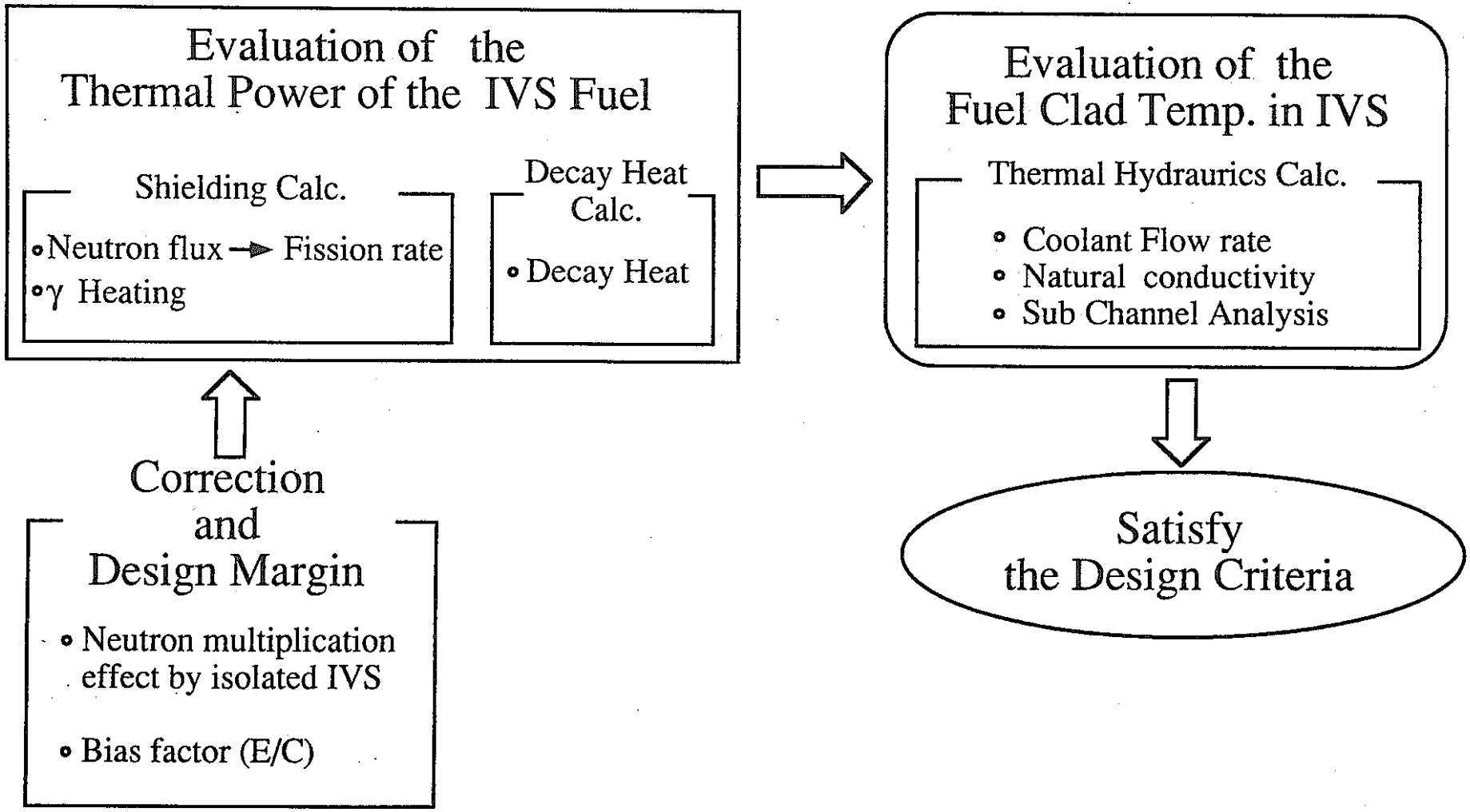

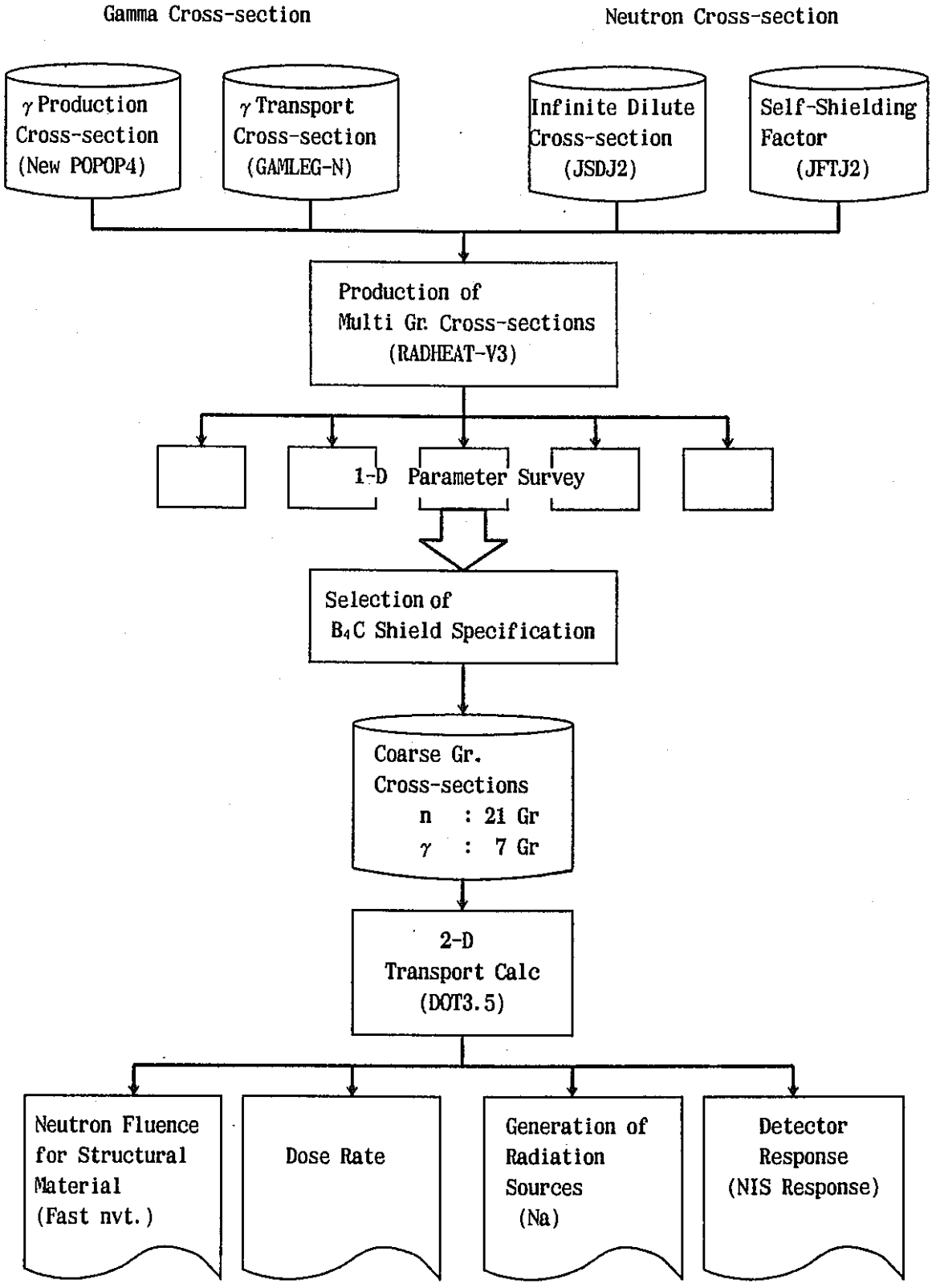

Fig. 2. Schematic Flow Diagram of Shielding Design

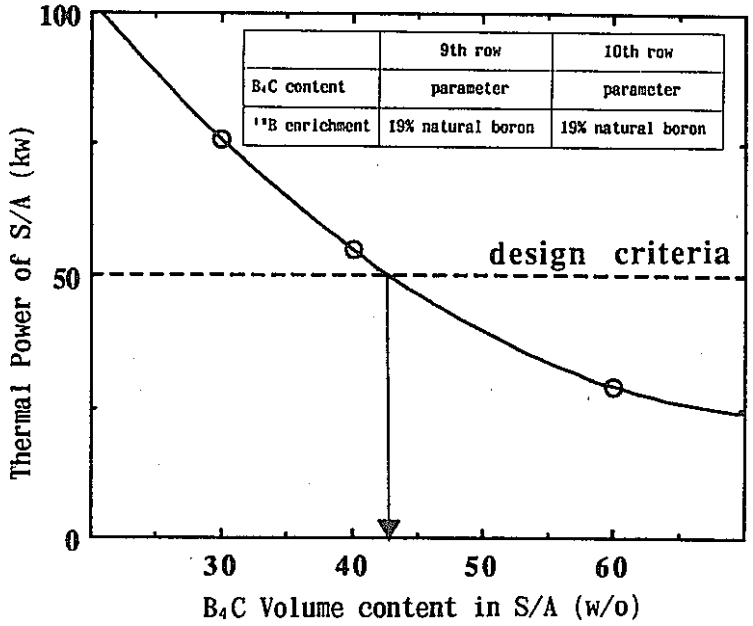

Fig. 3. Relationship between the thermal power of S/A in IVS and the B_4C volume content in B_4C shield S/A

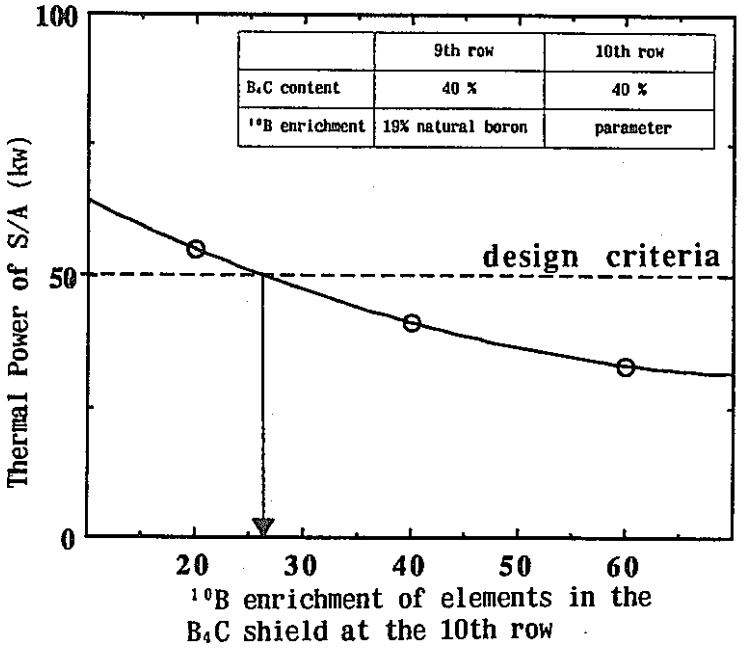

Fig. 4. Relationship between the thermal power of S/A in IVS and the ^{10}B enrichment of B_4C element

The specifications of the B_4C shield

- 96 B_4C shield S/A's in the outermost 2 rows.
- The B4C volume content in a S/A: 45%.
- The ^{10}B enrichment : 20% (natural boron)

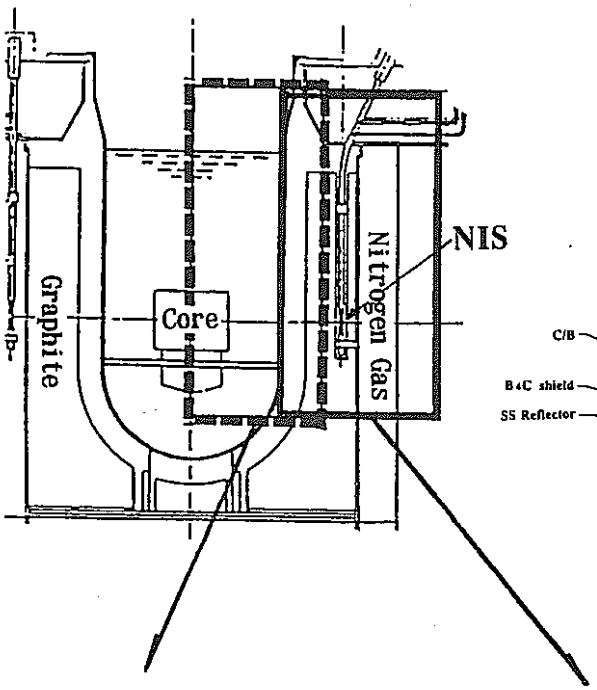

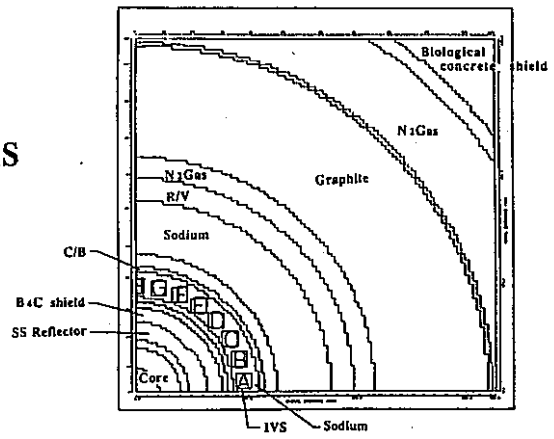

X-Y Model

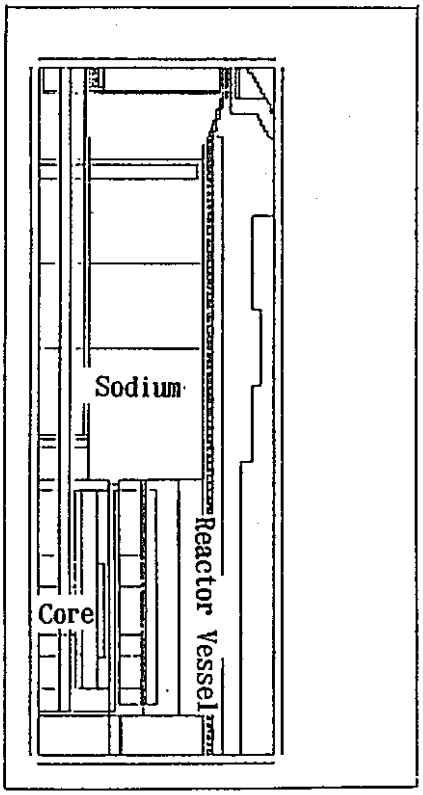

R-Z Model(STEP1)

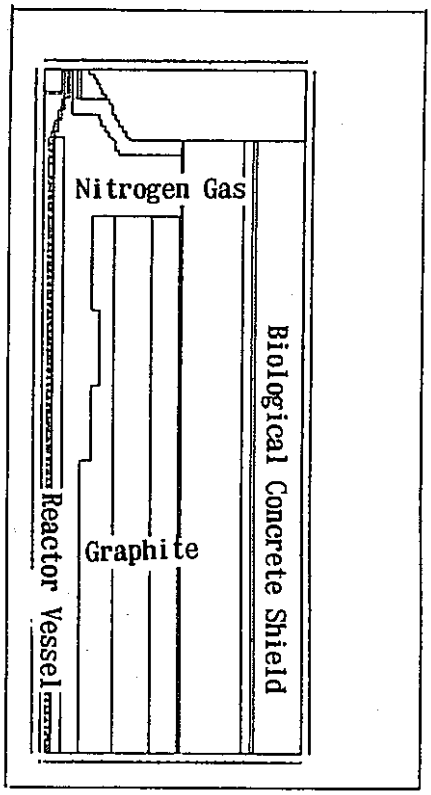

R-Z Model(STEP2)

Geometry modelings for 2-dimensional calculations

Table Parameters of Calculation by DOT3.5

Items \ Model	2D R-Z		2D X-Y
	Step 1	Step 2	
Objective of Calc.	In-Vessel radiation distribution	Ex-Vessel radiation distribution	The neutron multiplication effect by isolated IVS fuels
Number of Mesh	R: 96 Z: 200	R: 69 Z: 200	X: 107 Z: 107
PL SN	P3 S30	P3 S96	P3 S30
Neutron Source Calc.	2D Diff. Calc. (7 Gr.) (CITATION)	Ext. Boundary Source obtained in Step1	2D Diff. Calc.(7 Gr.) (CITATION)

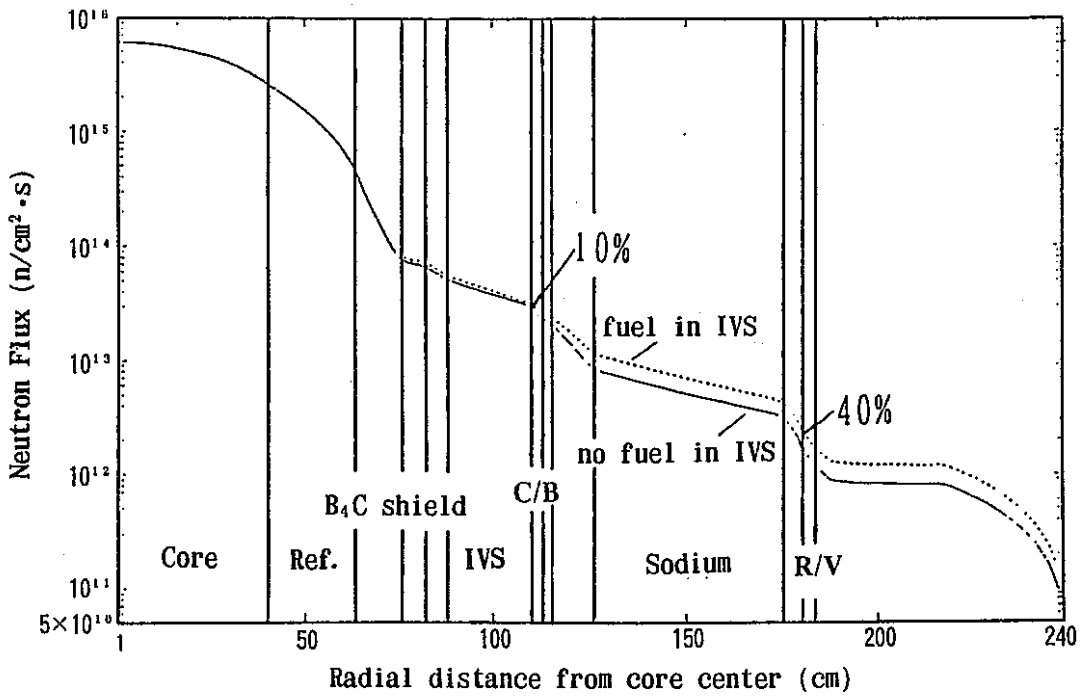

Fig. 6. Radial traverse of total neutron flux

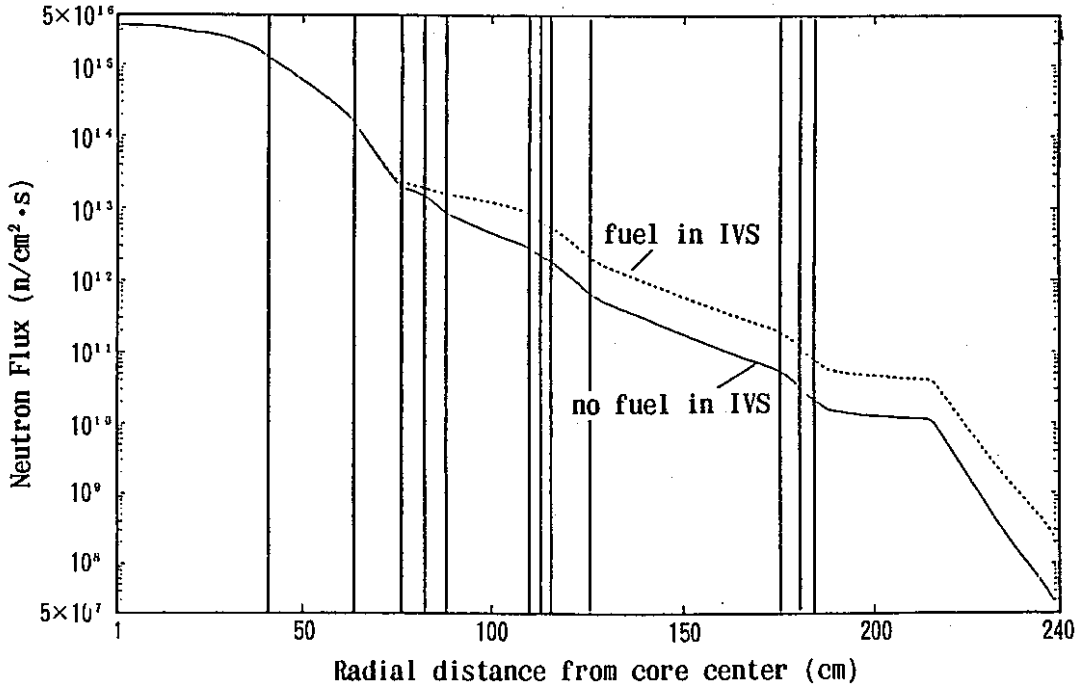

Fig. 7. Radial traverse of fast neutron flux

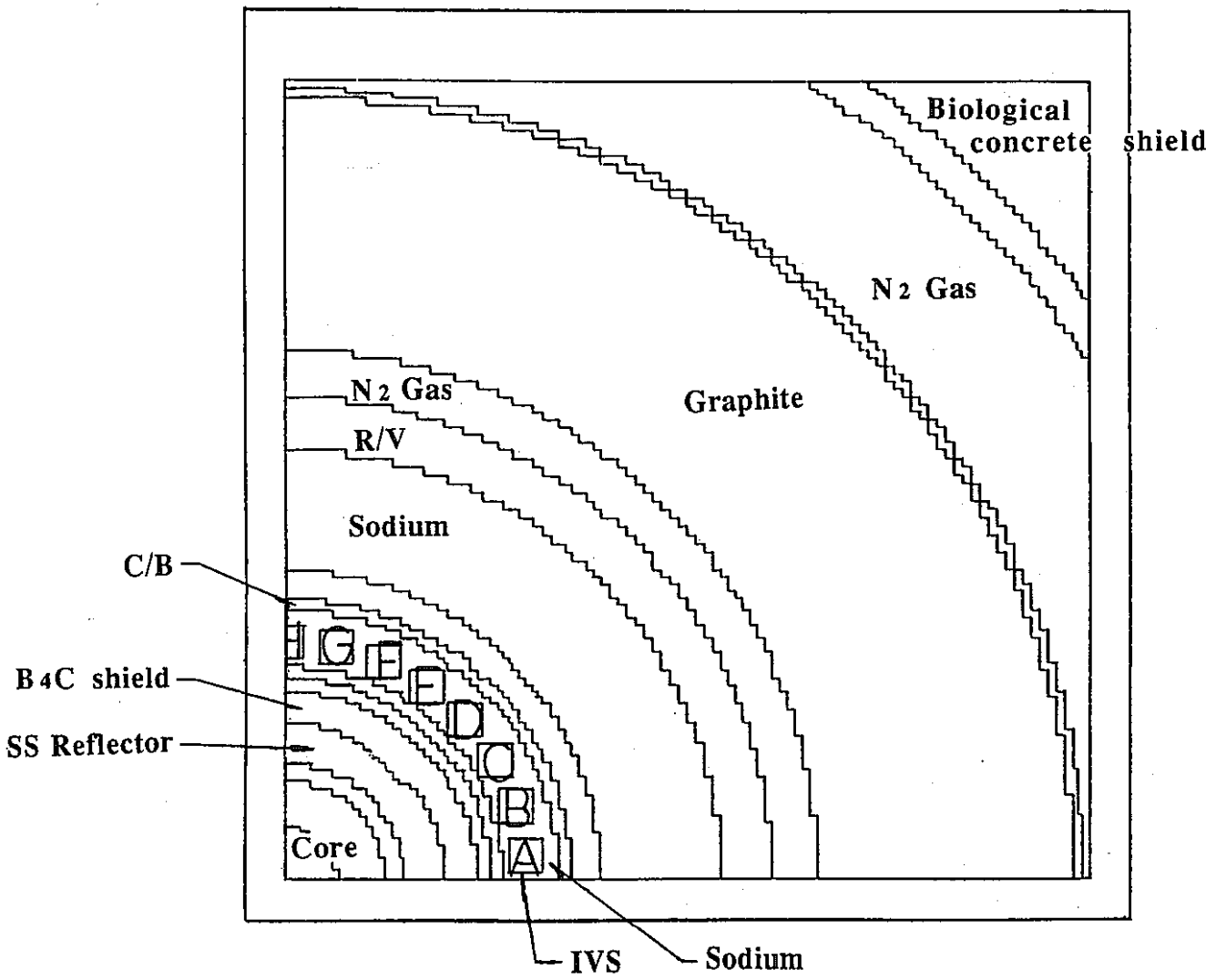

Geometry modeling for X-Y calculations

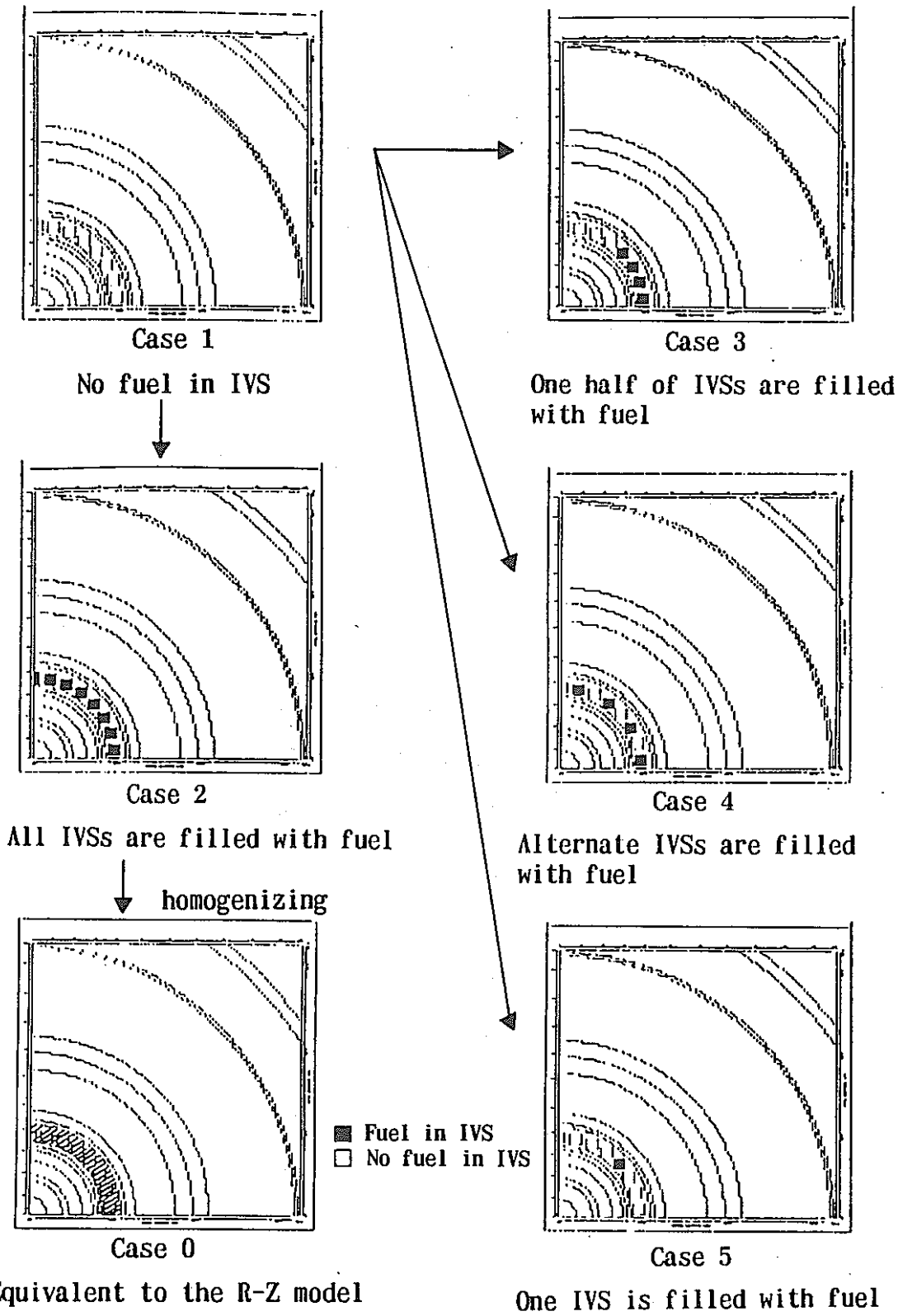

Fig.8 Models for the 2D X-Y calculations by DOT3.5

Correction for the Calculation

1 Neutron multiplication effect by Isolated IVS fuel

2 E/C factor (Design Margin)

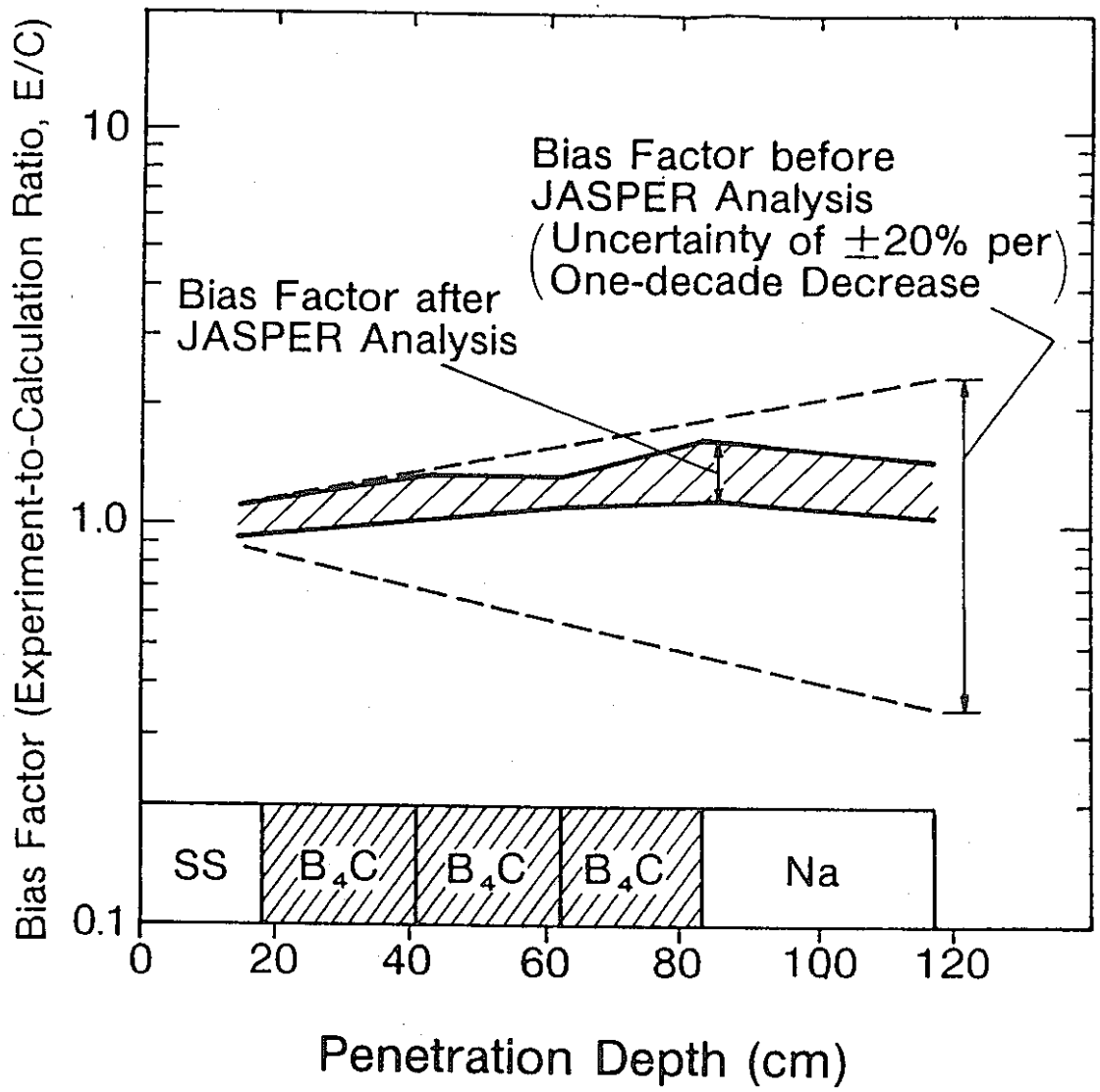

Fig.7 Comparison of Calculation Uncertainty between before and after JASPER Analysis

Japanese-American Shielding Program of Experimental Research (JASPER)

$$\frac{\text{Attenuation rate (3 SS Ref. + 2 } B_4C \text{ Shield)}}{\text{Attenuation rate (5 SS Ref.)}} = \frac{1}{5}$$

⬇

Uncertainty of Calc. = 7%

Table The maximum Clad Temp. of IVS Fuel

	Thermal Power of IVS Fuel		
	Fission	γ	Decay heat
Calc.	35.8kW	1.5kW	3.9kW
	DOT3.5 2D-R-Z (N:21Gr, γ :7Gr)		ORIGEN
Corr.	Isolated effect = 1.07		Uncertainty of calc. =1.30
	E/C from MK-II meas. = 1.10		
	E/C from JASPER = 1.07		
Total	45.1kW	1.9kW	5.1kW
	52.1kW		
Max Clad Temp. = 631.9°C (Hot Spot) < 675°C(Design Criteria)			

SUMMARY

- The basic specifications and arrangements of B4C shields were decided.

- The effects of isolated neutron sources could be evaluated from R-Z and X-Y calculations.

- The bias factor was evaluated from the results of the JOYO Reaction Rate Distribution Meas. Test and the JASPER program.

- It was confirmed that the max. thermal power of an IVS fuel satisfies the design criteria.

CONCLUSIONS

- By replacing two layers of SS reflectors by B4C shields, the heat generation of IVS fuel due to core-leakad neutron decreased, and the refueling procedure could be simplified.

To be presented at the ANS Topical Meeting on
New Horizons in Radiation Protection and Shielding

April 26-May 1,1992
Pasco, Washington, USA

EXPERIMENT AND ANALYSIS OF NEUTRON STREAMING THROUGH AN AXIAL SHIELD IN A FBR FUEL SUBASSEMBLY

K. CHATANI, A. SHONO, S. SUZUKI,
K. KINJO (PNC,Japan)
H. TSUNODA (MRI,Japan)

Table Objectives of JASPER Experiments

Experiments	Objectives	Remarks
1. Penetration Experiment for FBR Radial Shield	Weight and volume reduction of the shielding structure around the core	Experiment; Mar.,1986~Oct.,1986 Analysis; Completed
2. Fission Gas Plenum Experiment	Shorten the axial shield length in a fuel subassembly	Experiment; Jan.,1987~Feb.,1987 Analysis; Completed
3. Axial Shield Experiment	Same as above	Experiment; Aug.,1990~Dec.,1990 Analysis; Almost completed
4. In-Vessel Fuel Storage Experiment	Optimization of the radial shielding structure in reactor vessel	Experiment; Feb,1991~Sep.,1991 Analysis; Partly completed
5. IHX Activation Experiment	Reduction of the radiation level around the secondary cooling system	Experiment; Oct.,1991~Feb.,1992
6. Gap Streaming Experiment	Simplification of the shield around the roof slab	Experiment; Mar.,1992~
7. Flux Monitor Experiment	Optimization of the NIS location	
8. Special Material Experiment	Confirmation of the characteristics of the innovative shielding concept	

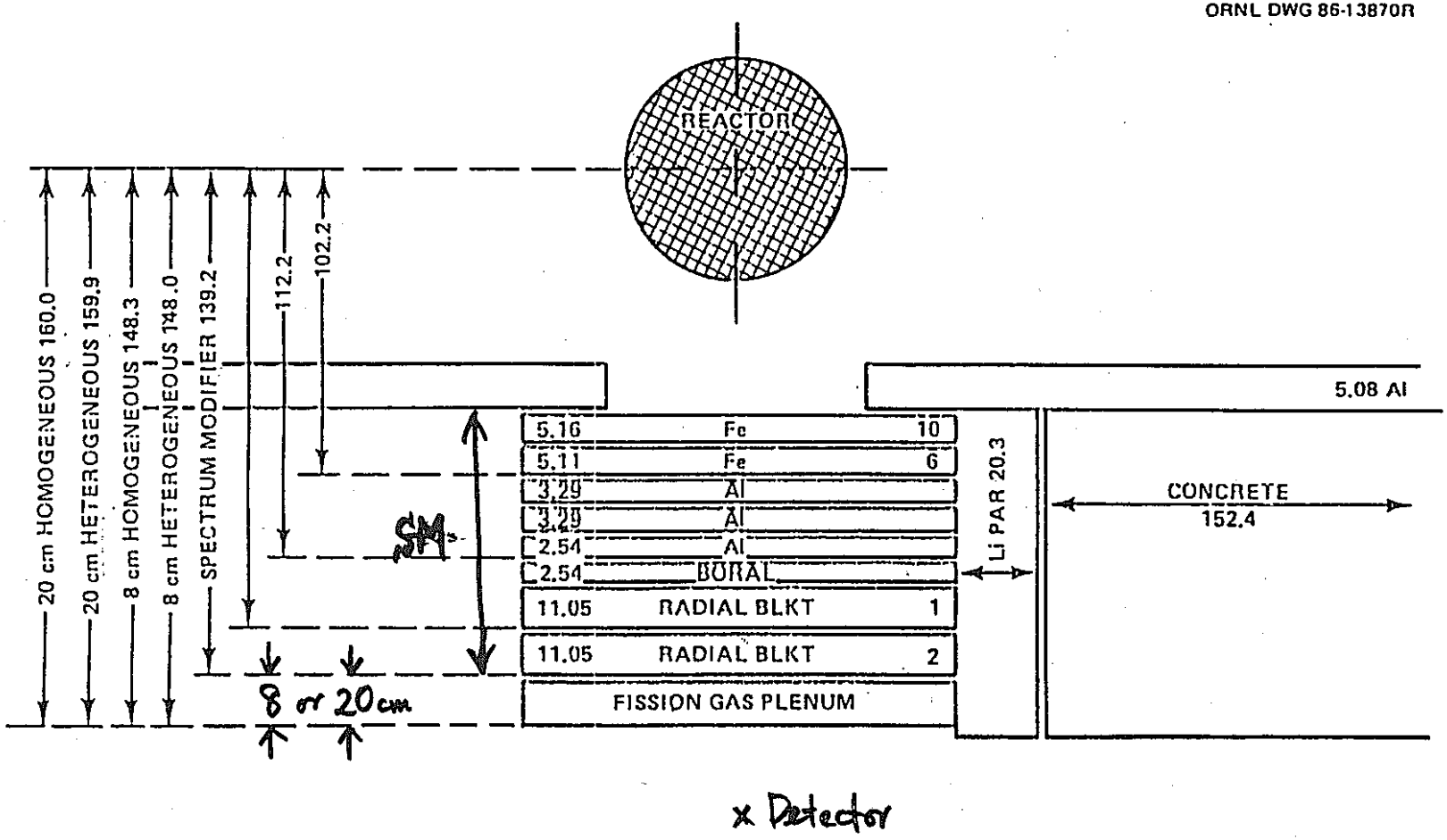

Fig. Schematic of Spectrum Modifier And Fission Gas Plenum Mockup

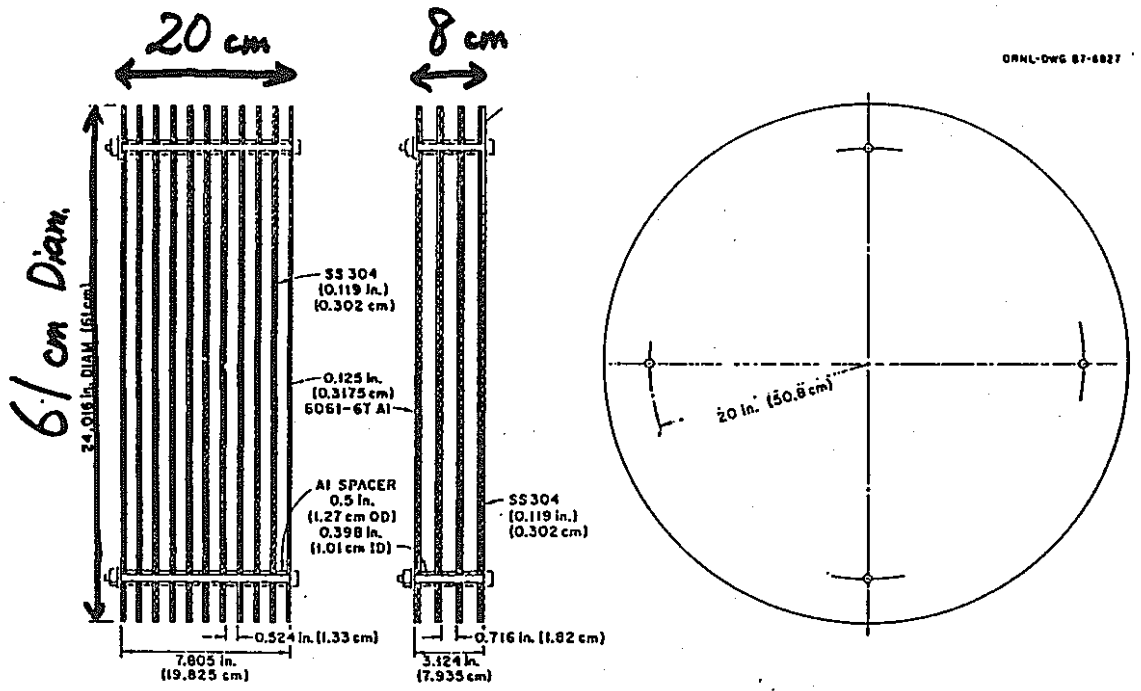

Homogeneous Gas Plenum Inserts

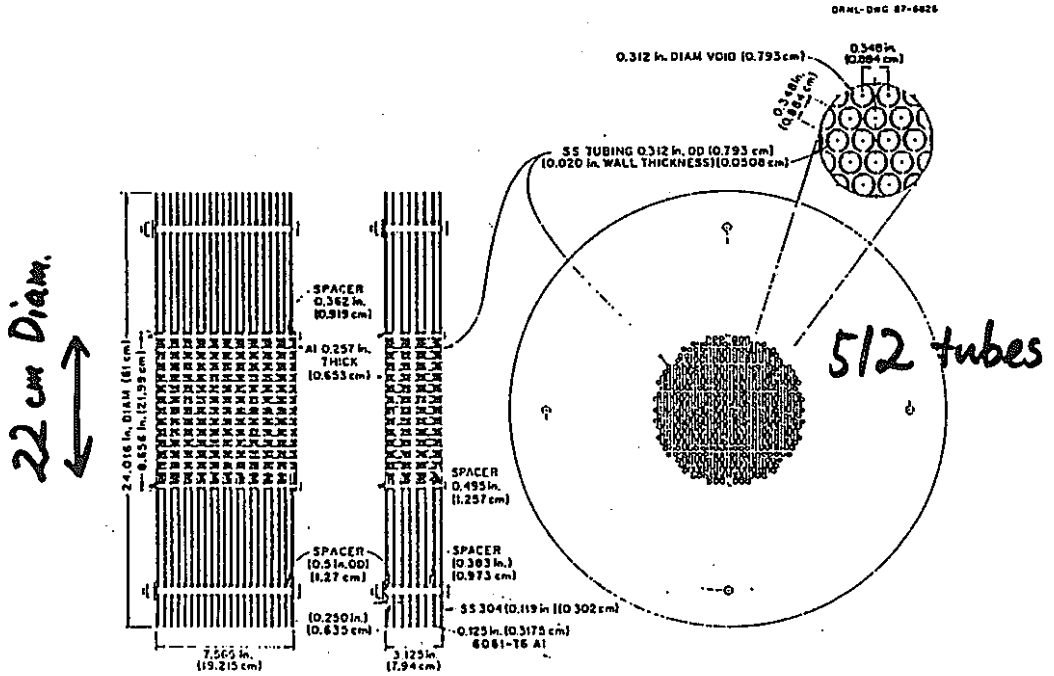

Heterogeneous Gas Plenum Inserts

Fig. Shematics of Fission Gas Plenums

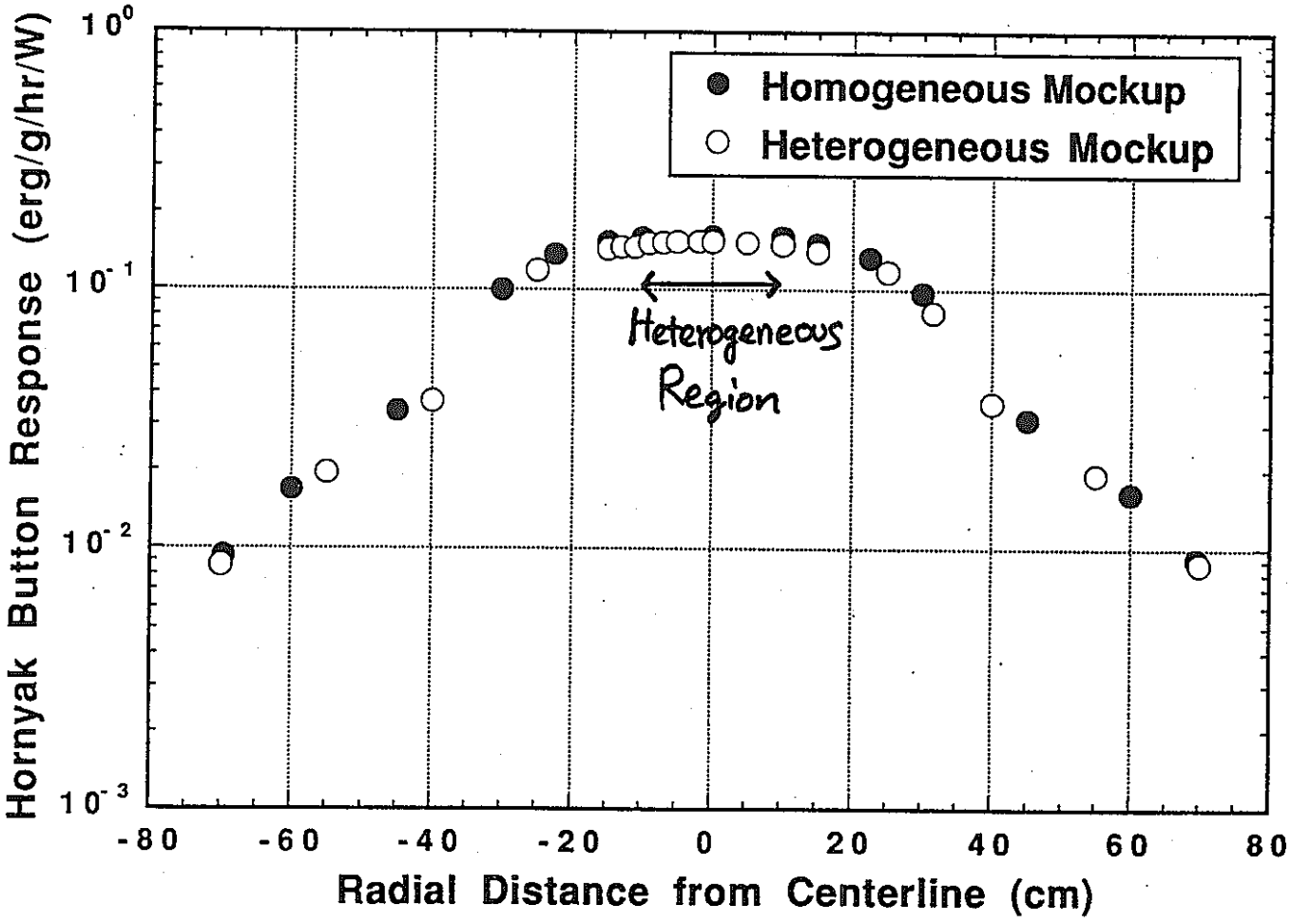

Fig. Dose Rate Profile for Hornyak Button Measurements along Horizontal Traverse

COMPARISON OF EXPERIMENT AND DESIGN SITUATION

	EXPERIMENT	DESIGN
VOLUME FRACTIONS	SS/Na/Void=16/33/51 (16Vol% Al)	SS/Na/Void=20/45/35
LENGTH OF PLENUM	8 and 20 cm	Upper Plenum ; about 20 cm Lower Plenum ; about 100 cm

Incident Neutron Spectrum

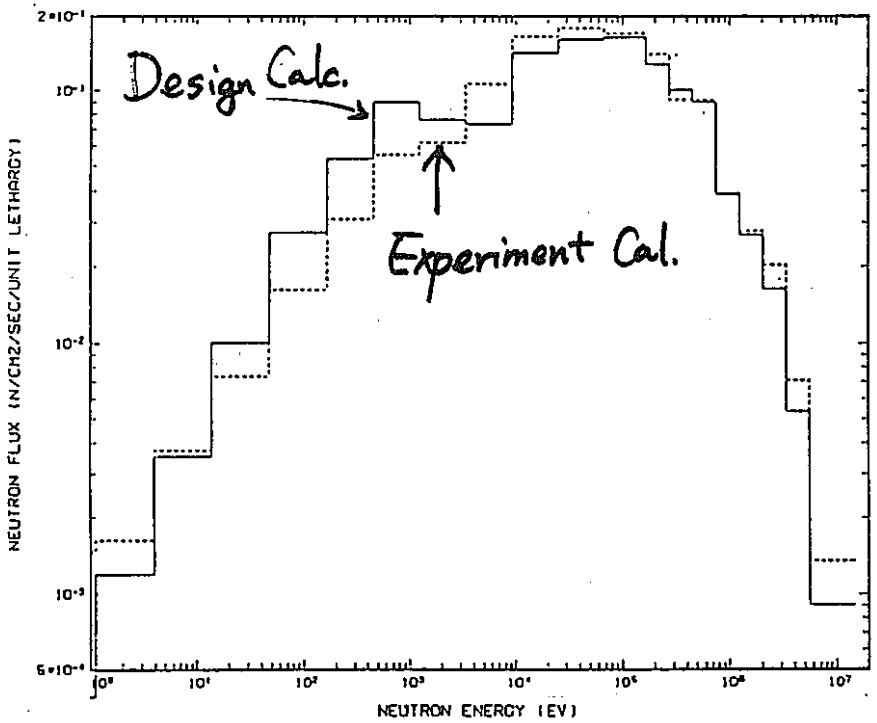

Incident Angular Flux Distribution

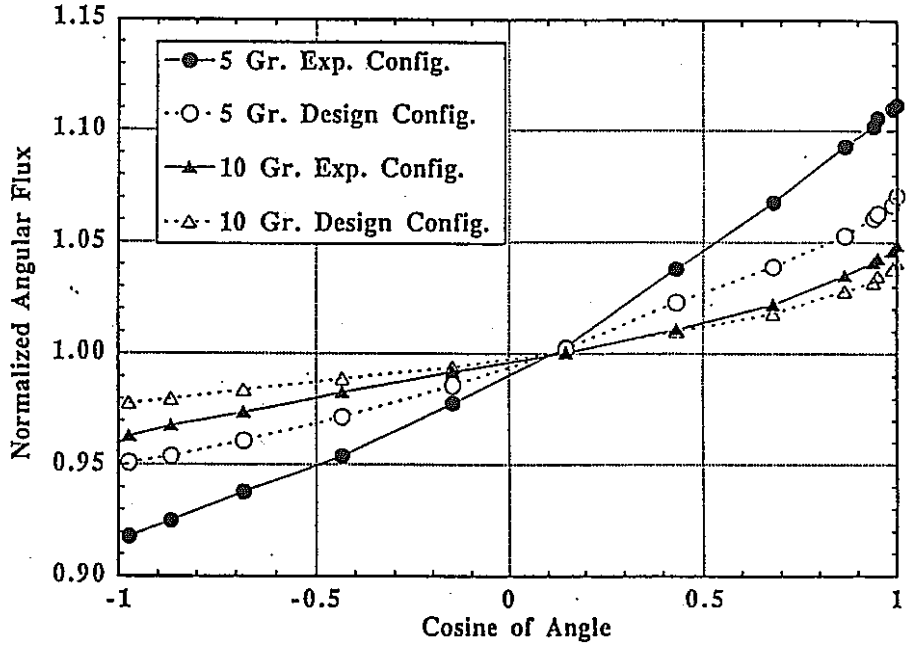

Angular Distribution of Incident Neutron Flux to Fission Gas Plenum Region
5 Gr.: 742keV - 1.22MeV
10 Gr.: 24.8keV - 67.4keV

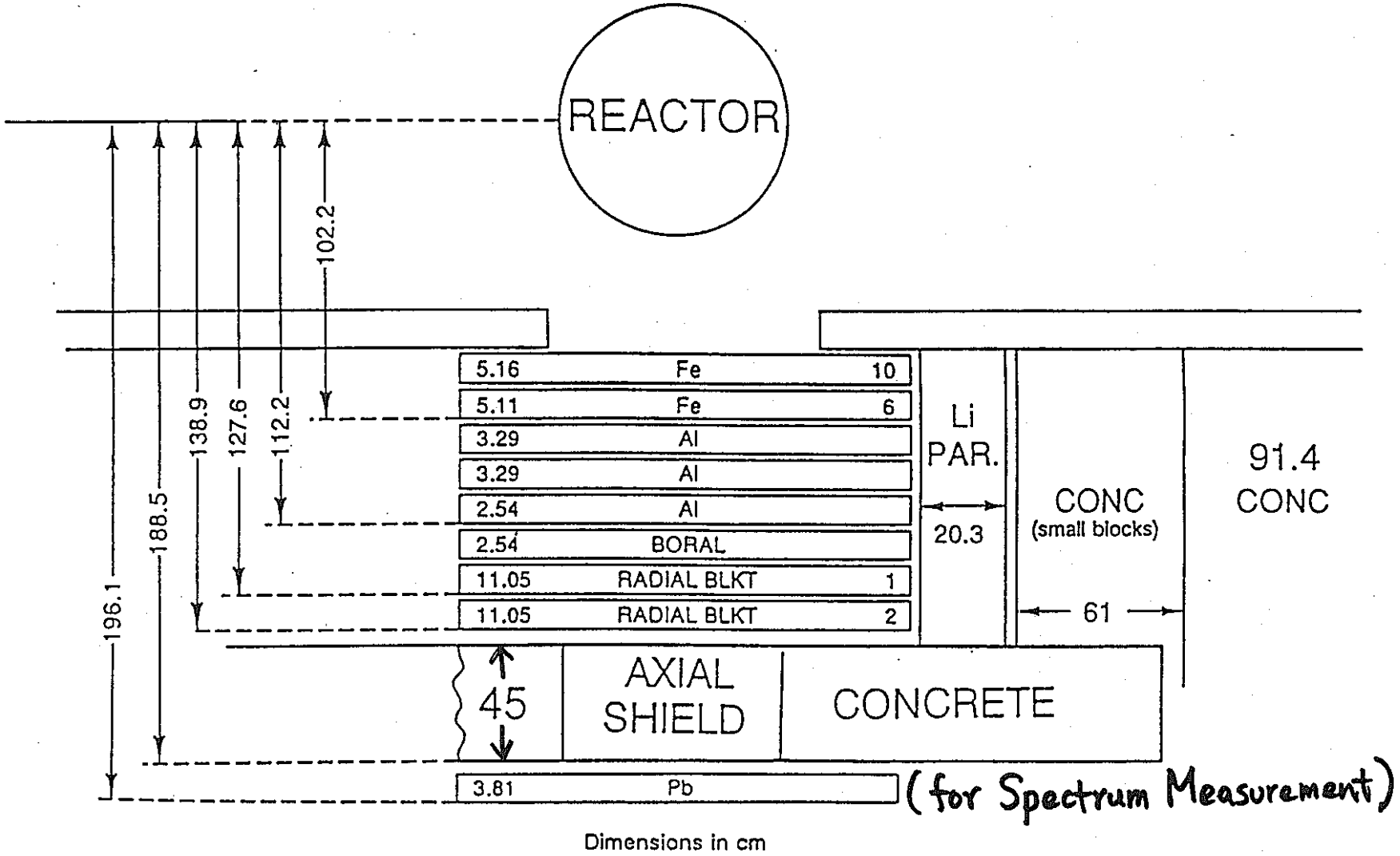

Fig. Schematic of the Axial Shield Mockup + Pb Slab

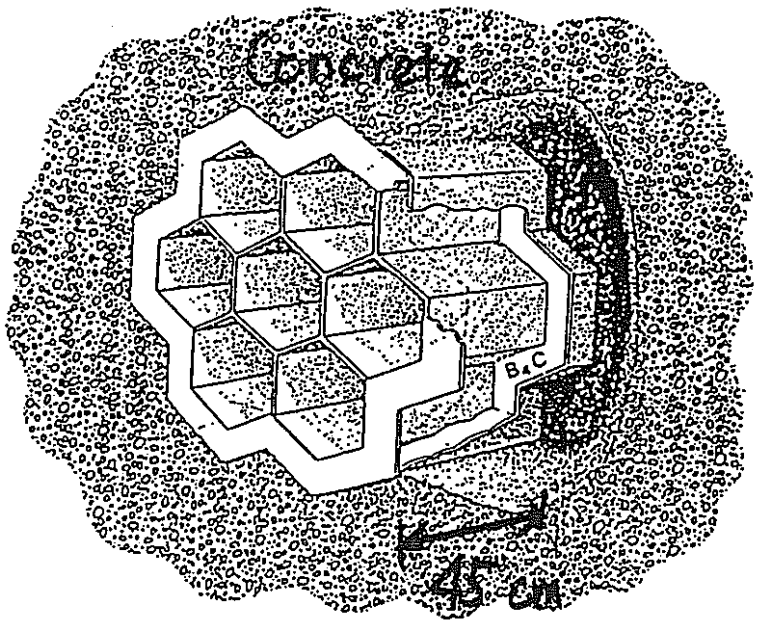

Support Structure for Experimental Assemblies

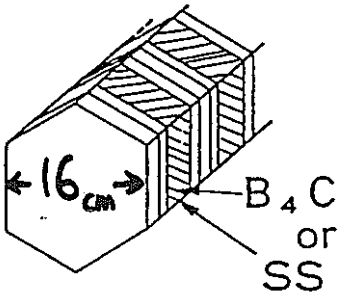

Homogeneous Type

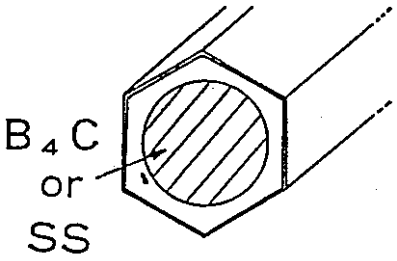

Central Blockage Type

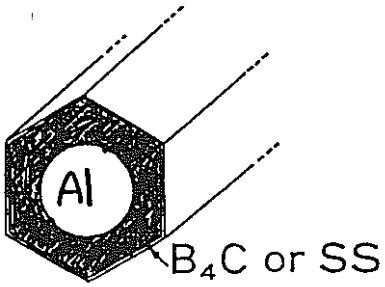

Central Na Channel Type

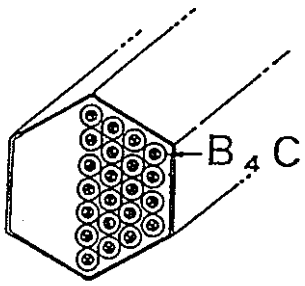

Rod Bundle Type

Fig. Experimental Assembly of Axial Shield Experiment

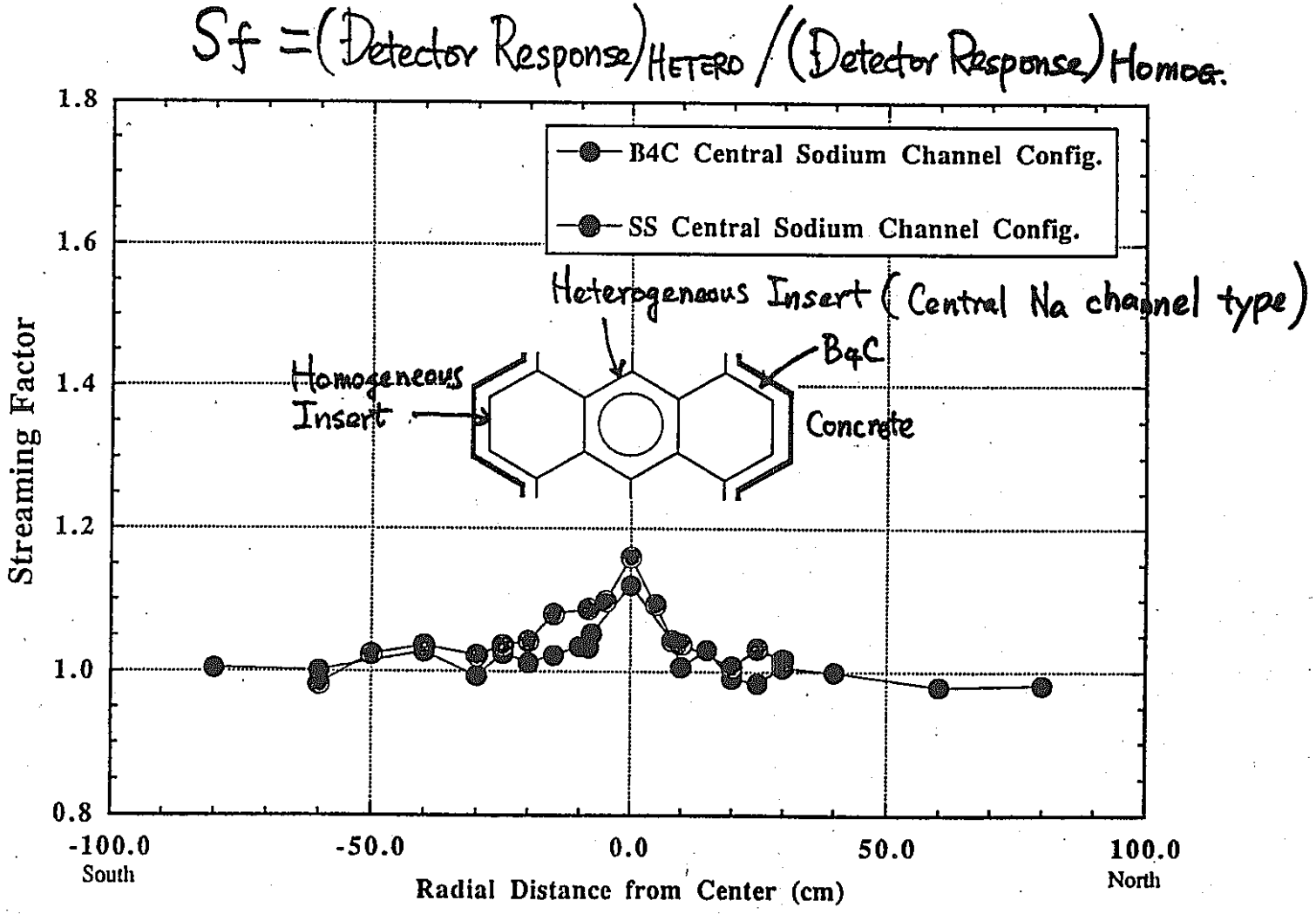

Radial Distributions of Streaming Factor derived from Measured Hornyak Button Responses

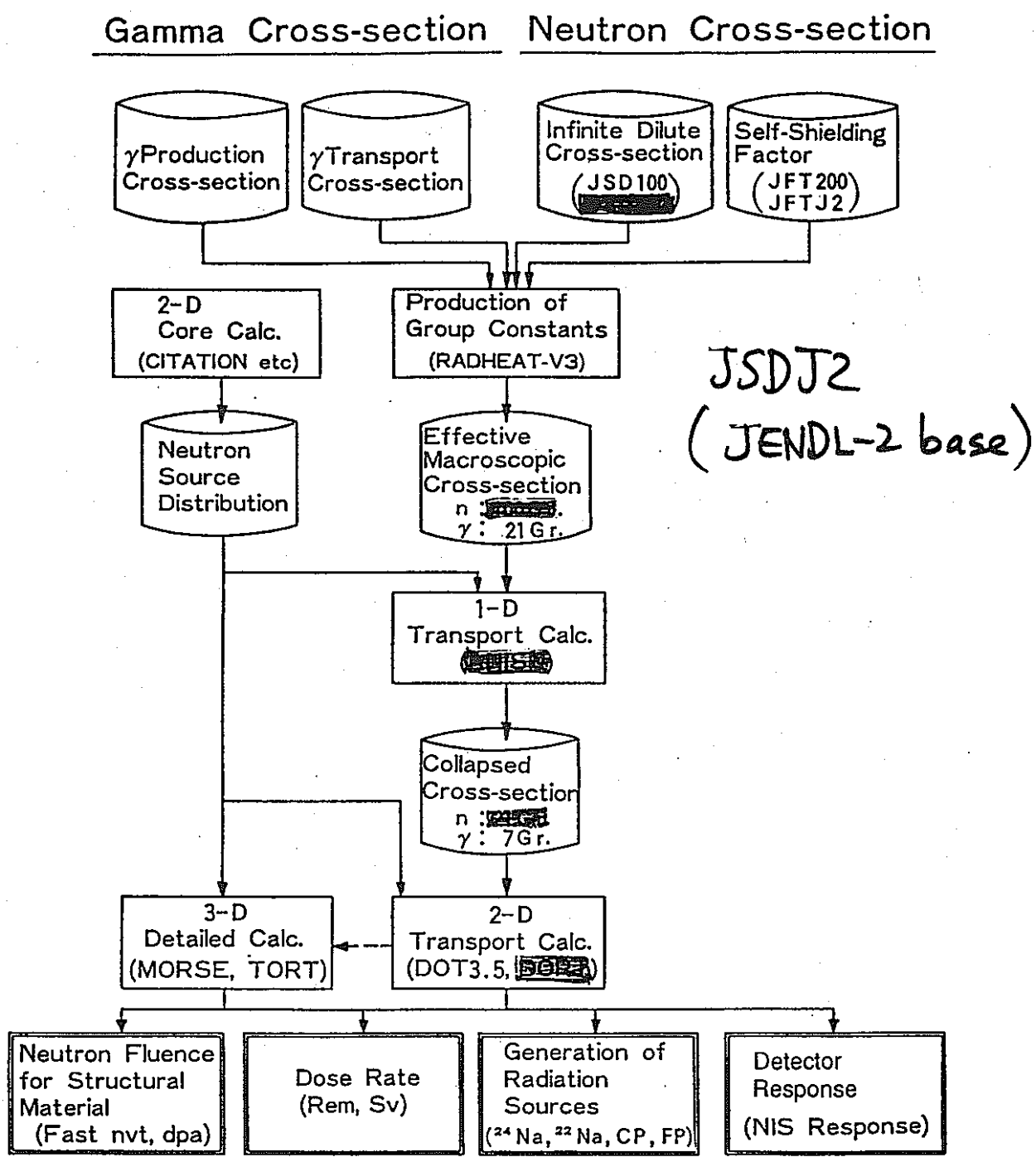

Fig. Schematic Flow Diagram for the Shielding Analysis in FBR Design

METHOD of CALCULATION

STANDARD SHIELDING ANALYSIS SYSTEM FOR FBR DESIGN IN JAPAN

- Start With 100 Group Cross Sections Generated From JENDL-2

- 1D Calculation for Cross Section Collapsing from 100 to 21 Gr.

- 2D Calculation for Comparison with Measured Data

- Numerical Approximations Emplyoed for DOT3.5 or DORT Calculation:
  - P3 Scattering Anisotopy
  - S100 Asymmetric Angular Quadrature Set
  - S96 Isotropic Angular Quadrature Set for Homogeneous Configurations

Table 1. Calculated to Measured Ratios (C/E) for B4C Central Sodium Channel Configuration

	Bonner Ball Detectors	Homogeneous Configuration	Heterogeneous Configuration
*1	3-inch BB	1.06	1.10
	4-inch BB	1.08	1.10
	5-inch BB	1.06	1.07
	8-inch BB	1.13	1.12
	10-inch BB	1.15	1.18
	12-inch BB	1.24	1.26
*2	3-inch BB	1.83	1.66
	4-inch BB	1.51	1.38
	5-inch BB	1.40	1.26
	8-inch BB	1.44	1.33
	10-inch BB	1.60	1.50
	12-inch BB	1.69	1.70

*1) 30 cm behind shield mockup
*2) 150 cm behind shield mockup

Table 3. Measured and Calculated Streaming Factors (Sf) Derived from Bonner Ball Response for B4C Central Sodium Channel Configuration

	Bonner Ball Detectors	Measured Sf's(E)	Calculated Sf's(C)	(C-E)/E
*1	3-inch BB	1.28	1.33	0.04
	4-inch BB	1.29	1.32	0.02
	5-inch BB	1.26	1.27	0.01
	8-inch BB	1.14	1.13	-0.01
	10-inch BB	1.07	1.09	0.02
	12-inch BB	1.05	1.07	0.01
*2	3-inch BB	1.19	1.08	-0.09
	4-inch BB	1.19	1.09	-0.09
	5-inch BB	1.20	1.08	-0.10
	8-inch BB	1.13	1.05	-0.07
	10-inch BB	1.09	1.03	-0.06
	12-inch BB	1.01	1.02	0.01

*1) 30 cm behind shield mockup
*2) 150 cm behind shield mockup

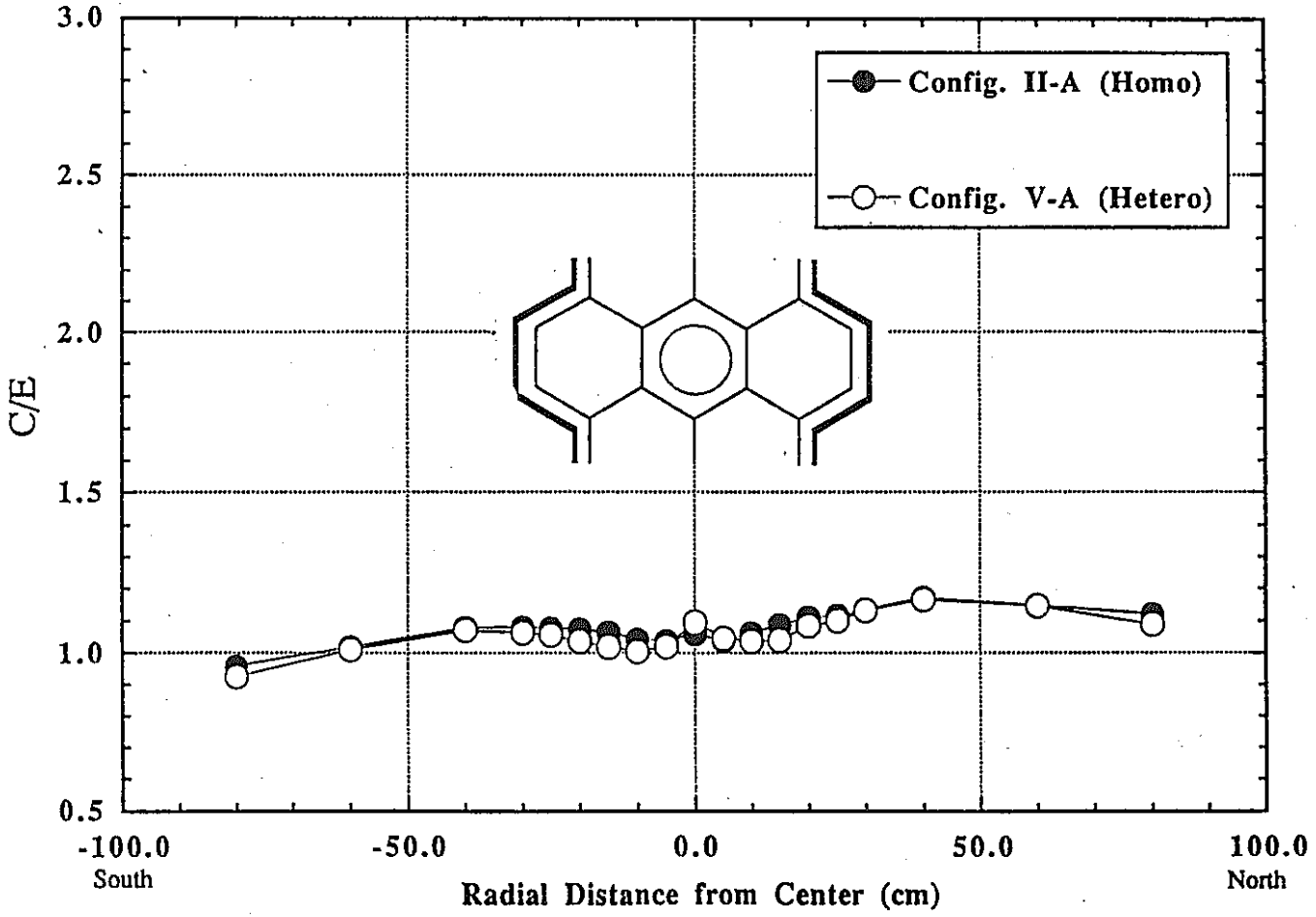

C/E Distributions of 5 inch Bonner Ball Response for B4C Type Axial Shield Configurations

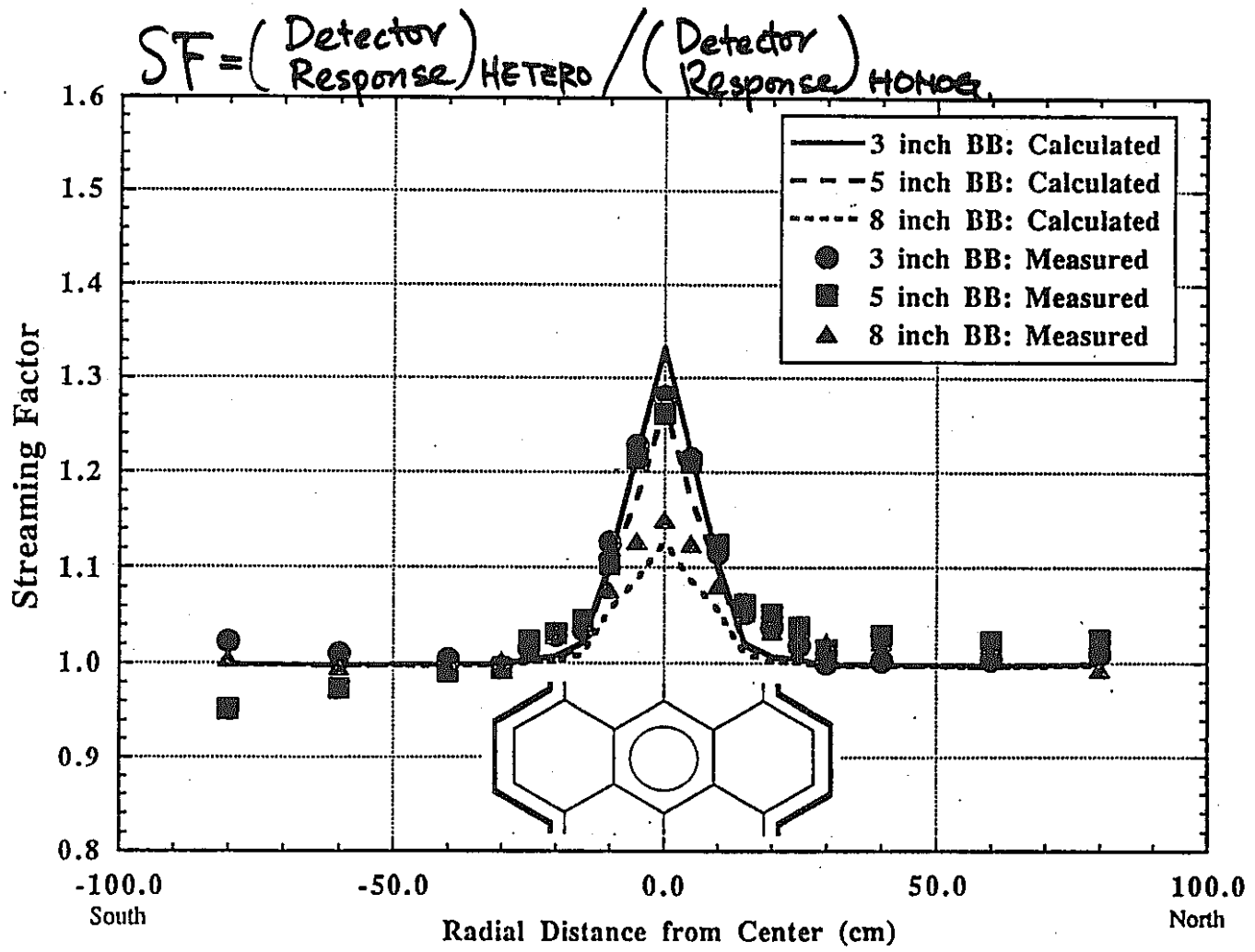

Radial Distributions of Streaming Factor derived from Bonner Ball Responses for B4C Type Axial Shield Configuration

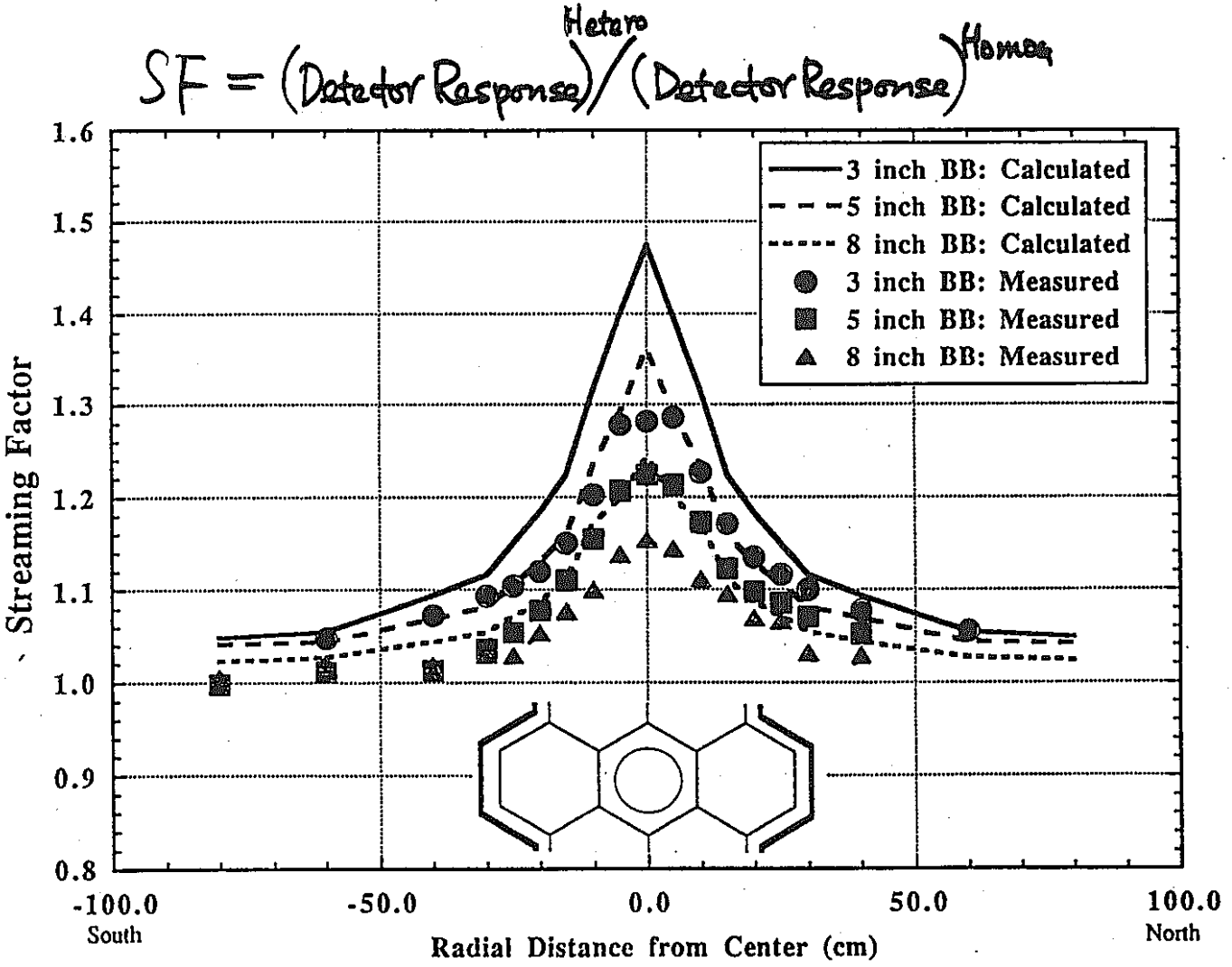

Radial Distributions of Streaming Factor derived from Bonner Ball Responses for SS Type Axial Shield Configuration

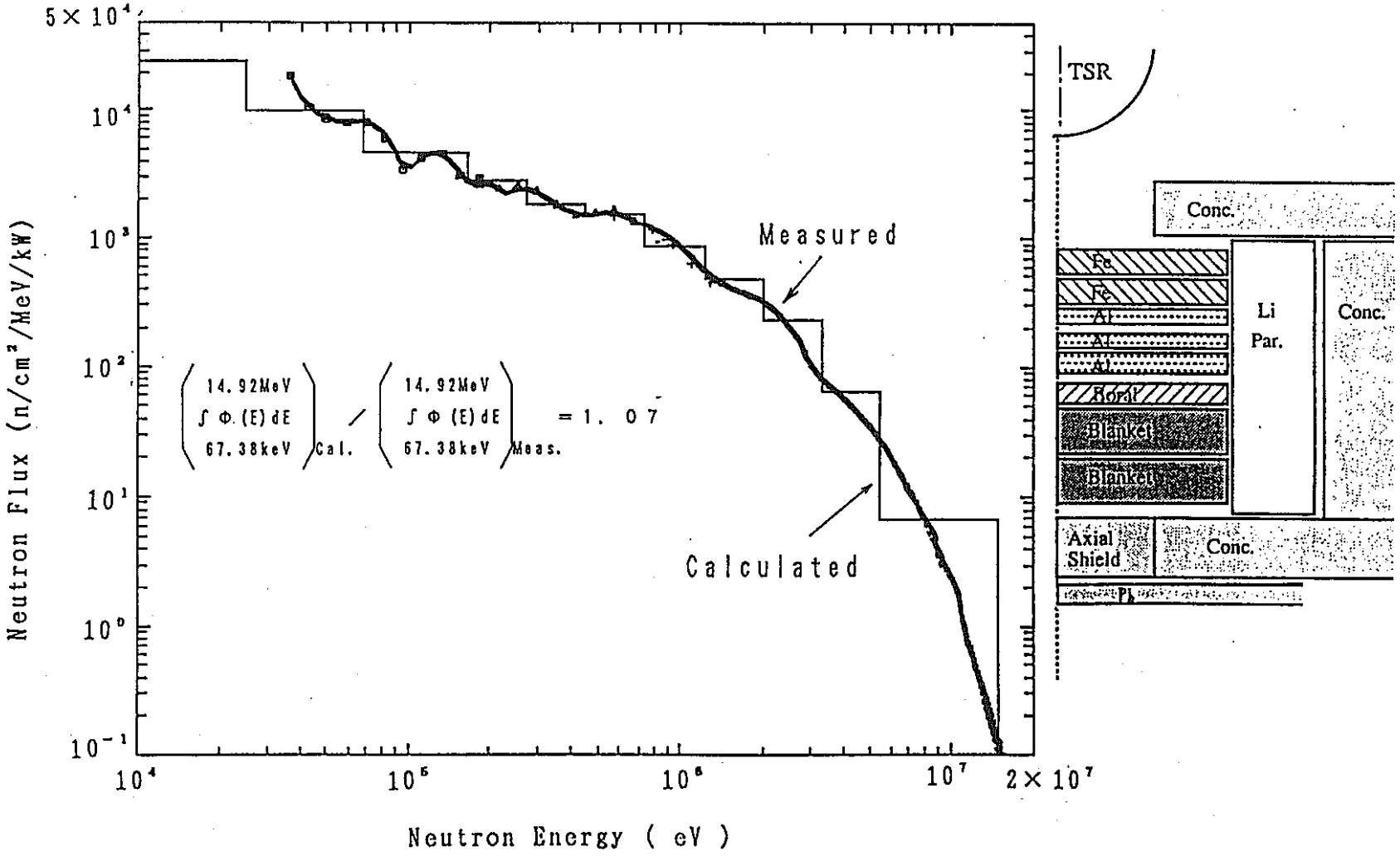

Fig. Comparison of Measured and Calculated Fast Neutron Spectra Behind Configuration II-A (B4C Type) with Lead Slabs.

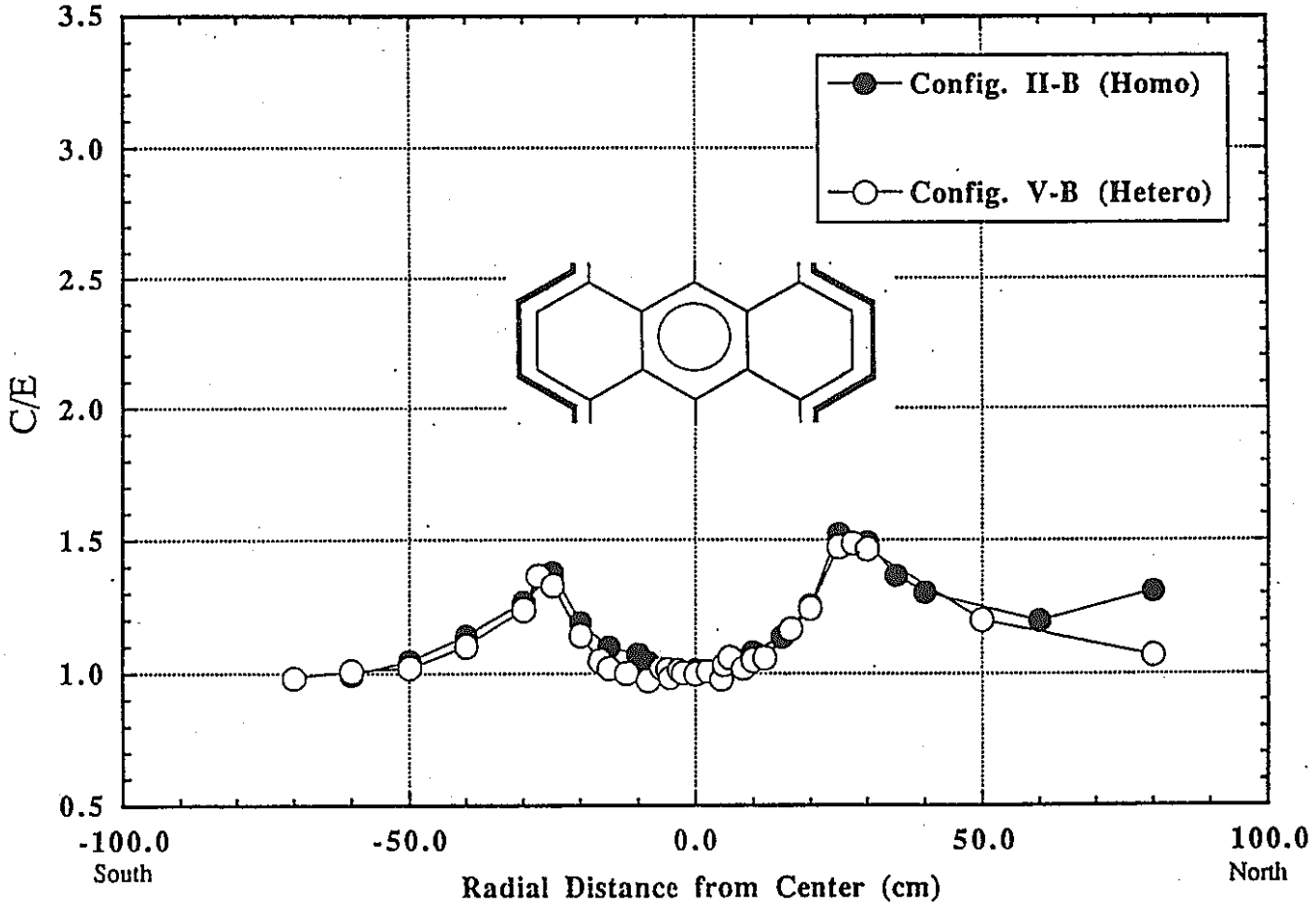

C/E Distributions of Hornyak Button Response for SS Type Axial Shield Configurations

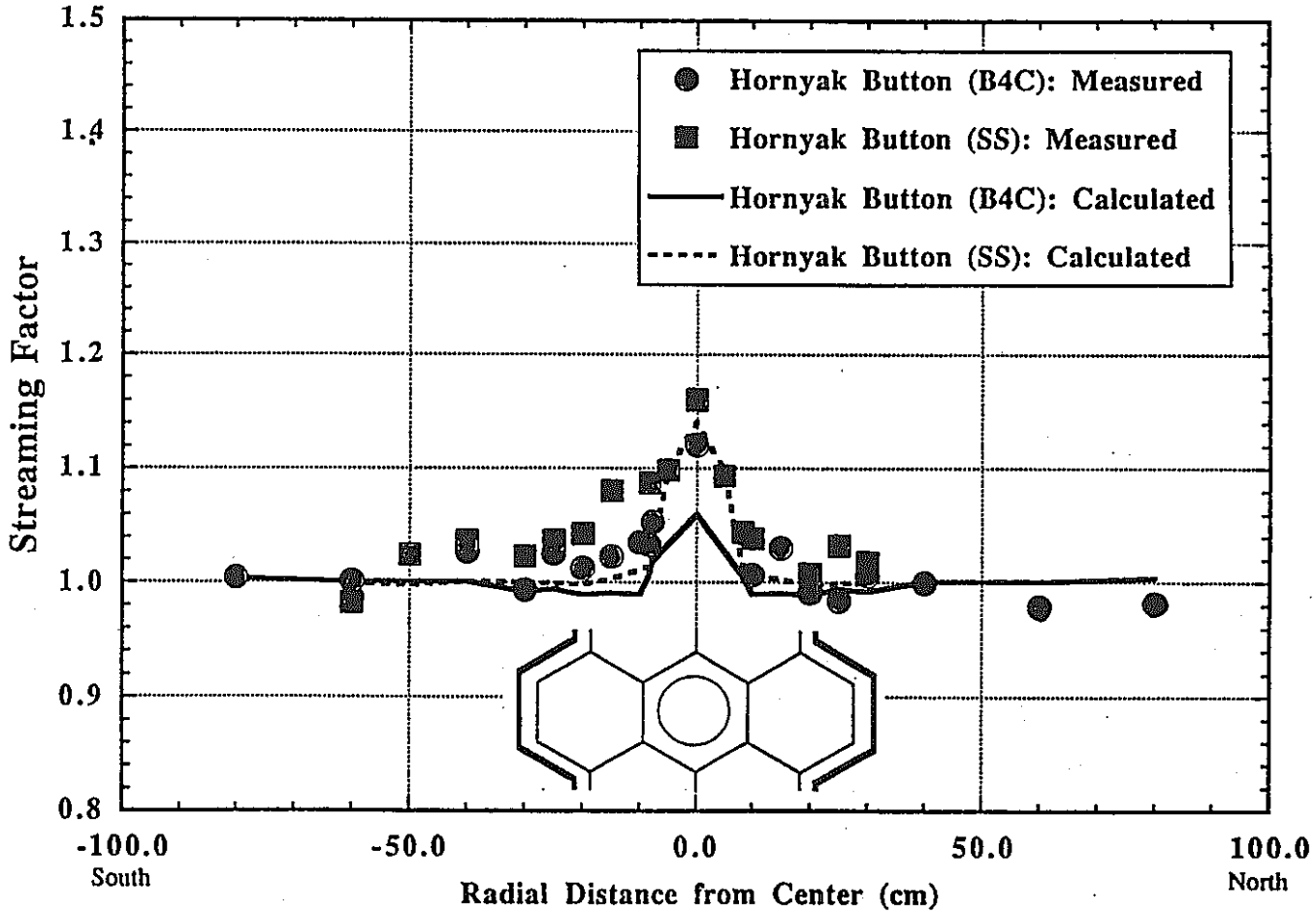

Radial Distributions of Streaming Factors derived from Hornyak Button Responses for B4C and SS Type Axial Shield Configurations

Items to Consider the Difference between Exp. and Design

1) Homogeneous Type Assembly is Not "Homogeneous Model" used for Design Calculation (Multi-layer Structure)

2) Substitute Material (Al) for Na

3) B_4C Theoretical Density (B_4C Type Assembly)

4) Size and Shape

5) Slightly Different Neutron Field

CONCLUSIONS

1. FISSION GAS PLENUM EXPERIMENT

- Neutron Streaming Can't Detected.
- It is Not Necessary to Change the Calculational Treatment of Homogening the Region Based on Volume Fractions of Each Materials.

2. AXIAL SHIELD EXPERIMENT

- Various Streaming Factors are Obtained from Measured Detector Responses.
- By Considering the Difference Between Shielding Design and Experiment, These Streaming Factors will be Used for DFBR Design Study in Japan.

3. ANALYSIS OF AXIAL SHIELD EXPERIMENT

- Japanese Analysis System of Shielding Design Can Predict Neutron Streaming Effect with Acceptable Level by Two-dimensional Model.

F. ALSMILLER
MARTIN MARIETTA ENERGY SYSTEMS, INC
P.O. BOX 2008
OAK RIDGE TN 37831-6364
USA

R. ALSMILLER, Jr.
MARTIN MARIETTA ENERGY SYSTEMS, INC
P.O. BOX 2008
OAK RIDGE TN 37831-6364
USA

DICK AMATO
BETTIS ATOMIC LAB

Y. ANAYAMA
SANOYA INDUSTRY CO. LTD.
2626 MORO KANUMA-SHI TOCHIGI
N/A N/A 322
JAPAN

MATTHEW APPLEBY
BOEING DEFENSE & SPACE GROUP
P.O. BOX 240002
HUNTSVILLE AL
USA

TONY ARMSTRONG
SCIENCE APPLICATIONS I
ROUTE 2
PROSPECT TN 38477
USA

KENNETH ASHE
DUKE ENGINEERING AND SERVICES INC
230 SOUTH TRYON STREET P.O. BOX 100
CHARLOTTE NC 28201-1004
USA

WILLIAM ATWELL
ROCKWELL SPACE SYSTEMS DIVISION
DOWNEY CA
USA

ALAN AVERY
AEA REACTOR SERVICES
WINFRITH TECHNOLOGY CE
WINFRITH, DORCHESTER,
ENGLAND

JOE BERRY
BATTELLE, PACIFIC NORTHWEST LABORAT
P.O. BOX 999
RICHLAND WA 99352
USA

THOMAS BLUE
OHIO STATE UNIVERSITY
206W. 18TH AVE.
COLUMBUS OH 43210
USA

LARRY BRACKENBUSH
BATTELLE - PNL
BATTELLE BLVD, P.O. BO
RICHLAND WA 99352
USA

B. BROADHEAD
MARTIN MARIETTA ENERGY SYSTEMS
P.O. BOX 2008
OAK RIDGE TN 37831-6370
USA

ROGER BROWN
WESTINGHOUSE HANFORD COMPANY
P.O. BOX BOX 1970 - G6-06
RICHLAND WA 99352
USA

THOMAS BROWN
LOS ALAMOS NATIONAL LA
MS K483
LOS ALAMOS NM 87545
USA

JEFFREY BULL
SUPERCONDUCTING SUPER COLLIDER LAB.
2550 BECKLEYMEADE AVENUE, MS-1071
DALLAS TX 75237
USA

WILBUR BUNCH
WESTINGHOUSE HANFORD CO.
P.O. BOX 1970, MSIN HO-35
RICHLAND WA 99352
USA

THOMAS BURNS
MARTIN MARIETTA ENERGY
P.O. BOX 2008, BLDG. 6
OAK RIDGE TN 37831
USA

JOHN BUTLER*
AEA TECHNOLOGY
WINFRITH TECHNOLOGY CENTER
WINFRITH, DORCHESTER, DORSET N/A DT
UNITED KINGDOM

DANIEL CALAMAND
COMMISSARIAT A L'ENERGIE ATOMIQUE
13108 SAINT-PAUL-LEZ-DURANCE CEDEX
CEN/CADARACHE N/A N/A
FRANCE

L. CARTER
WESTINGHOUSE HANFORD C
P.O. BOX 1970, MSIN HO
RICHLAND WA 99352
USA

P. CHEE
BOEING CO.
P.O. BOX 3707, MS-2T-50
SEATTLE WA 98124
USA

E. CHENG
TSI RESEARCH
225 STEVENS AVE., #110
SOLANA BEACH CA 92075
USA

EDWARD CHENG
TSI RESEARCH, INC
225 STEVENS AVE.,#110
SOLONA BEACH CA 92075
USA

STEVEN CHUCAS
AEA TECHNOLOGY
WINFIRTH, DORCHESTER
DORSET DT28DH
ENGLAND

MR COLLENS
LAWRENCE LIVERMORE NATIONAL LABORAT
P.O. BOX 808, L-298
LIVERMORE CA 94550
USA

TOM CONROY
BATTELLE - PNL
BATTELLE BLVD, P.O. BO
RICHLAND WA 99352
USA

DR. IAN CURL
AEA TECHNOLOGY
WINFIRTH, DORCHESTER
DORSET DT28DH
ENGLAND

ALBERT DAVIS
WASHINGTON PUBLIC POWER SUPPLY SYST
P.O. BOX 968 MS-927K
RICHLAND WA 99352
USA

PAUL, Jr. DELUCA
UNIVERSITY OF WISCONSI
DEPARTMENT OF MEDICAL
MADISON WI 53706
USA

LARRY DIETRICK
BISCO PRODUCTS
2300 E. DEVON AVE.
ELK GROVE IL 60007
USA

DON DUDZIAK
N.C. STATE UNIV.
DEPT. NUCLEAR ENGINEERING
RALEIGH NC 27695-7909
USA

MARGARET (PEGGY) EMMET
MARTIN MARIETTA ENERGY
P.O. BOX 2008, MS-6370
OAK RIDGE TN 37831-637
USA

GUY ESTES
LOS ALAMOS NATIONAL LABORATORY
MS B226
LOS ALAMOS NM 87432
USA

C. BRAD EVANS
EG&G ROCKY FLATS
P.O. BOX 464
GOLDEN CO 80402
USA

MADELINE FELTUS
THE PENNSYLVANIA STATE
231 SACKETT BUILDING
UNIVERSITY PARK PA 168
USA

GERALD FINK
TUV HANNOVER/SACHSEN-ANHALT
HANNOVER 81, P.O. BOX 81 05 51
HANNOVER N/A D 3000
FEDERAL REPUBLIC OF GERMANY

JOHN FIX
BATTELLE - PACIFIC NORTHWEST LABORA
P.O. BOX 999 MS P7-01
RICHLAND WA 99352
USA

R. FOX
BATTELLE - PNL
BATTELLE BLVD, P.O. BO
RICHLAND WA 99352
USA

CHIA FU
MARTIN MARIETTA ENERGY SYSTEMS, INC
P.O. BOX 2008
OAK RIDGE TN 37831-6356
USA

DR. AVIGDOR GAVRON
LOS ALAMOS NATIONAL LABORATORY
MS-H803
LOS ALAMOS NM 87545
USA

RAY GOLD
1982 GREENBROOK BLVD
RICHLAND WA 99352
USA

HARVEY GOLDBERG
WESTINGHOUSE HANFORD COMPANY
P.O. BOX 1970, MSIN HO-36
RICHLAND WA 99352
USA

JESS GREENBORG
WESTINGHOUSE HANFORD CO.
P.O. BOX 1970, MSIN HO-35
RICHLAND WA 99352
USA

EHUD GREENSPAN
UNIVERSITY OF CALIFORN
DEPARTMENT OF NUCLEAR
BERKELEY CA 94720
USA

HIROYUKI HANDA
HITACHI ENGINEERING, CO. LTD.
Z-1, SAIWAI-CHO 3-CHOME, HITACHI-SH
IBARAKI-KEN, 317
JAPAN

RICHARD HARTLEY (MAJ,USAF)
AIR FORCE - AIR UNIVERSITY
AIR FORCE INSTITUTE OF TECHNOLOGY/E
WRIGHT-PATTERSON AIR FORCE BASE OH
USA

WELLS HARVEY
LOS ALAMOS NATIONAL LA
2424 46 ST
LOS ALAMOS NM 87544
USA

TEROU HASHIMOTO
SANOYA INDUSTRY CO. LTD.
2626 MORO KANUMA-SHI, TOCHIGI
N/S N/S 322
JAPAN

PETER HASTINGS
DUKE ENGINEERING AND SERVICES, INC
230 SOUTH TRYON STREET
CHAROLETTE NC 28201-1004
USA

STANLEY HAYNES
WASHINGTON PUBLIC POWE
P.O. BOX 968
RICHLAND WA 99352
USA

NOLAN HERTEL
THE UNIVERSITY OF TEXAS AT AUSTIN
ETC5.160, MECHANICAL ENGINEERING DE
AUSTIN TX 78712-1063
USA

ROBIN HILL
BATTELLE - PNL
BATTELLE BLVD, P.O. BOX 999 MS K3-5
RICHLAND WA 99352
USA

ANDREW HODGDON
YANKEE ATOMIC ELECTRIC
580 MAIN ST.
BOLTON MA 01740
USA

WILLIAM HOPKINS
BECHTEL CORPORATION
9801 WASHINGTON BLVD
GAITHERSBURG MD 20878-5356
USA

HAMILTON HUNTER
MARTIN MARIETTA ENERGY SYSTEMS - OR
P.O. BOX 2008
OAK RIDGE TN 37831-6380
USA

DANIEL INGERSOLL
MARTIN MARIETTA ENERGY
P.O. BOX 2008
OAK RIDGE TN 37831
USA

NISY IPE
STANFORD LINEAR ACCELERATOR CENTER
BIN 48, SLAC, P.O. BOX 4349
STANFORD CA 94309
USA

TERRY JAMIESON
SCIENCE APPLICATIONS INTERNATIONAL
306-56 SPARKS STREET
OTTAWA ONTARIO K1P 5M9
CANADA

JEFFREY JOHNSON
MARTIN MARIETTA ENERGY
P.O. BOX 2008, BLDG. 6
OAK RIDGE TN 37831
USA

WILLIAM JOHNSON
SARGENT AND LUNDY
55 E. MONROE ST
CHICAGO IL 60603
USA

CARTER KIRK
WESTINGHOUSE HANFORD COMPANY
2706 W. MARGARET ST
PASCO WA 99301-4507
USA

JAMES LIVINGSTON
PNL
PNL
RICHLAND

S. MAO
STANFORD LINEAR ACCELERATOR CENTER
SLAC, BIN 48, P.O. BOX 4349
STANFORD CA 94309
USA

JOSEPH MCDONALD
BATTELLE - PACIFIC NORTHWEST LABORA
P.O. BOX 999
RICHLAND WA 99352
USA

LUTZ MORITZ
TRIUMF
4004 WESBROOK MALL
VANCOUVER, B.C. N/A V6T 2A3
CANADA

TAKASHI NAKAMURA
TOHOKU UNIVERSITY
CYCLOTRON AND RADIOISOTOPE CENTER,
AOBA, ARAMAKI, SENDAI N/A 980
JAPAN

DAVID NIGG
EG&G IDAHO. INEL
P.O. BOX 1625
IDAHO FALLS ID 83415-1575
USA

KERAN O'BRIEN
NORTHERN ARIZONA UNIVERSITY
1645 FABULOUS TEXAN WAY
SEDONA ARIZONA 86336
USA

CHERYL OXLEY
BATTELLE, PACIFIC NORTHWEST LABORAT
P.O. BOX 999
RICHLAND WA 99352
USA

JOHN JOHNSON*
BATTELLE - PNL
BATTELLE BLVD, P.O. BOX 999 K3-53
RICHLAND WA 99352
USA

KYLE KLEINHANS
MARTIN MARIETTA ENERGY SYSTEMS
P.O. BOX 2003, K-1020, MS-7404
OAK RIDGE TN 37831-7404
USA

ALLEN LU
WESTINGHOUSE HANFORD COMPANY
P.O. BOX 1970, MSIN HO-36
RICHLAND WA 99352
USA

WILLIAM MARTIN
DEPARTMENT OF ENGINEERING
COOLEY BLDG., NORTH CAMPUS (UNIV. O
ANN ARBOR MI 48109-2104
USA

BILL MCELROY
CONSULTANTS & TECHNOLOGY SERVICES
113 THAYER DRIVE
RICHLAND WA 99352
USA

MICHAEL MOYERS
LOMA LINDA UNIVERSITY MEDICAL CENTE
DEPT OF RAD. ONCOLOGY/11234 ANDERSO
LOMA LINDA CA 92354
USA

JOHN NEALY
NASA
NASA LANGLEY RESEARCH CENTER
HAMPTON VA 23665
USA

MASAYUKI NODAKA
KOBE STEEL
231 ARAICHO
TAKASAGO/HYDGO
JAPAN

YOSHIAKA OKA
NUCLEAR ENGINEERING RESEARCH LABORA
7-3-1 HONGO, BUNKYO-KU
TOKYO N/A 113
JAPAN

DONALD PALMROSE
EG&G IDAHO, INEL
P.O. BOX 1625 MS 2404
IDAHO FALLS ID 83415-2403
USA

BERNADETTE KIRK
MARTIN MARIETTA ENERGY
P.O. BOX 2008
OAK RIDGE TN 37831
USA

ROBERT LITTLE
LOS ALAMOS NATIONAL LA
P.O. BOX 1663, MS B226
LOS ALAMOS NM 87545
USA

ART LUCAS*
VICTOREEN
6000 COCHRAN ROAD
CLEVELAND OH 44139
USA

EDWARD MASON
UNIVERSITY OF CHICAGO
1101 E. 57TH ST.
CHICAGO IL
USA

ROBERT MORFORD
WESTINGHOUSE HANFORD C
P.O. BOX 1970, MSIN HO
RICHLAND WA 99352
USA

EARL MYOTT
WESTINGHOUSE HANFORD C
P.O. BOX 1970
RICHLAND WA 99352
USA

JAMES NICOLOSI
SCIENTIFIC ECOLOGY GRO
1560 BEAR CREEK RD
OAK RIDGE TN 37831
USA

EUGENE NORMAND
BOEING DEFENSE & SPACE
P.O. BOX 3999 MS 2T-50
SEATTLE WA 98124
USA

JERRY OSBORNE
WESTINGHOUSE HANFORD C
P.O. BOX 1970
RICHLAND WA 99352
USA

TED PARISH
TEXAS A&M UNIVERSITY

ERNEST PLECHATY
LAWRENCE LIVERMORE NATIONAL LABORAT
L-298, P.O. BOX 808
LIVERMORE CA 94550
USA

GERARD POLICASTRO
SCIENTIFIC ECOLOGY GROUP, INC
1560 BEAR CREEK RD
OAK RIDGE TN 37831
USA

R. PRIMM (III)
MARTIN MARIETTA ENERGY
P.O. BOX 2008, BLDG 60
OAK RIDGE TN 37831
USA

STEVE REESE
BATTELLE - PACIFIC NORTHWEST LABORA
P.O. BOX 999 MS P7-01
RICHLAND WA 99352
USA

RUSSELL RICHMAN
BATTELLE NORTHWEST
337 BUILDING, 300 AREA, P7-78
RICHLAND WA 99352
USA

PAUL RITTMANN
WESTINGHOUSE HANFORD C
P.O. BOX 1970, MSIN H4
RICHLAND WA 99352
USA

STEVE ROBYLER
WESTINGHOUSE HANFORD CO.
P.O. BOX 1970, HO-38
RICHLAND WA 99352
USA

KENT ROSENBERGER
WESTINGHOUSE SAVANNAH RIVER CO.
P.O. BOX 616 BUILDING 735-11A
AIKEN SC 29802
USA

WALLY RUFF
WESTINGHOUSE HANFORD C
P.O. BOX 1970
RICHLAND WA 99352
USA

WILLIAM SAILOR
LOS ALAMOS NATIONAL LABORATORY
MAIL STOP F607
LOS ALAMOS NM 87545
USA

TODD SAMUEL
WESTINGHOUSE HANFORD CO.
P.O. BOX 1970, HO-38
RICHLAND WA 99352
USA

MOHAMED SAWAN
UNIVERSITY OF WISCONSI
1500 JOHNSON DR.
MADISON WI 53706
USA

R. SCHERPELZ
BATTELLE - PNL
BATTELLE BLVD., P.O. BOX 999
RICHLAND WA 99352
USA

RANDY SCHWARZ
WESTINGHOUSE HANFORD COMPANY
P.O. BOX 1970, MSIN HO-35
RICHLAND WA 99352
USA

KEVIN SCHWINKENDORF
WESTINGHOUSE HANFORD C
P.O. BOX 1970, MSIN HO
RICHLAND WA 99352
USA

ROBERT SEAMON
LOS ALAMOS NATIONAL LABORATORY
GROUP X-6, MS B226
LOS ALAMOS NM 87544
USA

LOREN SHARP
WASHINGTON PUBLIC POWER SUPPLY SYST
P.O. BOX 968
RICHLAND WA 99352
USA

MARK SHAVERS
TEXAS A&M UNIVERSITY
DEPARTMENT OF NUCLEAR
COLLEGE STATION TX 778
USA

M. SHEA
HANSCOM AFB
GEOPHYSICS DIRECTORATE
BEDFORD MA 01731-5000
USA

YASUYUKI SHIMIZU
KAWASAKI HEAVY INDUSTRIES

KAZUO SHIN
KYOTO UNIVERSITY
DEPT OF NUCLEAR ENGINE
YOSHIDA, SAKYO-KU, KYO
JAPAN

JUDY SHINN
NASA
NASA LANGLEY RESEARCH CENTER
HAMPTON VA 23665-5225
USA

SCOTT SHIRAGA
WESTINGHOUSE HANFORD CO.
P.O. BOX 1970, N1-40
RICHLAND WA 99352
USA

AKIRA SHONO
MARTIN MARIETTA ENERGY
131 GOLFCREST LN.
OAK RIDGE TN 37830
USA

TED SIMMONS
SANDRA NATIONAL LABORATORIES
MS 5609, P.O. BOX 5800
ALBUQUERQUE NM 87185
USA

ROBERT SIMONS
WESTINGHOUSE HANFORD COMPANY
P.O. BOX 1970, MSIN HO-35
RICHLAND WA 99352
USA

LISA SIMONSEN
NASA
NASA LANGLEY RESEARCH
HAMPTON VA 23665
USA

GARY SLIPKE
BISCO PRODUCTS
2300 E. DEVON AVE.
ELK GROVE IL 60007
USA

DON SMART
HANSCOM AFB
SPACE PHYS. DIV., GEOPHYS. DIRECTOR
HANSCOM MA 01731
USA

JAMES SMATHERS
DEPT OF RADIATION ONCO
SUITE B265, 200 UCLA M
LOS ANGELES CA 90024-6
USA

NIGEL SMITH
AEA TECHNOLOGY
WINFIRTH, DORCHESTER
DORSET DT28DH
ENGLAND

MASAYUKI SUGIYAMA
CRC RESEARCH INSTITUTE
1-3-D17, NAKASE, CHIBA-SHI, CHIBA
CHIBA
JAPAN

KEIKO TADA
MISTUBISHI ATOMIC POWER INDUSTRIES,
4-1, SHIBAKQUEN 2-CHOME MINATO-KU
TOKYO N/A
JAPAN

JENNIFER TANNER
BATTELLE - PACIFIC NORTHWEST LABORA
P.O. BOX 999
RICHLAND WA 99352
USA

E. TRUMBLE
WESTINGHOUSE SAVANNAH RIVER COMPANY
116 DRIFTWOOD CIRLCE
AIKEN SC 29801
USA

WILLIAM URBAN
LOS ALAMOS NATIONAL LABORATORY
MS B226
LOS ALAMOS NM 87545
USA

FREJ WASASTJERNA
TECHNICAL RESEARCH CENTRE OF FINLAN
P. O. BOX 208
ESPOO SF-02151
FINLAND

J. WILKINS
CLARK ATLANTA UNIVERSITY
JAMES P. BRAWLEY DT. AND FAIR STR.,
ATLANTA GA 30314
USA

DAVE WOOTAN
WESTINGHOUSE HANFORD COMPANY
P.O. BOX 1970
RICHLAND WA 99352
USA

AKIHIRO YOSHIDA
POWER REACTOR AND NUCL FUEL DVLPMNT
O-ARAI ENGINEERING CENTER
4002, O-ARAI-MACHI, IBARAKI-KEN N/A
JAPAN

PAUL STANSBURY
BATTELLE - PACIFIC NORTHWEST LABORA
P.O. BOX 999 MS K3-55
RICHLAND WA 99352
USA

RAI-KO (DR.) SUN
UNIVERSITY OF CALIFORNIA
LAWRENCE BERKELEY LAB., 1 CYCLOTRON
BERKELEY CA 94720
USA

SHUN-ICHI TANAKA
JAPAN ATOMIC ENERGY RESEARCH INSTIT
SHIELDING LABORATORY
TOKAI-MURA, IBARAKI-KEN N/A 319-11
JAPAN

HANS TOFFER
WESTINGHOUSE HANFORD CO.
P.O. BOX 1970, HO-38
RICHLAND WA 99352
USA

HIROKAZU TSUNODA
MITSUBISHI RESEARCH INSTITUTE, INC
3-6 OTEMACHI 2-CHOME CHIYODA-KU
TOKYO
JAPAN

JOHN VAN KEUREN
WESTINGHOUSE HANFORD CO
N1-19, P.O. BOX 1970
RICHLAND WA 99352
USA

KIM WELSCH
WESTINGHOUSE HANFORD COMPANY
P.O. BOX 1970
RICHLAND WA 99352
USA

W. WILLINGHAM
KAISER ENGINEERS - HANFORD
P.O. BOX 888
RICHLAND WA 99352
USA

PETER WOOTTON
UNIVERSITY OF WASHINGTON
1959 NE PACIFIC ST, RAD. ONCOLOGY D
SEATTLE WA 98195
USA

RONALD ZELAC
LANDAUER INC
2 SCIENCE ROAD
GLENWOOD IL 60425
USA

ROB STEWART
BATTELLE - PACIFIC NOR
P.O. BOX 999
RICHLAND WA 99352
USA

MASAYUKI SUZUKI
TOYO ENGINEERING CORPO
8-1, 2 CHOME, AKANAHEM
CHIBA N/A 275
JAPAN

HIROAKI TANIUCHI
OAK RIDGE
158 GOLFCREST LN
OAK RIDGE TN 37830
USA

DAVID TRUBEY
10800 N. AIRWAY LOOP
CITRUS SPRINGS FL 3263
USA

K. UEKI
SHIP RESEARCH INSTITUT
NUCLEAR TECHNOLOGY DIV
6-38-1 SHINKAWA, MITAK
JAPAN

ALAN WALTAR
WESTINGHOUSE HANFORD C
P.O. BOX 1970, HO-32
RICHLAND WA 99352
USA

ARCHIE WILCOX
MOHR AND ASSOCIATES
228 INDIAN COURT
RICHLAND WA 99352
USA

JOHN WILSON
NASA
NASA LANGLEY RESEARCH
HAMPTON VA 23602
USA

NAOKI YAMANO
SUMITOMO ATOMIC ENERGY
DIVISION OF NUCLEAR DE
2-6-1 KAJI-CHO, CHIYOD
JAPAN

DOUG ZOUCHA
WESTINGHOUSE HANFORD C
P.O. BOX 1970
RICHLAND WA 99352
USA

TECHNICAL PROGRAM

Monday Morning, April 27, 1992
Plenary
Bronze/Silver Rooms

Chair: W. Ruff (Westinghouse Hanford Company)

8:15 *Welcome/Introductions*

H. Toffer, Manager
Reactor Physics and Special Studies
Westinghouse Hanford

W. Ruff, Deputy Director
Facility Operations Division
Westinghouse Hanford

J. D. Wagoner, Manager
U.S. Department of Energy
Richland Field Office

8:30 *Biomarkers and Their Potential Use in Radiation Protection*. John Johnson (PNL)

9:00 *The Horizons for Advanced Reactor Shielding Technology: Sunrise or Sunset?* Dan Ingersoll (ORNL)

9:30 *Instrumentation for a Secure Nuclear Future.* Arthur Lucas (Victoreen, Inc.)

10:00 *New Quantities for Use in Radiation Protection.* Charles Meinhold (NCRP)

10:30 *Beyond the Horizon in Radiation Shielding: A Stochastic World.* John Butler (AEA-Winfrith)

11:00 Open Discussion

Monday Afternoon, April 27, 1992
Advanced Computer Applications
Bronze Room

Chair: R. T. Primm III (ORNL)

2:00 *The Impact of Advances in Computer Technology on Particle Transport Monte Carlo.* William R. Martin (Univ of Michigan), James A. Rathkopf (LLNL), Forrest B. Brown (KAPL)

2:20 *Massively Parallel Monte Carlo Calculations with Workstations.* L. L. Carter, K. E. Hillesland (Westinghouse Hanford)

2:40 *Implementation of the Monte Carlo Charged Particle Transport Code EGS4 on the Hypercube.* Bernadette L. Kirk, Yousry Y. Azmy, T. A. Gabriel, C. Y. Fu (ORNL)

3:00 *Porting of Radiation Shielding Codes to Personal Computers.* Thomas M. Jordan (Experimental and Mathematical Physics Consultants)

3:20 **Break**

3:40 *Development of a Multi-Dimensional Coupled Neutron-Gamma Shielding Package for an Entry Level Workstation.* Donald E. Palmrose, Theodore A. Parish (Texas A&M)

4:00 *Graphical Debugging of Combinational Geometry.* Thomas J. Burns, Mark S. Smith (ORNL)

4:20 *Graphical Post-Processor Created for the Origen2 Code.* R. A. Schwarz, J. H. Lu, N. Shrivastava (Westinghouse Hanford)

4:40 *ChernoLit---Chernobyl Bibliographic Search System.* R. L. Hill, R. A. Kennedy, F. Carr, J. A. Mahaffey (PNL)

Monday Afternoon, April 27, 1992
Medical Applications
Silver Room

Chair: J. C. McDonald (PNL)

2:00 *Radiation Physics Aspects of Boron Neutron Capture Therapy.* David W. Nigg, Floyd J. Wheeler, Daniel E. Wessol, Carol A. Atkinson (INEL, EG&G Idaho)

2:20 *Boron Neutron Capture Supplementation of Fast Neutron Beam Therapy.* P. Wootton, S. Brossard, J. Livesey, R. Risler, G. Laramore, T. Griffin (Univ. of Wash.)

2:40 *Monte Carlo Analysis of an Accelerator Epithermal Neutron Irradiation Facility (AENIF) for Boron Neutron Capture Therapy.* T. E. Blue, T.-X. B. Qu, N. Gupta, R. A. Gahbauer (Ohio State)

3:00 *Neutron Beam Energy Transport Calculations by Combining Monte Carlo and Convolution Techniques.* Michael F. Moyers (Loma Linda Univ)

3:20 **Break**

3:40 *Fast Neutron Kerma Factors---Recent Determinations Below 100 MeV.* P. M. DeLuca, Jr., C. L. Hartmann, D. W. Pearson (Univ of Wisconsin - Madison)

4:00 *Comparison of Bonner Sphere Measurements with Shield Calculations for 46 MeV Be(p,xn) Neutron Sources.* James Smathers (UCLA), Nolan Hertel (Univ of Texas at Austin), Lee Myers (UCLA)

4:20 *K-Fluorescence X-ray Apparatus for the Calibration of Radiation Measuring Instruments.* R. A. Fox, J. C. McDonald, C. D. Hooker, K. K. Large (PNL)

4:40 *A Radioisotope Production Cyclotron Designed to Minimize Dose.* F. F. Szlavik, L. E. Moritz (TRIUMF--Canada)

6:00 **Vendor Show Open House**

Tuesday Morning, April 28, 1992
Radiation Effects and Analyses
Bronze Room

Chair: K. Ueki (Ship Resch Inst--Japan)

8:30 *Preview---a Fast Kernel-Based Program for Calculation of Pressure Vessel Irradiation.* Frej Wasastjerna (Technical Research Centre--Finland)

8:50 *Fast Flux Test Facility Irradiation Surveillance Assembly HM013: Dosimetry Analysis.* R. L. Simons, R. H. Webb (Westinghouse Hanford)

9:10 *SP-100 Reactor Cell Activation.* A. D. Wilcox (Westinghouse Hanford)

9:30 *Neutron Shielding Ability of KRAFTON N2-Manan-KRAFTON N2 Sandwich-type Material and Others.* K. Ueki, A. Ohashi (Ship Resch Inst--Japan), Y. Anayama (Sanoya Industry--Japan)

9:50 *SP-100 Inert Gas Activation.* A. D. Wilcox (Westinghouse Hanford)

10:10 **Break**

10:30 *Development of Neutron Shield Materials for Transport Packaging.* K. Tsuda, I. Iida, F. Matsuda (Kobe Steel--Japan), M. Nakazawa, T. Iguchi, Sjafruddin (Univ of Tokyo--Japan)

10:50 *Soil Density and Mass Attenuation Coefficients for Use in Shielding Calculations at the Hanford Waste Vitrification Plant.* Roger C. Brown (Westinghouse Hanford)

11:10 *Tank 101-SY Gamma Scan Evaluations Using Monte Carlo Techniques.* R. D. Crowe (Westinghouse Hanford)

11:30 *Effective Materials and Optimal Design for Radiation Shields.* Y. Karni (NRCN - Israel), E. Greenspan (Univ of California-- Berkeley), J. Bendahan, T. Gozani (SAIC)

Tuesday Morning, April 28, 1992
Radiation in Space
Silver Room

Chair: E. Normand (Boeing)

8:30 *Natural Radiation Environment Fluence and Dose Predictions for Missions to the Moon and Mars.* J. E. Nealy, L. C. Simonsen, S. A. Striepe (NASA Langley Research Center)

8:50 *Improved Radiation Environment Evaluation Technique: Application to the Redesigned Space Station.* M. H. Appleby (Boeing), M. J. Golightly, A. C. Hardy (NASA)

9:10 *Numerical Methods for High Energy Nucleon Transport.* S. L. Lamkin, G. S. Khandelwal (Old Dominion Univ), J. L. Shinn, J. W. Wilson (NASA Langley Research Center)

9:30 *Computationally Efficient Space Radiation Transport Codes.* J. L. Shinn, J. W. Wilson, L. W. Townsend, F. A. Cucinotta (NASA Langley Research Center), S. Y. Chun (Old Dominion Univ), F. F. Badavi (Christopher Newport College)

9:50 *Multi-Generation Transport Theory as an Analytical Heavy-Ion Transport Model.* M. R. Shavers, J. Miller, W. Schimmerling (LBL), J. W. Wilson, L. W. Townsend (NASA)

10:10 **Break**

10:30 *RTG Analysis Using MCNP 4/PC.* Thomas M. Jordan (E.M.P. Consultants), Matthew T. Wallace (Jet Propulsion Lab)

10:50 *New Direction in Heavy Ion Shielding.* J. W. Wilson (NASA Langley Research Center), F. F. Badavi (Christopher Newport College)

11:10 *Time Analysis of the October 1989 Proton Flare Using Computerized Anatomical Models.* Lisa C. Simonsen, Francis A. Cucinotta (NASA Langley Research Center), William Atwell (Rockwell International), John E. Nealy (NASA Langley Research Center)

11:30 *Potential Threat of Solar Proton Events to Missions in Space.* M. A. Shea, D. F. Smart (Hanscom AFB)

11:50 *Use of Tissue Equivalent Proportional Counters to Characterize Radiation Quality on the Space Shuttle.* L. A. Braby, T. J. Conroy, D. C. Elegy, L. W. Brackenbush (PNL)

Tuesday Afternoon, April 28, 1992
Monte Carlo Methods and Applications
Bronze Room

Chair: M. B. Emmett (ORNL)

2:00 *MOCAL, A Monte Carlo Albedo Code.* Robert J. Morford, Leland L. Carter, Edward R. Siciliano (Westinghouse Hanford)

2:20 *CASCADE---The System of Computer Codes for Monte Carlo Calculations of Electromagnetic Showers.* A. M. Kolchuzhkin, I. S. Tropin, S. A. Vorobyev, V. N. Zabaev, D. E. Chernov (Tomsk Polytechnical Univ)

2:40 *Analysis of the Fall-1989 Two-Meter Box Test Bed Experiments Performed at the Army Pulse Radiation Facility (APRF).* J. O. Johnson, J. D. Drischler, J. M. Barnes (ORNL)

3:00 *Development of Morse-AZA Code for Radiation Shielding Dose Calculation Using Albedo Monte Carlo Method.* T. Matsumura, K. Ishida (CRIEPI--Japan), M. Suzuki, M. Tsuji (Toyo Engineering--Japan)

3:20 *Nuclear Vulnerability of the U.S. M60A1 in an Initial Radiation Environment: MASH Code System Analysis.* J. O. Johnson, J. M. Barnes, T. J. Burns, J. D. Drischler (ORNL)

3:40 *Monte Carlo Calculations of Neutron Doses to Reactor Pressure Vessels.* A. F. Avery (AEA Technology--UK)

Tuesday Afternoon, April 28, 1992
Fast Reactor Shielding
Silver Room

Chair: D. T. Ingersoll (ORNL)

2:00 *The Role of the Janus Experimental Shielding Programme in the Assessment of the Shielding Methods Employed for EFR.* I. J. Curl (AEA Reactor Services--UK), D. Calamand (CEA-CEN Cadarache--France), K. Muller (Siemens/KWU--FRG)

2:20 *Experiment and Analysis of Neutron Streaming through an Axial Shield in an FBR Fuel Subassembly.* K. Chatani, H. Tsunoda, A. Shono, S. Suzuki, K. Kinjo (PNC--Japan)

2:40 *B_4C Shielding Design Study for the Joyo Reactor.* A. Yoshida, K. Chatani, S. Suzuki, K. Kinjo (PNC--Japan)

3:00 *French Contribution to the Analysis of the European Janus Experimental Programme for the Validation of New Shielding Concepts.* D. Calamand (CEA/CEN Cadarache--France)

3:20 *Current Status of JASPER: Japanese-American Shielding Program of Experimental Research.* J. V. Pace III (ORNL), A. Shono (PNC--Japan)

3:40 *Benchmark Calculation for FFTF Inner Radial Shield Damage Rates.* A. H. Lu, R. A. Schwarz, R. L. Simons (Westinghouse Hanford)

6:00 Social Hour

7:00 Banquet

Wednesday Morning, April 29, 1992
Radiation Protection
Bronze Room

Chairs: J. M. Selby (PNL)/K. L. Swinth (PNL)

8:30 *BREMCALC---A Computer Program for Calculating Electron and Positron Bremsstrahlung.* Paul D. Rittmann (Westinghouse Hanford)

8:50 *Radiation Protection Factor Calculations Using the VPF Computer Code.* F. J. Lemay, T. J. Jamieson (SAIC--Canada), T. Cousins (Defence Research Establishment--Canada)

9:10 *HESYRL Radiation Protection System Control and Data Acquisition.* Yuxiong Li, Juexin Li, Xinquan Ning, Can Wu (USTC--PRC)

9:30 *Neutron and Gamma Boundary Radiation Monitoring at Continuous Electron Beam Accelerator Facility.* R. J. Letizia, S. Pandey, E. M. Pollock (Nuclear Research Corp.), G. Stapleton (Southern Univ. Research Assoc.)

9:50 **Break**

Aircraft Radiation Environment

Chair: K. O'Brien (Northern Arizona Univ)

10:10 *The Distribution of Galactic Cosmic Rays and Solar Particle to Aircraft Altitudes.* D. F. Smart, M. A. Shea (Hanscom AFB)

10:30 *Extraterrestrial Radiation Exposure of Aircraft Crews.* Keran O'Brien (Northern Arizona Univ), Wallace Friedberg, Frances E. Duke, Lorrenza Snyder (FAA), Edgar B. Darden, Jr. (Oak Ridge Associated Universities), Herbert H. Sauer (NOAA)

10:50 *Model and Data Base for Background Radiation Exposure of High-Altitude Aircraft.* J. W. Wilson, J. E. Nealy (NASA Langley Research Center)

11:10 *Instruments to Measure Radiation Dose to Aircraft Crews and Passengers.* L. W. Brackenbush, L. A. Braby, R. I. Scherpelz (PNL)

12:00 **Luncheon**

Wednesday Morning, April 29, 1992
Evaluated Nuclear Data
Silver Room

Chair: R. C. Little (LANL)

8:30 *Validation of Beryllium Neutron Multiplication Cross Sections for ENDF/B-V.* Richard S. Hartley (Air Force Inst of Technology), Nolan E. Hertel (Univ of Texas at Austin), John Wiley Davidson (LANL) ★

8:50 *FSXLIB-J3: MCNP Continuous Cross Section Library Based on JENDL-3.* K. Kosako, Y. Oyama, H. Maekawa (JAERI)

9:10 *Integral Test of Cross Sections in JENDL-3 by Monte Carlo Analysis of Benchmark Experiments.* K. Ueki, A. Ohashi (Ship Resch Inst--Japan), M. Kawai (Toshiba--Japan)

9:30 *Key Changes in Nuclear Data in the Transition from ENDF/B-V to ENDF/B-VI.*
P. G. Young (LANL)

9:50 **Break**

10:10 *The ENDF/B-VI Photon Interaction Library.* Dermott E. Cullen, Sterrett T. Perkins, Ernest F. Plechaty (LLNL)

10:30 *Phase II Testing of ENDF/B-VI Shielding Data.* D. T. Ingersoll, R. Q. Wright, C. O. Slater (ORNL)

10:50 *Cross Sections from ENDF/B-VI for MCNP.* R. C. Little and R. E. Seamon (LANL)

11:10 *NEANSC Working Group on International Evaluation Cooperation.* D. C. Larson (ORNL), Claes Nordborg (NEA Data Bank--France), C. L. Dunford (BNL)

Wednesday Afternoon, April 29, 1992
Computer Codes and Methods
Silver Room

Chair: D. K. Trubey (Private Consultant)

2:00 *Simple Estimation Formula for Radiation Duct Streaming.* Kazuo Shin (Kyoto Univ), Y. Seki, H. Takatsu (JAERI--Japan)

2:20 *Verification of Broder's Formula Using One-Dimensional Discrete Ordinates Transport (ANISN) and Goldstein's Effective Z Methods.* Madeline Anne Feltus (Penn State) ★

2:40 *Transport Calculations Using STREAM.* F. J. Lemay, T. J. Jamieson (SAIC--Canada)

3:00 *Gamma Ray Exposure Buildup Factors in Polynomial Form for QADYA, a Point Kernel Shielding Code.* Andrew D. Hodgdon (YAEC)

3:20 *The Behavior of Gamma-Ray Buildup Factors in Stratified Shields.* Y. Harima (Tokyo Inst of Technology--Japan), H. Hirayama (National Lab for High Energy Physics--Japan), M. Sugiyama (CRC Research Inst --Japan), S. Tanaka (JAERI--Japan)

3:40 *Online Calculation of the Decay Heat of Assemblies at the Fast Flux Test Facility.* R. A. Schwarz, L. L. Carter, F. A. Schmittroth (Westinghouse Hanford), L. B. Brown (Consultant)

★ Best Paper Nominee

Wednesday Afternoon, April 29, 1992
Accelerator Sources and Shielding--I
Bronze Room

Chair: T. Nakamura (Tohoko University)

2:00 *Radiation Shielding for the Superconducting Super Collider.* Jeffrey S. Bull (Superconducting Super Collider Laboratory) ★

2:20 *Using the EGS4 Computer Code to Determine Radiation Sources Along Beam Lines at Electron Accelerators.* S. Mao, J. Liu, W. R. Nelson (Stanford Linear Accelerator Center)

2:40 *Particle Production Models in HETC88 in the Energy Range 3 to 30 GeV.* R. G. Alsmiller, Jr., F. S. Alsmiller, C. Y. Fu (ORNL)

3:00 *The Use of Delay Times in the Intranuclear Cascade Model of High-Energy (>~ 5 GeV) Hadron-Nucleus Collisions.* F. S. Alsmiller, R. G. Alsmiller, Jr., O. W. Hermann (ORNL)

3:20 *Transport Calculations of Radiation Streaming Through Shielding Penetrations for a Free-Electron Laser Accelerator Facility.* T. W. Armstrong (SAIC), D. L. Johnson (Boeing)

3:40 *Radiological Shielding Calculations for an Airborne Free-Electron Laser.* William C. Sailor, J. Wiley Davidson (LANL)

4:00 *Predictions of Induced Radioactivity in a Free-Electron Laser Wiggler Due to 80- and 180-MeV Electron Beam Losses.* T. W. Armstrong, B. L. Colborn (SAIC), D. L. Johnson (Boeing)

4:20 *Measurement on Electron Linac Prompt Radiation Field by Alanine/ESR Dosimetry.* Yuxiong Li (USTC--PRC), Renyou Liang (Academia Sinica-- PRC), Juexin Li (USTC--PRC), Yunhua Xu (Academia Sinica--PRC)

5:45 **Winery Tour and Dinner**

★ Best Paper Nominee

Thursday Morning, April 30, 1992
Radiation Sources and Dosimetry
Silver Room

Chair: N. E. Hertel (Univ of Texas at Austin)

8:30 *Adjustment Method for Neutron Energy Spectra Produced by (α,n) Reactions from Light Elements.* Naoki Yamano (Sumitomo--Japan)

8:50 *Radiation Spectra for a ^{238}Pu Heat Source.* H. J. Goldberg (Westinghouse Hanford)

9:10 *Methods for Calculating Dose Rates from Large Nuclear Reactor Fuel Arrays.* R. A. Schwarz, J. S. Lan (Westinghouse Hanford)

9:30 *Dose Calculations for Nuclear Criticality Accidents Shielded by Large Amounts of Water.* K. N. Schwinkendorf, A. D. Wilcox, S. P. Roblyer, H. Toffer (Westinghouse Hanford) ★

9:50 *Development of Real Time Personal Neutron Dosimeter with Two Silicon Detectors.* T. Nakamura, N. Tsujimura (Tohoku Univ-- Japan), T. Yamano (Fuji Electric--Japan)

10:10 **Break**

10:30 *Determination of Radionuclide Contents of an EBR-II Spent-Fuel Storage Cask.* R. I. Scherpelz, D. L. Haggard, R. D. Stewart (PNL)

10:50 *Shielding Data and Methods for Evaluating 1-cm Depth Dose Equivalent of Photons, β-Rays (Electrons), and Neutrons Based on ICRP-26 Recommendation.* Shun-ichi Tanaka, Hiroshi Kotegawa, Tomoo Suzuki, Akira Hasegawa (JAERI)

11:10 *Monte Carlo Calculations of Detector Responses Due to Plutonium-Oxide Sources.* L. L. Carter, R. F. Eggers, T. J. Samuel (Westinghouse Hanford), T. L. Williams (DOE)

★ Best Paper Nominee

Thursday Morning, April 30, 1992
Fusion Nucleonics and Shielding
Bronze Room

Chair: D. Dudziak (North Carolina State Univ)

8:30 *A Review of Shielding Experiments for Fusion Reactor at FNS/JAERI.* Hiroshi Maekawa, Yukio Oyama, Shun-ichi Tanaka (JAERI)

8:50 *Integral Fusion Neutronics Experiments and Analysis.* Anil Kumar, Mohamed A. Abdou (Univ California--Los Angeles), Jean Pierre Schneeberger (Ecole Polytechnique--Lausanne)

9:10 *Nuclear Data for Fusion Blanket Nucleonics and Shielding.* E. T. Cheng (TSI Research)

9:30 *Fusion Neutron Streaming Benchmark Experiment at Oktavian.* Y. Oka (Univ of Tokyo--Japan), K. Shin (Kyoto Univ--Japan), J. Yamamoto, A. Takahashi (Osaka Univ--Japan)

9:50 *Shielding Considerations for ITER: Current Status and Future Directions.* L. A. El-Guebaly, M. E. Sawan (Univ of Wisconsin-Madison)

10:10 **Break**

Accelerator Sources and Shielding--II

Chair: W. Davidson (LANL)

10:30 *Thick Target Neutron Yield for Charged Particles.* Kazuo Shin, Kagetomo Miyahara (Kyoto Univ), Yoshitomo Uwamino (Univ of Tokyo)

10:50 *Shielding and Radiation Protection at the SSRL 3 GeV Injector.* N. E. Ipe, J. C. Liu (Stanford Linear Accelerator Center)

11:10 *Neutron Skyshine from End Stations of the Continuous Electron Beam Accelerator Facility.* Rai-Ko S. Sun (LBL)

11:30 *Measurement and Calculation of Neutron Leakage Through a Labyrinth from a 40 MeV Proton Cyclotron Room.* Takashi Nakamura (Tohoku Univ--Japan), Toshio Ishikawa (Fujita Corp--Japan)